HYPOXIA-INDUCED RESPONSES OF PORCINE PULMONARY VEINS

AMY ARNOLD

PhD 2017

Hypoxia-Induced Responses of Porcine Pulmonary Veins

Amy Arnold

A thesis submitted in partial fulfilment of the requirements of Robert Gordon University for the degree of Doctor of Philosophy

January 2017

Declaration

I declare this thesis for degree of Doctor of Philosophy has been composed entirely by myself. The experimental work which is documented was conducted by myself. Verbatim extracts and information contained within this thesis which have not arisen from the results generated have been specifically acknowledged and referenced.

Contents

List of Figures

List of Tables

Acknowledgements

I would like to give thanks to a number of people who have contributed to and supported my rewarding yet challenging journey as a PhD student.

First and foremost, I would like to thank my principal supervisor, Dr. Stuart F. Cruickshank for his ongoing positivity and encouragement. He has helped me develop many vital and transferable skills in terms of scientific techniques and writing and has helped ensure I always look on the bright side and redirect energy to ensure optimal productivity when things do not work out as expected. I would like to thank my secondary supervisors: Dr. Helene Widmer for her invaluable help and patience during molecular profiling studies and Dr. Iain Rowe for support and advice regarding data analysis, electrophysiology and oxygen monitoring. Thanks also go to Prof. Alison Strath and Dr. Iain Rowe for their support and flexibility as employers over the last year - without their ongoing support I would most certainly not have finished my write-up by the deadline.

To all the staff at the School of Pharmacy and Life Sciences (and previously the Institute of Health and Wellbeing Research (IHWR)) including Margaret Brown, Tina Lowes, Mairi Thomson and Chris Fletcher for technical help. To Andrea MacMillan for administrative support and for always helping keep a smile on my face. To Prof. Cherry Wainwright (in her role as Director of IHWR) and Dr Rachel Knott (in her role as Graduate School Leader of IHWR) for their support throughout my PhD project. I also thank Sarah, Karen and Emma who all provided advice and encouragement throughout the journey.

Thanks go to Robert Gordon University (IHWR) for funding my three-year studentship and to The Physiological Society and The British Pharmacological Society for travel grants which allowed me to attend a number of national and international conferences.

I thank Heather McClafferty (from Professor Mike Shipston's group, Centre of Integrative Physiology, University of Edinburgh) for her kind help and expert advice regarding molecular biology techniques.

To my mother, for her unquestionable strength, love and guidance and to my father for his love and continuing help and support. To my younger sister Lisa who was always there to provide words of encouragement and wisdom (beyond her years). To my grandparents, both absent and present who

have all been influential throughout my childhood and adult life. I know they are all very proud of everything I have achieved to date despite my seemingly perpetual life as a student. To my partner Darren, who, when we first met, was blissfully unaware of the consequences of dating a PhD student. In spite of this, he has remained resolute in his understanding throughout the long evenings in the lab and during the write-up, not to mention the emotional rollercoaster that seems to go hand-in-hand with scientific experimentation. To Darren's family also who were always interested to hear my progress and lend a word of encouragement.

To my dear friend Bernadette, who encouraged me to return to study and helped develop my critical thinking skills with all her questions. Last but not at all least, to my PhD partner in crime, Olivia, we laughed, we cried and it was always nice to know there was someone by my side who understood exactly how I felt. I feel extremely lucky that not only has this journey allowed me to develop academically, it has brought me a friend for life.

Publications

Arnold, A., Hannon, C., Dospinescu, C., Widmer, H., Rowe, I. & Cruickshank, S.F. *Hyperoxic-induced contraction in porcine pulmonary veins* (July 2013) (Abstracts, quadrennial meeting of the International Union of Physiological Sciences, Birmingham, UK)

Arnold, A., Widmer, H., Rowe, I. & Cruickshank, S.F. *Organ culture: impact on agonist- and hypoxia-induced responses of porcine inferior pulmonary veins* (December 2013) (Abstracts, annual meeting of the British Pharmacological Society, London, UK)

Arnold, A., Widmer, H., Rowe, I. & Cruickshank, S.F. *Ketamine: impact on hypoxic vasoconstriction responses in porcine intrapulmonary veins* (December 2014) (Abstracts, annual meeting of the British Pharmacological Society, London, UK)

Arnold, A., Linklater, L., Widmer, H., Rowe, I. & Cruickshank, S.F. *Lysosomal calcium: impact on serotonin-induced contractions of ovine pulmonary arteries* (March 2015) (Abstracts, annual Experimental Biology conference, Boston, Massachusetts, USA)

Abstract

The pulmonary vein (PV) constricts to hypoxia however little is known about the underlying mechanisms. Hypoxic PV constriction is proposed to recruit upstream capillary beds and optimise gas exchange in healthy humans and may play a role in high altitude pulmonary oedema. The PV is also intrinsic to disease states including pulmonary hypertension and pulmonary veno-occlusive disease. Blood vessel culture can be a powerful tool to enable assessment of the impact of environmental factors on vessel function and as a disease model. However culture conditions alone affect vessel contractility; the effect of culture conditions on PV function remained to be established. The aim of this project was to investigate hypoxic responses of porcine PVs including the impact of maintenance in culture.

Maintenance of PVs in culture conditions for 24 hours increased contraction to hypoxia and inhibited hypoxic relaxation post-contraction. These changes to PV hypoxic responses were thought to result from endothelial dysfunction. However, the endothelial nitric oxide synthase inhibitor L-NAME inhibited PV hypoxic contraction and enhanced relaxation. The impact of K^+ channel inhibitors on hypoxic contraction was also investigated. Penitrem A, 4AP, DPO-1, $ZnCl_2$ and glyburide had no significant effect however TEA and BDM inhibited the hypoxic contraction. This suggested that TASK, $K_V1.5$, BK_{Ca} and K_{ATP} do not play a role in the mechanism of hypoxic pulmonary venoconstriction however K_V channels containing $K_V2.1$ α subunits may modulate the response.

Results with L-NAME suggested endothelial dysfunction may not fully account for the change in PV function after exposure to culture. Therefore the impact of PV maintenance in culture was further explored using an isolated PV smooth muscle cell (PVSMC) model. Maintenance of PVs in culture conditions had minimal impact on morphology and electrical properties of PVSMCs. Notably, resting membrane potential and hypoxia-induced depolarisation were not significantly different.

Based on the findings of this study, the endothelium in PVs appears to a) play a major role in modulation of the hypoxic response b) be sensitive to short-term exposure to culture conditions. K^+ channels appear to play a minor role in PV hypoxic contraction and SMCs isolated from PVs maintained in culture conditions have similar morphological and electrophysiological characteristics to freshly isolated PVSMCs. Taking all this into account, endothelial regulation of contractility should be a key focus for future PV research.

Keywords: hypoxia; pulmonary vein; potassium channels; nitric oxide; vasoconstriction; smooth muscle cells; blood vessel culture; endothelium

Chapter 1

General Introduction

The pulmonary vein (PV) constricts to hypoxia however little is known about the underlying mechanisms. Hypoxic PV constriction is proposed to recruit upstream capillary beds and optimise gas exchange in healthy humans (Taylor *et al.,* 2011) and may play a role in disease states including high altitude pulmonary oedema (Bärtsch and Gibbs, 2007, Maggiorini *et al.,* 2001).

Pulmonary Circulation

The function of the lung is respiratory gas exchange and the pulmonary circulation is designed to aid with this function. Systemic venous blood (oxygen saturation 70-80%) (Muralidhar, 2002, Reyer, 2013) is returned to the right side of the heart and pumped to the lungs for oxygenation via pulmonary arteries and arterioles to capillary beds that surround the respiratory units of the lung (alveoli). At the interface between the alveoli and capillary bed, oxygen moves from the alveoli into blood and carbon dioxide moves in the opposite direction. Oxygenated blood then travels from the capillary beds via pulmonary venules and veins back to the left atrium to be pumped round the systemic circulation (Tortora and Derrickson, 2006).

Pulmonary blood vessels have thinner walls and less smooth muscle than their systemic counterparts resulting in lower pressures (Dembinski *et al.,* 2004). Pulmonary arterial pressure (systolic/diastolic) is approximately 23/9 mmHg and pulmonary capillary wedge pressure is approximately 10 mmHg in healthy humans (Muralidhar, 2002). Pulmonary venous pressure is suggested to lie somewhere between pulmonary arterial and pulmonary capillary wedge pressure (Chaliki *et al.,* 2002). In contrast, pressures within the systemic circulation are approximately six times higher than those recorded in the pulmonary circulation (Dembinski *et al.,* 2004) with anything up to 120/80 mmHg (systolic/diastolic) being considered normal (Viera, 2007). Resistance values are also approximately six times higher in the systemic circulation (900-1400 dyne.sec.cm^{-5}) than in the pulmonary

circulation (150-250 dyne.sec.cm^{-5})(Muralidhar, 2002). The lower resistance in the pulmonary circulation is attributable to the shorter blood vessels present within the blood vessel network and the larger diameter of pulmonary vessels compared with systemic vessels (Boron and Boulpaep, 2005). Diameter in particular makes a significant contribution to resistance with resistance being inversely proportional to (diameter)^4 (Tortora and Derrickson, 2006).

Anatomy and Structure of the Pulmonary Vein

The primary role of the pulmonary vein (PV) as the last segment of the pulmonary circulation is to return oxygenated blood from the lungs to the left atrium the heart. In humans, the pulmonary venous tree comprises 15 branching orders with the first formed by post-capillary venules. These small PVs merge and form one PV for each lobule of the lung and eventually, one PV for each lobe of the lung (Hughes and Morrell, 2001). Four extrapulmonary veins leave the lung and empty into the left atrium and are named: right superior, right inferior, left superior and left inferior pulmonary veins (Porres *et al.,* 2013).

Similar to all other veins, PVs have endothelial, smooth muscle and adventitial layers and have less smooth muscle than size-matched pulmonary arteries (PAs) (Hughes and Morrell, 2001). In humans, PVs larger than 100μm diameter have an internal elastic lamina lined by the endothelial layer and a disorganised medial layer composed of smooth muscle, collagen and elastic fibres with no clearly marked adventitial layer (Kay, 1983). Small PVs located near capillaries are "partially muscular" whereas larger PVs have a continuous layer of smooth muscle (Hislop and Reid, 1973).

Regulation of Tone in the Pulmonary Vein

Historically, PVs have been regarded as passive conduit blood vessels with no significant impact on regulation of blood flow or total vascular resistance within the lung. Consequently, in comparison to PAs, relatively little research has been conducted in order to understand the underlying functions and mechanisms of PVs involved in normal physiology and pathophysiology.

There is a significant body of research suggesting PVs as an important origin of ectopic beats and arrythmogenic activity in patients with atrial fibrillation (Haissaguerre *et al.,* 1998, reviewed by Fynn and Kalman, 2004, Khan, 2004,). However, there is an outstanding gap in the field in terms of

pulmonary venous contribution to pulmonary hypertension (Tuder *et al.,* 2013) highlighting the need for a better understanding of pulmonary venous tone regulation and contribution to disease states. PVs demonstrate vasoconstriction in response to a number of agonists and in some cases to a greater extent than PAs. Histamine (acting on smooth muscle H_1 receptors; Shi *et al.*, 1998, Toda, 1990) has a more specific/exclusive constrictor effect on PVs when compared with size-matched PAs in isolated lungs and lung slices (Glazier and Murray, 1971, Hasebe *et al*., 1992, Shi *et al.,* 1998). *In vivo* canine studies showed increased PA and PV pressure (Kadowitz *et al.,* 1975) and pulmonary vascular resistance (PVR) (Hyman *et al.,* 1978) on administration of $PGF_{2\alpha}$ (FP receptor agonist; Walch *et al.,* 2001). However in isolated canine pulmonary vessels, $PGF_{2\alpha}$ was a more potent vasoconstrictor in PVs than in PAs (Kadowitz *et al.,* 1975) and in isolated goat PAs, $PGF_{2\alpha}$ constricted PVs but PAs were unresponsive (Chand, 1981). U46619 (thromboxane A_2 mimetic, TP receptor agonist; Walch *et al.,* 2001) is a known robust, potent and dose-dependent vasoconstrictor of human and canine PVs (Ding and Murray, 2005, Walch *et al.,* 2001) and PVs from piglets are more reactive to U46619 than PAs (Arrigoni *et al.,* 1999).

Substantial innervation of the pulmonary vasculature exists and is likely to play an important role in regulation of tone within PVs and PAs. Neuronal input is mainly derived from branches of vagus and cervicothoracic sympathetic nerves including adrenergic, cholinergic and sensory fibers. In general, across species, adrenergic innervation of the pulmonary circulation is greater than cholinergic. Neuropeptidic transmission is also present with contributions from neuropeptide Y, vasoactive intestinal peptide and substance P. Neuropeptides are either co-expressed in autonomic fibers or expressed within sensory nerves. Nerve fibers extend from a plexus at the hilus of the lung (which contains parasympathetic ganglia as well as sympathetic fibers) to form a perivascular neural network within the adventitial layer of pulmonary blood vessels. A small number of nerve fibers within PAs and PVs extend into the medial layer. Innervation of the pulmonary vasculature extends down into small PAs and PVs (approximately 50 to 100µm diameter) however less autonomic/substance P containing nerves are present in PVs compared with size-matched PAs (reviewed in Townsley, 2012).

These data suggest PVs are not merely passive conduits but are intrinsically vasoactive, involved in blood flow regulation and therefore likely contribute to disease states including pulmonary hypertension.

Contribution of Pulmonary Veins to Total Pulmonary Vascular Resistance

In contrast to the systemic circulation where arteries contribute to approximately 70% of total vascular resistance, PVR is divided more equally between PAs, capillaries and PVs (Levitzky, 2002). This would suggest that PVs play a vital role in blood flow regulation with PV resistance directly impacting on flow within the pulmonary circulation (Fung and Huang, 2004). A review by Gao and Raj (2005) considered a wide range of studies which investigated contributions of blood vessels across the pulmonary circulation towards total PVR. The conclusions were that PVs appear to make a significant contribution to total PVR and that this percentage contribution decreases with increasing age in animals. There is a general shift from the main contributors to PVR being larger pulmonary vessels (PAs and PVs) in infant lungs towards more contribution from microvessels and capillaries in the adult lung. This may be due to increased alveolar size with age resulting in compression of capillary lumen and increased resistance. In addition, the smooth muscle layer is thicker in neonatal PAs and vascular smooth muscle decreases in mass with increasing age leading to larger PA lumen (reviewed by Gao and Raj, 2005) which may explain the reduced contribution of PAs to PVR. A similar reduction in vascular smooth muscle mass and increased lumen diameter may occur in PVs.

Contribution of PVs to total PVR ranged from 7% in a study using lung micropuncture in rabbits (Raj *et al.,* 1986) to 49% when using morphometric measurements in cats (Zhuang *et al.,* 1983). It is difficult to determine whether the wide range of values were a result of the different experimental techniques or species differences.

Endothelial Contribution to Pulmonary Venous Tone

The endothelium plays a vital role in regulation of pulmonary and systemic vascular tone (Barnes and Liu, 1995) . A range of contractile and relaxant mediators are released from the endothelium which all have a significant effect on vasoactivity.

Endothelin-1 (ET-1, ET_A/ET_B receptor agonist; Lopez-Valverde *et al.,* 2005) is a more potent vasoconstrictor in PVs than PAs in the rat (Rodman *et al.,* 1992), sheep (Toga *et al.,* 1992) and human (Brink *et al.,* 1991). In very low concentrations (1-100 pM), ET-1 caused relaxation in porcine pulmonary vessels and the magnitude of relaxations were greater in PVs than PAs (Zellers *et al.,* 1994). ET-1 mediated relaxations were inhibited by blocking endothelial nitric oxide synthase (eNOS) and the release of endothelium-derived nitric oxide (NO) appeared higher in PVs than PAs (Zellers *et al.,* 1994). In a different study also using a pig model, the amount and activity of eNOS protein were

greater in PVs than PAs (Bina *et al.,* 1998). Inhibition of eNOS caused an increase in baseline tension in PVs from newborn lambs with no effect on PAs and endothelium-dependent relaxations mediated by NO were larger in PVs than PAs (Gao *et al.,* 1995). The process of NO-mediated regulation of pulmonary venous tone during the perinatal period is an oxygen-dependent process which is suggested to contribute to the reduction in PVR on birth when pO_2 increases from <25mmHg (*in utero*) to 100 mmHg (reviewed by Gao and Raj, 2005). Hence, PV activity appears to be more sensitive to modulation by endothelium-derived constricting and relaxing factors than PA activity.

Effects of Hypoxia in the Systemic Circulation

Hypoxic vasoconstriction is a physiological response which is generally considered specific to the pulmonary circulation; blood vessels in the systemic circulation normally respond to hypoxia with vasodilation (Staub, 1985, Leach *et al.,* 1994). The physiological function of this dilation is to ensure adequate oxygenated blood flow towards hypoxic tissues and organs (Hampl *et al.*, 2002). Risso *et al.* (2012) proposed the physiological relevance of hypoxic dilation within systemic veins was to ensure maintenance of blood flow away from hypoxic tissue in order to avoid an increase in post-capillary resistance.

In some instances, blood vessels in the systemic circulation constrict when exposed to hypoxia; one example is the foetoplacental vasculature. This makes sense, bearing in mind that the physiological function of the placenta is to oxygenate foetal blood (Hampl *et al.*, 2002, Jakoubek *et al.*, 2006); the placenta *in utero* has a function similar to the lung upon birth. Hypoxic foetoplacental vasoconstriction (HFPV) ensures diversion of foetal blood flow to better maternally perfused (and therefore oxygenated) areas of the placenta to ensure maximal oxygenation of foetal blood (Hampl *et al.*, 2002). The phenomenon has been demonstrated in isolated human cotyledons where exposure to hypoxia results in an increased perfusion pressure due to HFPV (Hampl *et al.*, 2002, Jakoubek *et al.,* 2006). Microvessels are proposed as the most likely mediators of HFPV; larger conduit arteries and veins play less of a role. The specific microvessels involved in HFPV were not identified but microvessels on the venous side could play a role.

Hypoxic constriction in the systemic circulation has also been demonstrated within the bovine digital vein (Risso *et al.,* 2012) but is dependent on the priming vasoconstrictor. Preconstriction with KCl and phenylephrine (α_1-adrenoceptor agonist) resulted in hypoxic vasodilation and constriction, respectively. The investigators proposed that the use of phenylephrine as a priming agent may

demonstrate more closely the hypoxic response *in vivo*. They reasoned that vascular tone is normally maintained via activation of α-adrenoceptors by the sympathetic nervous system. The physiological role of hypoxic constriction in the bovine digital vein still remains to be established although it is thought to contribute to the pathophysiology of laminitis (Risso *et al.,* 2012).

These documented effects of hypoxia on the systemic circulation suggest that, in certain circumstances, hypoxia may cause vasoconstriction and that this response may involve veins (Risso *et al.,* 2012) however the physiological implications are not fully understood.

Effects of Hypoxia in the Pulmonary Circulation

The physiological purpose of hypoxic vasoconstriction within the pulmonary circulation is to maintain ventilation-perfusion matching within the lung by diverting blood flow from hypoxic to better oxygenated areas (von Euler and Liljestrand, 1946 cited from Hillier *et al.,* 1997). Hypoxic pulmonary vasoconstriction (HPV) is more efficient in situations where the hypoxic area is smaller because this increases the fraction of blood redirected to areas with better ventilation (Marshall *et al.,* 1981 cited from Hillier *et al.,* 1997). The current consensus within the field of HPV research is that small resistance pulmonary arteries are the most important mediators (Archer *et al.,* 1996, Archer *et al.*, 2004, Sylvester *et al.,* 2012); vasoconstriction of the pulmonary artery (PA) results in redirection of blood flow away from hypoxic areas (Hillier *et al.,* 1997). More specifically, the underlying mechanism is thought to reside within the PA smooth muscle cell (PASMC) (Sylvester *et al.,* 2012). Research to date has therefore focussed on underlying mechanisms of HPV within the PA (reviewed by Sylvester *et al.* (2012)).

Effects of Hypoxia in the Pulmonary Vein and Comparison to Pulmonary Artery

Despite the focus of research on the PA, the PV is also known to constrict in response to hypoxia. One of the earliest studies suggesting hypoxic pulmonary venoconstriction was an *in vivo* canine study showing hypoxia-induced increases in pulmonary arterial wedge and venous pressures with little increase in left atrial pressure indicating active venoconstriction (Rivera-Estrada *et al.,* 1958). The magnitude of PV contraction to hypoxia has been shown to be similar to and often greater than the PA response (Bressack and Bland, 1980, Félétou *et al.,* 1995, Miller *et al.,* 1989, Raj *et al.,* 1990, Sheehan *et al.,* 1992, Zhao *et al.,* 1993, Zhao *et al.,* 1996). Furthermore, HPV is triggered by alveolar

hypoxia as opposed to PA hypoxaemia therefore the logical sensor would be pulmonary capillaries or downstream vessels i.e. PVs (Dawson, 1984). Many of the studies showing robust hypoxic contraction in isolated PVs did so in large diameter PVs (3 to 7mm) from both rat (Zhao *et al.,* 1993, Zhao *et al.,* 1996) and pig (Félétou *et al.,* 1995, Miller *et al.,* 1989) in contrast to the smaller resistance vessels which are considered more important on the arterial side of the pulmonary circulation (Archer *et al.,* 1996, Archer *et al.*, 2004, Sylvester *et al.,* 2012). Isolated lung studies in lamb (Raj and Chen, 1986), ferrets (Raj *et al.*, 1990) and cats (Nagasaka *et al.*, 1984) have all shown an increase in pulmonary venous resistance in response to hypoxia, further implicating a role for the PV in the overall HPV response. PVs and PAs appear to contribute equally to the increase in PVR under hypoxic conditions in lamb and ferret lungs (Raj and Chen, 1986, Raj *et al.*, 1990) whereas, in cats, PAs contribute more than PVs (Nagasaka *et al.*, 1984). This could indicate a species and/or developmental variation in HPV. Developmental variation in the hypoxic response was identified and characterised within the ovine pulmonary circulation (Bland *et al.,* 1977, Bressack and Bland, 1980). *In vivo* studies of lamb showed an increase in PA pressure and lung lymph flow and decrease in lymph protein concentration in response to hypoxia suggesting a rise in transvascular pressure due to HPV in post-capillary vessels (Bressack and Bland, 1980). Similar studies in adult sheep showed only an increase in PA pressure in response to hypoxia suggesting predominance of HPV in PAs (Bland *et al.,* 1977).

Hasebe *et al.* (1992) demonstrated HPV in both arterial and venous sides of the canine pulmonary circulation in an isolated caudal lobe system using antegrade and retrograde pulsatile perfusion techniques. Their results indicated that the main sites of HPV were the small pulmonary arterioles and venules located between more muscular vessels. Audi *et al.* (1991) used a constant flow perfusion system and arterial/venous occlusion techniques in canine lung lobes and concluded that the main site of HPV was in the small resistance arteries with limited contribution of PVs. These differences are most likely linked to the different experimental conditions used by the two groups. Notably, the conditions used by Hasebe *et al.* (1992) could be considered more physiologically relevant as they used pulsatile perfusion rather than constant perfusion (Audi *et al.,* 1991) and also used a ventilator with a respirator to maintain normal ventilatory movement.

Further evidence supporting the involvement of small venous vessels in the HPV response came from studies of the effect of hypoxia directly on pulmonary venules in dogs (Hillier *et al,* 1997) and guinea pigs (Tracey *et al.,* 1989a, Tracey *et al.,* 1989b). In the canine study subpleural venules (< 70 µM diameter) were visualised using a videomicroscopic technique in an intact lung lobe; hypoxia caused active venoconstriction with a mean reduction in vessel diameter of ~25% (Hillier *et al.,* 1997).

Myography studies in guinea pig pulmonary venules revealed larger contractions when PO_2 ~ 0 Torr compared to PO_2 ~ 25 Torr but under both conditions the response was fast in onset and sustained without the need for pharmacological preconstriction (Tracey *et al.,* 1989a, Tracey *et al.,* 1989b).

These findings in pulmonary venules dispute the assumption that venules are unable to contract due to having an incomplete vascular media (Fishman, 1961 cited from Hiller *et al.,* 1997, Hillier *et al.,* 1997). Interestingly, Hillier *et al.* (1997, p. 1089) proposed that:

> "*hypoxic venoconstriction occurs predominantly in venules <200μM and most likely tapers to insignificance by the time veins of several millimetres are reached"*

Taking into account results from larger veins discussed earlier, this does not appear to be the case. Therefore investigation of HPV responses along the pulmonary venous system is warranted.

A recent review (Sylvester *et al.,* 2012) largely disregarded the PV as having an important role in the overall hypoxic response. As limited research has been undertaken there is still a large degree of uncertainty around the physiological role of PV hypoxic contraction. However, the hypoxic response in PV is robust and appears to contribute to the overall response in the lung and therefore requires further attention in its own right.

Other characteristics of HPV, in addition to magnitude, are different when comparing PAs and PVs. The hypoxic contraction of isolated PVs is monophasic, generally involving one peak of contraction followed by relaxation (Dospinescu *et al.,* 2012, Uzun and Demiryürek, 2003, Zhao *et al.*, 1993, Zhao *et al.*, 1996). HPV in the isolated PA is often biphasic involving an initial, short-lived peak of contraction (phase 1) followed by relaxation then a gradually developing second prolonged contraction (phase 2) (Dipp and Evans, 2001, Dipp *et al.*, 2001, Leach *et al.,* 1994, Robertson *et al.*, 2004, Zhao *et al.*, 1993, Zhao *et al.*, 1996). However some research groups have found hypoxic PA contraction to be monophasic and sustained (Archer *et al.*, 1996, Archer *et al.*, 2001, Archer *et al.*, 2004).

Furthermore, Miller *et al.* (1989) found vast differences in the sensitivity of porcine PAs and PVs to hypoxia. The constrictor response in PAs was poor in 7.5% oxygen; exposure to 0% oxygen was required for substantial contraction whereas robust constriction of the PV was elicited in 7.5% oxygen. They discovered that PAs required pharmacological preconstriction in order to develop a contractile response to hypoxia whereas PVs did not; a finding confirmed by Félétou *et al.* (1995).

PVs and PAs also differ in terms of the mechanism of energy generation for hypoxic contraction. PVs rely more on oxidative phosphorylation to generate ATP for hypoxic contraction whereas in PAs,

phase 1 requires oxidative phosphorylation and glycolysis and phase 2 requires glycolysis but not oxidative phosphorylation (Zhao *et al.,* 1996). Importantly, phase 2 is the prolonged phase (Dipp and Evans, 2001, Dipp *et al.*, 2001, Leach *et al.,* 1994, Robertson *et al.*, 2004, Zhao *et al.*, 1993, Zhao *et al.*, 1996) thereby maintaining the HPV response in PAs and contributing more to the overall pulmonary vascular response to hypoxia (Dipp and Evans, 2001). Hence the predominating mechanism of energy production during HPV is completely different between PVs and PAs (Zhao *et al.,* 1996).

These differential features of hypoxic contraction in PAs and PVs suggest that underlying mechanisms may be different. These findings further support the rationale for investigating the underlying mechanisms and regulation of hypoxic responses in the PV specifically.

Underlying Mechanisms of Hypoxic Contraction – Potassium Channels

Despite extensive study, a degree of debate remains with regard to the underlying mechanisms of hypoxic contraction in resistance PAs. However one potential mechanism involving voltage-gated potassium (K^+) channels (K_V) is well consolidated. The mechanism is thought to involve hypoxic inhibition of a rapidly-activating, noninactivating potassium current through one or more delayed rectifier K^+ channels. This ultimately results in depolarisation of the PASMC membrane, calcium (Ca^{2+}) influx via L-type voltage-gated Ca^{2+} channels (VGCC) and vasoconstriction of the PA (Archer *et al.,* 1996, Archer *et al.,* 1998, Archer and Michelakis, 2002, Archer *et al.,* 2004, Leach *et al.,* 1994, McMurtry *et al.*, 1976, Moudgil *et al.,* 2005, Platoshyn *et al.,* 2006). The delayed rectifier channel involved was later identified as a K_V channel (Archer *et al.,* 2004) and further investigation revealed that these hypoxia sensitive channels contain $K_V1.5$ and $K_V2.1$ α subunits (Archer *et al.,* 1998, Archer *et al.,* 2004, Moudgil *et al.,* 2005). The hypoxia-sensitive current in PASMCs is sensitive to 4-aminopyridine (4AP, (K_V inhibitor (Dospinescu *et al.,* 2012)) and correolide ($K_V1.x$ inhibitor, Archer *et al.,* 2004) confirming the involvement of K_V channels and those containing α subunits from the $K_V1.x$ family specifically (Archer *et al.,* 1996, Archer *et al.,* 2001, Archer and Michelakis, 2002, Archer *et al.,* 2004).

Antibodies for both $K_V1.5$ and $K_V2.1$ can inhibit a portion of the hypoxia-sensitive current in PASMCs; hypoxic depolarisation is completely abolished when the antibodies are administered together and $K_V1.5$ appears to play a larger role than $K_V2.1$ (Archer *et al.,* 2004). $K_V1.5$ knockout mice have a reduced response to hypoxia in both isolated perfused lung and isolated PA ring studies (Archer *et*

al., 2001). Current flow through homomeric $K_V1.5$ channels is inhibited during hypoxia in rat PASMCs over-expressing the $K_V1.5$ gene. Overexpression of the gene in other cell types including rat mesenteric artery smooth muscle cells, HEK-293 and COS-7 did not confer a hypoxia-sensitive current suggesting that block of $K_V1.5$ channels under hypoxic conditions is a PASMC specific mechanism (Platoshyn *et al.,* 2006). Taking all this into account, K_V channels (specifically containing $K_V1.5$ and 2.1 α subunits) play an important role in the mechanism of HPV in PAs.

TASK-1 (acid-sensitive member of the two-pore domain K^+ channel family) is another K^+ channel candidate proposed to mediate hypoxic contraction of the PA. In human PA smooth muscle, TASK-1 is involved in controlling resting membrane potential (RMP) and is inhibited by hypoxia. Knockdown of TASK-1 mRNA caused depolarisation of the RMP and inhibited depolarisation in response to hypoxia in primary cultures of human PASMCs (Olschewski *et al.,* 2006). However, large conductance Ca^{2+}-sensitive K^+ (BK_{Ca}) channels are thought to make a negligible contribution to the mechanism of HPV in PAs as the hypoxia-sensitive current in PASMCs is insensitive to the BK_{Ca} channel inhibitors iberiotoxin, charybdotoxin and tetraethylammonium chloride (TEA) (Archer *et al.,* 1996, Archer and Michelakis 2002, Archer *et al.,* 2004).

As discussed, inhibition of K_V currents is proposed to mediate hypoxic vasoconstriction of PAs via Ca^{2+} entry through L-type Ca^{2+} channels (Archer *et al.,* 1996, Archer *et al.,* 1998, Archer and Michelakis, 2002, Archer *et al.,* 2004, Leach *et al.,* 1994, McMurtry *et al.*, 1976, Moudgil *et al.,* 2005, Platoshyn *et al.,* 2006), however there is some dispute over the importance of L-type calcium channels during HPV. Some researchers have found that Ca^{2+} release from the sarcoplasmic reticulum (SR) plays a more prominent role in HPV in PAs (Dipp and Evans, 2001, Dipp *et al.*, 2001). Others argue that these results may be due to the use of a pharmacological preconstrictor before initiation of HPV whereby the preconstrictor may itself cause Ca^{2+} release which might be misinterpreted as being a result of HPV (Archer and Michelakis, 2002). However Dipp and Evans (2001) and Dipp *et al.* (2001) showed abolition of the HPV response by inhibiting Ca^{2+} release from the SR (with ryanodine and caffeine) in the absence of preconstriction.

Inhibition of K^+ channels (K_V and/or TASK) appears to play an important role in hypoxic responses of the PASMC yet controversy remains over the signalling pathways linking PASMC depolarisation to PA constriction. Porcine pulmonary vein smooth muscle cells (PVSMCs) demonstrate a K^+ current which is sensitive to hypoxia and 4AP. In contrast to PASMCs, this hypoxia-sensitive current in PVSMCs is also sensitive to TEA. 4-aminopyridine (4AP) and TEA reduced contractile responses to hypoxia in isolated PVs however Penitrem-A (a more selective BK_{Ca} channel inhibitor than TEA) failed to alter

hypoxic contraction which may suggest BK_{Ca} channels are not involved in the underlying mechanism (Dospinescu *et al.,* 2012).

In addition to functional characterisation of the PV, Dospinescu *et al.* (2012) provided a comparative mRNA expression profile for K^+ channels between PVs and size-matched PAs. A hypoxia sensitive BK_{Ca} channel variant (STREX) (McCartney *et al.,* 2005) was identified in porcine PVs and STREX, K_V1.5 and 2.1 mRNA were all expressed to a greater extent in PVs than in PAs (Dospinescu *et al.,* 2012). These findings highlight further differences between PAs and PVs however it is not possible to conclude whether these increased levels of K_V1.5, K_V2.1 and STREX mRNA would result in increased expression at the cell membrane. Archer *et al.* (2004) found that the mRNA expression of K_V1.2, K_V1.5, K_V2.1, K_V4.3, K_V9.3 and BK_{Ca} was significantly greater in small PAs (<40μM) compared to large PAs (100-200μM) but immunoblotting revealed that only K_V1.5 showed increased expression at the protein level. Further investigation of K^+ channel expression and function in the PV is warranted as preliminary research suggests an important role for K^+ channels during PV hypoxic responses.

Underlying Mechanisms of Hypoxic Contraction – Reactive Oxygen Species and AMP Kinase

K^+ channels appear to be effectors of hypoxic contraction however mitochondria have been proposed as the sensors of hypoxia in PASMCs (Archer *et al.,* 1993, Leach *et al.,* 2001, Rounds and McMurtry, 1981, Waypa *et al.,* 2001, Weissman *et al.,* 2003). This theory is substantiated by the strategic positioning of mitochondria in PASMCs when compared with mesenteric artery smooth muscle cells. In PASMCs, mitochondria are located near the plasma membrane and mitochondrial by-products are thought to have an effect on K_V channels in the membrane (Firth *et al.,* 2009). Despite most investigators being in agreement about the sensor of hypoxia within PASMCs, there is some controversy over the trigger for HPV. Some authors have found that HPV increases reactive oxygen species (ROS) production at complex III of the mitochondrial electron transport chain (Leach *et al.,* 2001, Waypa *et al.,* 2001). An increase in ROS causes an increase in cytosolic Ca^{2+} in PASMCs (Waypa *et al.,* 2002) and this Ca^{2+} may lead to inhibition of K_V channels and cell depolarisation (Post *et al.,* 1995). The opposing HPV theory involves reduced ROS production which is proposed to inhibit K^+ channels (Archer *et al.,* 1993) causing membrane depolarisation (Yuan, 1995, Michelakis *et al.,* 2001) and VGCC influx (McMurtry *et al.*, 1976). K_V channels have a high cysteine content (sulfhydryl groups) and could be controlled by the redox balance within the cell, channels would be open when oxidised and closed when reduced which ties in with the reduced ROS theory (Conforti and Millhorn, 2000).

Mitochondrial hyperpolarisation and reduced ROS have been suggested as an underlying mechanism of pulmonary arterial hypertension (PAH). Decreased ROS are hypothesised to activate the transcription factor hypoxia-inducible factor-1α (HIF-1α) which results in reduced expression of $K_V1.5$, membrane depolarisation, calcium influx, vasoconstriction and ultimately, PAH (Bonnet *et al.,* 2006).

AMP-activated kinase (AMPK) may provide a link between mitochondrial oxygen sensing and Ca^{2+} signalling during HPV in PAs (Evans *et al.,* 2005). Hypoxia is suggested to activate AMPK via inhibition of mitochondrial oxidative phosphorylation (Archer *et al.,* 1993, Evans, 2006, Rounds and McMurtry, 1981) resulting in reduced ATP levels, an elevated AMP/ATP ratio and activation of AMPK (Hardie and Hawley, 2001). Whether by this mechanism or another, hypoxia has been demonstrated to double the AMP/ATP ratio in PASMC (Evans *et al.,* 2005) and inhibition of AMPK with Compound C inhibits HPV in rat pulmonary artery (Robertson *et al.,* 2008). AMPK activation is proposed thereafter to cause cyclic ADP-ribose (cADPr)-mediated Ca^{2+} release via the ryanodine receptor on the SR in PASMCs (Evans *et al.,* 2005). An overview diagram of the proposed mechanisms of HPV in PASMCs highlighting the link between mitochondria, AMPK, Ca^{2+} signalling and K^+ channels is shown in Figure 1.

Another notable finding of Evans *et al.* (2005) was that a particular isoform of AMPK (AMPK-α1) is predominant within resistance PAs and expression of this isoform was reduced in systemic arteries. Expression of this particular isoform may help towards explaining the differential response of pulmonary and systemic vascular beds to hypoxia.

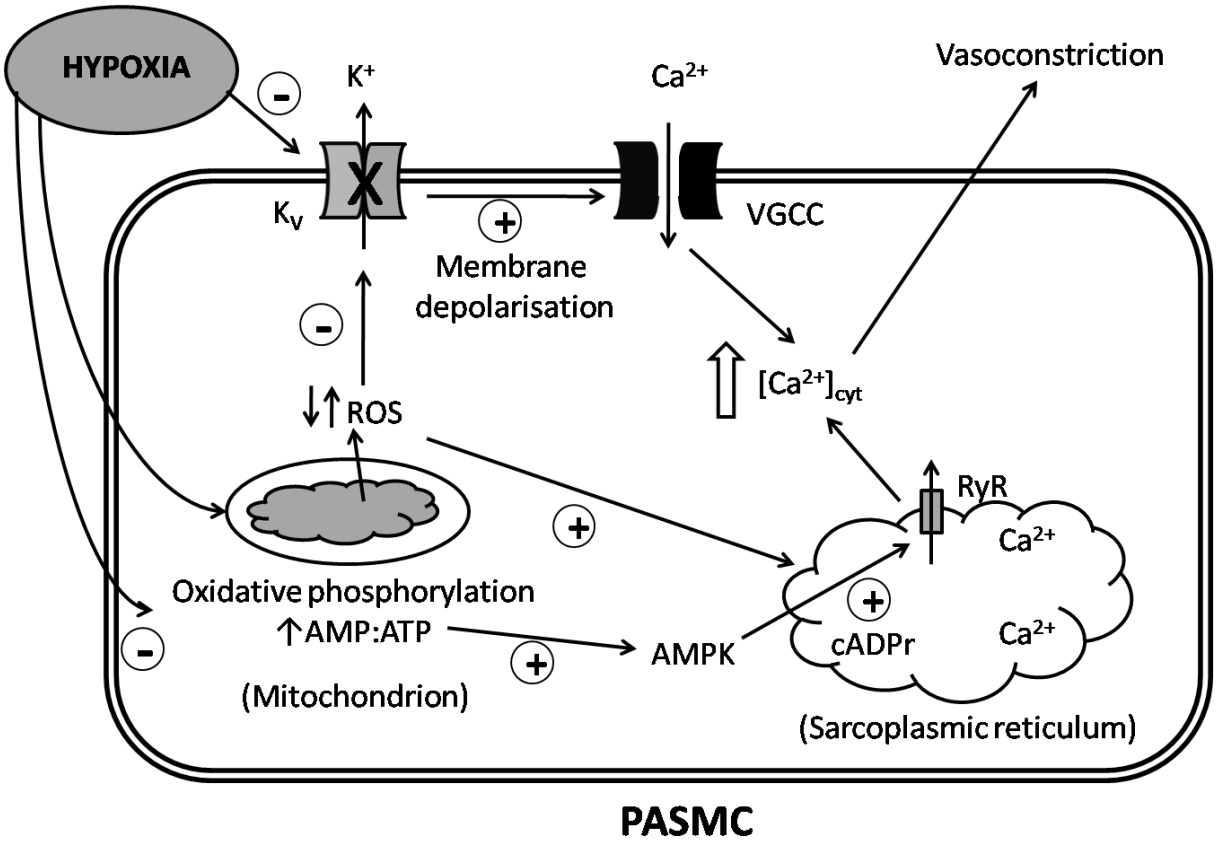

Figure 1. Diagram showing the proposed roles of K^+ channels, Ca^{2+} signalling, mitochondria and AMPK in the hypoxic response of PASMCs. N.B. K_V – voltage-activated K^+ channels, VGCC – L-type voltage-gated Ca^{2+} channels, ROS –reactive oxygen species, AMPK – AMP-activated kinase, cADPr – cyclic ADP ribose. Adapted from Murray *et al.*(2006).

Differential Responses to Hypoxia Along the Vascular Tree

Studies of hypoxic contraction in PAs have identified a difference in responses along the vascular tree. Conduit/proximal PAs tend to exhibit relaxation or a small contraction in response to hypoxia. In contrast small resistance/distal PAs show a strong hypoxic contraction (Archer *et al.,* 1996, Archer *et al.,* 2004, Audi *et al.,* 1991). These findings have been disputed by others who demonstrated that large PAs do constrict in response to hypoxia (Leach *et al.,* 1994) however HPV remains primarily associated with resistance PAs. Archer *et al.* (2004) proposed that by having the strongest HPV response in small resistance PAs this would aid ventilation-perfusion matching without raising PVR as would be the case if larger PAs were the main site of HPV. Furthermore, if larger PAs had a strong HPV response, this could be detrimental to the right heart by increasing afterload.

Small resistance venules have been proposed as a site of HPV (Hillier *et al.,* 1997, Tracey *et al.,* 1989a, Tracey *et al.,* 1989b) however large diameter PVs (3 to 7mm) also exhibit robust hypoxic contraction (Félétou *et al.,* 1995, Miller *et al.,* 1989, Zhao *et al.,* 1993, Zhao *et al.,* 1996). Hypoxic constriction of small veins or venules too close to the capillary bed could result in oedema formation (Gao and Raj, 2005, Maggiorini *et al.,* 2001). If hypoxic contraction was stronger further downstream from the capillary bed then this could help with upstream capillary recruitment (Taylor *et al.,* 2011) and redistribution of perfusion within a larger section of the lobe. This could maximise oxygenation whilst minimising any increase in capillary pressure. A strong HPV response occurring closer to the left atrium could result in redistribution of blood into a larger lung area and restriction of oxygenated blood outflow from the lungs to the left heart and would therefore be less beneficial.

Proposed Physiological Relevance of Hypoxic Pulmonary Venoconstriction

The importance of hypoxic pulmonary venoconstriction has been largely disregarded and therefore the potential physiological relevance has not been explored. Hypoxia-induced contraction of the PV has been proposed to facilitate capillary recruitment and optimise gas exchange capacity within the lung in healthy human subjects (Taylor *et al.*, 2011). The underlying mechanism is thought to involve an increase in upstream pressure resulting from downstream PV constriction. This theory requires further investigation as it was founded on a study which excluded a number of factors in combination (other than direct pulmonary venoconstriction) as fully accounting for capillary recruitment during hypoxia in healthy human subjects. Less than 40% of the observed hypoxia-induced increase in pulmonary capillary blood volume was attributable to changes in cardiac output, pulmonary arterial pressure or left ventricular diastolic function (Taylor *et al.,* 2011). Hypoxic contraction of the PV may also play a role in the manifestation of disease including the rise in capillary pressure seen during high altitude pulmonary oedema (Bärtsch and Gibbs, 2007).

The theory of capillary recruitment is disputed by the findings of others who have found hypoxic exposure reduces overall pulmonary blood volume and microvascular volume specifically (Bressack and Bland, 1980, Clough *et al.,* 2000). This may suggest a process involving reduced capillary recruitment and is more in keeping with the body of research supporting pre-capillary constriction of small pulmonary arteries as the predominant response during hypoxia. Due to this dispute and general lack of knowledge in the area, research is required to explore the potential physiological role for hypoxic pulmonary venoconstriction and the role it may play in pulmonary disease states.

Morphological Changes in Pulmonary Arteries and Veins Exposed to Chronic Hypoxia

Chronic hypoxia can result in structural remodelling of both PAs and PVs; one physiological example of chronic hypoxia is high-altitude. Exposure of cattle to high-altitude resulted in hyperplasia and hypertrophy of the smooth muscle in the media of PA yet only hyperplasia was evident in PVs (Naeye *et al.,* 1965). Moreover, in humans, high-altitude exposure resulted in hypertrophy and thickening of the media particularly in small PVs (less than 150 μM diameter). Small PVs became arterialised in nature and the findings were suggested to indicate a prolonged increase in tone within these vessels under conditions of high-altitude (Wagenvoort and Wagenvoort, 1976, Wagenvoort and Wagenvoort, 1982). Notably, the study only included subjects with no pre-existing left cardiac dysfunction or failure or heart valve disease which could have been alternative causes of the morphological changes observed in PVs (Wagenvoort and Wagenvoort, 1976). This may suggest that high-altitude/chronic hypoxia exposure has a direct effect on the PV causing increased basal tone and structural alterations.

Experimental models of chronic hypoxia in rats (using animal-holding chambers with 10-11% O_2) have demonstrated medial thickening in small PVs and medial hypertrophy in pulmonary arteries, arterioles, veins and venules (Takahashi *et al.,* 2001, Dingemans and Wagenvoort, 1978). Crenation of the vascular walls and excrescences (protrusion of SMCs into the intimal layer) indicated constriction of both arteries and veins in response to hypoxia (Dingemans and Wagenvoort, 1978). Hence, morphological changes in PVs exposed to chronic hypoxia are consistent across a range of methods, species and researchers and appear similar to the changes seen in PAs.

Pathological Consequences of Hypoxic Exposure

HPV is an essential physiological response in healthy humans however it can also contribute to a number of disease states. HPV tends to be more beneficial in diseases affecting a smaller, more focussed area of the lung such as pneumonia and atelectasis. In these cases, HPV results in optimisation of blood oxygenation by diverting flow away from the small hypoxic area to other better ventilated areas without significantly raising PVR. When the whole lung is exposed to hypoxia (for example under high altitude conditions or sleep apnoea), HPV is global and can result in elevated PVR, pulmonary hypertension and ultimately right ventricular hypertrophy if the exposure is prolonged (Archer and Michelakis, 2002, Dingemans and Wagenvoort, 1978, Félétou *et al.,* 1995, Lal *et al*., 1999, Moudgil *et al.,* 2005, Sheehan *et al.,* 1992).

Increased resistance in small pulmonary veins and venules during hypoxia can result in increased microvascular pressure leading to an increase in fluid and/or protein filtration and oedema formation (Gao and Raj, 2005, Hillier *et al.,* 1997, Raj *et al.,* 1990). Global hypoxic exposure in lamb lungs resulted in an increased rate of weight gain representing increased fluid filtration and interstitial oedema (Raj and Chen, 1986).

PVs are proposed to play a role in the pathological manifestations of high altitude pulmonary oedema. One theory is that high altitude pulmonary oedema results from inhomogeneous hypoxic pulmonary venoconstriction and subsequent regional overperfusion in the lung (Bärtsch and Gibbs, 2007). Others postulated that hypoxic contraction occurs in the smallest venules resulting in increased upstream capillary pressure and hydrostatic pulmonary oedema (Maggiorini *et al.,* 2001). Investigation of underlying mechanisms of the hypoxic response in PVs is required to help identify potential therapeutic targets during diseases resulting from hypoxic exposure.

The Role of the Pulmonary Vein in Disease

In addition to high altitude pulmonary oedema, evidence from other areas of clinical research suggests the PV is an area worthy of investigation. Elevated pulmonary venous resistance is strongly correlated with the increase in pressure gradient across the pulmonary circulation seen in morbidly obese patients without daytime hypoxia undergoing bariatric surgery and those with acute respiratory distress syndrome (ARDS). The increased resistance within the pulmonary venous system in patients undergoing bariatric surgery was thought to be caused by increased prostanoid production and thromboxane (TP) receptor expression in morbid obesity. In ARDS endotoxin-mediated venoconstriction and leukocyte aggregation are proposed to contribute (Her *et al.*, 2005, Her *et al.*, 2010). In each of these groups there was no history of left heart failure therefore it may be the case that the increased resistance generated was attributable to an intrinsic PV mechanism involving constriction and/or remodelling.

Furthermore, hypoxaemia in human inferior PVs is positively correlated with body mass index (BMI) (Yamane *et al.,* 2008) yet there was no such relationship in superior PVs. This may be due to impairment of HPV and ventilation-perfusion mismatch in inferior PVs specifically. This proposes not only a difference between inferior and superior PVs but also a role for inferior PVs specifically in obesity-related respiratory disorders including sleep apnoea.

Additionally, a link between metabolic syndrome and pulmonary venous hypertension (PVH) resulting from left ventricular diastolic dysfunction (LVDD) has been identified by Robbins *et al.* (2009). Compared to patients with PAH, patients with PVH due to LVDD showed a higher prevalence of hypertension, obesity, diabetes mellitus and hyperlipidaemia (characteristics of metabolic syndrome). In this study, patient numbers were small (17 patients with PVH; 35 patients with PAH), however the finding is still important. Interestingly, the authors' acknowledged that their assessment of left ventricular diastolic dysfunction was suboptimal and this could suggest metabolic dysregulation in PVs may contribute to PVH independently of heart dysfunction.

It is unclear whether the observations by Her *et al.,* 2005, Her *et al.,* 2010*,* Robbins *et al.*, 2009 and Yamane *et al.,* 2008 indicate intrinsic pathophysiological mechanisms within the PV however pullmonary veno-occlusive disease (PVOD) is a disease known to originate in the PV. Lesions occur primarily in the PV and involve fibrotic tissue occlusion of the lumen and an increased production of smooth muscle, elastic fibers and myofibroblasts (Montani *et al.*, 2009, Pietra *et al.*, 2004) leading to the development of interstitial oedema (Palmer *et al.,* 1998). The PV itself is directly involved in the changes in compliance and structure which occur with these conditions. Patients may present in a similar manner to patients with idiopathic PAH (Simonneau *et al.,* 2004) with approximately 5-10% of cases initially diagnosed as PAH being later identified histologically as PVOD (Iwaki *et al.,* 2009, Montani *et al.*, 2009). This can have significant clinical implications as a number of treatments for PAH may precipitate pulmonary oedema in PVOD patients including prostacyclin (epoprostenol, a vasodilatory prostanoid), bosentan (endothelin receptor antagonist) and calcium channel blockers (Creagh-Brown *et al.,* 2008, Montani *et al.,* 2008, Palmer *et al.,* 1998). In the case of prostacyclin, a low dose infusion has resulted in fatal pulmonary oedema in a patient with PVOD (Palmer *et al.,* 1998). This highlights the importance of diseases originating in the PV and the difference between PA and PV pathophysiology.

Hence there is direct evidence (from PVOD patients and high-altitude exposure studies) and indirect evidence (from the studies of Her *et al.,* 2005, Her *et al.,* 2010*,* Robbins *et al.*, 2009 and Yamane *et al.,* 2008) for the PV as an origin of disease. However a sound scientific knowledge base of regulatory mechanisms within the PV is lacking. Further exploration of the underlying regulatory and metabolic pathways within isolated vessels and cells is essential and could help identify potential therapeutic targets which could contribute to the development of treatments for PV-related disease.

Blood Vessel Culture as a Model for Disease

The maintenance of functional, isolated blood vessels under culture conditions is a potentially powerful tool to enable assessment of the impact of various environmental conditions on vessel function. For example, it has been used to investigate the effects of high glucose on mouse aorta function (Tian *et al.,* 2012). However culture conditions alone can affect blood vessel function including examples from both pulmonary (Guibert *et al.,* 2005, Manoury *et al.*, 2009) and systemic vascular beds (Alm *et al.*, 2002, Binko *et al.*, 1999, Cao *et al.*, 2005, De Mey *et al.,* 1989, Morita *et al.,* 2013, Thorne *et al.,* 2001, Thorne *et al.,* 2002, Thorne and Paul, 2003).

In PAs, exposure to culture conditions for 3-4 days appears to mimic chronic hypoxia (Manoury *et al.,* 2009) in terms of reduced functional K^+ channels (Osipenko *et al.*, 1998, Platoshyn *et al.*, 2001), smooth muscle cell depolarisation (Bonnet *et al.*, 2001, Osipenko *et al.*, 1998, Platoshyn *et al.*, 2001), and the emergence of basal tone due to Ca^{2+} influx (Bonnet *et al.*, 2001, Platoshyn *et al.*, 2001).

Isolated PVSMCs exposed to culture conditions for 4-6 days exhibit store-operated Ca^{2+} entry and raised intracellular Ca^{2+} in response to acute hypoxia (Peng *et al*., 2013). Unfortunately these Ca^{2+} responses were not directly compared to those of freshly isolated PVSMCs so no further conclusions can be drawn. The effect of maintaining isolated PVs in culture conditions remains to be established.

Sex and Species Differences in Pulmonary Vasculature and Utililty of the Porcine Model

Human epidemiological studies have revealed a higher prevalance of PAH in females compared to males (Martin and Pabelick, 2014). However, opposing sex differences exist within rat models of hypoxic pulmonary hypertension where male rats have increased disease severity compared with females (Rabinovitch *et al.,* 1981) and 17β-oestradiol and oestrogen receptors have protective effects (Lahm *et al.,* 2012). This is known within the field as the "oestrogen paradox" whereby oestrogen is protective within experimental rodent models yet clinically, the female sex is associated with a higher risk of PAH occurrence (Martin and Pabelick, 2014). This paradox raises potential questions as to the relevance of rodent models in the study of pulmonary vasculature and disease.

Despite this, the majority of the fundamental research in the area of pulmonary circulation (including hypoxic pulmonary vasoconstriction) has been conducted in rodent models. Reliance on rodents to investigate the pulmonary circulation has been challenged due to profound differences from human physiology in terms of K^+ channel function (Manoury *et al.*, 2011) and anatomy in terms of

cardiomyocyte distribution (Bonnet and Archer, 2007, Michelakis *et al.*, 2001, Roux *et al.*, 2004). Cardiomyocytes within the rat extend into fifth order PVs (Michelakis *et al.*, 2001) whereas, in humans, cardiomyocytes are confined to extrapulmonary veins (Bonnet and Archer, 2007, Roux *et al.*, 2004). The distribution of cardiomyocytes in PVs in large domestic mammals including sheep and pigs are similar to that seen in humans (Nathan and Gloobe, 1970).

Morphological studies of fibrous tissue, collagen and smooth muscle content of mammalian PVs revealed that PVs in cat, dog, ferret, goat, rabbit and human were less distensible and contained a higher proportion of fibrous tissue and collagen (Kay, 1983) indicating they were less vasoactive. PVs from cow, sheep, guinea pig and pig were more highly muscularised (Kay, 1983) indicating increased vasoactivity compared with other mammals. However, Taylor *et al.* (2011) challenged the suggestion of reduced vasoactivity in humans PVs when they proposed a role for hypoxic pulmonary venoconstriction in hypoxic pulmonary capillary recruitment suggesting human PVs may be more vasoactive than first suspected.

Therefore the pulmonary vascular system in large domestic mammals such as pigs may more closely represent the human model and provide a suitable alternative for study of PV function. Porcine PVs are also known to have a robust hypoxic vasoconstrictor response (Miller *et al*., 1989) and a hypoxia-sensitive K^+ current is present within PVSMCs (Dospinescu *et al.,* 2012).

Aims and Objectives

As previous HPV research has focussed on PAs, there is relatively less known about the mechanism of hypoxic contraction in PVs. Hypoxic pulmonary venoconstriction is proposed to recruit upstream capillary beds and optimise gas exchange in the lungs of healthy human subjects (Taylor *et al.,* 2011) and also to play an important role in disease states, for example, pulmonary oedema (Bärtsch and Gibbs, 2007, Maggiorini *et al.,* 2001). The PV directly contributes to disease states including pulmonary hypertension (Iwaki *et al.,* 2009, Montani *et al.*, 2009, Tuder *et al.,* 2013) and pulmonary-veno occlusive disease (Pietra *et al.*, 2004, Montani *et al.*, 2009). Blood vessel culture can be a powerful tool to enable assessment of the impact of environmental factors on vessel function (e.g. high glucose (Tian *et al.,* 2012) and as a model for disease. However culture conditions alone affect vessel contractility (Manoury *et al.,* 2009); the effect of culture conditions alone on PV function remains to be established.

Hypoxaemia is positively correlated with BMI in inferior but not superior PVs (Yamane *et al.,* 2008) however it is unknown whether functional differences exist between PVs from different locations. Previous research has characterised contractile function and SMC morphology and electrophysiology in superior/middle PVs (Dospinescu, 2009) therefore work presented here will have a focus on inferior PVs. Characterisation of the inferior PV in terms of underlying functional mechanisms and regulation at the isolated vessel and cellular level and gene expression is required before potential therapeutic targets can be identified.

The aim of this project was to investigate hypoxic responses of porcine intrapulmonary veins and PVSMCs (with a focus on inferior PVs) including the impact of PV maintenance in culture.

Objectives

The objectives detailed below were proposed to address this aim:

1. to characterise contractile responses of porcine inferior and superior PVs to pharmacological agonists and hypoxia
2. to investigate underlying mechanisms and pathways of hypoxia-induced responses in inferior PVs
3. to investigate the mRNA expression profile of K^+ channels in inferior and superior PVs
4. to develop a protocol to freshly isolate PVSMCs from inferior PVs in order to examine morphological and passive electrical properties

5. to characterise electrical properties of inferior PVSMCs in terms of membrane potential and voltage-activated whole-cell currents
6. to develop an appropriate blood vessel culture technique for PVs and evaluate the impact of maintenance in culture conditions on contractile function, K^+ channel expression and PVSMC morphology and electrical properties

Chapter 2

General Methods

Porcine Abattoir Tissue

All experiments were performed in accordance with UK legislation. Porcine heart and lung tissue (*sus scrofa domesticus*) was obtained from either Scotch Premier Meat Ltd (Inverurie, Aberdeenshire) or Quality Pork Producers Ltd (Brechin, Angus). Tissue was obtained from animals aged between 18 – 28 weeks, weighing 70-80kg of either sex.

Dissection Procedure

Heart and lung tissue (see Figure 2) from Scotch Premier Meat Ltd arrived in the lab for dissection within ~1 hour of kill. Tissue from Quality Pork Producers Ltd arrived in the lab for dissection within ~1-2 hours of kill.

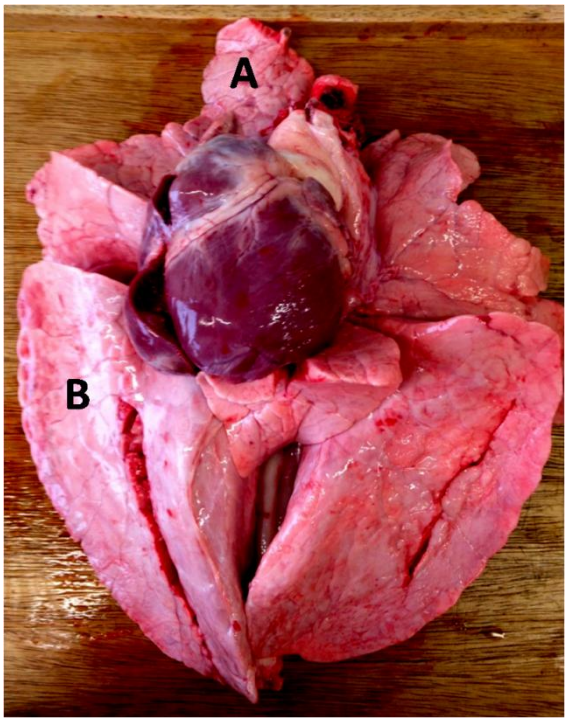

Figure 2. Porcine heart and lungs. Ventral view of heart and lungs *en bloc*. Pulmonary veins were mainly dissected from right cranial (A) and caudal (B) lobes for use in all experiments.

Pulmonary veins (PVs) were dissected from the right cranial (A in Figure 2) and caudal (B in Figure 2) lobes and cleared of any adherent tissue. For clarity, in terms of anatomy, cranial lobes will be considered analogous to superior and caudal to inferior for the purpose of this study and will be referred to as such from this point forwards (Srebnik, 2002). If these lobes were unavailable or badly damaged then the corresponding veins from the left lung were used instead. Size-matched 3^{rd}-4^{th} order superior and 4^{th}-5^{th} order inferior PVs of external diameter 3.4 ± 1.0 mm (mean ± SD, N=49) were used for isolated vessel experiments (see Figure 3).

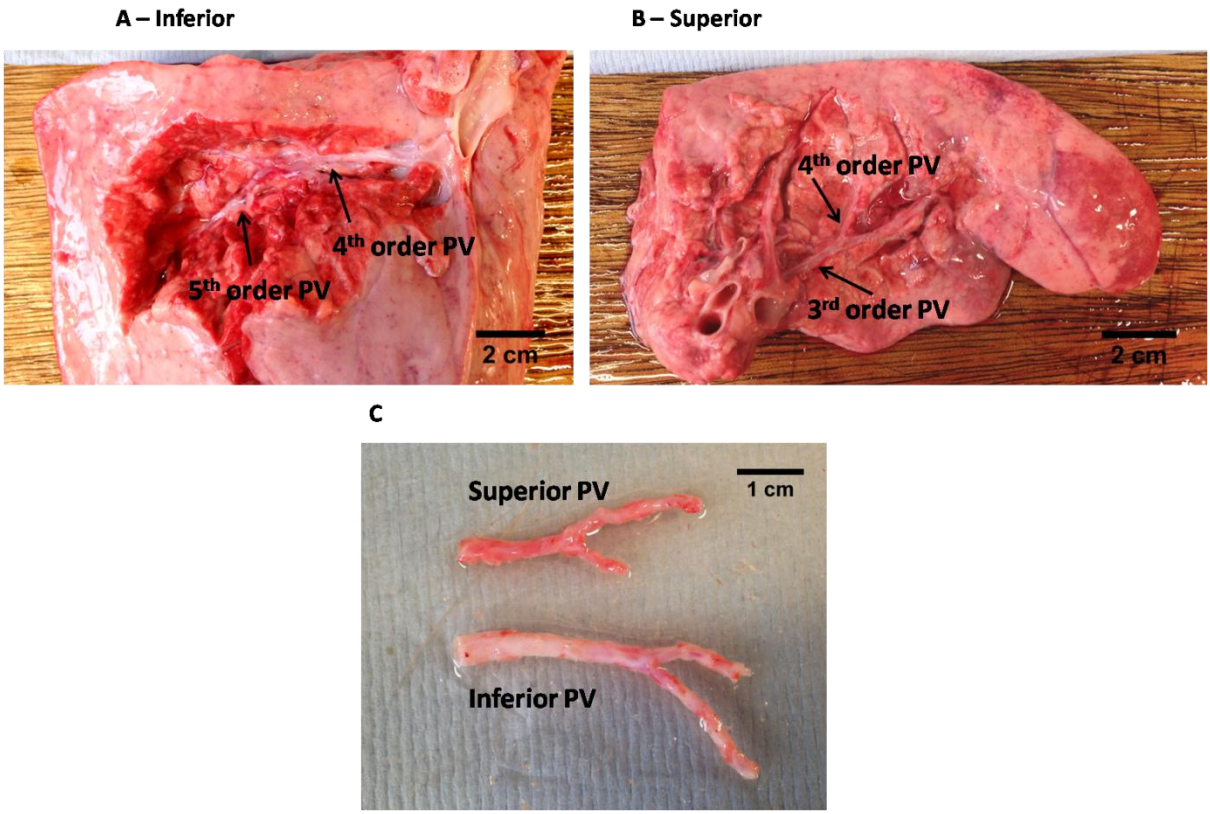

Figure 3. Dissection of inferior and superior pulmonary veins . A: Right inferior pulmonary lobe with 4th and 5th order pulmonary veins (PVs) shown *in situ*. B: Left superior pulmonary lobe with 3rd and 4th order PVs shown *in situ*. C: Isolated segments of 3rd-4th order superior and 4th-5th order inferior PVs shown side-by-side to illustrate size matching.

Vein were dissected free from lung tissue. To maintain tissue during dissection for myography experiments, tissue was regularly washed with KREB's solution (composition in mM: 119 NaCl, 4.7 KCl, 1.18 KH_2PO_4, 1.18 $MgSO_4$, 25 $NaHCO_3$, 2.52 $CaCl_2$, 10.88 glucose). During dissection for electrophysiology experiments tissue was regularly washed with calcium-free dissecting solution (composition in mM: 119 NaCl, 4.7 KCl, 1.18 KH_2PO_4, 1.17 $MgSO_4$, 25 $NaHCO_3$, 10HEPES, 5.5 glucose; pH adjusted to 7.4 with NaOH). PVs were used immediately for experiments or kept in KREB's or calcium-free dissection solution as above before placing in culture conditions.

Culture Conditions

In order to develop a tool for use as a disease model and for investigation of the effects of a range of environmental conditions (e.g. high glucose) on vessel function (Tian *et al.,* 2012), vessels were maintained under tissue culture conditions. Culture conditions alone affect contractile function of blood vessels including PAs, where they appear to mimic chronic hypoxia (Manoury *et al.,* 2009). Therefore the effect of culture conditions alone on PVs needed to be established.

PVs to be maintained in culture conditions were transferred to a laminar flow hood (Bioair Instruments, Italy). Vessels were removed from KREB's/dissection solution using sterile forceps and placed in a sterile bijou tube containing approximately 6mL Eagle Minimum Essential Medium (Sigma Aldrich, UK) supplemented with 2% penicillin-streptomycin for rinsing. This rinsing procedure was repeated before placing the unpressurised vessels in sterile untreated 6-well tissue culture plates containing approximately 3mL of the supplemented medium per well. The plates were maintained in a humidified Galaxy S incubator (Wolf Laboratories, UK) at 37^{o}C in 95%air/5%CO_2 for 24 hours.

Myography

Myography provides a convenient way to study *in vitro* physiology and pharmacology of a range of tissues, including blood vessels. Experiments can be performed over several hours in a temperature controlled, oxygenated environment. Blood vessels were attached to a force transducer via a pair of stainless steel hooks allowing for measurement of isometric tension responses under fixed strain to a range of stimuli.

Equipment and Calibration

Each 4-channel Myobath (World Precision Instruments, UK) consisted of four individual 25mL glass baths which meant different stimuli could be used in each bath and adjacent time controls were readily achievable. The baths were filled with KREB's solution and bubbled with 95%O_2/5%CO_2 in order to maintain pH at 7.4. Temperature was maintained at 36.7 ± 0.3°C (mean ± SD, N=8) by a thermocycler (Grant FH16-D) which heated water in the external water jacket.

A two-point calibration of each myograph channel was performed at 0 and 5g (using a 5g calibration weight). PVs were cut into rings of length 4.0 ± 1.0mm (mean ± SD, N=49) and two tissue hooks were

passed through the lumen of the vessel rings. One tissue hook was attached to a tissue holder and the other was connected to a force-transducer. Mounted PV rings were then lowered into the baths. The force-transducer signal was amplified via a TBM4M trans-bridge amplifier (World Precision Instruments, UK) set to gain of x10. The amplified signal was recorded by PowerLab 4/25 data acquisition system (ADInstruments, UK) and LabChart 7 software (©ADInstruments 2010). Data readings were acquired at a frequency of 20Hz. Figure 4 shows the equipment used during myography experiments.

A

B

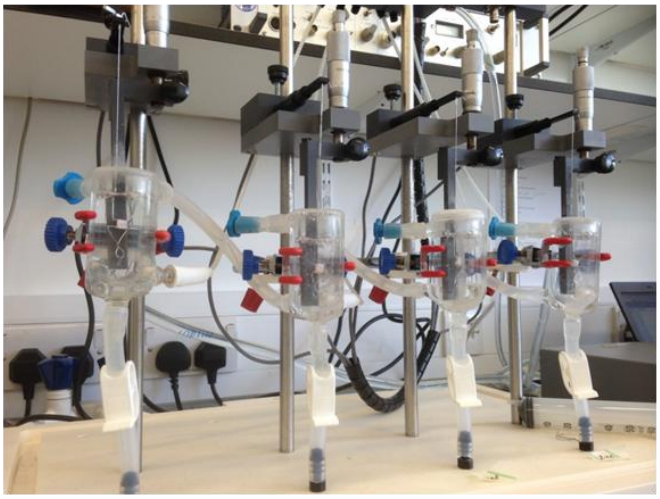

C

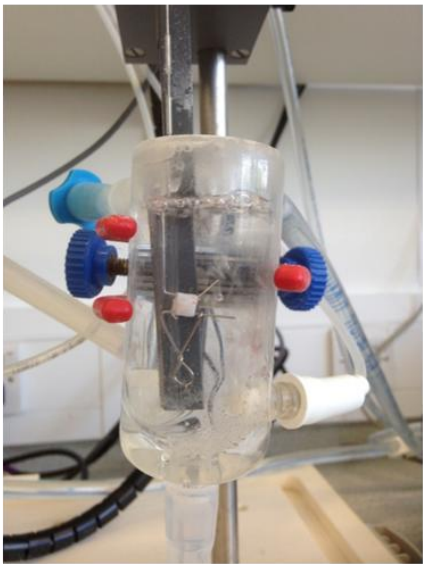

Figure 4. Equipment used during myography. A: Equipment used for myography - trans-bridge amplifier, thermocycler, myograph baths and gas cylinder. B: Four myograph channels mounted with vessel rings. C: Myograph bath showing mounted vessel between two stainless steel hooks.

Equilibration, Optimal Resting Tension and Calculation of Equivalent Pressure

After mounting and submerging in the bath the vein rings were allowed to equilibrate for 60 minutes at 1.5g resting tension. This tension was determined to produce optimal responses to 80mM KCl during preliminary experiments and was set manually using tensiometers.

As part of evaluation of the experimental model, approximate equivalent physiological pressures for this tension (1.5g) were calculated using the Laplace equation (Thomas, 2003):

$$Pressure\ (mmHg) = \frac{Force(Newtons)}{Radius\ (m) x\ Vessel\ Wall\ Length\ (m)}\ x\ 0.0075$$

(Equation 1)

Note that 1.5g was converted to Kg force (0.0015Kg) and then to Newtons using a conversion factor of 0.102 (0.0147 Newtons). Using a radius of 1.7mm (0.0017m) and a vessel wall length of 4.0mm (0.004m) which were the mean values for PVs used in this study, this gave an equivalent pressure of 16.2 mmHg. Within *in vivo* canine studies, pulmonary venous pressure was 17.1 ± 6.5 mmHg which was between PA pressure (20.2 ± 6.2 mmHg) and pulmonary wedge pressure (13.3 ± 6.2 mmHg) (Chaliki *et al.*, 2002). Therefore a pressure of 16.2 mmHg seems reasonable when compared to physiological values in canine studies. Human values for PA pressure range between 10 and 20 mmHg and pulmonary capillary wedge pressure between 5 and 15 mmHg (Muralidhar, 2002) therefore according to canine studies, human pulmonary venous pressure would lie somewhere between these values (Chaliki *et al*., 2002). Although these pressures cannot be directly extrapolated to the pig, both dogs and humans are also large mammals so it seems likely that a pressure of 16.2 mmHg may lie within physiological range for a pig.

Functional Testing

After a 60 minute equilibration period, viability of the tissue was tested by exposing to 80mM KCl three times. Endothelial function was checked by preconstricting with a submaximal concentration of a vasoconstriction (either 2 µM Prostagandin $F2_{\alpha}$ ($PGF2_{\alpha}$) or 1µM histamine) then applying 10µM carbamoylcholine chloride (carbachol (synthetic acetylcholine analogue, cholinergic agonist)).

Hypoxic Exposures

The gas mixture bubbling the bath was changed from 95%O_2/5%CO_2 (normoxia) to 95%N_2/5%CO_2 in order to achieve hypoxic levels in the bath. The exposures lasted for 15-20 minutes with at least 30 minutes for recovery (in 95%O_2/5%CO_2) between exposures.

Oxygen Monitoring in Myography

Oxygen was monitored during myography experiments in Chapter 4 on separate days in different channels each time using a thin flexible needle-type housing (NTH) trace oxygen microsensor connected to a Single Channel Fiber-Optic Oxygen Meter (Microx TX3-trace, Precision Sensing GmbH, Germany). A two point calibration of the Microx TX3-trace was performed by first exposing the oxygen and temperature sensors to deionised water bubbled with 95%N_2/5%CO_2 for 40 minutes at room temperature for a 0% air saturation reading. The sensors were then placed in deionised water exposed to room air for 40 minutes at room temperature for a 100% air saturation reading.

Oxygen measurements were recorded within the OxyView-TX3 v5.31 software (© PreSens GmbH) as % air saturation at a sampling rate of 1Hz. All recorded values were normalised as a percentage of the mean %air saturation over the first 15 minutes of normoxia for all recordings as it was assumed that the oxygen level was stable at this point as the bath had been bubbled with 95%O_2/5%CO_2 for at least 1 hour. During the first 15 minutes of recording under normoxic conditions, oxygen tension was 101.3 ± 1.2 %mean normoxic air saturation (mean ± standard error of the mean (S.E.M), N=8). Over the 15 minute hypoxic exposure the mean oxygen tension reached was 7.2 ± 1.1 % mean normoxic air saturation (N=8, P<0.001 compared to normoxia). The average time taken to reach minimum oxygen tension on exposure to hypoxia was 724.6 ± 45.3s. On reoxygenation, oxygen tension recovered to 89.2 ± 2.1 %mean normoxic air saturation (N=8, P<0.001 compared to initial normoxia and hypoxia). After reinstating 95%O_2/5%CO_2, oxygen levels reached a steady state in 199.8 ± 39.7s. The time course for mean oxygen levels before, during and after hypoxia exposure is shown in Figure 5.

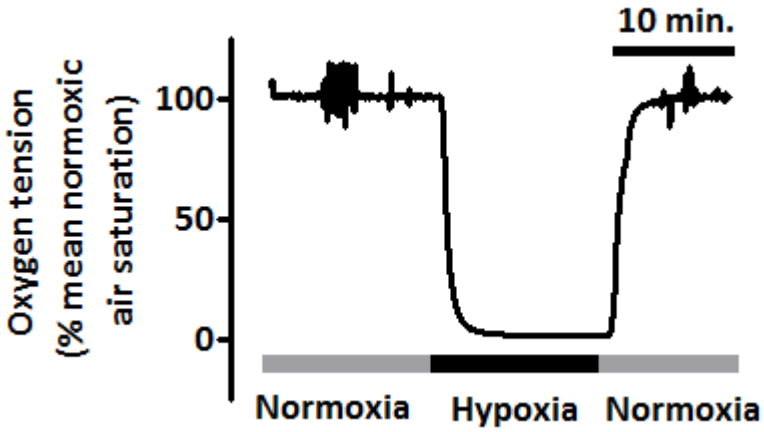

Figure 5. Mean oxygen tension before, during and after exposure to hypoxia within the myograph bath. Trace represents mean oxygen levels over 15 minutes normoxia (95%O_2/5%CO_2), 15 minutes hypoxia (95%N_2/5%CO_2) and approximately 11 minutes reoxygenation with 95%O_2/5%CO_2 (N=8). Data are normalised to mean %air saturation over the first 15 minutes of normoxia for all recordings. Grey and black bars represent normoxia and hypoxia, respectively.

Oxygen readings were made by placing the fibre-optic recording electrode within the myobath which allowed for simultaneous recording of oxygen and tension. Figure 6 shows a representative trace illustrating simultaneous recording.

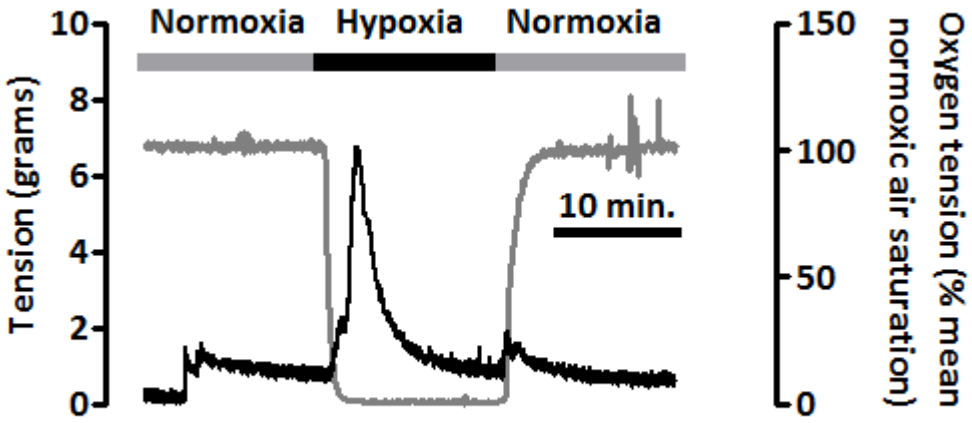

Figure 6. Representative sample trace for pulmonary vein tension and oxygen tension before, during and after hypoxia. Black trace represents tension (left y-axis) and grey trace represents mean oxygen levels (right y-axis) over 15 minutes normoxia (95%O_2/5%CO_2), 15 minutes hypoxia (95%N_2/5%CO_2) and approximately 15 minutes reoxygenation with 95%O_2/5%CO_2. Oxygen tension is normalised to mean %air saturation over the first 15 minutes of normoxia for all recordings. Grey and black bars at top of figure represent normoxia and hypoxia, respectively.

Temperature Monitoring in Myography

The Microx TX3-trace oxygen meter also measured temperature simultaneously. Temperature was stable over time during hypoxic/normoxic conditions (36.7 ± 0.3°C, mean ± SD, N=8) therefore it is unlikely that this acted as a stimulus for the contractile responses observed within PVs.

pH Monitoring in Myography

A digital pH meter (SevenEasy, Mettler-Toledo Ltd., Leicester, UK) was used to measure pH within different myograph baths to determine the effect of changing bubbling from hypoxic to normoxic gas mixtures both immediately and at 1-5 minute intervals thereafter. During experiments with 4AP in Chapter 4, HEPES bath solution (composition in mM: 150 NaCl, 5.4 KCl, 1.2 $MgCl_2$, 1.8 $CaCl_2$, 10 HEPES, 10 glucose) was used therefore similar pH measurements were taken in this solution bubbled with 95%O_2/5% CO_2 and 95%N_2/5%CO_2.

In Kreb's solution, the mean pH over the initial 15 minutes of normoxia before hypoxia exposure was 7.45 ± 0.01. During the 15 minutes of hypoxia, the mean pH was 7.45 ± 0.01 and then during the final 15 minutes of normoxia pH remained at 7.45 ± 0.01 (P<0.05, N=3). The time course for mean pH levels before, during and after hypoxia exposure in Kreb's is shown in Figure 7.

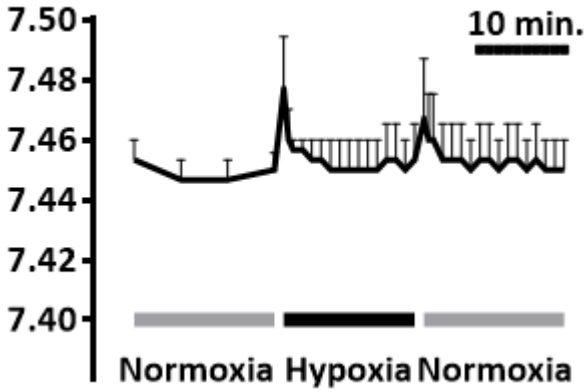

Figure 7. Mean pH before, during and after exposure to hypoxia in Kreb's solution. Trace represents mean (±S.E.M) pH levels over 15 minutes normoxia (95%O_2/5%CO_2), 15 minutes hypoxia (95%N_2/5%CO_2) and 15 minutes reoxygenation with 95%O_2/5%CO_2 (N=3). Grey and black bars represent normoxia and hypoxia, respectively.

As can be seen from Figure 7 there was a sharp change in pH of Kreb's solution on gas changeover at hypoxia and normoxia. When gas was changed from normoxia to hypoxia pH increased from 7.45 ± 0.01 (1 minute before gas change) to 7.48 ± 0.02 (immediately after gas change), however this difference in pH was not statistically significant (P>0.05, N=3). When gas was changed from hypoxia back to normoxia pH increased from 7.45 ± 0.01 (1 minute before gas change) to 7.47 ± 0.02 (immediately after gas change) and again this was not statistically significant (P>0.05). These sharp increases on gas changeover are most likely because the buffer within Kreb's solution is a bicarbonate buffer which requires 5% CO_2 for maintenance at pH 7.4. On gas changeover this 5% CO_2 is absent and it takes a period of time of bubbling for the level to rise to 5%. Generally, during gas changeover, pH levels had stabilised after 5 minutes (see Figure 7).

In HEPES solution, the mean pH increased over time. During the initial 10 minutes of normoxia before hypoxia exposure, the mean pH was 6.56 ± 0.02. During the 15 minutes of hypoxia, the mean pH increased to 6.58 ± 0.03 although this was not statistically significant (P>0.05, N=3). In the final 15 minutes of normoxia pH increased further to 6.59 ± 0.03, a level significantly higher than initial

period of normoxia (P<0.05, N=3). The time course for mean pH levels before, during and after hypoxia exposure in HEPES is shown in Figure 8.

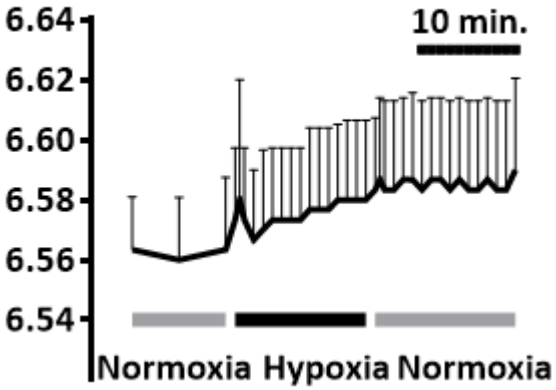

Figure 8. Mean pH before, during and after exposure to hypoxia in HEPES solution. Trace represents mean (±S.E.M) pH levels over 10 minutes normoxia (95%O_2/5%CO_2), 15 minutes hypoxia (95%N_2/5%CO_2) and 15 minutes reoxygenation with 95%O_2/5%CO_2 (N=3). Grey and black bars represent normoxia and hypoxia, respectively.

When gas was changed from normoxia to hypoxia in HEPES solution pH increased slightly from 6.56 ± 0.02 (1 minute before gas change) to 6.57 ± 0.02 (immediately after gas change), but this was not statistically significant (P>0.05, N=3). When gas was changed from hypoxia back to normoxia pH did not change (hypoxia (1 minute before gas change): 6.58 ± 0.03, normoxia (immediately after gas change): 6.58 ± 0.02, P>0.05).

In HEPES solution, pH gradually increased over time. As the HEPES solution was bubbled with 5% CO_2, pH would be expected to decrease (Elder *et al.,* 2015). HEPES solutions were prepared and pH buffered at room temperature and then used in myography experiments at 37°C; the increase in temperature could have caused the increase in pH (Barron *et al.,* 2006).

To investigate whether there was a relationship between O_2 levels and pH, an x-y scatter graph (O_2 vs. pH) was plotted however there was no significant correlation between O_2 level and pH (P>0.05).

Reverse Transcriptase Polymerase Chain Reaction

Reverse Transcriptase Polymerase Chain Reaction (RT-PCR) was used to investigate the molecular basis of K^+ channels in PVs in order to help identify potential targets for electrophysiology studies. Details of RNA extraction and RT-PCR are covered within Appendix 1.

Smooth Muscle Cell Isolation from PVs

Smooth muscle cells (SMCs) were isolated either from freshly dissected inferior PVs or from inferior PVs maintained in tissue culture conditions for 24 hours for use in electrophysiology studies. SMCs were identified based on morphological and functional responses; no other identification of cell phenotype was undertaken.

A protocol was developed and optimised in order to yield healthy, functional cells for whole-cell patch clamping. Ideally, the protocol would achieve a high yield (10-20 cells per field at 20x magnification) of spindle-like relaxed cells with intact membranes however partially contracted cells could also be used as this was considered another indicator of viability.

Cell Isolation Optimisation

A modified version of a protocol devised by Dospinescu (2009) was used in order to effectively isolate viable smooth muscle cells as this protocol was devised using porcine PV. However optimisation was required as the size and order of PVs used was different; Dospinescu (2009) used 5^{th} to 7^{th} order superior PVs which were much smaller and had thinner walls than the 4^{th} to 5^{th} order inferior PVs used in this study.

The main modifications involved removing rinsing steps, amending the order of enzyme addition and changing enzyme digestion times (described in more detail later). Yield and quality were documented for every batch of cells produced. Yield was rated on a scale from 0 to 5, with 0 being no cells to 5 being very many cells. Quality was a descriptive comment on the membrane appearance (healthy, fragile, blebbed) and contractile state (contracted/partially contracted, relaxed) of the cells. Optimal digestion times produced a yield high enough for numerous patch-clamping attempts and also cells healthy enough to withstand patch clamping protocols for approximately 20-

30 minutes. Under-digestion resulted in few cells with blebbed membranes and over-digestion produced a high yield of poor quality, fragile cells (refer to Figure 9 for examples of different qualities of isolated cells).

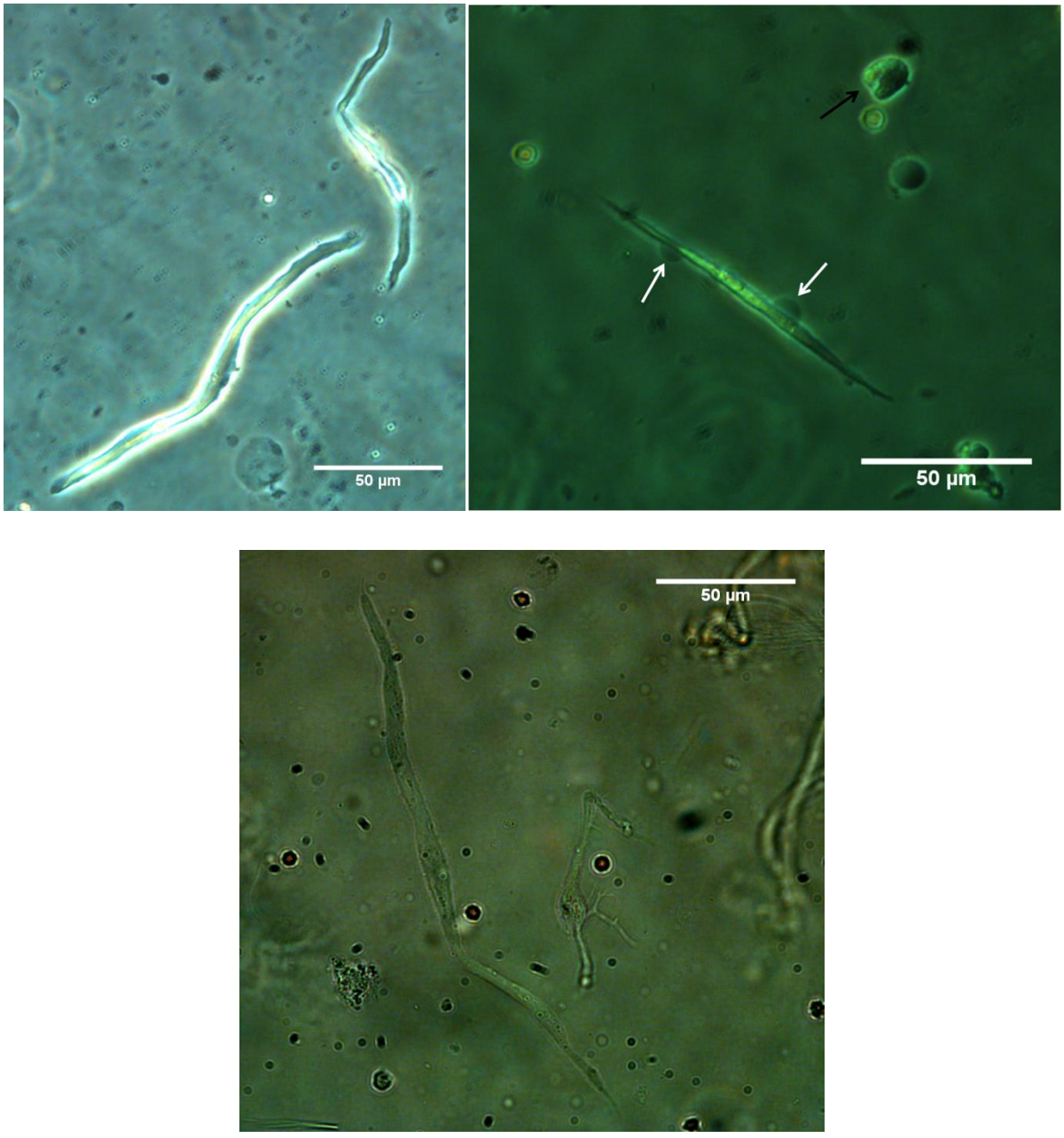

Figure 9. Various qualities of freshly isolated inferior pulmonary venous smooth muscle cells (phase contrast microscopy). (*top left*) Two relaxed elongated single smooth muscle cells with bright halos indicating intact and healthy cell membranes. (*top right*) Smooth muscle cell with blebs of membrane shown by white arrows. Contracted smooth muscle cell with bright halo indicating intact membrane shown by black arrow. (*bottom*) Cell on left - poor quality translucent smooth muscle cell with fragile membrane.

Cell Isolation Protocol

Inferior PVs (4^{th}-5^{th} order) with an outer diameter of 3.0 ± 0.7 mm (mean ± SD, N= 87) were dissected from the right lung as earlier described for use in cell isolation experiments. If these lobes were unavailable or badly damaged then the corresponding veins from the left lung were used instead without any noticeable variation in results.

PVs were then cut open longitudinally and pinned out in a dish containing Ca^{2+} free dissecting solution. A razor blade was used to gently scrape off the endothelial layer then the vein was turned over, pinned again and the adventitial layer was carefully removed using a pair of forceps and scissors. At this stage the vessel was then cut using the "feathering" technique (alternating cuts on either side of the pinned out vessel) which increased the surface area for enzymatic activity.

Smooth Muscle Cell Dispersion from PV Segments

After removing endothelial and adventitial layers and "feathering", the vein was cut into segments approximately 0.5-0.75cm long and then placed into a 1.5mL microcentrifuge tube containing Ca^{2+} free dissociation solution (composition in mM: 128 NaCl, 5.4 KCl, 0.95 KH_2PO_4, 0.35 Na_2HPO_4, 4.16 $NaHCO_3$, 10 HEPES, 10 glucose, 2.9 sucrose; pH adjusted to 7.3 with NaOH) supplemented with 1.5mg/mL papain from Papaya latex (Sigma Aldrich, UK).

Vessel segments were then placed in a refrigerator (2 to 8°C) for 1-2 hours followed by addition of 0.75mg/mL DL-dithiothreitol and incubation in a dri-block (DB-2A, Techne, UK) at 37°C for 10 minutes (original protocol by Dospinescu (2009) involved addition of both papain and DL-dithiothreitol before incubation on ice). Vessel samples were then transferred to a separate 1.5mL microcentrifuge tube containing Ca^{2+} free dissociation solution supplemented with 1.5mg/ml collagenase from *Collagenase histolyticum* Type VIII (Sigma Aldrich, UK) using a wide bore fire-polished glass Pasteur pipette. Following transfer, the vein segment was incubated in a dri-block at 37°C for approximately 25-40 minutes depending on prior assessment of vessel wall thickness and segment size.

After this final digestion stage vein samples were transferred into 1mL enzyme free fresh dissociation solution and rinsed three times before final transfer into 0.5mL enzyme free fresh dissociation solution. Tissue was left at room temperature for 30-60 minutes followed by trituration via a fire polished glass Pasteur pipette (usually 5 times) which produced viable SMCs. At this stage cells were visualised using a Leica DMI4000B microscope, images were taken using attached Leica DFC 300 FX

camera and yield and quality were recorded as previously described. Triturated cells were stored at room temperature and used for patch clamping over 4-6 hours.

Whole-Cell Patch Clamping

Whole-cell patch clamping was used to record resting membrane potential (in current-clamp mode) and whole-cell voltage activated currents (in voltage-clamp mode) within inferior PVSMCs. Changes in membrane potential and voltage activated currents were characterised in response to pharmacological agents which modify K^+ currents. The effect of hypoxia on resting membrane potential (RMP) was also investigated.

Preparation of Pulmonary Vein Smooth Muscle Cells

Patch clamping experiments were performed at room temperature. Approximately 80-100µL of cell suspension was pipetted onto a glass coverslip. The glass coverslip was attached to a low profile large bath recording chamber (RC-26GPL, Harvard Apparatus, Kent, UK) with silicon grease (Dow Corning, Belgium). Cells were allowed to settle onto the coverslip for 15-20 minutes. The recording chamber was mounted on the stage of a Nikon Eclipse inverted microscope TS100 using a platform (PH-1, Harvard Apparatus, Kent, UK) and Nikon stage adaptor (TS1M, Harvard Apparatus, Kent, UK). Once cells had settled, the recording chamber was filled with HEPES-based extracellular bath solution (of composition (in mM): 150 NaCl, 5.4 KCl, 1.2 $MgCl_2$, 1.8 $CaCl_2$, 10 HEPES, 10 glucose; pH adjusted to 7.4 with NaOH) with a plastic Pasteur pipette.

Patch Pipette Pulling

Pipettes were pulled from Clark borosilicate standard wall glass capillaries with filament (1.5mm O.D. x 0.86mm I.D.; Biochrom Ltd, Cambridge, UK) using a Flaming Brown P-87 micropipette puller (Sutter Instruments Co., USA). Fire-polishing of the pipettes was then performed using a microforge (MF-830, Narishige, Tokyo, Japan) to a final resistance of approximately 2-6 MΩ when filled with intracellular pipette solution (composition (mM): 110 KCl, 2.5 $MgCl_2$, 10 HEPES, 3.6 ATP (magnesium salt); pH adjusted to 7.2 with KOH) through a Nalgene 0.2µM syringe filter (25 mm surfactant free

cellulose acetate membrane). Small batches of 8-10 pipettes were made prior to immediate use during the course of each experimental day. Making pipettes in small batches reduced the chances of pipette tips becoming blocked with dust and debris.

Electrode Preparation and Reference Electrode

The main electrode consisted of a piece of thin silver wire (diameter 0.25mm) soldered to a brass pin; the brass pin made contact with the CV 201A/CV 203BU Axopatch headstage (Axon Instruments, California, USA) which allowed for current to flow and hence be amplified (via Axopatch 200A/200B amplifier) and recorded. This combination in turn was connected to a plastic airtight pipette holder. The silver wire was placed in concentrated chloride solution (Presept tablets, Fisher, UK) at the start of every experimental day to produce a silver chloride (AgCl) outer layer on the silver wire in order to reduce electrode polarisation which can increase resistance and delay potential changes. Changing pipettes can lead to the AgCl layer being scraped off hence the need for regular maintenance (Molleman, 2003). A reference electrode was required for recording intracellular potential relative to extracellular. The reference electrode was also connected to the Axopatch headstage by a brass pin and placed directly into the bath solution beside the outflow point of the recording chamber.

Giga-Seal Formation

Cells were selected for attempting giga-seal formation based on their appearance - the aim was to find cells with healthy, intact membranes (relaxed or partially contracted). After selection of a suitable cell, filled intracellular pipettes were mounted onto the pipette holder (attached to the Axopatch headstage); this reduced the period of time the pipette was exposed to the air to prevent blockage of the tip. Positive pressure was applied via mouth through a plastic pipette tip and silicon tubing (1mm I.D., 2mm O.D.) attached to a side arm of the pipette holder before the pipette was lowered into solution in the chamber using a coarse micromanipulator (Narishige, Tokyo, Japan). Applying positive pressure helped prevent blockage of the pipette tip with fibres and extracellular material when moving through the bath solution.

Progress of the patch clamp attempt was monitored through the “pipette seal test/signal monitor” function of the WinEDR software v3.7.0 (© John Dempster, University of Strathclyde). The voltage-clamp mode of the amplifier was selected with an initial holding voltage of 0mV with a 5mV voltage

step of 50ms duration; this allowed for monitoring of seal formation and for the software to calculate pipette resistance. When the pipette was near the cell, a three-axes vernier-type water hydraulic micromanipulator (MHW-3, Narishige, Tokyo, Japan) for finer adjustment to move it closer. Pipette resistance was logged 3-4 times to give an average value of 3.7 ± 0.9 MΩ (mean ± SD, n=1064). Pipette offset control of the Axopatch was used to adjust the offset current to zero. Series resistance was not compensated electronically however pipette resistance was compensated using Fast TAU and Fast MAG controls.

The hydraulic micromanipulator was then used to bring the pipette into contact with the cell and then press the pipette down gently on the membrane. To attempt formation of a giga-seal, positive pressure was switched to negative suction whilst observing resistance on WinEDR software – the aim was for a resistance greater than 1GΩ (cell-attached configuration). Once a giga-seal was formed, holding voltage was changed to -80mV with no voltage step. The known RMP of SMCs is more positive than -80mV therefore this protocol was used to stabilise the giga-seal and prevent depolarisation of the membrane prior to attempting going to whole-cell configuration (Molleman, 2003). Before this, WinEDR was switched to either -80mV with a 90mV step to +10mV or -80mV with a small 10mV voltage to -70mV (50ms duration) which allowed for monitoring the transition from seal to whole-cell configuration. A larger voltage step often resulted in seal break therefore the smaller voltage step was used in latter experiments.

When the seal was stable, resistance was logged with an average value of 6.5 ± 5.5 GΩ (mean ± SD, n=379) before attempting to achieve the whole-cell configuration. If the final outcome was a seal or patch break, pipettes were removed from the chamber and discarded before the next attempt.

Whole-cell configuration

For whole-cell configuration, the area of cell membrane (patch) attached to the pipette tip has to be ruptured to allow for full contact between the intracellular pipette solution and the cytosol of the cell. In order to achieve this, a short, sharp application of negative suction was applied whilst monitoring the progression from cell-attached to whole-cell; successful breakthrough was indicated by a dramatic increase in the capacitance transients at the start and end of the voltage step. Thereafter, the cell and pipette solution were allowed to exchange contents by diffusion for approximately 4 minutes. During this time the hydraulic manipulator was used to lift the cell off the base of the coverslip and into the main body of solution. Access conductance (G_a), membrane

conductance (G_m) and membrane capacitance (C_m) were logged for the cell and the amplifier was then switched to current-clamp mode to check initial RMP. The bath was perfused and any RMP changes recorded over a 30 second period. All subsequent voltage protocols and resting RMP recordings were made under constant perfusion.

Liquid Junction Potentials

Liquid junction potentials (LJPs) occur when two solutions of different ionic concentrations and mobilities come into contact (Figl *et al.,* 2004). Some ions move faster than others down their concentration gradients and if, for example, the anions move faster than the cations in solution then a potential difference (LJP) can be set up. In the case of these electrophysiology experiments, the LJP may arise between the bath and pipette solutions and could result in a difference between the measured and the actual membrane potential of the smooth muscle cell.

LJPs were calculated using an Excel spread sheet developed by Jim Kenyon, University of Nevada (2007) using the ionic concentrations of the bath and pipette solutions and the temperature in degrees Kelvin and a number of constants: the mobilities and valences for each ion and physical constants R and F. The LJP between the bath and pipette solutions was calculated as 4.91 mV and therefore considered negligible when compared to previously published values (Selyanko *et al.,* 1995, Selyanko *et al.,* 2000). On this basis, measured membrane potentials/voltages were not corrected for errors resulting from LJPs.

Perfusion System

Multiple syringe barrels were used to create a perfusion system for continuous flow of bath solution to the chamber and to supply hypoxic solution (bubbled with 100% N_2) where appropriate. The system consisted of two 60mL syringes and one 5mL syringe connected using three-way taps and some flexible thin tubing which transported solution to the inflow point of the chamber (see image in Figure 10). Excess bath solution was drained through the outflow point connected to more tubing and a Dymax 30 pump (Charles Austen Pumps, UK).

All experiments were carried out under maximum, unrestricted flow conditions which had a mean flow rate of 5.31 ± 0.57 mL/min. The volume of liquid required to prime/fill the inflow tubing was

1.17 ± 0.06 mL and after priming the tubing it took 7.33 ± 1.53 seconds to fill the chamber at maximum flow (values are mean ± SD, N=3).

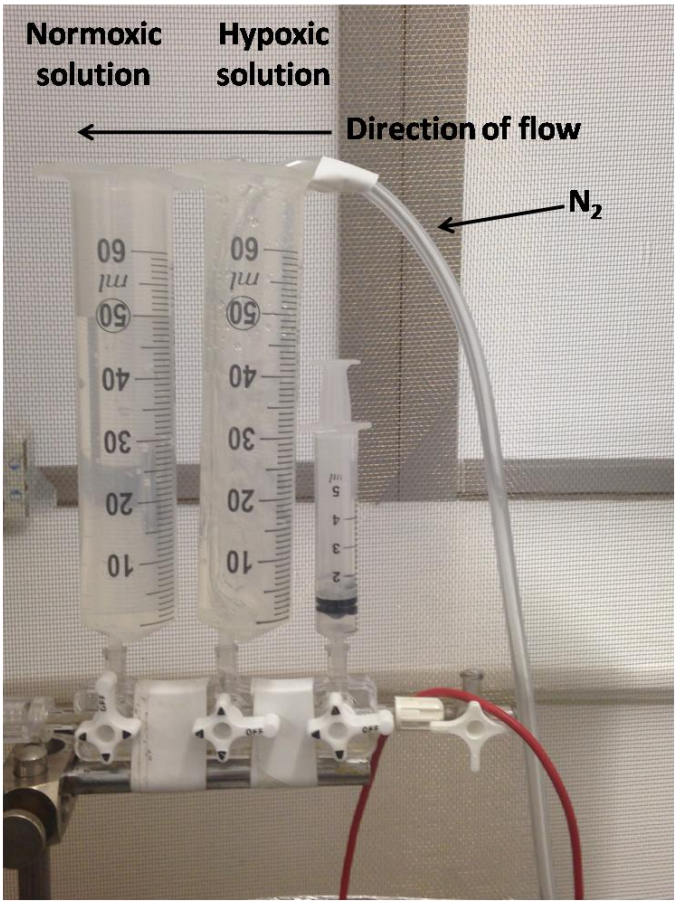

Figure 10. Flow system for electrophysiology bath solution. Direction of flow of solution and tubing for supply of nitrogen to solution in syringe barrel are shown by black arrows. Left 60mL syringe contains normoxic solution (equilibrated with room air) and right 60mL syringe contains hypoxic solution (bubbled with 100% nitrogen). Three-way taps were used to change from normoxic to hypoxic flow.

Picospritzer® Drug Application

All pharmacological agents were applied by Picospritzer® (Model III, Parker Instruments, USA). The inflow point of the Picospritzer® was connected to a compressed air cylinder by rigid plastic tubing. The outflow was attached by flexible tubing to a micropipette holder mounted onto a coarse micromanipulator on the opposite side of the microscope platform to the Axopatch headstage.

Pipettes were pulled and fire polished as previously described and filled with drug solution before mounting in the holder. For drug application, after a suitable cell was identified, the Picospritzer® pipette was placed into solution (before the microelectrode pipette) above the base of the chamber. Pipettes were regularly checked for blockage at the tip. After whole-cell configuration was achieved and drug application was required, the Picospritzer® pipette was brought into the same focal plane as the cell and moved to within approximately 25-50µM of the cell membrane (see Figure 11). The duration of application was set on the system and the manual button was pressed to apply the drug directly onto the cell.

The Picospritzer® system was connected to the Axopatch 200A/200B amplifier which in turn meant that a 3rd channel could be set up on WinEDR for logging Picospritzer® ON/OFF modes accurately.

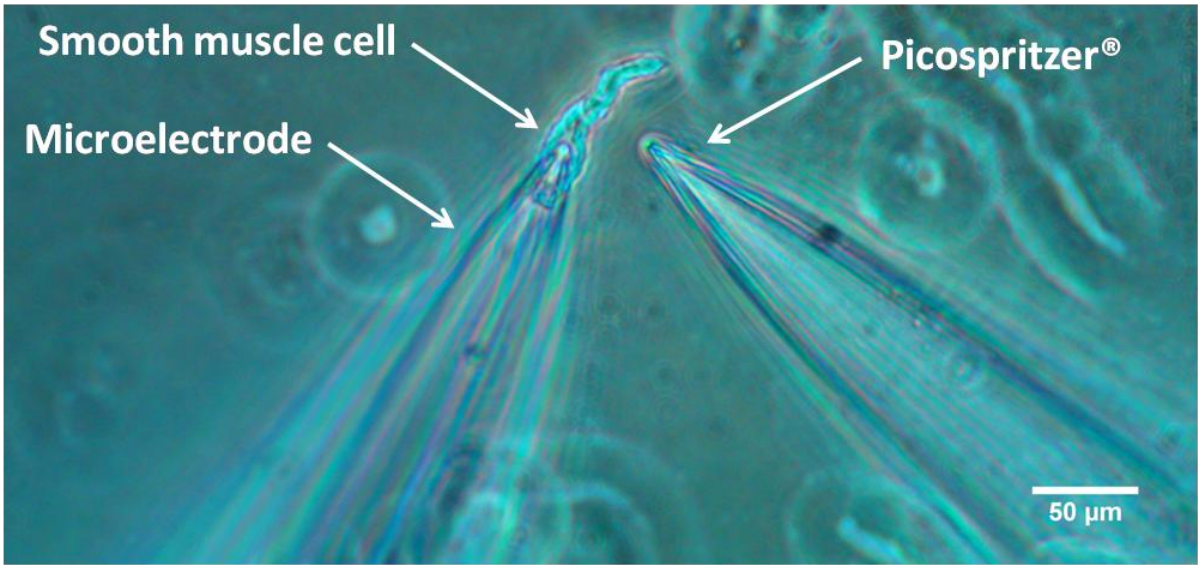

Figure 11. Microelectrode attached to smooth muscle cell and Picospritzer® in position for drug application. White arrows show microelectrode pipette attached to cell (left) and Picospritzer® pipette filled with drug solution (right) in the same focal plane.

Oxygen Monitoring in the Electrophysiology Chamber

Oxygen monitoring was performed in the recording chamber using the Microx TX3-trace after calibration (described earlier in this chapter). Control experiments (in the absence of cells and recordings) were performed on three separate experimental days. Recordings were made at different locations and depths in the bath as it was likely that flow and distance from the surface (and hence potential for re-equilibration with room air) could have an impact on the level of hypoxia

reached. Normoxia in these set of experiments means the perfusing bath solution was passively oxygenated with room air (i.e. not bubbled with oxygen as in myography experiments). Hypoxic solutions were bubbled with 100% N_2 for at least 10 minutes before flow into the recording chamber commenced. Previous work suggests that 10 minutes bubbling is adequate to reach maximal hypoxic levels with 5 minutes N_2 bubbling producing an O_2 level of 5-6% (Dospinescu, 2009). The different locations for recordings in the bath are indicated in Figure 12.

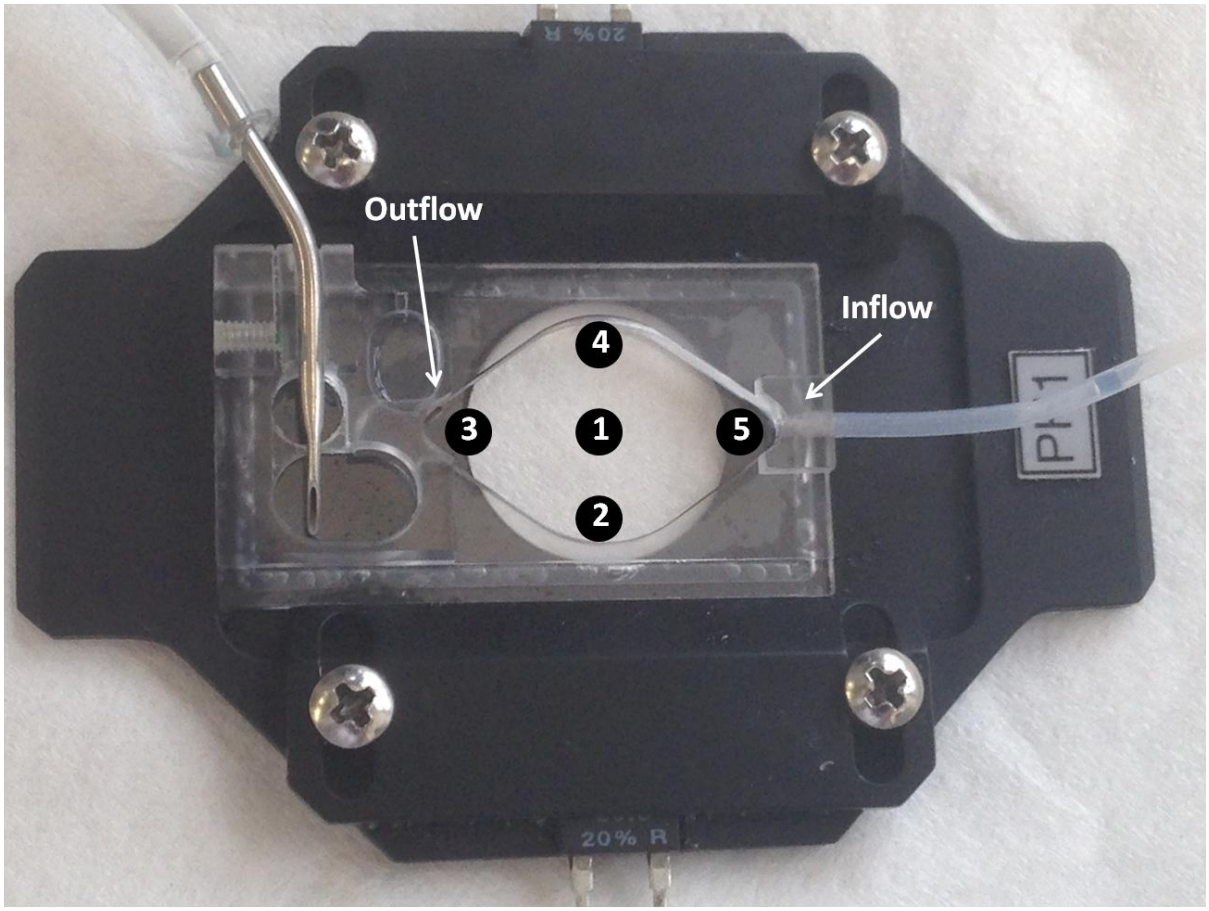

Figure 12. The RC-26GPL bath recording chamber labelled with sites of oxygen measurement. White arrows highlight inflow and outflow sites; numbers 1-5 represent sites within the chamber that were used for measurements during control oxygen monitoring experiments.

Oxygen measurements were recorded as described previously. Measurements were made for a total of 11 minutes: 1 minute normoxia followed by 5 minutes hypoxia and 5 minutes reoxygenation. Values were normalised as a percentage of the mean %air saturation over the initial 1 minute of normoxia for all recordings.

In the first set of control oxygen monitoring experiments, measurements were taken at each location (1-5) at a similar depth to where cell recordings were made. During the first minute of recording under normoxic conditions, mean oxygen tension across all locations was 101.8 ± 1.8% mean normoxic air saturation (mean ± S.E.M, N=3). Over the 5 minute hypoxic exposure the mean oxygen tension was 36.9 ± 1.5% mean normoxic air saturation (N=3, P<0.001 compared to normoxia). The average time taken to reach minimum oxygen tension on exposure to hypoxia was 188.5 ± 18.9s. On returning to normoxia, oxygen tension then recovered to 96.2 ± 1.8 %mean normoxic air saturation (N=3, P<0.001 compared to hypoxia). After stopping hypoxic perfusion, oxygen levels reached a steady state in 119.9 ± 27.0s. On hypoxic perfusion, temperature fell from 22.3 ± 0.3°C to 21.3 ± 0.3°C (mean ± SD, N=3, P<0.01 compared to during initial normoxia) and then recovered to 22.1 ± 0.2°C when hypoxic perfusion was stopped (P<0.05 compared to during hypoxia). The time course for mean oxygen levels before, during and after hypoxia exposure alongside corresponding temperature readings are shown in Figure 13.

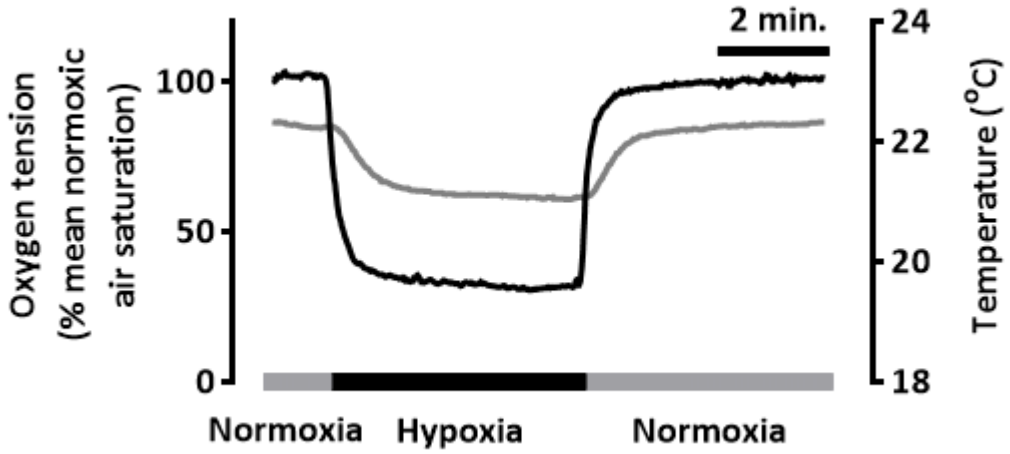

Figure 13. Mean oxygen tension and temperature before, during and after exposure to hypoxia within the electrophysiology chamber. Black trace represents mean oxygen levels over 1 minute normoxia (room air), 5 minutes hypoxia (100% N_2) and approximately 5 minutes reoxygenation with room air (N=3). Data are normalised to mean %air saturation over the first minute of normoxia for all recordings performed. Grey trace represents mean temperature over the same time course. Grey and black bars represent normoxia and hypoxia, respectively.

Oxygen levels during hypoxic perfusion at the same depth in all 5 locations (shown in Figure 12) were compared to assess whether assumed differences in laminar flow had an effect on the tensions reached (Figure 14).

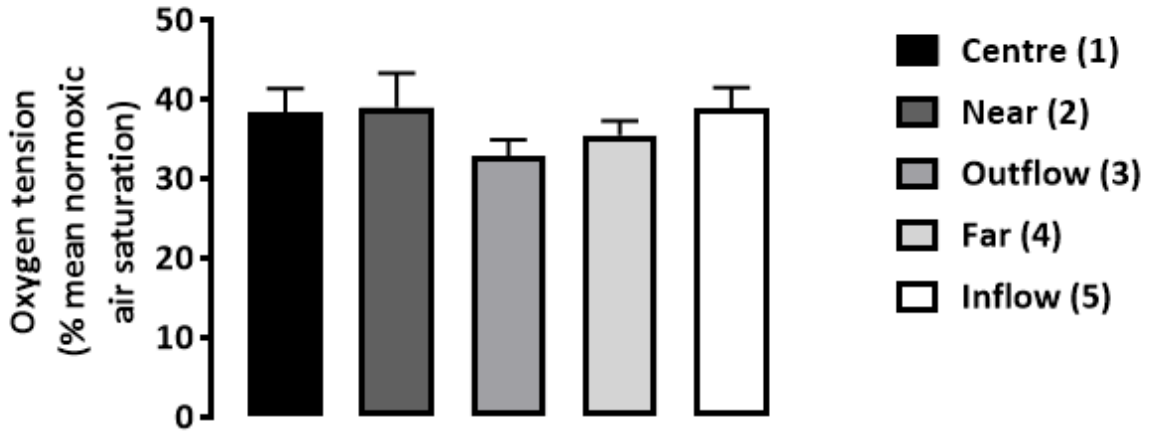

Figure 14. Oxygen levels during hypoxic perfusion at different locations within the electrophysiology chamber. Mean oxygen levels reached during hypoxia at each of the 5 locations (shown in Figure 12). Data are normalised to mean %air saturation over the first minute of normoxia for all recordings performed (N=3 for each location tested).

There was no significant difference between the oxygen levels reached during hypoxic perfusion at any of the locations tested (data shown in Figure 14). However, it is worthy of note that oxygen levels reached during hypoxia (30-40 %mean normoxic air saturation) were much higher than the low levels seen in similar control experiments performed by Dospinescu (2009): 5-6% after 5 minute hypoxic flow. The oxygen level reached could be influenced by flow rates and depth in the bath solution. Flow rates were comparable (5.31 mL/min compared to 3.53-6.06 mL/min (Dospinescu, 2009). Measurements of oxygen levels reached during hypoxia at different depths in the chamber bath solution are shown in Figure 15. All measurements at different depths were recorded at the central point (position 1 in Figure 12).

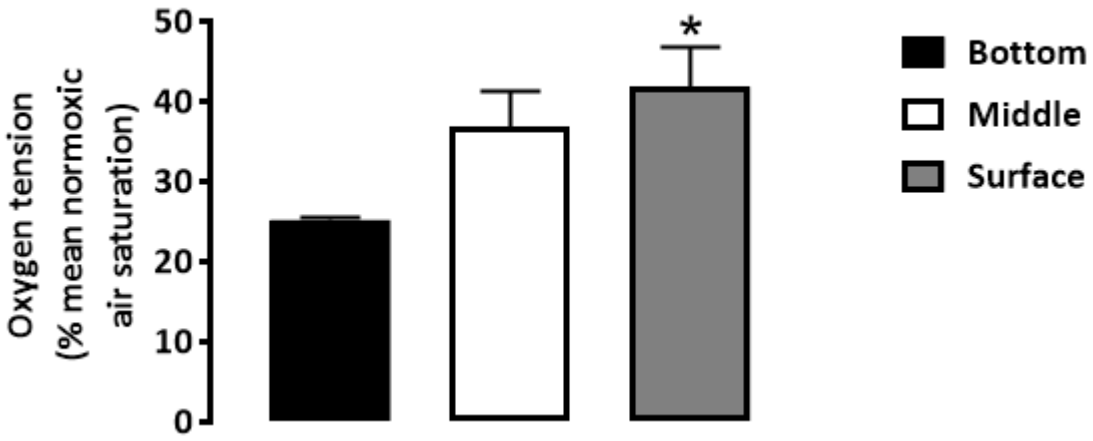

Figure 15. Oxygen levels during hypoxic perfusion at different depths within the electrophysiology chamber bath solution. Mean oxygen levels during hypoxia at each of the 3 depths – all recordings performed at position 1 in Figure 12. Data are normalised to mean %air saturation over the first minute of normoxia for all recordings (N=3 for each depth tested). *P<0.05 compared with mean oxygen level measured during hypoxic perfusion at bottom of chamber.

The oxygen levels reached during hypoxic perfusion were lower with increasing depth in the chamber bath solution; oxygen levels were significantly greater during hypoxia at the surface compared to the bottom of the chamber (P<0.05). This indicates that reoxygenation and re-equilibration with room air occurs more readily at the surface meaning lower levels of oxygen cannot be reached. Despite levels of oxygen being lowest at the bottom of the chamber, they still did not reach the levels seen by Dospinescu (2009). Oxygen levels were averaged over the full 5 minute hypoxic exposure rather than taken from a minimum point which may partially explain the higher levels seen in these experiments. However the mean time course plot for oxygen (Figure 13) shows levels remained around 30% mean normoxic air saturation at the minimum point.

Statistical Analysis

Data were stored, processed and statistically analysed using Microsoft Excel 2007 (Microsoft Corporation, USA) and GraphPad Prism 5/7 software (GraphPad Software Inc., USA). Data are mainly presented as mean ± S.E.M unless otherwise stated; N represents number of different pigs used and n represents number of cells, where appropriate. Mean data were analysed using either Students

unpaired *t*-test, repeated measures one-way ANOVA or standard one-way ANOVA with Tukey's post test or repeated measures two-way ANOVA with Bonferroni's post test, as appropriate (see individual chapters). A *P* value of less than 0.05 was considered statistically significant.

Solutions

KREB's solution (mM): 119 NaCl, 4.7 KCl, 1.18 KH_2PO_4, 1.18 $MgSO_4$, 25 $NaHCO_3$, 2.52 $CaCl_2$, 10.88 glucose

Ca^{2+} free KREB's solution (mM): 119 NaCl, 4.7 KCl, 1.18 KH_2PO_4, 1.18 $MgSO_4$, 25 $NaHCO_3$, 2.52 $MgCl_2$, 10.88 glucose

Dissecting solution (mM): 119 NaCl, 4.7 KCl, 1.18 KH_2PO_4, 1.17 $MgSO_4$, 25 $NaHCO_3$, 10 HEPES, 5.5 glucose; pH adjusted to 7.4 with NaOH

HEPES-based extracellular (bath) solution (mM): 150 NaCl, 5.4 KCl, 1.2 $MgCl_2$, 1.8 $CaCl_2$, 10 HEPES, 10 glucose; pH adjusted to 7.4 with NaOH

Dissociation solution (mM): 128 NaCl, 5.4 KCl, 0.95 KH_2PO_4 , 0.35 Na_2HPO_4, 4.16 $NaHCO_3$, 10 HEPES, 10 glucose, 2.9 sucrose; pH adjusted to 7.3 with NaOH

Intracellular pipette solution (mM): 110 KCl, 2.5 $MgCl_2$, 10 HEPES, 3.6 ATP (magnesium salt); pH adjusted to 7.2 with KOH and filtered through a Nalgene 0.2µM syringe filter (25 mm surfactant free cellulose acetate membrane).

All solutions were prepared in deionised water and all except KREB's and intracellular solution were titrated to the desired pH with 1-2M NaOH and HCl and stored in a refrigerator at 2-8°C. Intracellular solution was titrated with 1M KOH and divided into 1mL aliquots in 1.5mL microcentrifuge tubes which were frozen at -20°C and defrosted on day of use. All pH measurements were made using a digital pH meter (SevenEasy, Mettler-Toledo Ltd., UK).

As solutions were used over a range of temperatures, pH of bath and dissociation solutions were checked at fridge temperature (7.2 ± 0.3°C), room temperature (21.6 ± 1.6°C) and approximately 37°C (36.8 ± 0.2°C). All temperature values mean ± SD, N=3. The pH results are shown in Table 1.

Table 1. Effect of Temperature on pH of HEPES-based Bath and Dissociation Solutions

	Fridge Temperature	Room Temperature	37°C
Bath Solution pH	7.55 ± 0.02	7.40 ± 0.02	7.24 ± 0.01
Dissociation Solution pH	7.49 ± 0.04	7.36 ± 0.03	7.23 ± 0.02

Drugs

4AP (Sigma Aldrich, UK): final concentration of 5mM by dissolving in 0.4706g of 4AP in 1L HEPES bath for organ bath (stored in fridge) or 0.047g in 100mL HEPES bath for electrophysiology (aliquoted in 1mL aliquots and frozen). The 4AP solution in HEPES was pH adjusted to 7.4 with HCl (at room temperature).

BDM (Sigma Aldrich, UK): 1M stock prepared in KREB's, final concentration of 0.1 - 10mM in KREB's (for 0.1mM concentration stock was diluted 1 in 10 before use)

Caffeine (Sigma Aldrich, UK): final concentration of 20mM by dissolving in 3.8838g of caffeine in 1L KREB's

Carbamoylcholine (Carbachol) (Sigma Aldrich, UK): 10mM stock prepared in KREB's, final concentration of 10µM by adding 25µL to 25mL KREB's

DPO-1 (Tocris Bioscience, UK): 10mM stock prepared in ethanol, final concentration of 10µM by adding 25µL to 25mL KREB's

Glyburide (Enzo Life Sciences (UK) LTD., UK): 10mM stock prepared in DMSO, final concentration of 10µM by adding 25µL to 25mL KREB's

Histamine (Sigma Aldrich, UK): 10mM stock prepared in KREB's, final concentration 1nM to 100µM by diluting original stock as required (1 in 10 to 1 in 10000) for a measurable volume to add to 25mL KREB's (minimum 22.5µL). For endothelial tests stock was diluted 1 in 10 in KREB's before adding by adding 25µL to 25mL KREB's to give a final concentration of 1µM.

KCl (Sigma Aldrich, UK): 2M stock prepared in deionised water. Myograph - final concentration of 80mM by adding 1mL stock to 25mL KREB's. Electrophysiology - final concentration of 80mM by diluting 40µL in 1mL HEPES bath solution.

L-NAME (Sigma Aldrich, UK): 100mM stock prepared in KREB's, final concentration of 100µM by adding 25µL to 25mL KREB's

Penitrem A (Enzo Life Sciences (UK) LTD., UK): 5mM stock prepared in DMSO, diluted 1 in 10 in KREB's before adding by adding 25µL to 25mL KREB's to give a final concentration of 500nM

$PGF_{2\alpha}$ (Enzo Life Sciences (UK) LTD., UK): 1mM stock prepared in ethanol, final concentration 10nM to 10µM by diluting original stock as required (1 in 10 to 1 in 1000) for a measurable volume to add to 25mL KREB's (minimum 22.5µL). Alternatively a 2mM stock was prepared in ethanol, final concentration of 2µM by adding 25µL to 25mL KREB's for endothelial function tests.

Ryanodine (Enzo Life Sciences (UK) LTD., UK): 2mM stock prepared in DMSO, final concentration of 2µM by adding 25µL to 25mL KREB's

TEA (Sigma Aldrich, UK): final concentration of 5mM by dissolving in 0.0828g of TEA in 100mL KREB's for organ bath (made fresh daily) or 100mL HEPES bath for electrophysiology (aliquoted in 1mL aliquots and frozen)

U46619 (Enzo Life Sciences (UK) LTD., UK): 10mM stock prepared in DMSO, final concentration 10pM to 1µM by diluting original stock as required (1 in 10 to 1 in 100000) for a measurable volume to add to 25mL KREB's (minimum 22.5µL).

Zinc Chloride (Fisher Scientific, UK): 1M stock prepared in KREB's, final concentration of 1mM by adding 25µL to 25mL KREB's (organ bath); 1mM stock prepared in HEPES bath by dissolving 0.0136g in 100mL for electrophysiology (aliquoted in 1mL aliquots and frozen)

See Table 2 for details of concentration values for half maximal inhibition of target (IC_{50} values) for drugs used in myography and electrophysiology experiments.

Table 2. IC_{50} values for inhibitors used in myography and electrophysiology experiments.

Drug	Target for inhibition	IC_{50} value	Cell/tissue type and species	Reference (s)
4AP	K_V	232µM	Conduit PASMCs (rat)	Smirnov *et al.*, 2002
BDM	$K_V2.1$	16.7mM	*Xenopus* oocytes expressing rat $K_V2.1$	Lopatin and Nichols, 1993
DPO-1	$K_V1.5$	0.16-0.76µM	Chinese hamster ovary cells expressing human $K_V1.5$	Lagrutta *et al.,* 2006
Glyburide	K_{ATP}	86 ± 17nM	A10 cells (vascular smooth muscle cell line derived from rat thoracic aorta)	Russ *et al.,* 1997
L-NAME	Nitric oxide synthase (NOS)	0.87 ± 0.02 µM	Mouse cerebellar NOS	Moore *et al.,* 1993
Penitrem A	BK_{Ca}	64.4 nM	Human embryonic kidney 293 cells expressing human BK_{Ca}	Asano *et al.,* 2012
Ryanodine	Ryanodine receptor	4.5-5.5µM	Ileal smooth muscle cells (rabbit)	Sakai *et al.,* 1988
TEA	BK_{Ca}	~0.3mM	Skeletal muscle cells (rat)	Blatz and Magleby, 1984
Zinc chloride	TASK-1 TASK-3	175µM ~12-20µM	*Xenopus* oocytes expressing rat TASK-1 Human embryonic kidney 293 cells/ *Xenopus* oocytes expressing TASK-3	Leonoudakis, 1998 Gruss *et al.,* 2004, Clarke *et al.,* 2004

Solvent Controls

Levels of ethanol and DMSO did not exceed 0.1% total organ bath volume; the effect of the maximal level of solvent on baseline tension was investigated.

Dissociation Enzymes

Papain (from Papaya Latex, product number P4762), collagenase from *Clostridium histolyticum* (Type VIII, product number C2139) and DL-Dithiothreitol (product number D0632) were all acquired from Sigma Aldrich, UK. Another batch of papain was also used for some experiments (Acros Organics, Fisher Scientific, UK, product number 10701262). Enzymes were dissolved in HEPES-based dissociation solution at a concentration of 10mg/mL and aliquoted in volumes between 350µL and 1mL and stored at -20°C. Stock aliquots were defrosted on a daily basis and an appropriate volume was added to 1mL dissociation solution to give the desired concentration.

Chapter 3

Impact of Maintenance in Culture Conditions on Hypoxia and Agonist Induced Responses in Porcine Inferior and Superior Pulmonary Veins

Introduction

The maintenance of functional, isolated blood vessels under culture conditions is a potentially powerful tool to enable assessment of the impact of various environmental conditions on vessel function as outlined in Chapter 1 – General Introduction. However culture conditions alone can affect blood vessel function (Alm *et al.*, 2002, Binko *et al.*, 1999, Cao *et al.*, 2005, De Mey *et al.,* 1989, Manoury *et al.*, 2009, Morita *et al.,* 2013, Guibert *et al.,* 2005, Thorne *et al.,* 2001, Thorne *et al.,* 2002, Thorne and Paul, 2003).

Receptor mediated contractility can be affected when blood vessels are maintained in culture. For example, contractions to 5HT in rat mesenteric arteries are enhanced within 6 hours and in rat pulmonary arteries (PAs) after 4 days exposure to culture conditions (Cao *et al.*, 2005, Guibert *et al.,* 2005). In contrast, others have shown that rat mesenteric arteries display a similar contractile response to 5HT after 3 days in serum-free culture conditions (Morita *et al.,* 2010). Responses to other contractile agonists including U46619 (in rat mesenteric arteries and porcine coronary arteries), endothelin-1 (in rat PAs) and phenylephrine (in rat aorta) are unchanged after maintenance in culture conditions as compared with responses of freshly isolated vessels (Alm *et al.*, 2002, Binko *et al.*, 1999, Guibert *et al.,* 2005, Thorne *et al.*, 2001).

Receptor independent mechanisms may also be affected. KCl-mediated contractions (between 10 and 40mM) are significantly increased in rat PAs after 3-4 days (Guibert *et al.,* 2005, Manoury *et al.*, 2009) whereas contraction to 50mM KCl is diminished after 3 days maintenance in culture conditions (Manoury *et al.,* 2009). In addition, KCl sensitivity is reduced in rat renal arteries after 6 days and porcine coronary arteries after 24 hours exposure to culture conditions (De Mey *et al.,* 1989, Thorne *et al.*, 2002). 4AP mediated contraction is significantly reduced and caffeine contraction significantly

increased in porcine coronary artery after exposure to 24 hours in culture conditions at 37°C as compared to control arteries stored in culture medium for 24 hours at 4°C (Thorne *et al.,* 2002, Thorne and Paul, 2003). Storing vessels for 24 hours at 4°C in culture medium appears to have no significant impact on function compared to freshly isolated vessels (Thorne *et al.,* 2001).

Contraction is not the only functional mechanism affected by maintenance in culture conditions; relaxation may also be altered. Exposure to serum-free culture conditions for as little as 20-24 hours impairs cholinergic-mediated endothelial dependent relaxation in both pulmonary and mesenteric arteries (Alm *et al.*, 2002, Manoury *et al.*, 2009). Addition of adult serum to the culture medium can normalise this impairment of endothelial dependent relaxation (Morita *et al.,* 2013). Hypoxia-induced relaxation is significantly inhibited by 24 hours in culture conditions at 37°C in porcine coronary and carotid arteries and rat and mouse aorta as compared to vessels stored in culture medium for 24 hours at 4°C (Thorne *et al.,* 2001, Thorne *et al.,* 2002). Relaxation via K^+ channel activation with pinacidil is also impaired in porcine coronary artery (Thorne *et al.,* 2002) however relaxation with SNP (nitric oxide donor), isoproterenol (β-adrenoceptor agonist) and forskolin (adenylate cyclase activator) remains unchanged (Thorne *et al.,* 2001) after maintenance in culture conditions.

Maintenance in culture conditions has a significant impact on blood vessel function. Before using the method for future applications, the impact of maintenance in culture conditions alone on pulmonary vein (PV) contractility required investigation.

In PAs, exposure to culture conditions appears to mimic chronic hypoxia (Manoury *et al.,* 2009) as discussed in Chapter 1 – General Introduction. The potential for mimicry between culture conditions and chronic hypoxic requires further investigation in PVs. Exposure to culture conditions augments responses to KCl in PAs within 3-4 days (Guibert *et al.,* 2005, Manoury *et al.*, 2009) yet exposure of rats to chronic hypoxia (10% O_2 for 2-7 days) has no effect on KCl responses (20-100mM) in PVs (Zhao *et al.,* 1995). PVs isolated from rats kept in a normobaric hypoxic chamber (10% pO_2) for 3 weeks behave differently to PAs isolated from hypoxic rats when compared to their respective normoxic controls (Lal *et al.*, 1999). Exposure of rats to chronic hypoxia augmented PV responses to the endothelin ET_B receptor agonist sarafotoxin-6c compared to normoxic controls; this effect was not observed in PAs. PAs from chronically hypoxic rats showed reduced sensitivity to U46619 than control rats whereas potency in the PV was unchanged (Lal *et al.*, 1999). In PVs, acute hypoxia-mediated contraction appears to be enhanced after exposure to chronic hypoxia, yet contractile responses to angiotensin II (AT_1 receptor agonist; Ardaillou, 1999), phenylephrine and KCl are significantly reduced after 2, 7 and 14 days of chronic global hypoxia, respectively (Zhao *et al*., 1995).

After 20 hours lobar hypoxia (as opposed to global), acute hypoxic contractions of ovine PVs were also enhanced compared to PVs from the normoxic control lobe. This enhancement did not occur in PAs from the lobe exposed to chronic hypoxia compared to control PAs (Sheehan *et al*., 1992). Selective maintenance/enhancement of this intrinsic pulmonary venous response to hypoxia may indicate the clinical importance of the PV as suggested by Taylor *et al.* (2011). The hypoxic response of the porcine PV required further characterisation.

As PV contraction during hypoxia may facilitate recruitment of lung capillaries and therefore maximise surface area for gas exchange (Taylor *et al.,* 2011); maintenance of this response under chronic hypoxic conditions would be advantageous. However, in obese patients undergoing surgical procedures, evidence suggests an inverse relationship between body BMI and PO_2 values in inferior PVs, with no such relationship existing in superior PVs (Yamane *et al*., 2008). This may be due to impairment of hypoxia-induced contraction and V-Q mismatch in inferior PVs specifically. Differences in the function of inferior and superior PVs required identification and characterisation, specifically in relation to hypoxic PV responses.

PVs are also known to contract in response to a number of agonists and in some cases to a greater extent than PAs, for example, histamine (Shi *et al.*, 1998, Toda, 1990), $PGF_{2\alpha}$ (Chand, 1981, Kadowitz *et al.,* 1975) and U46619 (Arrigoni *et al.,* 1999). These enhanced responses are described in more detail within Chapter 1 – General Introduction.

The aim of this study was to investigate the impact of maintenance in culture conditions on inferior and superior PV function including endothelial function and contractile responses to pharmacological agonists (histamine, $PGF_{2\alpha}$ and U46619) and hypoxia.

Methods and Experimental Protocols

Myography was used to investigate the contractility of porcine 3^{rd}-4^{th} order superior and 4^{th}-5^{th} order inferior intrapulmonary veins. Tissue for experiments in this chapter was obtained from Scotch Premier Meat Ltd (Inverurie, Aberdeenshire). Contractile responses to KCl, histamine, $PGF_{2\alpha}$, U46619 and hypoxia were explored. Possible mechanisms underlying the PV hypoxic response were also investigated using Ca^{2+} free conditions, by depleting SR Ca^{2+} with ryanodine and caffeine (Jabr *et al.,* 1997) and by blocking BK_{Ca} channels with Penitrem A (Dospinescu *et al.,* 2012).

Inferior and superior PVs were size-matched and were dissected from porcine lungs as described in Chapter 2. After dissection 3-4^{th} order vessels were used fresh and 4^{th}-5^{th} order were maintained in culture conditions for 24 hours (see Chapter 2 for more details).

On each experimental day, two myograph set-ups were used, each comprising of four channels. One set-up contained 4 vessel rings from a superior PV and the other 4 rings from an inferior PV; on alternate days fresh vessels and those maintained in culture were mounted and tested. Set-ups were also swapped on a daily basis, i.e. one day set-up 1 would be inferior PV and the next superior PV.

Equilibration, Resting Tone and Functional Testing

Once PVs were mounted and set to optimal resting tension of 1.5g (see Chapter 2), they were left to equilibrate for 60 minutes. After this time the vessels were checked for viability by exposing to 80mM KCl three times. If no constriction occurred in response to 80mM KCl then vessels were considered non-viable and not included in further analysis however endothelial integrity and responses to hypoxia were still assessed.

Endothelial integrity was assessed by preconstricting with a sub-maximal level of contractile agonist (2µM $PGF_{2\alpha}$) followed by application of a cholinergic agonist (acetylcholine synthetic analogue carbamoylcholine chloride- carbachol (10µM)). If the blood vessel relaxed in response to the cholinergic agonist this confirmed endothelial function; if further contraction occurred then this indicated endothelial damage (Furchgott and Zawadzki, 1980). PVs which failed to relax in response to carbachol were not excluded from further testing.

Concentration-Dependent Responses to Histamine, $PGF_{2\alpha}$ and U46619

Concentration response studies were performed with histamine, PGF_{α} and U46619. The aim of these studies was to identify any differences in contractile responses between inferior and superior PVs and those which were fresh or exposed to culture conditions for 24 hours. Drugs were applied cumulatively to determine response curves. Concentration ranges used were 1nM - 100µM for histamine, 10nM- 10µM for $PGF_{2\alpha}$ and 10pM - 1µM for U46619. Contractions were allowed to reach steady state before addition of the next concentration. Agonist response studies were either conducted before or after hypoxia studies as described below.

Hypoxia Response Studies

Pulmonary veins were exposed to hypoxia by changing the myograph bubbling from 95%O_2/5%CO_2 to 95%N_2/5%CO_2. CO_2 levels were maintained at 5% to maintain the pH of KREB's at 7.4. Hypoxic exposures lasted approximately 15-20 minutes and at least 30 minutes in 95%O_2/5%CO_2 were allowed for recovery between exposures. Tension was re-adjusted to the optimal resting tension of 1.5g before the first exposure to hypoxia. Two initial hypoxic exposures were conducted before PVs were exposed to pharmacological agents or altered Ca^{2+} conditions; this was due to the second hypoxic response being a more robust response and therefore control for comparison with the third "test" response. More information is provided in Results section.

Initial Investigation of Pathways Underlying the Hypoxic Response

To investigate the role of extracellular Ca^{2+} in hypoxic responses of inferior and superior PVs, KREB's was washed out and vessels were incubated in Ca^{2+} free KREB's solution ($CaCl_2$ substituted with equimolar $MgCl_2$).

Ryanodine and caffeine have been previously used to investigate the effect of SR depletion on the hypoxic response in canine PAs (Jabr *et al.*, 1997). For SR depletion, PVs were exposed to 20mM caffeine four times at 15-20 minute intervals. For exposure to caffeine, KREB's was washed out and replaced with KREB's solution containing 20mM caffeine. On the 3rd caffeine exposure 2µM ryanodine was added.

BK_{Ca} channels have been proposed to play a role in attenuating HPV in PAs (Peinado *et al.,* 2008, Yan *et al.,* 2014). A positive correlation between RNA expression of BK_{Ca} and HPV magnitude has been established in human PAs (Peinado *et al.,* 2008). Furthermore, activation of BK_{Ca} by docosahexaenoic acid has been suggested to attenuate HPV in rat PAs; the inhibitory effect of docosahexaenoic acid on hypoxic contraction was reversed by the BK_{Ca} blocker iberiotoxin (Yan *et al.,* 2014). The potential for BK_{Ca} inhibition of the hypoxic response was investigated using the blocker Penitrem A (500nm) (Dospinescu *et al.*, 2012).

PVs were incubated in these conditions for at least 20 minutes before the third hypoxic "test" exposure.

Solvent Controls

Experiments using ryanodine, Penitrem A and U46619 involved adding 25µL of DMSO to the bath and those using $PGF_{2\alpha}$ involved adding 25µL ethanol. Therefore the impact of these volumes of solvent alone (absence of drug) on baseline tension was investigated.

Data Analysis

Hypoxic/reoxygenation (see Results) magnitude data are expressed normalised to baseline tension (A.U). For the sake of clarity hypoxic relaxation is expressed with a value of 1 subtracted to more clearly illustrate where relaxation below baseline occurs. Contractile data for KCl and agonists were standardised to final mean 80mM KCl response (FMKCl) in fresh inferior/superior PVs as appropriate and expressed as %FMKCl. Where appropriate data are presented as mean ± S.E.M and N represents the number of vessels from different animals. Statistical significance was determined at $P<0.05$ using Students unpaired *t*-test, repeated measures one-way ANOVA or one-way ANOVA with Tukey's post-test (GraphPad Prism 5, CA, USA).

Results

KCl Viability Testing

To test for smooth muscle viability, at the start of each experimental day, PVs were exposed to 80mM KCl three times. In fresh inferior PVs, 100% contracted to 80mM KCl and first (3.2 ± 0.4 g), second (3.6 ± 0.4 g) and third (3.8 ± 0.4g) responses were not significantly different from one another (P>0.05, N=11). In fresh superior PVs there was also no significant difference between first (1.9± 0.4g), second (2.1 ± 0.4g) and third (2.1 ± 0.4g) KCl responses (P>0.05, N=11). First, second and third responses to 80mM KCl were significantly larger in magnitude in fresh inferior PVs than superior PVs (P<0.05).

PVs maintained in culture for 24 hours also did not show a significant increase in KCl contraction with repeated exposure; 97.5% of inferior and 85% of superior PVs successfully responded. In inferior PVs, first (5.0 ± 0.6g), second (5.1 ± 0.6g) and third (5.0 ± 0.6g) responses did not differ in magnitude (P>0.05, N=10). The same trend was observed in superior PVs (2.3 ± 0.4g, 2.2 ± 0.3g, 2.3 ± 0.3g; 1^{st}, 2^{nd} and 3^{rd} responses, respectively, P>0.05, N=10). Similar to fresh PVs all three responses to 80mM KCl were significantly larger in magnitude in inferior PVs than superior PVs (P<0.01).

Maintenance in culture conditions significantly increased the first KCl contraction in inferior PVs (P<0.05) but did not alter KCl responses in superior PVs or subsequent KCl contractions (second/third) in inferior PVs (P>0.05). All further agonist data were standardised to mean 3^{rd}/final KCl response (FMKCl) in fresh inferior/superior PVs (as appropriate) demonstrating absolute changes as a result of exposure to 24 hours of culture conditions. The final KCl response was used for standardisation as it was demonstrably reproducible and considered more stable than 1^{st} and 2^{nd} responses as Ca^{2+}-sensitisation occurs in response to KCl (Ratz *et al.*, 2005).

Endothelial Function Testing

In order to test for endothelial function, PVs were preconstricted with a submaximal concentration of $PGF_{2\alpha}$ (2µM) before exposing to a synthetic analogue of acetylcholine- carbachol (10µM). If vessels relaxed to carbachol, this indicated a functional endothelium.

In fresh PVs, 2µM $PGF_{2\alpha}$ produced a sustained contraction in 100% of vessels tested before assessment of endothelial relaxation with 10µM carbachol. The level of preconstriction produced

with a submaximal concentration of $PGF_{2\alpha}$ (2μM) was not significantly different between inferior and superior PVs (1.5 ± 0.4g and 1.0 ± 0.2g, inferior and superior, respectively, *P*>0.05, N=8). When standardised to FMKCl, the difference was still not significant, response magnitude was 39.1 ± 11.3%FMKCl (inferior) and 46.9 ± 8.8%FMKCl (superior).

$PGF_{2\alpha}$ (2μM) produced a contraction in 81.25% of both inferior and superior PVs maintained in culture. Unfortunately, this was a transient contraction in 46.2% of inferior PVs and 73.0% of superior PVs which responded. This made subsequent analysis of endothelial relaxation challenging. The level of preconstriction before carbachol was applied was 1.1 ± 0.3g in inferior and 0.8 ± 0.2g in superior PVs maintained in culture for 24 hours (N=8). When standardised to FMKCl the magnitude was 29.5 ± 7.9% in inferior PVs and 39.0 ± 9.5% in superior PVs. Contraction to $PGF_{2\alpha}$ was not significantly different between inferior and superior PVs maintained in culture and there was also no difference between the level of preconstriction achieved in fresh PVs and those maintained in culture (*P*>0.05). However as stated earlier the contraction in PVs exposed to culture conditions was transient therefore results should be interpreted with caution.

To calculate % endothelial relaxation, the following equation was used:

$$\%\ Endothelial\ Relaxation = \frac{Contraction\ (g) - Relaxation\ (g)}{Contraction\ (g)} \times 100$$

(Equation 2)

Contraction was the absolute value of tension in response to $PGF_{2\alpha}$ before carbachol was applied (i.e. not a Δ value). Relaxation was the absolute value of tension once the response to carbachol had reached a steady plateau.

Almost all fresh PVs (96.9%) successfully relaxed in response to 10μM carbachol. Fresh inferior PVs produced a greater relaxation in response to carbachol than superior PVs (79.0 ± 3.4% and 62.7 ± 6.2%, inferior and superior respectively, *P*<0.001, N=8). When maintained in culture 96.9% of inferior and 87.5% of superior PVs relaxed in response to carbachol. There was no significant difference in endothelial-mediated relaxation between inferior/superior; inferior PVs produced a relaxation of 55.5 ± 7.7% and superior PVs relaxed 49.8 ± 7.2% (*P*>0.05, N=8). Notably, the endothelial relaxation was significantly impaired in PVs maintained in culture for 24 hours compared to fresh PVs (inferior PVs: *P*<0.001, superior PVs: *P*<0.01). To reiterate, these data should still be interpreted with caution as the $PGF_{2\alpha}$ contraction was often not sustained and this could influence results. Example traces from superior PVs illustrating the difference between preconstriction to

$PGF_{2\alpha}$ and endothelial relaxation to carbachol are shown in Figure 16. Similar results were observed in inferior PV.

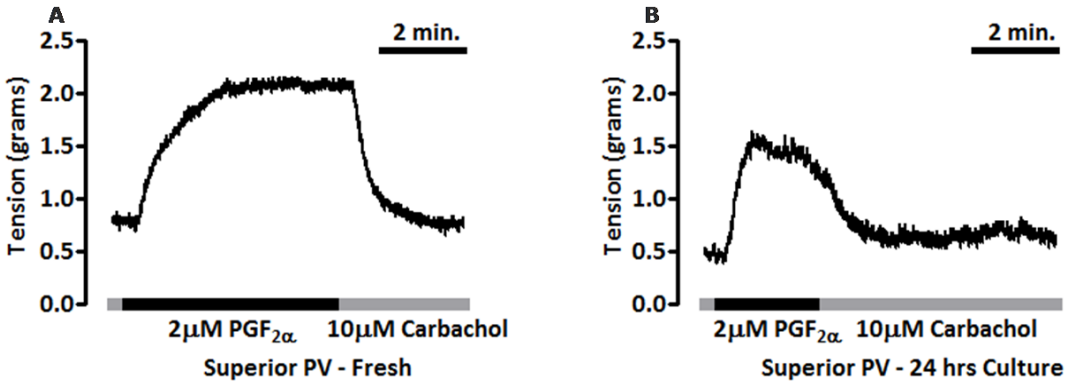

Figure 16. Representation of endothelial relaxation responses in fresh superior pulmonary vein and those maintained in culture for 24 hours. Preconstriction to 2μM $PGF_{2\alpha}$ and relaxation with 10μM carbachol in fresh superior PV and after maintenance in culture conditions for 24 hours. Sample traces for A: fresh superior PV and B: superior PV maintained in culture for 24 hours. Black and grey bars represent $PGF_{2\alpha}$ and carbachol exposure, respectively. N.B sustained constriction to $PGF_{2\alpha}$ in fresh superior PVs and transient constriction in superior PVs maintained in culture which is relaxing before application of carbachol. However an increase in the relaxation slope seen after application of carbachol suggests a functional endothelium.

Agonist Cumulative Concentration-Dependent Responses

Concentration-dependent responses to histamine, $PGF_{2\alpha}$ and U46619 were investigated in fresh PVs and those maintained in culture for 24 hours by applying drugs cumulatively.

Response curves were fitted with the sigmoidal dose-response curve function within GraphPad Prism 5 (California, USA); equation as follows:

$$Y = Bottom + \frac{(Top - Bottom)}{1 + 10^{Log\ EC50 - X}}$$

(Equation 3)

Where *bottom* is the y value at bottom sigmoid plateau, *top* is y value at top sigmoid plateau and *log* EC_{50} is x value for y response at half distance between bottom and top plateaus.

Histamine

Maximum contractile responses to histamine were significantly increased in inferior PVs maintained in culture (292.6 ± 11.3%FMKCl) compared to fresh (167.2 ± 10.5% FMKCl; $P<0.001$, N=7). Superior PVs maintained in culture for 24 hours also showed an increased maximum response to histamine compared to fresh PVs (308.5 ± 25.9 and 194.6 ± 30.6%FMKCl, respectively; $P<0.05$, N=6-7). There was no difference in maximum responses between inferior and superior PVs or between EC_{50} values for any of the four groups ($P>0.05$, see Figure 17 C&D and Table 3).

$PGF_{2\alpha}$

Maximum contractile responses to $PGF_{2\alpha}$ were not different in inferior PVs maintained in culture (115.1 ± 13.6%FMKCl) compared to fresh (94.1 ± 16.9%FMKCl; $P>0.05$, N=7). Maximum contractions were also not significantly altered in fresh superior PVs (197 ± 127%FMKCl) compared to those maintained in culture for 24 hours (117.2 ± 22.7%FMKCl $P>0.05$, N=6-7). Maximum contractions between inferior and superior PVs and EC_{50} values between groups were not significantly different ($P>0.05$, N=6-7, see Figure 17 E&F and Table 3).

U46619

Maintenance of inferior PVs in culture conditions for 24 hours significantly augmented the maximum contractile response to U46619 (225.7 ± 11.2% and 173.4 ± 7.1%FMKCl, culture/fresh, respectively; $P<0.01$, N=7). There was no significant effect of maintaining superior PVs in culture conditions on maximum U46619 contraction (181.2 ± 19.6% and 227.5 ± 22%FMKCl, culture/fresh, respectively; $P>0.05$, N=7). However fresh superior PVs showed a greater maximal response to U46619 than fresh inferior PVs ($P<0.05$, N=7). Maximum contractions between superior and inferior PVs kept in culture and U46619 potency between groups were not significantly changed ($P>0.05$, N=7, see Figure 17 G&H and Table 3).

Table 3. EC_{50} values for fresh inferior and superior pulmonary veins and those maintained in culture for 24 hours. Values for histamine, $PGF_{2\alpha}$ and U46619 quoted as mean with 95% confidence intervals (in brackets) and taken from fitting concentration-response curves with sigmoidal dose-response curve equation (GraphPad Prism 5, CA, USA) – see Equation 3. EC_{50} values for all agonists across all groups were not significantly different (P>0.05 using Students unpaired t-tests, N=6-7).

EC_{50} values (M)	**Fresh Inferior PV**	**Fresh Superior PV**	**Inferior PV – 24 hours culture**	**Superior PV – 24 hours culture**
Histamine	$2.2x10^{-7}$ ($8.5x10^{-8}$ - $6.0x10^{-7}$)	$2.3x10^{-7}$ ($1.9x10^{-8}$ - $2.8x10^{-6}$)	$1.8x10^{-7}$ ($1.0x10^{-7}$-$3.3x\ 10^{-7}$)	$7.1x10^{-8}$ ($1.9x10^{-8}$ - $2.7x10^{-7}$)
$PGF_{2\alpha}$	$2.3x10^{-6}$ ($7.0x10^{-7}$ - $7.6x10^{-6}$)	$8.6x10^{-6}$ ($6.1x10^{-7}$ - $1.2x10^{-4}$)	$1.3x10^{-6}$ ($5.1x10^{-7}$ - $3.4x10^{-6}$)	$8.6x10^{-7}$ ($1.3x10^{-7}$ - $5.6x10^{-6}$)
U46619	$3.1x10^{-9}$ ($1.7x10^{-9}$ - $5.7x10^{-9}$)	$3.7x10^{-9}$ ($9.5x10^{-10}$ - $1.5x10^{-8}$)	$3.5x10^{-9}$ ($1.6x10^{-9}$ - $7.3x10^{-9}$)	$1.4x10^{-9}$ ($2.9x10^{-10}$- $6.8x10^{-9}$)

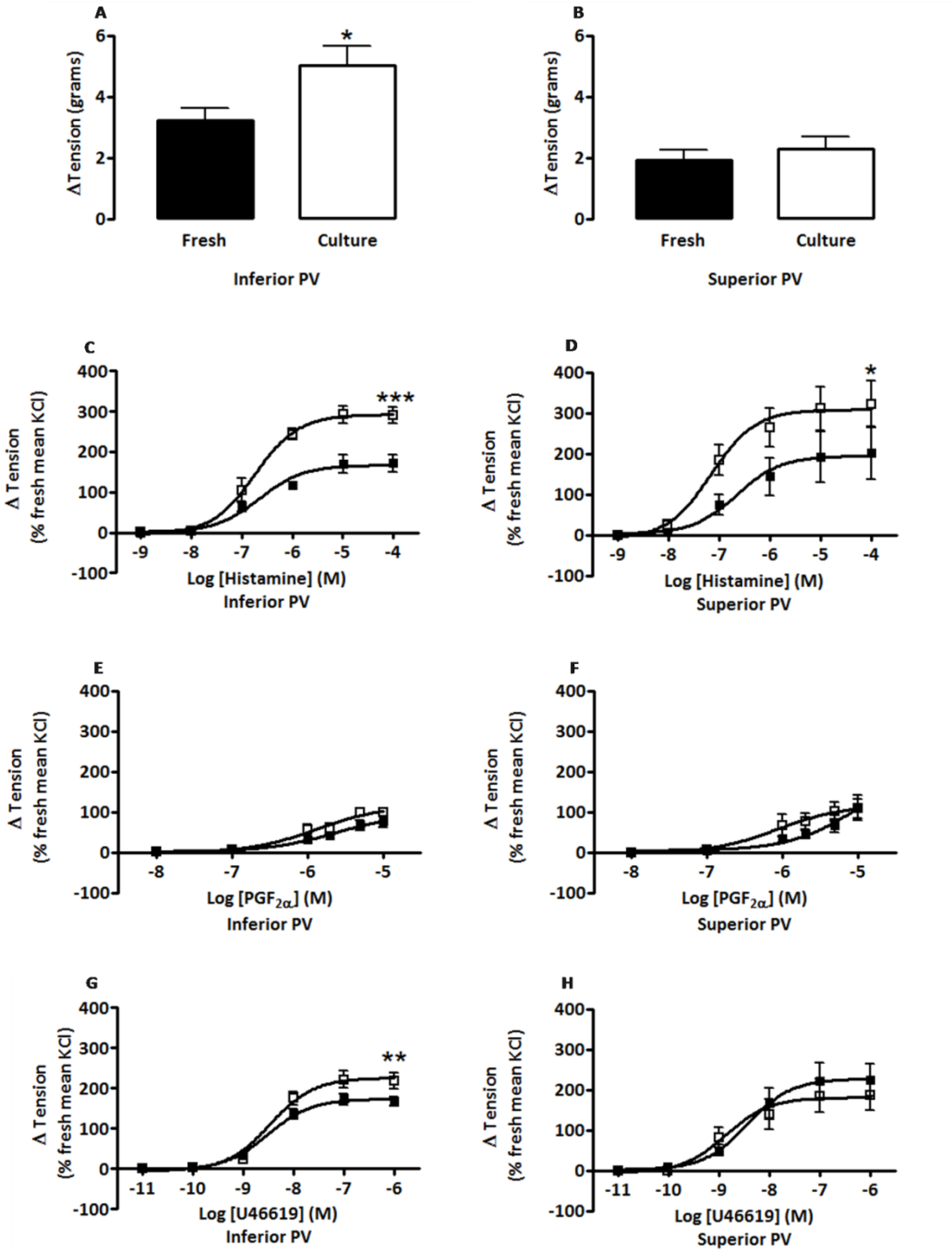

Figure 17. Impact of 24 hours maintenance in culture conditions on pulmonary vein contractile responses. Impact of maintenance in culture on 1st 80mM KCl response in inferior (A) and superior (B) pulmonary veins (PVs), N=9-10. Impact of maintenance in culture on responses to histamine (C: inferior and D: superior PVs), $PGF_{2\alpha}$ (E: inferior and F: superior PVs) and U46619 (G: inferior and H: superior PVs). All data for concentration-response curves expressed are standardised to mean 3rd response to KCl in fresh inferior/superior PV, N=6-7. N.B. ■ = fresh, □ = 24 hours in culture conditions. All data represent mean ± S.E.M. **P*<0.05, ** *P*<0.01, ****P*<0.001 compared to fresh PV (analysis using Students unpaired *t*-test).

Characterisation of PV Hypoxic Responses

Hypoxia caused a transient contraction in 88% and 99% of fresh PVs (1^{st} and 2^{nd} exposure respectively). In PVs maintained in culture conditions for 24 hours, hypoxia caused a transient contraction in 57% and 86% (1^{st} and 2^{nd} exposure respectively). Hence 2^{nd} exposures were used for further analysis and as controls. The consistency of these contractile hypoxic responses is clearly demonstrated in Figures 17 and 18 with all raw traces plotted standardise to baseline on the same axes. After contraction, relaxation to below baseline occurred in 94% of fresh PVs but only 37% of PVs maintained in culture during 2^{nd} hypoxic exposure (highlighted in Figures 19 and 20).

The hypoxic peak was significantly larger in inferior PVs maintained in culture for 24 hours (6.4 ± 1.5 A.U, N=10) than fresh inferior PVs (2.8 ± 0.4 A.U, N=9; $P<0.05$). Hypoxic peak was not significantly augmented in superior PVs kept in culture (4.3 ± 1.1 A.U, N=10) compared to fresh (2.0 ± 0.3 A.U, N=9; $P>0.05$). There was no difference in hypoxic peak magnitude between fresh inferior and to superior PVs ($P>0.05$); there was also no change in magnitude between inferior and superior PVs maintained under culture conditions ($P>0.05$). Peak magnitude data are expressed standardised to baseline (A.U), see Figure 22A.

There was a significant reduction in the magnitude of hypoxic relaxation when inferior PVs were exposed to culture conditions (0.16 ±0.15 and -0.4 ± 0.1 A.U, culture/fresh respectively, $P<0.01$). The same was also observed in superior PVs (0.1 ± 0.1 and -0.3 ± 0.1 A.U, culture/fresh respectively, $P<0.01$). Hypoxic relaxation was not significantly different between inferior and superior PVs either fresh or maintained in culture ($P>0.05$). For the sake of clarity hypoxic relaxation data are expressed standardised to baseline with a value of 1 subtracted to more clearly illustrate where relaxation below baseline occurs, see Figure 22B.

With regard to hypoxic response dynamics, time to 50% peak magnitude ($T_{0.5}$ peak) was not significantly different between fresh inferior (181.0 ± 26.0s) and superior PVs (141.0 ± 24.0s; $P>0.05$); the same was seen in vessels exposed to 24 hours culture conditions (146.2 ± 26.7 and 163.2 ± 37.6, inferior/superior PVs, respectively; $P>0.05$). There was also no significant difference in $T_{0.5}$ peak between fresh PVs and those maintained in culture ($P>0.05$). Time to 75% maximal relaxation ($T_{0.75}$ relaxation) was no different in inferior PVs kept in culture (384.4 ± 31.0s) than in fresh (461.6 ± 38.2s; $P>0.05$) and maintenance in culture did not significantly change $T_{0.75}$ relaxation in superior PVs (448.1 ± 61.9 and 480.5 ± 55.2s, culture/fresh, respectively; $P>0.05$). There was also no significant difference for $T_{0.75}$ relaxation between superior and inferior PVs either fresh or maintained in culture conditions ($P>0.05$). To investigate whether there was a time dependency of hypoxic response

according to vessel size, x-y scatter graphs were plotted with external diameter against $T_{0.5}$ peak or$T_{0.75}$ relaxation. There was no significant correlation between external diameter and either of these parameters of response dynamics (*P*>0.05).

Area under the curve (AUC) was increased in inferior PVs kept in culture (2044.4 ± 327.0) compared to fresh (969.7 ± 64.4, *P*<0.01). AUC was also augmented in superior PVs maintained in culture (1449.9 ± 248.9) compared to superior PVs (869.2 ± 58.0; *P*<0.05). As for all other parameters analysed, there was no significant change in AUC between inferior and superior PVs either fresh or after maintenance in culture conditions (*P*>0.05). See Figure 22 C-E.

Novel Reoxygenation Contraction

Under control conditions, oxygenation did not induce contraction. However, unexpectedly, it was discovered that reoxygenation after the 2nd hypoxic insult caused a further contraction in 97% of fresh PVs and 81% of those maintained in culture. The reoxygenation peak was not significantly different between inferior (2.5 ± 0.4 A.U) and superior PVs maintained in culture (1.8 ± 0.2; *P*>0.05); there was also no change in magnitude when comparing fresh inferior PVs (3.2 ± 0.5 A.U) to superior PVs (2.8 ± 0.4 A.U, *P*>0.05). Reoxygenation peak was significantly reduced in superior PVs exposed to culture conditions compared to fresh (*P*<0.05). There was no significant difference in reoxygenation peak magnitude between fresh inferior PVs and those kept in culture (*P*>0.05). Peak magnitude data are also expressed standardised to baseline (A.U).

Maintenance in culture conditions altered reoxygenation response dynamics, significantly reducing AUC in inferior (from 839.7 ± 113.8 (fresh) to 424.7 ± 61.7 (culture)) and superior PVs (from 728.6 ± 94.6 (fresh) to 432.5 ± 28.4 (culture); *P*<0.01). Maintenance in culture shortened $T_{0.5}$ peak in inferior PVs (from 80.2 ± 10.6s (fresh) to 39.8 ± 6.3s (culture); *P*<0.01). $T_{0.5}$ peak was not significantly different in inferior compared to superior PVs maintained in culture (39.8 ± 6.3s and 64.3 ± 13.4s, respectively; *P*>0.05). There was also no significant change in $T_{0.5}$ peak between fresh superior PVs (85.2 ± 16.3s) and those exposed to 24 hours culture conditions or in AUC or $T_{0.5}$ peak for fresh inferior and superior PVs (*P*>0.05). These data are illustrated in Figures 19, 20 and 22.

To investigate whether there was a time dependency of reoxygenation response according to vessel size, x-y scatter graphs were plotted with external diameter against $T_{0.5}$ peak. There was no significant correlation between external diameter and $T_{0.5}$ peak (*P*>0.05).

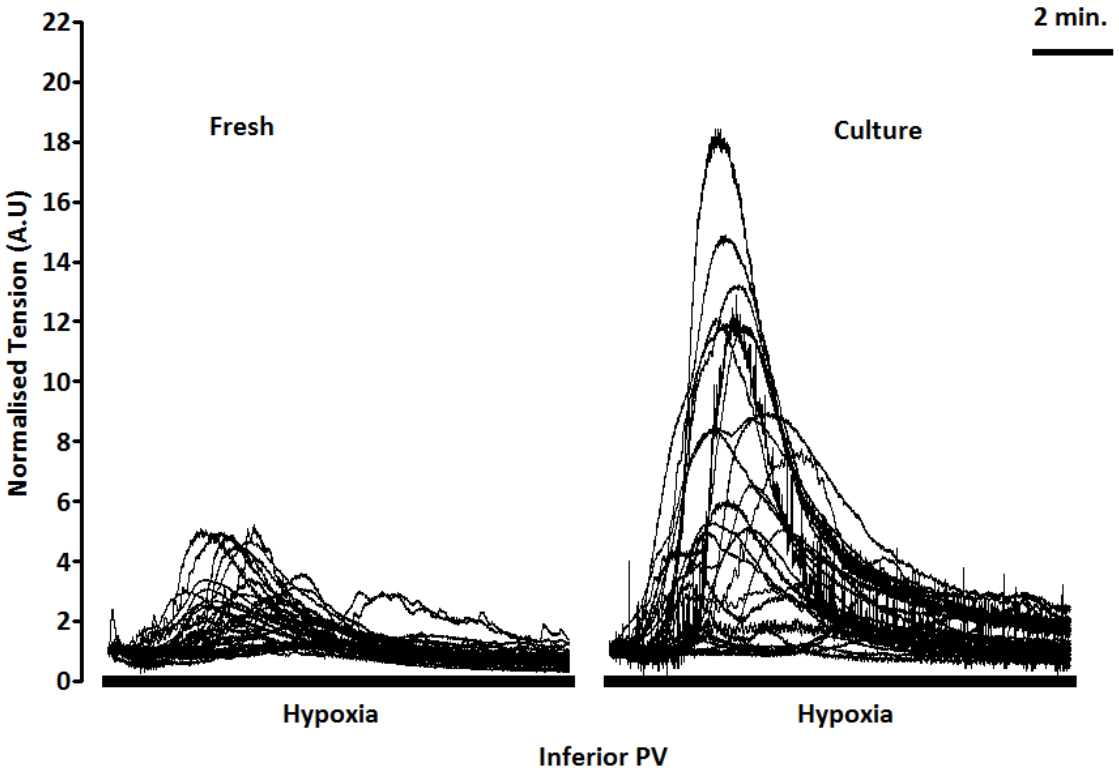

Figure 18. Standardised raw traces of hypoxia-induced contractions in fresh inferior pulmonary veins (PVs) and those maintained in culture for 24 hours. Hypoxic contraction of fresh inferior pulmonary veins (left) and those maintained in culture conditions for 24 hours (right). Raw traces plotted on same graph over same time period (12.26 minutes). Tension values are standardised to the initial baseline tension (A.U). Black bars represent hypoxia exposure. N=9 for fresh inferior PVs and N=10 for those maintained in culture.

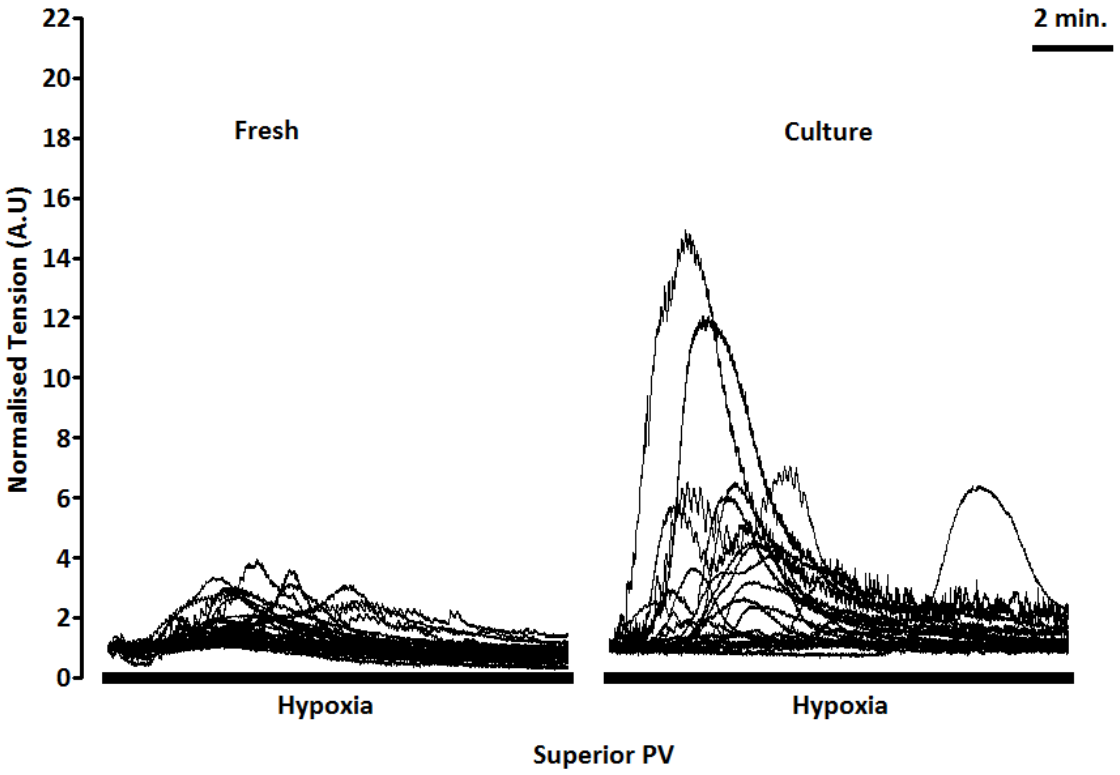

Figure 19. Standardised raw traces of hypoxia-induced contractions in fresh superior pulmonary veins (PVs) and those maintained in culture for 24 hours. Hypoxic contraction of fresh superior pulmonary veins (left) and those maintained in culture conditions for 24 hours (on right). Raw traces plotted on same graph over same time period (12.22 minutes). Tension values are standardised to the initial baseline tension (A.U). Black bars represent hypoxia exposure. N=9 for fresh superior PVs and N=10 for those maintained in culture.

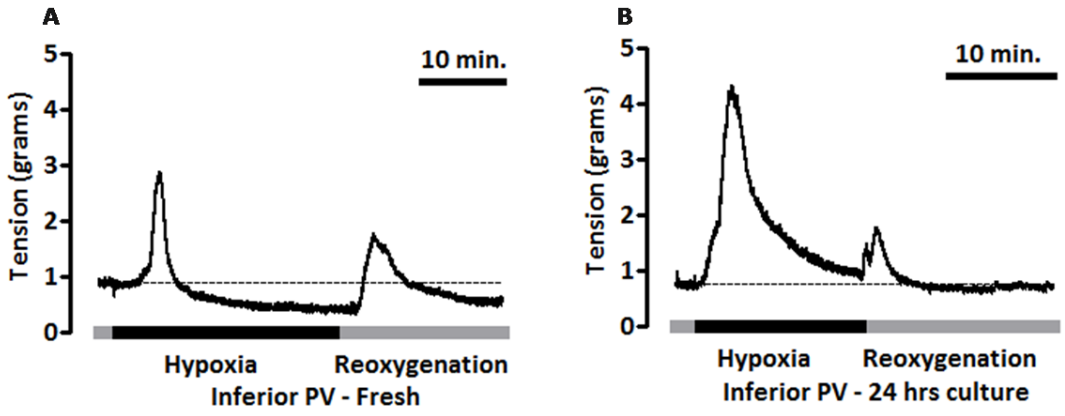

Figure 20. Representation of hypoxic and reoxygenation responses in fresh inferior pulmonary veins and those maintained in culture for 24 hours. Sample traces for hypoxic and reoxygenation responses in fresh inferior pulmonary vein (A) and after maintenance in culture conditions for 24 hours (B). Grey and black bars represent reoxygenation and hypoxia, respectively. Dotted line highlights level of baseline before hypoxic exposure initiated.

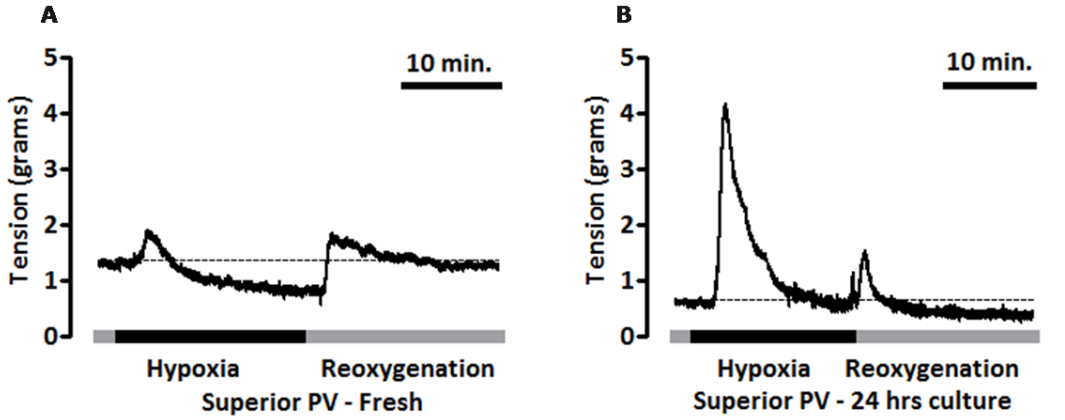

Figure 21. Representation of hypoxic and reoxygenation responses in fresh superior pulmonary veins and those maintained in culture for 24 hours. Sample traces for hypoxic and reoxygenation responses in fresh superior pulmonary vein (A) and after maintenance in culture conditions for 24 hours (B). Grey and black bars represent reoxygenation and hypoxia, respectively. Dotted line highlights level of baseline before hypoxic exposure initiated.

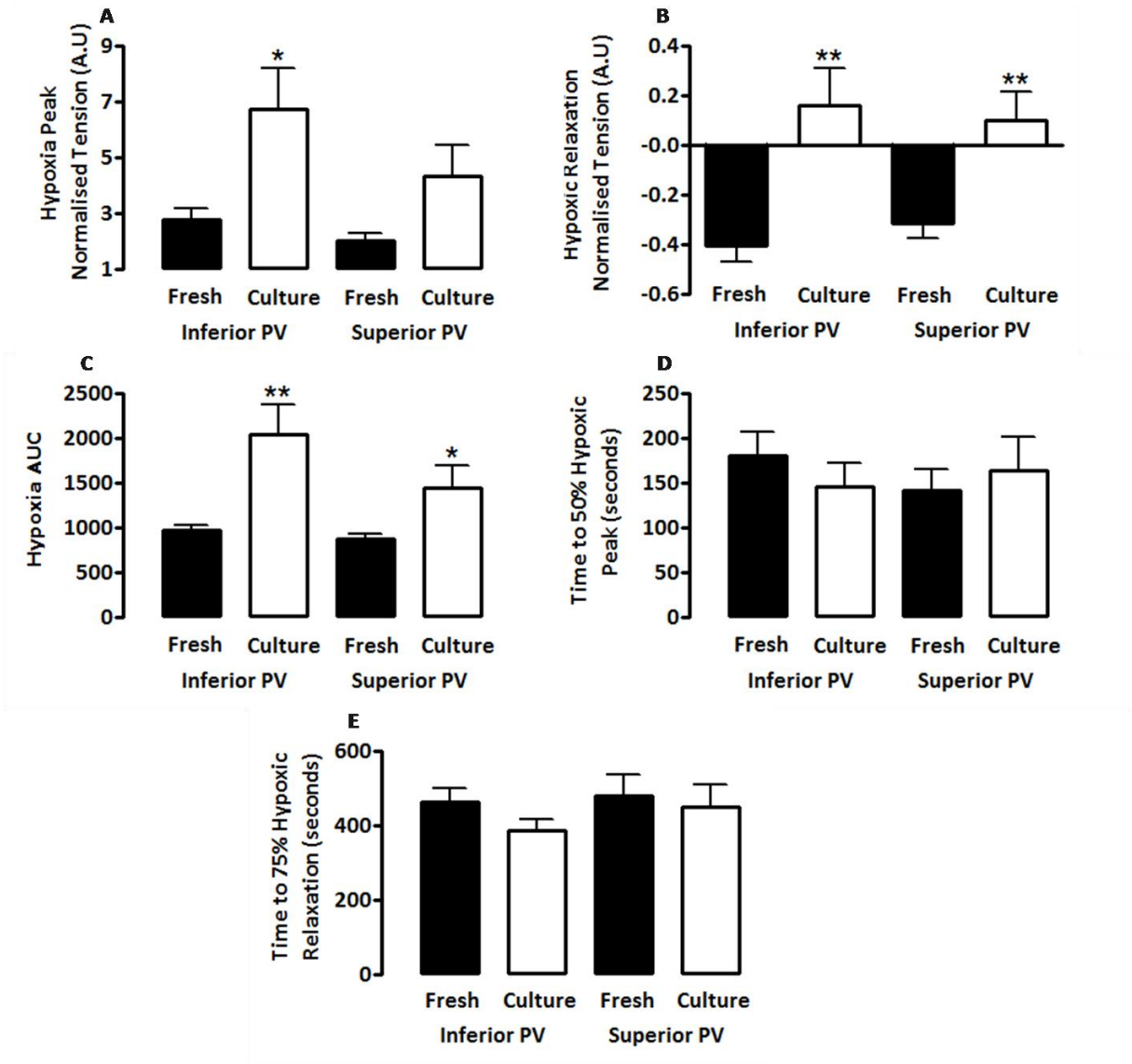

Figure 22. Hypoxic responses: differences between inferior and superior pulmonary veins and effect of maintenance in culture conditions for 24 hours. A: magnitude of hypoxic peak and B: magnitude of hypoxic relaxation post-contraction expressed as tension normalised to baseline tension. For the sake of clarity hypoxic relaxation data are expressed with a value of 1 subtracted to more clearly illustrate when relaxation below baseline occurs. C: area under the curve (AUC) for the hypoxic response (traces for AUC were plotted standardised to baseline over a time period of 759 seconds); D: time to 50% peak magnitude and E: time to 75% maximal relaxation post-contraction peak. All data represent mean ± S.E.M. *P<0.05, ** P<0.01 (analysis using Students unpaired t-tests), compared to fresh inferior/superior pulmonary vein (PV), N=9 for fresh inferior and superior PV and superior PV maintained in culture; N=10 for inferior PV maintained in culture.

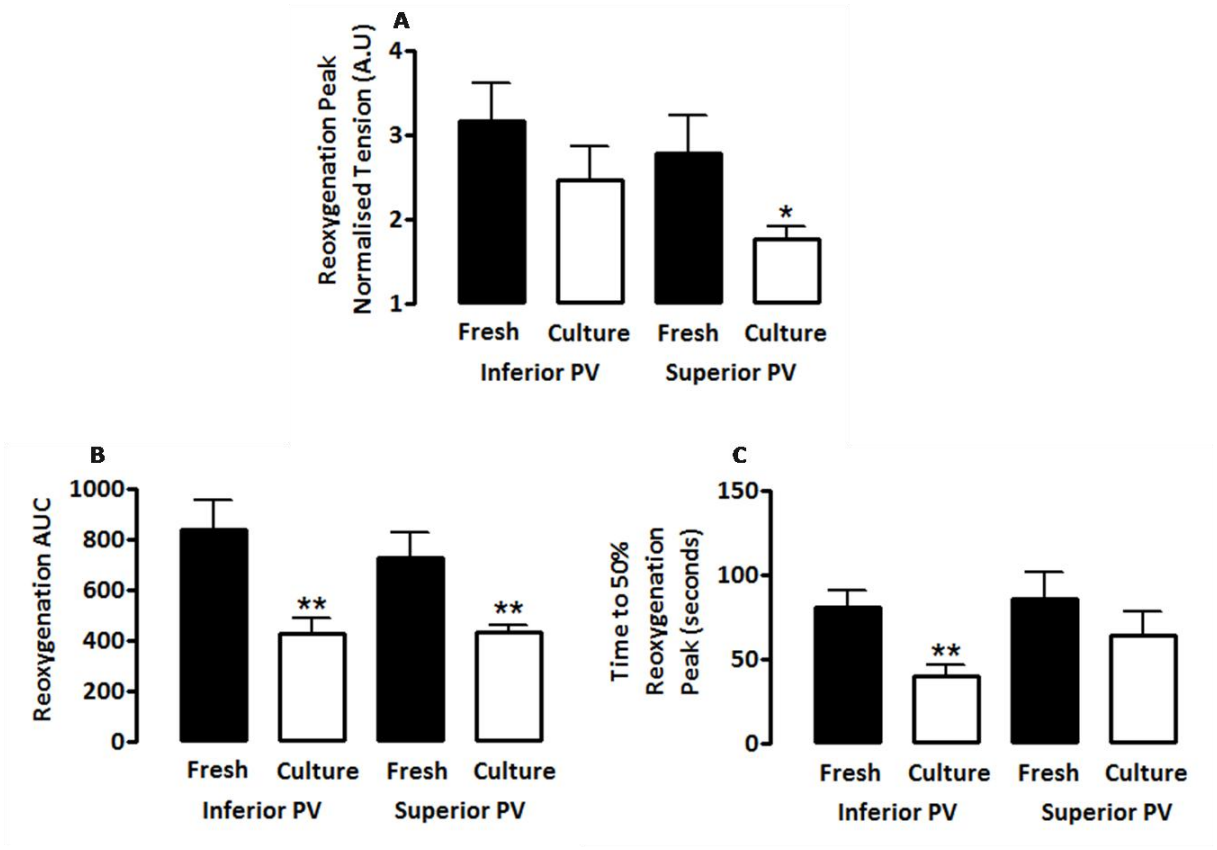

Figure 23. Reoxygenation contraction: differences between inferior and superior pulmonary veins and effect of maintenance in culture conditions for 24 hours. A: magnitude of the reoxygenation contraction after hypoxic exposure. Data are expressed as tension normalised to baseline tension. B: area under the curve (AUC) for reoxygenation contraction (traces for AUC were plotted standardised to baseline over a time period of 371.75 seconds) and C: time to 50% peak magnitude. Data represent mean ± S.E.M.*P<0.05, ** P<0.01 compared to fresh inferior/superior pulmonary vein (PV) (analysis using Students unpaired t-tests). N=9 for fresh inferior and superior PV and superior PV maintained in culture; N=10 for inferior PV maintained in culture.

Underlying Mechanisms of Hypoxic and Reoxygenation Responses

Ca^{2+} free conditions were used to investigate Ca^{2+} influx pathways involved in hypoxic and reoxygenation responses; ryanodine (2μM) and caffeine (20mM) were used to investigate SR Ca^{2+} release (all data is taken from fresh inferior/superior PVs). The hypoxic contraction in inferior PVs (2.8 ± 0.4 A.U, N=9) was not significantly reduced by Ca^{2+} free conditions (2.9 ± 0.5 A.U, N=5; *P*>0.05). The same was seen in superior PVs (2.0 ± 0.3 (N=9) and 1.8 ± 0.2 A.U (N=7), control/Ca^{2+} free respectively; *P*>0.05). On the other hand exposure to ryanodine (and caffeine) significantly inhibited the hypoxic contraction in both inferior and superior PVs (from 2.8 ± 0.4 to 1.2 ± 0.1 A.U (N=6) in inferior PVs (*P*<0.01) and from 2.0 ± 0.3 to 1.0 ± 0.1 A.U in superior PVs (*P*<0.05)) – see Figure 24.

In inferior PVs hypoxic relaxation was significantly reduced from -0.4 ± 0.1 to 0.1 ± 0.1 and -0.01 ± 0.1 A.U using ryanodine and Ca^{2+} free conditions, respectively (*P*<0.05 for Ca^{2+} free; *P*<0.001 for ryanodine). Relaxation was significantly inhibited in superior PVs from -0.3 ± 0.1 to and -0.04 ± 0.1 A.U in the presence of ryanodine (*P*<0.05) whereas Ca^{2+} free conditions had no significant effect (-0.1 ± 0.1 A.U, *P*>0.05). Reoxygenation peak was significantly inhibited by ryanodine in inferior PVs (from 3.2 ± 0.5 (N=9) to 1.0 ± 0.1(N=7); *P*<0.01) and superior PVs (from 2.8 ± 0.4 (N=9) to 1.1 ± 0.1 (N=5); *P*<0.05) whereas Ca^{2+} free conditions had no significant effect (hyperoxia peak 2.5 ± 0.5 A.U in inferior PVs (N=5) and 3.2 ± 0.6 A.U in superior PVs (N=6); *P*>0.05). See Figure 25.

Penitrem A (500nM) was used to investigate BK_{Ca} channel contribution to hypoxic and reoxygenation responses of fresh PVs. The hypoxic peak in the presence of Penitrem A was 3.1 ± 0.7 and 2.0 ± 0.5 A.U (inferior and superior, respectively, inferior: N=6, superior: N=5) and not significantly different (*P*>0.05) from controls (2.8 ± 0.4 (inferior) and 2.0 ± 0.3 A.U (superior); both N=9). Hypoxic relaxation was -0.3 ± 0.1 and -0.2 ± 0.1A.U (inferior and superior, respectively): again not significantly different (*P*>0.05) from controls (-0.40 ± 0.1 (inferior) and -0.3 ± 0.1 A.U (superior)). See Figure 26. The reoxygenation response was similarly unaffected by Penitrem A: 2.9 ± 0.5 and 2.3 ± 1.0 A.U (inferior (N=6) and superior (N=3), respectively) compared to controls: 3.2 ± 0.5 (inferior) and 2.8 ± 0.4 A.U (superior); N=9, *P*>0.05). See Figure 27.

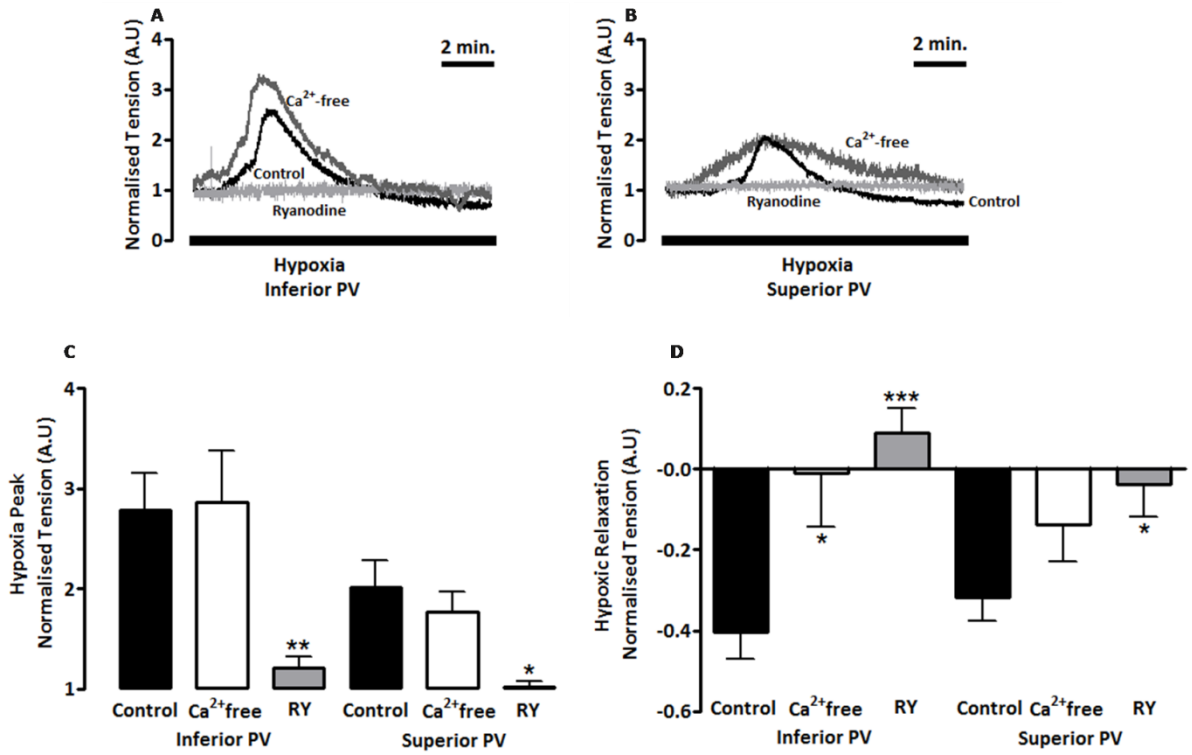

Figure 24. Hypoxic contraction of fresh inferior and superior pulmonary veins in control and Ca^{2+} free conditions and after exposure to 2µM ryanodine. Representative traces from A: inferior and B: superior pulmonary vein (PV). N.B. control (black), Ca^{2+} free (dark grey) and ryanodine (light grey). Black bar at bottom shows hypoxic exposure duration. C: Hypoxic peak magnitude and D: hypoxic relaxation post peak seen with control (N=9), Ca^{2+} free (N=4(inferior); N=6(superior)) and 2µM ryanodine (N=6(inferior); N=5(superior)) for inferior and superior PVs. All data expressed as tension normalised to baseline tension. For the sake of clarity hypoxic relaxation data are expressed with a value of 1 subtracted to more clearly illustrate when relaxation below baseline occurs. In C and D data represent mean ± S.E.M., **P*<0.05, ***P*<0.01 and ****P*<0.001 compared to control inferior or superior PV (analysis using Students unpaired *t*-tests).

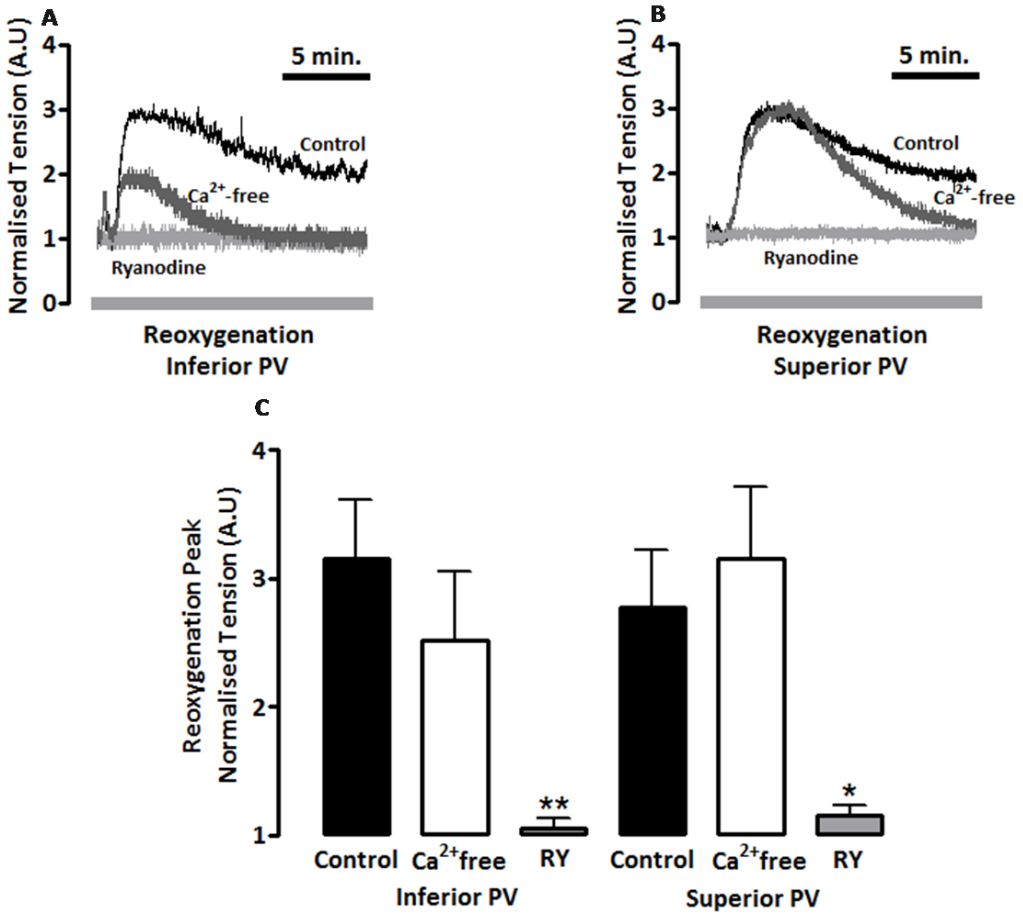

Figure 25. Reoxygenation contraction of fresh inferior and superior pulmonary veins in control and Ca^{2+} free conditions and after exposure to 2µM ryanodine. Representative traces from A: inferior and B: superior pulmonary veins (PVs). N.B. control (black), Ca^{2+} free (dark grey) and ryanodine (light grey). Grey bar at bottom shows reoxygenation exposure duration. C: Reoxygenation peak magnitudes (mean ± S.E.M.) seen with control (N=9), Ca^{2+} free (N=5(inferior); N=6(superior)) and 2µM ryanodine (N=7(inferior); N=5 (superior)). All data expressed as tension normalised to baseline tension. **P*<0.05; ***P*<0.01 compared to control inferior or superior PV (analysis using Students unpaired *t*-tests).

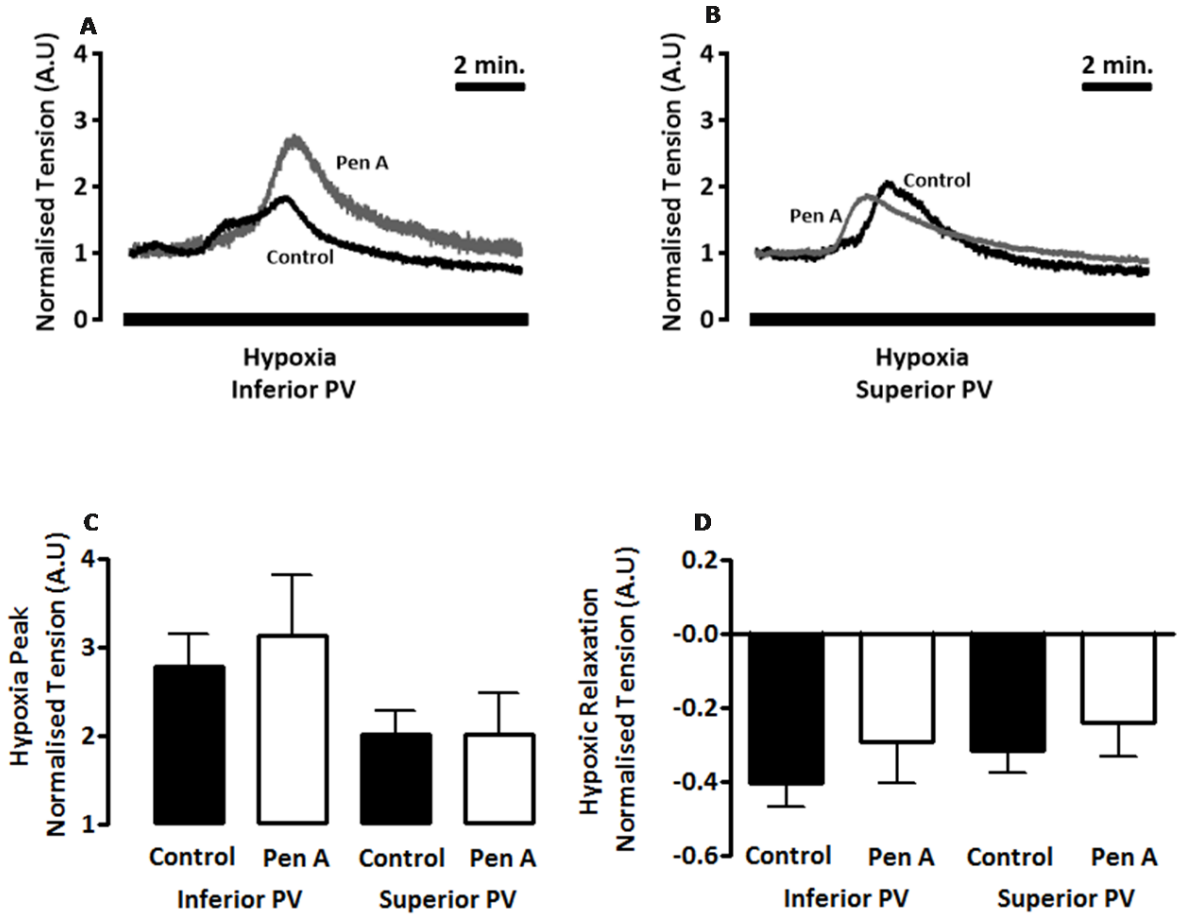

Figure 26. Hypoxic contraction of fresh inferior and superior pulmonary veins in control conditions and after exposure to 500nM Penitrem A. Representative traces from A: inferior and B: superior pulmonary vein (PV). N.B. control (black) and Penitrem A (Pen A, dark grey). Black bar at bottom shows hypoxic exposure duration. C: Hypoxic peak magnitude and D: hypoxic relaxation post peak seen with control (N=9) and 500nM Penitrem A (N=6(inferior); N=5(superior)). All data expressed as tension normalised to baseline tension. For the sake of clarity hypoxic relaxation data are expressed with a value of 1 subtracted to more clearly illustrate when relaxation below baseline occurs. In C and D data represent mean ± S.E.M (analysis using Students unpaired *t*-tests).

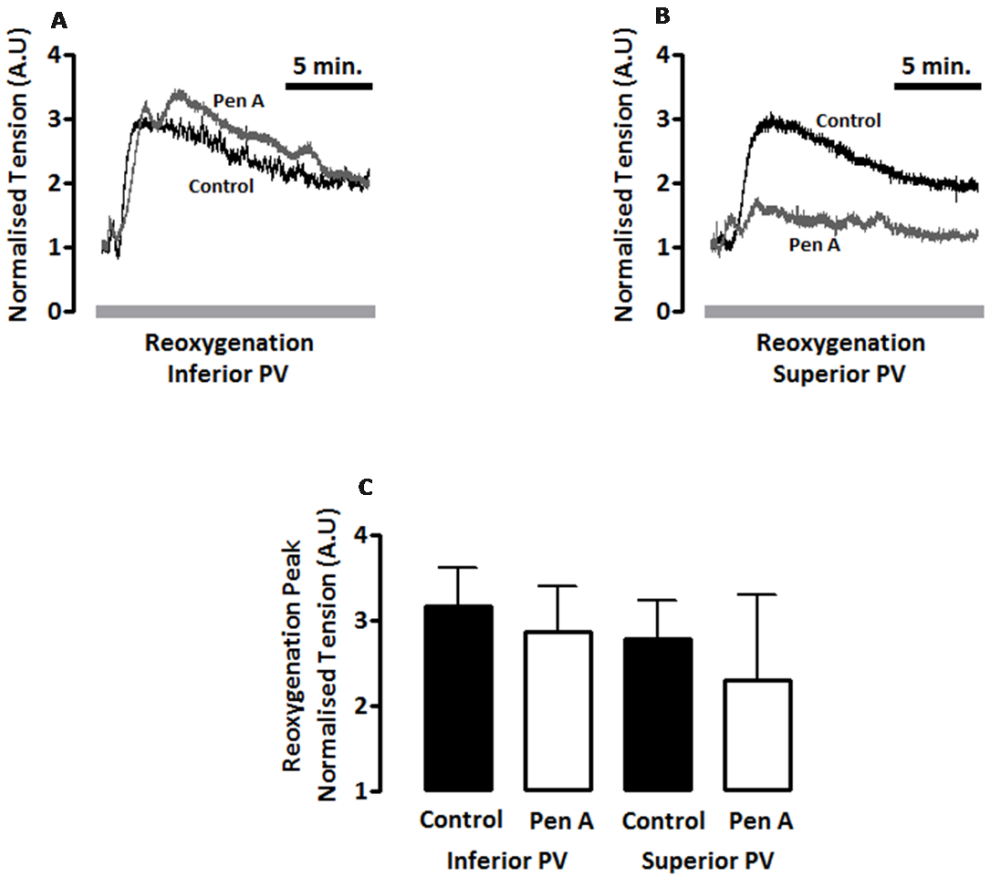

Figure 27. Reoxygenation contraction of fresh inferior and superior pulmonary veins in control conditions and after exposure to 500nM Penitrem A. Representative traces from A: inferior and B: superior pulmonary veins (PVs). N.B. control (black) and Penitrem A (Pen A, dark grey). Grey bar at bottom shows reoxygenation exposure duration. C: Reoxygenation peak magnitudes (mean ± S.E.M.) seen with control (N=9) and Penitrem A (N=6(inferior); N=3(superior)) in inferior and superior PVs. All data expressed as tension normalised to baseline tension (analysis using Students unpaired *t*-tests).

Solvent Controls

Adding 25µL of ethanol to the bath solution caused fresh inferior PVs to relax to a level significantly lower than baseline tension ($P<0.05$, N=3). All other PVs showed no change in baseline tension on application of 25µL ethanol and 25µL DMSO also had no impact on baseline tension ($P>0.05$, N=3). The results are shown in Table 4.

Table 4. Impact of solvents on baseline tension of pulmonary veins. Impact of adding solvents ethanol (25µL) and DMSO (25µL) on baseline tension in fresh inferior and superior PVs and those maintained in culture conditions for 24 hours (N=3). *P<0.05 compared to baseline tension (analysis using Students unpaired *t*-tests).

Ethanol (25µL)	Baseline Tension (g)	Tension after adding solvent (g)
Inferior - Fresh	1.4 ± 0.3	1.1 ± 0.2*
Superior - Fresh	1.5 ± 0.3	1.4 ± 0.3
Inferior – Culture	0.5 ± 0.1	0.6 ± 0.1
Superior - Culture	0.8 ± 0.3	0.8 ± 0.3
DMSO (25µL)		
Inferior - Fresh	1.5 ± 0.4	1.3 ± 0.3
Superior - Fresh	1.7 ± 0.4	1.6 ± 0.4
Inferior – Culture	0.5 ± 0.1	0.4 ± 0.1
Superior - Culture	0.8 ± 0.4	1.0 ± 0.2

It appears from Table 4 that baseline tension is lower in PVs kept in culture than fresh PVs. Tension data from before addition of either ethanol or DMSO were combined for comparison of baseline tension fresh PVs and those kept in culture. The average baseline tension level in fresh inferior PVs was significantly greater (1.5 ± 0.3g) and in inferior PVs kept in culture was (0.5 ± 0.1g, P<0.05, N=3). The baseline tension was also greater in fresh superior PVs (1.6 ± 0.3g) compared to those kept in culture (0.8 ± 0.3g) but this trend did not reach statistical significance (P>0.05, N=3).

Discussion

This study set out to identify the impact of maintenance in culture conditions on inferior and superior PV contractile responses to KCl, histamine, $PGF_{2\alpha}$, U46619 and hypoxia. Possible mechanisms underlying the PV hypoxic response were also investigated using Ca^{2+} free conditions, by depleting SR Ca^{2+} with ryanodine and caffeine and by blocking BK_{Ca} channels with Penitrem A.

Maintenance in culture conditions for 24 hours enhanced contractile responses to KCl and U46619 in inferior PVs and histamine in both inferior and superior PVs and impaired endothelial-mediated relaxation. Hypoxia-mediated contraction was augmented in terms of peak magnitude in inferior and AUC in inferior and superior PVs. Hypoxic relaxation after peak response was inhibited in both inferior and superior PVs. There was no significant change in dynamics of the hypoxic response (time taken to 50% contraction or 75% relaxation).

Differences were also seen between inferior and superior PVs. In fresh vessels, maximal contraction to U46619 was larger in superior than inferior PVs and contractile responses to KCl were greater in inferior PVs. There was no significant difference in magnitude or dynamics of the hypoxic response between inferior and superior PVs. In vessels maintained in culture, KCl responses were greater in inferior PVs compared to superior PVs. Similar to fresh PVs, there was no difference in the hypoxic response between inferior and superior PVs.

Ca^{2+} release from a ryanodine-sensitive store contributes to hypoxia-mediated contraction in PVs however Ca^{2+} influx and BK_{Ca} channels appear to play less of a role. The relaxation phase of the hypoxic response is impaired in Ca^{2+} free conditions in inferior PVs and by depleting the SR in both inferior and superior PVs.

Whilst carrying out these experiments, a novel PV contractile response was uncovered on reoxygenation after hypoxic exposure. This response was inhibited when ryanodine and caffeine were present during hypoxia and reoxygenation but Ca^{2+} free conditions and blocking BK_{Ca} channels had no effect. Maintenance in culture for 24 hours reduced peak magnitude and AUC of the reoxygenation contraction in superior PVs; AUC and time taken to 50% peak were reduced in inferior PVs.

Maintenance in Culture Conditions: Influence on PV Functional Responses

Maintaining PVs in culture conditions for 24 hours enhanced contractile responses to a range of stimuli including KCl, histamine and U46619 in inferior PVs and histamine in superior PVs and endothelial-mediated relaxation was impaired.

KCl

Maintenance of blood vessels in culture is suggested to mimic chronic hypoxia (Manoury *et al*., 2009). Exposure of rats to 10% O_2 for 2-7 days had no effect on KCl responses (20-100mM) in PVs (Zhao *et al.,* 1995); this agrees with the findings from this study in superior but not inferior PVs. Hypersensitivity to 10mM KCl is evident in PAs after 3-4 days of culture (Guibert *et al.,* 2005, Manoury *et al.,* 2009) however the augmented first response to 80mM KCl in inferior PVs contrasts with PA studies showing no change in contraction to higher KCl concentrations (50mM) after 1 day culture (similar to superior PVs) and diminished responses by day 3 (Manoury *et al.*, 2009). KCl contractions are mediated by smooth muscle membrane depolarisation and Ca^{2+} influx (Zhao *et al.*, 1995) therefore the results of these experiments may suggest inferior PV smooth muscle is more sensitive to the depolarising effects of culture conditions than that of PAs or superior PVs. On the other hand, there may be an alteration of Ca^{2+} channel expression or activation.

Endothelial Function Testing

Maintenance in serum-free culture conditions impairs endothelium-dependent relaxation in both rat pulmonary and mesenteric arteries (Alm *et al.*, 2002, Manoury *et al.,* 2009, Morita *et al.,* 2013) and the same occurred in this study in porcine PVs. Endothelial function was still present but was significantly reduced in PVs kept in culture compared to freshly isolated PVs. Unfortunately, the submaximal constriction with $PGF_{2\alpha}$ (before addition of carbachol) was often not sustained after PVs had been maintained in culture. This must be borne in mind and results should be interpreted with caution. In PVs which showed this type of response, the relaxation slope changed on addition of carbachol indicating that endothelial function remained. However, the value for contraction for calculations was taken from a transient point in the response (i.e. not a plateau) and this could influence results.

Optimisation of the PV culture method could involve addition of adult serum to the culture medium which can normalise endothelium-dependent relaxation in rat mesenteric arteries (Morita *et al.,* 2013). This method would be difficult to apply to the current procedure as tissue is acquired from an abattoir and fresh blood is not available in order to obtain porcine serum through centrifugation as suggested by Morita *et al*. (2013).

Alternatively, the endothelium could be removed prior to culture as this has been demonstrated to provide partial protection against PA smooth muscle cell depolarisation thought to be caused by altered endothelial function (Manoury *et al.,* 2009). Endothelium could be removed by rubbing the intimal layer with a cotton wool swab, stainless steel wire or emery paper. Removing PV endothelium was attempted in later experiments with both metal wire and emery paper but was problematic as the result was either failure (confirmed by a positive endothelial function test) or complete loss of contractile function. Further optimisation of endothelial denudation in PVs is required before this can be used as a potential means of protection against the effects of maintenance in culture conditions. This could help reduce variation in responses between fresh PVs and those maintained in culture for future studies.

Agonist Cumulative Concentration-Dependent Responses

Histamine

There appears to be no published research investigating histamine responses before and after maintenance of blood vessels in culture. The main focus of pulmonary vascular research is PAs and histamine has a more specific constrictor effect on PVs (Hasebe *et al*., 1992). Maximum contractile responses to histamine in inferior and superior PVs are augmented after 24 hours maintenance in culture conditions and there may be several possible explanations for this. Contractile histamine receptors in smooth muscle (Shi *et al.*, 1998, Toda, 1990) may be upregulated after 1 day exposure to culture. Alternatively, histamine responses in fresh tissue may be a balance between endothelial relaxation and smooth muscle contraction; after maintenance in culture there is a balance shift due to impaired endothelial-derived relaxation therefore contraction is potentiated. The latter possibility ties in with the impairment in cholinergic-mediated endothelial relaxation also observed in PVs after maintenance in culture.

$PGF_{2\alpha}$

There appears to be no readily available research which has investigated the direct impact of maintenance in culture conditions on contractile responses to $PGF_{2\alpha}$. As already mentioned, organ culture has been suggested to mimic chronic hypoxia in PAs (Manoury *et al.,* 2009)and exposure of rats to chronic hypoxia (4-6 weeks at high altitude, 4270m) lead to increased lung pressor responses to $PGF_{2\alpha}$ compared to control (low altitude, 1520m) (McMurtry *et al.*, 1978). The current study suggests maintenance in culture for 24 hours has no impact on $PGF_{2\alpha}$ contractile responses. This may contest the link between culture and chronic hypoxia or may suggest that the duration of maintenance in culture may be important. It is difficult to draw any solid conclusions due to the lack of previous research.

U46619

Responses to U46619 were enhanced in inferior PVs but were not different in superior PVs after maintenance in culture conditions. There was no significant effect on contractile responses to U46619 in mesenteric arteries exposed to serum-free culture conditions for 20 hours (Alm *et al.,* 2002) in accordance with the results observed in superior PVs. Similarly, coronary arteries exposed to serum-free culture media at 37°C for 24 hours showed no difference in response to 10^{-6}M U46619 compared to control arteries stored in the same media at 4°C (Thorne *et al.*, 2001). Therefore the augmented response appears unique to inferior PVs.

Global hypoxia in rats (10% O_2 for 3 weeks) caused no change in U46619 responses over the same concentration range used in this study (Lal *et al.,* 1999) suggesting that mimicry between maintenance in culture and chronic hypoxia may exist in porcine superior PVs. In contrast, exposure to lobar hypoxia for 20 hours significantly augmented contraction to U46619 in sheep (Sheehan *et al.,* 1992), more in keeping with the findings from inferior PVs. Unfortunately this does not help explain the differences between U46619 responses in inferior and superior PVs or provide further insight into the link between organ culture and chronic hypoxia. When different methodologies are used (for example in chronic hypoxia studies), this only raises confusion when comparing results and makes drawing conclusions difficult.

Maximum contractile responses to U46619 were significantly greater in fresh superior PVs than inferior PVs. There is currently no known research comparing inferior/superior PVs specifically. Contractions to U46619 in ovine medium (1^{st} order) and large (main) PVs are known to be similar (73.9 ± 3.0% and 74.3 ± 6.6% response to 75mM KCl). In contrast, ovine PAs larger than 200µM

diameter showed no response to U46619; smaller PAs around 200µM diameter contracted but to a lower level than PVs (45.0 ± 11.8% response to 75mM KCl) (Kemp *et al.*, 1997). Other researchers have compared U46619 responses of systemic arteries from different locations. Angus *et al.* (1986) demonstrated significantly larger maximal contraction to U46619 in canine mesenteric and renal arteries than femoral, coronary and carotid arteries. EC_{50} values also varied between artery types with the lowest value in mesenteric arteries and highest in carotid arteries; in contrast, there was no difference in EC_{50} values between inferior and superior PVs.

Within vascular smooth muscle, U46619 is an agonist at TP receptors (G_q protein), which leads to activation of phospholipase C, increased IP_3 production, Ca^{2+} release and contraction. TP receptors are also present in vascular endothelial cells however signalling pathways and their role in vasomotion is less well established (Coleman *et al.*, 1994). They may play a regulatory role in dampening contraction which could be one explanation for the enhanced responses after maintenance in culture in inferior PVs and the difference between fresh superior and inferior PVs. Upregulation or different expression levels of TP receptors at the smooth muscle level may be an alternative explanation.

There are many possible reasons why PV contractile function changes after maintenance in culture conditions. As seen in this study, endothelial function is impaired and contractions enhanced after PV maintenance in culture. In normal conditions endothelium is in contact with blood including essential nutritional components (e.g. proteins, vitamins) for maintenance of vascular homeostasis. Serum-free culture media does not contain these components hence why endothelial/vascular function may be altered (Morita *et al.*, 2013). PV function may also change due to moving vessels from *in vivo* to serum-free conditions and the resulting loss of shear stress (Cao *et al.*, 2005) or distension (De Mey *et al.*, 1989). Comparison of undistended and distended rat renal arteries after 6 days maintenance in culture conditions revealed contraction to phenylephrine and angiotensin II was reduced to a greater extent in the undistended arteries (De Mey *et al.*, 1989).

Despite maintenance in culture conditions for 24 hours enhancing PV contractile responses to KCl, U46619 and histamine, overall contractile phenotype remained intact. Unfortunately, maintenance in culture conditions for 24 hours also appears to impair endothelial function hence use of the method for manipulation of environmental conditions would require appropriate controls. One example is, for high glucose, use of PV kept in isosmotic culture medium as a control instead of making direct comparison to freshly isolated vessels. If the protocol is applied in this way, the maintenance in culture technique remains feasible for further studies.

Hypoxia-induced Contraction in Porcine Inferior and Superior PVs

This study found no difference in hypoxia-induced constriction between inferior and superior PVs in terms of peak magnitude, AUC and response dynamics (time taken to 50% maximum contraction and 75% relaxation). There was a trend for hypoxic peak contraction to be larger in inferior PVs than superior as can be seen from sample traces but this did not reach statistical significance.

The occurrence of hypoxia-induced contraction in PVs is well established. The transient, monophasic nature of hypoxic contraction in fresh inferior and superior PVs (Figure 18-21) was similar to that seen by other researchers (Dospinescu *et al.,* 2012, Félétou *et al.,* 1995, Miller *et al.,* 1989, Sheehan *et al.,* 1992, Uzun and Demiryürek, 2003, Zhao *et al.,* 1993, Zhao *et al.,* 1996). In accordance with other studies, hypoxia-induced contraction in PVs did not require pharmacological preconstriction (Dospinescu *et al.,* 2012, Félétou *et al.,* 1995, Miller *et al.,* 1989, Sheehan *et al.,* 1992, Uzun and Demiryürek, 2003). Preconstriction can help replicate the basal pulmonary vascular tone seen to fall during exercise (Merkus *et al.,* 2008) however the level and type of preconstriction agent are likely to significantly affect properties of the hypoxic contraction (Connolly *et al.,* 2013).

The increase in AUC (non-significant trend) seen in fresh inferior compared to superior PV is likely due to both an increased peak magnitude and $T_{0.5}$ peak (trends also did not reach significance) suggesting a slightly longer duration of response. Sample traces clearly demonstrate the larger peak in fresh inferior PV.

The consistent relaxation below baseline post hypoxic-contraction in PVs has not been demonstrated or analysed in previous published research. Physiologically, transient contraction and subsequent relaxation below baseline tone may be relevant to minimise the upstream pressure generated by 3^{rd}-5^{th} order PV constriction (Taylor *et al.*, 2011) and prevent pulmonary oedema (Gao and Raj, 2005, Maggiorini *et al.,* 2001). In addition, a prolonged hypoxic contraction occurring closer to the left atrium could result in back-up of blood to a larger area of the lung and restriction of oxygenated blood outflow. There are no known publications directly comparing hypoxia-induced contraction in inferior and superior PVs and often the lobe from which PVs are sourced is not specified (Félétou *et al.,* 1995, Uzun and Demiryürek, 2003). Sheehan *et al.* (1992) compared hypoxic contraction of PVs from apical (cranial) and cardiac (middle) ovine lung lobes however this was in the context of chronic apical lobar hypoxia with PVs from the cardiac lobe acting as controls. The increased response in apical PVs was therefore most likely due to chronic hypoxia exposure rather than spatial variation. The similar hypoxic responses observed in this study comparing PVs from inferior and superior lobes

is not in keeping with previous work suggesting a stronger hypoxic contraction in cranial lobes (Hlastala *et al.,* 2004, Hopkins *et al.,* 2007, Starr *et al.,* 2005).

Constriction of PVs in Response to Reoxygenation: A Novel Finding

An unexpected and novel finding of this study was that inferior and superior PVs constrict in response to reoxygenation after a hypoxic insult. Previous research has identified a transient, reversible constriction in response to reoxygenation after hypoxia in PAs (Liu *et al.*, 2001). Unfortunately this information was only included as a discussion point and no analysis was conducted, however the authors did propose that it may be mediated by reactive oxygen species (ROS; Liu *et al.*, 2001). Reoxygenation constriction after 30 minutes hypoxic exposure (described by the authors as "hyperoxic constriction") was also identified in human PAs by Ariyaratnam *et al.* (2013). The authors suggested that this may contribute to acutely elevated PA pressure in patients with post infarction ventricular septal defects resulting from PA exposure to highly oxygenated blood. However, as alveolar gas content is the stimulus for hypoxic contraction (Dawson, 1984) and PVs are normally exposed to highly oxygenated blood (Widmaier *et al.,* 2006), this is an unlikely clinical context for PV constriction on reoxygenation. Physiologically, pulmonary venoconstriction as a result of reoxygenation post hypoxic insult may allow for capillary recruitment (as in hypoxia-induced contraction (Taylor *et al.,* 2011) and subsequent CO_2 offloading.

Long term hyperoxic exposure, in an experimental setting, is detrimental to PVs, resulting in morphology changes (including increased medial thickness), narrowing and occlusion (Hu and Jones, 1989). Clinically, hyperoxic exposure can contribute to pulmonary oedema in hyperbaric O_2 therapy (Weaver and Churchill, 2001) and after inhalation of hyperoxic gas mixtures by SCUBA divers during immersion (Coulange *et al.,* 2010). Furthermore, cardio-pulmonary bypass and hypoxia-reoxygenation lung injury can result in pulmonary oedema (Asimakopoulos *et al.,* 1999, reviewed in den Hengst *et al.,* 2010). Hypoxic pulmonary venoconstriction is thought to increase upstream capillary pressure which increases fluid and/or protein filtration resulting in oedema (Gao and Raj, 2005, Hillier *et al.,* 1997, Lal *et al*., 1999, Maggiorini *et al.,* 2001, Raj and Chen, 1986, Raj *et al.,* 1990). Pulmonary venoconstriction on reoxygenation could contribute to oedema in a similar way, providing a potential clinical context for this phenomenon.

Reoxygenation peak magnitude, AUC and time to 50% peak magnitude were not significantly different between superior and inferior PVs. The term "reoxygenation" was chosen as studies have

shown that high oxygen tension (for example 95% O_2) is required to adequately oxygenate cells deepest within isolated vessels (Pittman and Duling, 1973 cf Gao *et al.,* 2008). The use of 94-95%O_2 for oxygenation is commonplace in the study of isolated PVs (Dospinescu *et al.,* 2012, Félétou *et al.,* 1995, Gao *et al.,* 2008, Miller *et al.,* 1989, Sheehan *et al.,* 1992, Zhao *et al.,* 1993, Zhao *et al.,* 1996). However others have used room air or 20-21%O_2 for normoxic conditions suggesting 95% may be hyperoxic (Archer *et al.,* 1996, Archer *et al.,* 1998, Connolly *et al.,* 2013, Dipp and Evans, 2001, Dipp *et al.,* 2001, Ng *et al.,* 2005). The level of oxygen reaching the tissues by physical diffusion (Pittman and Duling, 1973 cf Gao *et al.,* 2008) may be affected by vessel wall thickness. Considering veins have thinner walls than arteries (Widmaier *et al.,* 2006) this is an important methodological consideration. Leach *et al.* (1994) found the magnitude of hypoxic contraction in PAs was reduced after equilibration with 21% compared to 95% O_2. This comparative approach could be adopted in future experiments to investigate whether contraction would also occur on restoration of 21% O_2.

Maintenance in Culture Conditions: Significant Influence on Hypoxia/Reoxygenation Responses

This findings of this study suggest that maintenance of PVs in culture conditions for 24 hours alters hypoxic and reoxygenation response magnitude and dynamics. Hypoxia-induced contraction was increased in terms of magnitude in inferior PVs and AUC in inferior and superior PVs and hypoxic relaxation post-peak was inhibited in both inferior and superior PVs exposed to culture conditions for 24 hours. There was no significant change in dynamics (time taken to 50% maximum relaxation and 75% relaxation) of the hypoxic response after maintenance in culture conditions.

As previously mentioned, earlier research investigating the impact of organ culture on rat PAs suggested it mimics chronic hypoxia (Manoury *et al.,* 2009). Taking this into consideration, the results of Sheehan *et al.* (1992) who found 20 hours lobar hypoxia in sheep increased acute HPV in isolated apical PVs are in disagreement with this study which found no change in hypoxia peak after maintenance in culture in superior PVs (anatomically correspond to apical). However, an increase in AUC was observed which may be interpreted as an increased overall contraction. Zhao *et al.* (1995) found no change in the absolute magnitude of acute hypoxic pulmonary venoconstriction in rats exposed to 10% O_2 for 14 days compared to normoxic controls (room air). However, Zhao *et al.* (1995) interpreted that PVs may actually have an increased acute hypoxic response because smooth muscle content relative to connective tissue may be decreased after 14 days exposure to hypoxia. This explanation was deduced from their results showing that general contractility for example, in response to KCl, was impaired after 14 days and KCl was used as the preconstricting agent yet the

hypoxic contraction itself was maintained. Another proposal was that PVs were already constricted in response to chronic hypoxia therefore further contraction to acute hypoxia was expected to be impaired but this was not the case. Caution must be used when interpreting results from chronic hypoxia studies as there are a number of differing factors. These factors include the nature of chronic hypoxia (local vs. global), duration, species differences and methods of data normalisation. Hence maintenance of PVs in 24 hours culture conditions may mimic the effects of chronic hypoxia in terms of acute hypoxic responses yet further investigation is required.

Maintenance of blood vessels in serum-free culture conditions impairs endothelium-dependent relaxation (EDR) (Manoury *et al.,* 2009, Morita *et al.,* 2013). Endothelial function also appears to be impaired in PVs kept in serum-free culture media in this study. However as $PGF_{2\alpha}$ did not always reach a stable plateau, results must be interpreted with caution. Perhaps using KCl for submaximal constriction instead of $PGF_{2\alpha}$ (Morita *et al.,* 2013) may have optimised this test as 80mM KCl produced a stable contraction in inferior and superior PVs after maintenance in culture conditions. Preconstriction agents for endothelial function testing therefore must be considered carefully.

There is a lack of consensus on endothelial contribution to hypoxic pulmonary venoconstriction. Some have found hypoxic response magnitude is endothelium-dependent (Félétou *et al.,* 1995, Sheehan *et al.,* 1992); others showed no endothelial contribution (Zhao *et al.,* 1993). This could be due to different HPV mechanisms between PV branches (main PV branch (Zhao *et al.,* 1993) vs. intralobar PVs (Félétou *et al.,* 1995, Sheehan *et al.,* 1992)) or species differences (rat (Zhao *et al*., 1993), pig (Félétou *et al*., 1995) and sheep (Sheehan *et al*., 1992)). Similar controversy exists over the endothelial-dependence of HPV in PAs. Hypoxic contractions in PAs preconstricted with $PGF_{2\alpha}$ show a biphasic response. Denuding the endothelium in rat and rabbit PAs (using 1μM for $PGF_{2\alpha}$ preconstriction) did not affect transient phase 1 of the response but full development of sustained phase 2 was impaired (Dipp *et al.*, 2001, Dipp and Evans, 2001). Removal of endothelium in rat PAs (preconstricted with 10μM $PGF_{2\alpha}$) had no impact on phase 1 in large PAs (~2mm) but inhibited phase 1 in small PAs (100-350μm); phase 2 was abolished in both (Leach *et al.*, 1994).

When no pharmacological preconstriction is used, PA hypoxic responses are monophasic. Research in rats suggests the PA hypoxic response in the absence of preconstriction is endothelium independent (Archer *et al.,* 2004) whereas in pig it is endothelium dependent (Liu *et al.*, 2001). Hence, absence/presence and level of preconstriction affects both response dynamics and endothelial dependence of responses and species differences likely play a role. Interestingly, PV studies showing an endothelial contribution to hypoxic responses did so in the absence of preconstriction (Félétou *et al.,* 1995, Sheehan *et al.,* 1992) whereas those showing no endothelial

dependence used preconstriction (20mM KCl, Zhao *et al.,* 1993). A possible candidate for endothelial mediation of hypoxic contraction is endothelin-1. Blocking endothelin-1 ET_A receptors (with BQ-123) and removal of the endothelium both abolished hypoxic PA constriction yet introduction of endothelin-1 as a priming agent in endothelium-denuded PAs restored hypoxic contraction (Liu *et al.*, 2001). This possible candidate could be investigated further by testing the impact the ET_A antagonist BQ-123 in PV hypoxic studies.

Since maintenance in culture conditions appears to alter PV endothelial function in this study, the results may suggest endothelial regulation of hypoxic contraction in inferior/superior PVs however this would require further investigation by performing experiments after endothelial denudation. Removal of endothelium was attempted in later experiments, however this was unsuccessful. The increased hypoxic contraction and reduced relaxation after maintenance in culture conditions could result from reduced production of an endothelial relaxing factor. This could be investigated using a nitric oxide (NO) synthase inhibitor (e.g. L-nitro-arginine (L-NAME)) and/or cyclooxygenase inhibitor (e.g. indomethacin) (Félétou *et al.,* 1995). If NO synthase or cyclooxygenase inhibition increase hypoxic contraction in fresh PVs to a similar extent as seen after maintenance in culture this could help suggest the possible mechanism. The effect of L-NAME on hypoxic contraction of inferior PVs was investigated in later experiments (see Chapter 4). A positive control to investigate impact of NO on hypoxic responses in PVs would involve the use of ionomycin to stimulate NO release from endothelial cells (Cosentino *et al.*, 1997). Manoury *et al.* (2009) speculate that maintenance in culture changes the activity of an endothelial mediator resulting in PA smooth muscle cell depolarisation; this may provide an alternative explanation for the findings of this study.

The variation in magnitude of hypoxic responses observed after PVs were maintained in culture conditions for 24 hours (see Figures 17 and 18) could be explained by sex differences as pigs of either sex were killed at the abattoir and used for experiments. Unfortunately, the sex of pig tissue used on a daily basis was unknown therefore specific conclusions cannot be drawn. Sex differences are known to exist within rat models of hypoxic pulmonary hypertension with male rats having increased disease severity compared with females (Rabinovitch *et al.,* 1981) and 17β-oestradiol and oestrogen receptors having protective effects (Lahm *et al.,* 2012).

Reoxygenation contraction was reduced in terms of AUC (inferior and superior PVs) and magnitude (superior PV only) after maintenance in culture conditions for 24 hours. Dynamics of the reoxygenation contraction were also affected in inferior PVs with time taken to 50% peak being significantly shortened after maintenance in culture. As maintenance in culture disrupts endothelial function, a possible explanation for this reduced reoxygenation response could be reduced

production of an endothelial contracting factor. Endothelin-1 may be a potential candidate; damaged endothelial cells may produce less endothelin-1 which in turn results in less contraction via ET_A receptors in smooth muscle (Liu *et al.*, 2001). This could be explored by introducing a low level of endothelin-1 in the bath solution to see whether the response can be restored (Liu *et al.*, 2001). Another suggestion is that the normoxic contraction is reduced simply because the hypoxic contraction was larger meaning the ability of the venous smooth muscle to contract further is impaired. Others have proposed that ROS are involved in normoxic contraction (Liu *et al.*, 2001). Use of antioxidants such as pyrrolidinedithiocarbamate and ebselen or the superoxide dismutase (SOD) inhibitor diethyldithiocarbamate (Waypa *et al.,* 2001) could help uncover whether ROS have a role to play in normoxic contraction. For example, if antioxidants/SOD inhibitors reduced normoxic contraction in fresh PVs to a similar extent as seen after maintenance in culture this could help suggest the possible mechanism. However extensive further characterisation of the normoxic contraction itself is required before the mechanism of inhibition via maintenance in culture can be uncovered.

Ryanodine-sensitive Ca^{2+} Source: Key to Hypoxic and Reoxygenation Responses

This study found that application of ryanodine abolished hypoxic and normoxic contractions along with hypoxic relaxation post peak in both inferior and superior porcine PVs. Exposure of inferior/superior PVs to Ca^{2+} free conditions had no significant effect on hypoxic or normoxic contraction but inhibited hypoxic relaxation in inferior PVs. Application of Penitrem A had no effect on any of the hypoxic/normoxic responses investigated.

Hence from these results, hypoxic contraction in porcine inferior and superior PVs appears to require an intact ryanodine-sensitive Ca^{2+} store. This is important as little is known about the underlying mechanisms of hypoxic contraction in PVs. Many researchers have shown SR release of Ca^{2+} (Connolly *et al.,* 2013, Dipp and Evans, 2001, Dipp *et al.,* 2001, Jabr *et al.,* 1997) is essential for hypoxic responses in PAs. The lack of an inhibitory effect in the absence of extracellular Ca^{2+} contrasts with previous work in PVs (Dospinescu *et al.,* 2012) and PAs (Archer and Michelakis, 2002, Connolly *et al.,* 2013, Leach *et al.,* 1994, McMurtry *et al.,* 1976, Moudgil *et al.,* 2005, Ng *et al.,* 2005). In fact, in inferior PVs, Ca^{2+} free conditions appeared to enhance the hypoxic response (although this trend was not statistically significant). A potential explanation for this may lie in the experimental protocol as control data were taken from the second hypoxic response and test data from the 3rd

response. If hypoxic responses increase with repeated exposure then this may be why the response appears to be enhanced slightly.

Speculatively, as Ca^{2+} free conditions significantly impaired hypoxic relaxation in inferior PVs and ryanodine reduced relaxation in both inferior and superior PVs, it could be suggested that BK_{Ca} channels play a role in hypoxic relaxation. However, the application of Penitrem A had no effect suggesting that BK_{Ca} were not involved.

Contraction of PVs on reoxygenation also appeared dependent on an intact ryanodine-sensitive Ca^{2+} store. However, it could be argued that the overall contractility of the tissue was impaired because the hypoxic response was inhibited therefore it was unlikely that normoxic contraction would occur. Unfortunately, the protocol did not involve a final viability test with 80mM KCl which could prove/disprove this theory. Further experiments would be required and good practice would involve a final KCl test for all PVs. Ca^{2+} free conditions failed to have an inhibitory effect and there was a non-significant trend for enhancement of reoxygenation contraction in superior PVs in the absence of Ca^{2+}; this may also be a result of time-dependency of the responses. The contractile response to hyperoxia/reoxygenation in PAs is dependent on voltage gated Ca^{2+} channels (Ariyaratnam *et al.,* 2013); further studies with voltage gated Ca^{2+} channel blockers (e.g. nifedipine) could be used to investigate their contribution to PV reoxygenation responses.

Solvent controls

Solvent controls showed ethanol and DMSO (at a level of 0.1% in the bath solution) had no impact on baseline tension apart from ethanol (25µL) which caused significant relaxation in fresh inferior PVs. Ethanol was only used a solvent for $PGF_{2\alpha}$ in this set of experiments and overall response was contraction, therefore the response to $PGF_{2\alpha}$ in these vessels is most likely due to the drug itself rather than the solvent. Therefore, these controls provide reassurance that the responses seen are caused by the drugs being used and not the solvent. Interestingly, baseline tension levels were lower in PVs maintained in culture compared to fresh PVs, but this trend only reached statistical significance in inferior PVs. This contrasts with previous findings in PAs where maintenance in culture appeared to result in a level of basal tone from Ca^{2+} influx. PAs kept under culture conditions relaxed in response to removal of extracellular Ca^{2+} whereas fresh PAs did not (Manoury *et al.*, 2009). However, it should be noted that PAs were maintained in culture for 4 days therefore the results are not directly comparable with this study.

Another point to note is that tension levels were measured at the same time point each day for fresh PVs (after 2nd hypoxic exposure) whereas tension was measured at various time points for PVs which had been maintained in culture. One day it was after the 2nd hypoxic response, another after the 2nd hypoxic response and cumulative concentration response curves to $PGF_{2\alpha}$ and the third after only one hypoxic exposure. This variability adds a time factor which could influence baseline tension and may be the reason for the difference rather than maintenance in culture *per se*. The N numbers are also small – results from only 3 different animals hence results should be interpreted with caution. All hypoxia/normoxia data were standardised to baseline before further analysis so baseline tension was already taken into account.

Key Findings

Maintenance of PVs in culture conditions augmented contractions to agonists and hypoxia and may be a result of impaired endothelial function. A ryanodine-sensitive Ca^{2+} source appears central to the hypoxic responses of PVs whereas influx of extracellular Ca^{2+} and BK_{Ca} channels play less of a role. Little was previously known as to the underlying mechanism of hypoxic responses in PVs and the impact of maintenance in culture conditions on PV function had not been investigated. The experimental protocol also revealed a novel PV normoxic contraction post-hypoxic exposure.

Understanding more about functional regulation of PVs and particularly the hypoxic response could help identify pathways contributing to hypoxia-related diseases such as high altitude pulmonary oedema (Bärtsch and Gibbs, 2007, Maggiorini *et al.,* 2001) and ultimately, potential therapeutic targets.

Further Work

Endothelial contribution to hypoxic responses of the PV will be further investigated and the impact of PV maintenance in culture will be explored at the smooth muscle level in terms of morphology and electrophysiology. Pathways underlying the hypoxic response in porcine PVs are not fully understood based on these initial studies and require further investigation, particularly the contribution of different K^+ channels since a hypoxia-sensitive K^+ current has already been identified in porcine PVs from superior/middle lobes (Dospinescu *et al.*, 2012).

The main focus of remaining studies will be on PVs from inferior lobes as little is known about mechanisms of hypoxic contraction in PVs from this location. As mentioned previously, there is a positive correlation between BMI and level of hypoxaemia in inferior PVs in obese patients which is not observed in superior PVs suggesting a clinical difference between PVs from these locations (Yamane *et al.*, 2008).

Chapter 4

Investigation of Underlying Pathways and Mechanisms of Hypoxia-Induced Responses in Porcine Inferior Pulmonary Veins

Introduction

Hypoxaemia in human inferior PVs is positively correlated with BMI in supine obese subjects (Yamane *et al.,* 2008) but this relationship is not evident in superior PVs. This suggests insufficient gas exchange in regions of the lung linked to inferior PVs and could be due to impairment of hypoxic pulmonary venoconstriction and ventilation-perfusion mismatch in inferior PVs specifically. Previous research has highlighted spatial variation in hypoxic responses within the lung during *in vivo* experiments in human and pig however the techniques used in these studies did not allow for identification of the specific blood vessels involved (Dehnert *et al.,* 2006, Hlastala *et al.,* 2004, Hopkins *et al*., 2007*,* Starr *et al.,* 2005). Results from Chapter 3 suggest that hypoxic contraction in isolated inferior and superior PVs was similar in terms of magnitude and response dynamics. However *in vivo* studies suggest a stronger HPV response exists in superior than inferior blood vessels (from cranial and caudal lobes, respectively) (Hlastala *et al.,* 2004, Hopkins *et al*., 2007*,* Starr *et al.,* 2005). To date, little is known as to the pathways and mechanisms of hypoxic responses within PVs and in particular, the potential for variation in responses between PVs from different locations.

Characterisation of underlying mechanisms of PV hypoxic contraction was previously performed in superior/middle PVs (Dospinescu *et al.,* 2012) although some investigators do not state the lung location from which they dissect PVs (Félétou *et al.,* 1995, Zhao *et al.,* 1993, Zhao *et al.,* 1996). It cannot be assumed that mechanisms underlying the hypoxic response are the same in PVs from different lung lobes since there appears to be spatial variation in HPV (Dehnert *et al.,* 2006, Hlastala *et al.,* 2004, Hopkins *et al*., 2007*,* Starr *et al.,* 2005) and differences between inferior and superior PVs in a clinical setting (Yamane *et al.,* 2008). This spatial variation identified in lung lobes and PVs highlights the need for characterisation of mechanisms and pathways underlying hypoxic responses within the inferior PV specifically.

The current consensus within the field of HPV is that small resistance PAs are the main vessels involved (Archer *et al.,* 1996, Archer *et al.*, 2004) and the majority of research into the underlying mechanisms has focused on PAs. Comparatively little is established about the mechanisms of hypoxic contraction in PVs yet PVs are known to constrict to hypoxia with a magnitude similar to or greater than PAs (Bressack and Bland, 1980, Félétou *et al.,* 1995, Miller *et al.,* 1989, Raj *et al.,* 1990, Sheehan *et al.,* 1992, Zhao *et al.,* 1993, Zhao *et al.,* 1996).

Despite extensive research, there is no overall consensus on the mechanism of HPV in PAs. One proposed mechanism involves inhibition of K_V channels (particularly $K_V1.5$ and $K_V2.1$) by hypoxia (Archer *et al.,* 1996, Archer *et al.,* 1998, Archer and Michelakis, 2002, Archer *et al.,* 2004, Moudgil *et al.,* 2005, Platoshyn *et al.,* 2006). TASK-1 may also be involved as it controls RMP and is inhibited by hypoxia in human PA smooth muscle (Olschewski *et al.,* 2006).

A K^+ current sensitive to hypoxia, 4-aminopyridine (4AP) and tetraethylammonium chloride (TEA) has been identified within superior/middle PVSMCs suggesting a role for K_V and possibly large BK_{Ca} channels in hypoxic contraction. RT-PCR studies identified the presence of BK_{Ca} at the mRNA level in PV tissue and the BK_{Ca} blocker Penitrem A reduced outward currents in single PVSMC however it had no effect on hypoxic contraction of isolated PVs (Dospinescu *et al.,* 2012). Experiments in Chapter 3 also showed that Penitrem A had no effect on hypoxic contraction of superior/inferior PVs. In rats, basal PV tone and RMP in PVSMCs are regulated by K_V channels (Michelakis *et al.,* 2001) and inhibiting K_V with 4AP resulted in an increase in baseline tension within superior/middle porcine PVs (Dospinescu *et al.,* 2012). K^+ channels appear to play a role in the regulation of basal tone and hypoxic responses of PVs hence investigation of the role of different K^+ channels, especially within the inferior PV, will be explored within this study.

Experiments exploring the impact of maintenance of PVs in culture conditions (Chapter 3) proposed the idea that endothelial damage or dysfunction may be involved in enhancement of the hypoxic response compared to fresh PVs. Within PVs, there is a lack of consensus on endothelial contribution to hypoxic contraction. Some have found the magnitude of contraction is endothelium-dependent (Félétou *et al*., 1995, Sheehan *et al*., 1992); others showed no endothelial contribution (Zhao *et al*., 1993). L-NAME is commonly used as a NOS inhibitor to investigate the role of endothelial NO production/endothelial dysfunction (Bardou *et al.,* 2001, Félétou *et al.,* 1995) therefore it was used in an attempt to simulate the effects of maintenance in culture.

The aim of this study was to investigate the involvement of K^+ channels and NOS in pathways and mechanisms regulating hypoxia-induced responses in inferior PVs.

Methods and Experimental Protocols

Myography was used to investigate the contractility of porcine 4^{th}-5^{th} order inferior intrapulmonary veins (as described previously). Tissue for experiments in this chapter was obtained from Quality Pork Producers Ltd (Brechin, Angus). Initially, two sets of heart and lungs were transported together but this procedure was found to compromise tissue viability hence only one set of heart and lungs were collected daily (see Results section). All 4^{th}-5^{th} order inferior PVs were used immediately after dissection within this study.

The contribution of different K^+ channels to the hypoxia-induced response of inferior pulmonary veins was investigated. Hypoxic responses were measured in the presence of the K_V channel inhibitor 4AP (Dospinescu *et al.*, 2012), BK_{Ca} inhibitor TEA (Archer *et al.,* 1996, Moudgil *et al.,* 2005), K_{ATP} channel blocker glyburide (Yuan, 1995), TASK-1/3 blocker zinc chloride ($ZnCl_2$) (Ali *et al.,* 2014, Patel *et al.,* 2013), K_V2.1 channel inhibitor BDM (Lopatin and Nichols, 1993) and K_V1.5 inhibitor DPO-1 (Lagrutta *et al.*, 2006).

As endothelial damage was proposed to enhance hypoxic contraction after maintenance in culture (see Chapter 3), L-NAME was used to study the impact of inhibiting nitric oxide synthase (NOS) (MacLean and Morecroft, 2001, Bardou *et al.*, 2001) on the hypoxic response.

Equilibration, Resting Tone and Functional Testing

Optimal resting tension (1.5g) and KCl viability tests were the same as described in Chapters 2&3. Due to inconsistent contractile responses with $PGF_{2\alpha}$ seen within this series of experiments, histamine (1µM) was used as the preconstriction agent for endothelial integrity testing followed by application of carbachol (10µM). As the NOS inhibitor L-NAME (MacLean and Morecroft, 2001, Bardou *et al.*, 2001) was being used to simulate endothelium dysfunction, endothelial integrity tests were conducted before and after application of L-NAME (100µM). Vessel rings which had a successful endothelial function test were selected and exposed to L-NAME (100µM) for 10 minutes after which another endothelial test was performed. Time controls were also conducted whereby a second endothelial test was performed but vessels were not exposed to L-NAME.

Hypoxia Response Studies

PVs were exposed to hypoxia as described in Chapter 2. Hypoxic exposures lasted 15 minutes with at least 30 minutes for recovery (in 95%O_2/5%CO_2) between exposures. Tension was readjusted to the optimal resting tension of 1.5g (as determined during preliminary experiments) before the first two exposures to hypoxia (in the absence of drugs). These two initial hypoxic exposures were conducted, followed by 15 minutes of normoxia and then 30 minutes incubation with a pharmacological agent. A third hypoxic exposure was then performed in the presence of the pharmacological agent, followed by 15 minutes normoxia and a single washout of drug with fresh bath solution. PVs were left in fresh solution under normoxia for 30 minutes then exposed to a final 15 minutes of hypoxia before normoxic washout. This final step was added to the pre-existing protocol to assess whether drug actions were reversible.

Investigation of Pathways Underlying the Hypoxic Response

K^+ Channel Inhibitors

K^+ channels are known to regulate tone in rat PVs with 4AP increasing basal tone, TEA causing minimal constriction and glyburide and the BK_{Ca} blocker iberiotoxin having no effect on resting tension (Michelakis *et al*., 2001). 4AP and TEA can also inhibit hypoxic contraction in superior/middle lobe PVs and a current identified in SMCs from these vessels was hypoxia, 4AP and TEA sensitive (Dospinescu *et al.,* 2012). Therefore, TEA and 4AP were chosen in order to confirm whether similar mechanisms of hypoxic contraction exist in inferior PVs. As K_V1.5 and K_V2.1 are proposed mediators of hypoxic contraction in PAs (Archer *et al.*, 1998, Archer and Michelakis, 2002, Archer *et al.,* 2004, Moudgil *et al.,* 2005, Platoshyn *et al.,* 2006), antagonists of these two channel subunits (DPO-1 and BDM, respectively; Lagrutta *et al.*, 2006, Lopatin and Nichols, 1993) were used to investigate whether they are also involved in hypoxic contraction of PVs (Archer *et al.,* 1998, Archer and Michelakis, 2002).

Concentrations of drugs were chosen based on values in the literature; TEA is documented as preferential for BK_{Ca} channels at 5mM (Archer *et al.,* 1996, Moudgil *et al.,* 2005). Although Penitrem A had no effect on hypoxic responses (see Chapter 3), it was decided to investigate this further because BK_{Ca} channels have a proposed role in attenuating HPV in PAs (Peinado *et al.,* 2008, Yan *et al.,* 2014). 4AP used at a concentration of 5mM is preferential for K_V channels (Archer *et al.,* 1996, Yuan, 1995). BDM inhibits K_V2.1 channels with an IC_{50} of 16.7mM (Lopatin and Nichols, 1993)

however preliminary experiments showed inhibition of the PV hypoxic response with concentrations as low as 10mM therefore concentrations of 1, 5 and 10mM were chosen. DPO-1 inhibits $K_V1.5$ current with an IC_{50} of 30 – 266nM (Lagrutta *et al.,* 2006, Karczewski *et al.*, 2009) and myography experiments in arteries from brain and skeletal muscle showed contractile responses to DPO-1 in the range of 10nm to 10µM (Fancher *et al.,* 2015) therefore a concentration of 10µM was chosen to achieve effective block of the channel.

Glyburide (also known as glibenclamide) blocks K_{ATP} channels and has been shown to potentiate hypoxic vasoconstriction in rat main pulmonary artery (Bardou *et al.*, 2001) and small intrapulmonary arteries (Lopez-Valverde *et al.*, 2005) at concentrations of 1 and 10µM, respectively. Exposure to 10µM glyburide in superior/middle lobe porcine PVs did not alter hypoxia-induced contraction and the hypoxia sensitive current in SMCs was insensitive to glyburide (Dospinescu *et al.*, 2012) however mechanisms of the hypoxic response are yet to be established in inferior PV. A concentration of 10µM was chosen, as per the literature. TASK-1 has also been suggested to be involved in hypoxic contraction (Olschewski *et al.,* 2006). $ZnCl_2$ was chosen to investigate TASK-1 involvement in hypoxic contraction of the porcine PV at a concentration of 1mM as this has been used for inhibition of TASK-1/3 in isolated chorionic plate arteries (Ali *et al.,* 2014).

L-NAME

L-NAME was chosen to investigate the impact of NOS inhibition (MacLean and Morecroft, 2001, Bardou *et al.*, 2001) on the hypoxic response of inferior PVs. The hypoxic response of PVs was potentiated after maintenance in culture conditions and this was suspected to occur due to endothelial dysfunction. It was thought that interfering with NO production may mimic the effects of culture and support the proposed mechanism of enhanced hypoxic contraction. Inhibition of NO synthesis significantly inhibits hypoxic contraction in pig PVs (5-7mm) (Félétou *et al.,* 1995).

Data Analysis

Hypoxia/reoxygenation response magnitude data are expressed normalised to baseline tension (A.U). For the sake of clarity hypoxic relaxation is expressed with a value of 1 subtracted to more clearly illustrate where relaxation below baseline occurs. Raw traces had tension normalised to baseline tension before AUC was calculated. In experiments where drugs were applied peak

magnitude and AUC data were further standardised to the mean time control data to take account for changes in responses over time. This helped identify changes which occurred due to the drug exposure specifically. Where appropriate data are presented as mean ± S.E.M and N represents the number of vessels from different animals. Statistical significance was determined at $P<0.05$ using Students unpaired *t*-test, repeated measures one-way ANOVA or one-way ANOVA with Tukey's post-test (GraphPad Prism 5, CA, USA).

Please note that for experiments which were considered preliminary or for control purposes, only peak magnitude and relaxation were calculated. These traces were not analysed in terms of response dynamics (AUC, time to 50% peak and time to 75% relaxation) as this in-depth analysis was prioritised for other experiments which were more integral to the main objectives.

Parameters of response dynamics (AUC, time to 50% peak and time to 75% relaxation) were measured in order to fully characterise the hypoxic contractile response within PVs where current research is lacking. Furthermore, pharmacological agents may not change the absolute magnitude of the response but could alter the response dynamics/time course and this could have a physiological impact by advancing or delaying the onset of hypoxic venoconstriction. The measurements also acted as surrogate markers for example time to 75% relaxation ($T_{0.75}$ relax) could act as a surrogate marker for absolute relaxation where the PV did not fully relax within the 15 minute exposure to hypoxia.

Results

KCl Viability Testing

KCl viability testing was conducted as described previously (Chapters 2&3). On exposure to 80mM KCl 95.3% of inferior PV rings contracted. There was no significant difference in the magnitude of 80mM KCl responses comparing 1st, 2nd and 3rd exposures to 80mM KCl (4.3 ± 0.5g, 5.1 ± 0.5g and 5.2 ± 0.6, respectively, P>0.05, N=30).

Endothelial Function Testing and Impact of L-NAME

During this set of experiments $PGF_{2\alpha}$ produced inconsistent results therefore histamine was chosen as an alternative preconstrictor for endothelial tests. Histamine (1μM) produced a mean (± S.E.M) change in tension of 3.6 ± 0.5g (N=28) in 92.6% of inferior PVs. When carbachol (10μM) was applied after histamine exposure, 87.8% of inferior PVs relaxed with a mean relaxation of 50.9 ± 3.7% (N=29).

To test whether L-NAME impaired endothelial relaxation via carbachol, endothelial function tests were performed in the presence of the drug. Endothelial relaxation was significantly inhibited in the presence of 100μM L-NAME (before: 48.8 ± 6.4%, after: -13.7 ± 8.4% (negative relaxation indicating contraction with carbachol), P<0.001, N=5). Time controls were also conducted whereby no L-NAME was applied but a second endothelial test was performed. Endothelial relaxation in the time control PV ring was not significantly different than the initial endothelial test (before: 59.8 ± 8.6%, after: 50.2 ± 9.1%, P>0.05, N=4) but significantly greater than the relaxation seen in the presence of L-NAME (P<0.01).

It was also observed that introducing L-NAME significantly enhanced contraction to 1μM histamine (before: 1.7 ± 0.5g, after: 4.0 ± 2.0g, P<0.01, N=5) however in the time control, histamine contraction was significantly reduced (before: 4.8 ± 1.6g, after: 2.7 ± 1.3g, P<0.01, N=4). There was no significant difference when comparing the contraction to histamine in the presence of L-NAME compared to time control directly (P>0.05).

Hypoxic Responses in Fresh Inferior PV from New Tissue Source

Initially, two heart and lungs were transported from the abattoir daily for testing. The success rate for hypoxic contractions was reduced to only 23% on 1st exposure and 37.5% on 2nd exposure (N=12). Because of the poor response rate, from this point onwards, only one heart and lungs was collected per day. Success rates for hypoxia-induced contraction then increased to 82% (1st exposure) and 91% (2nd exposure) which was a lot closer to the success seen in previous experiments (88 and 99%, respectively).

As per previous results (Chapter 3), 2nd exposures to hypoxia were more consistent and robust hence they were used for further analysis and as controls (2nd exposures will be referred to as 1st exposures for time control data or "Before" responses where PVs were exposed to drugs).

Comparison of Responses to Repeated Hypoxic Exposure in Inferior PV

Time control data showed that contractile responses of inferior PVs to hypoxia increased in magnitude on repeated exposure. Time controls were not exposed to any drug other than initial KCl viability tests and drugs used in endothelial function tests. Third hypoxic responses were significantly larger than responses on 1st exposure; 2nd hypoxic responses were not significantly different from either first or third response. Both hypoxic peak magnitude and AUC values were larger in 3rd than 1st exposures. Peak magnitudes were 7.2 ± 1.0 A.U and 3.4 ± 0.6 A.U, respectively (P<0.01). AUC values were 2203.3 ± 232.7 and 1394.9 ± 175.6, respectively (P<0.05). For 2nd exposures, peak magnitude was 5.9 ± 0.9 A.U and AUC was 1941.7 ± 163.1. Hypoxic relaxation post contraction did not change significantly over time; 1st, 2nd and 3rd exposures resulted in relaxations of 0.01 ± 0.04 A.U, 0.3 ± 0.1 A.U and 0.06 ± 0.09 A.U, respectively (P>0.05). See Figure 28 for representative traces and mean data.

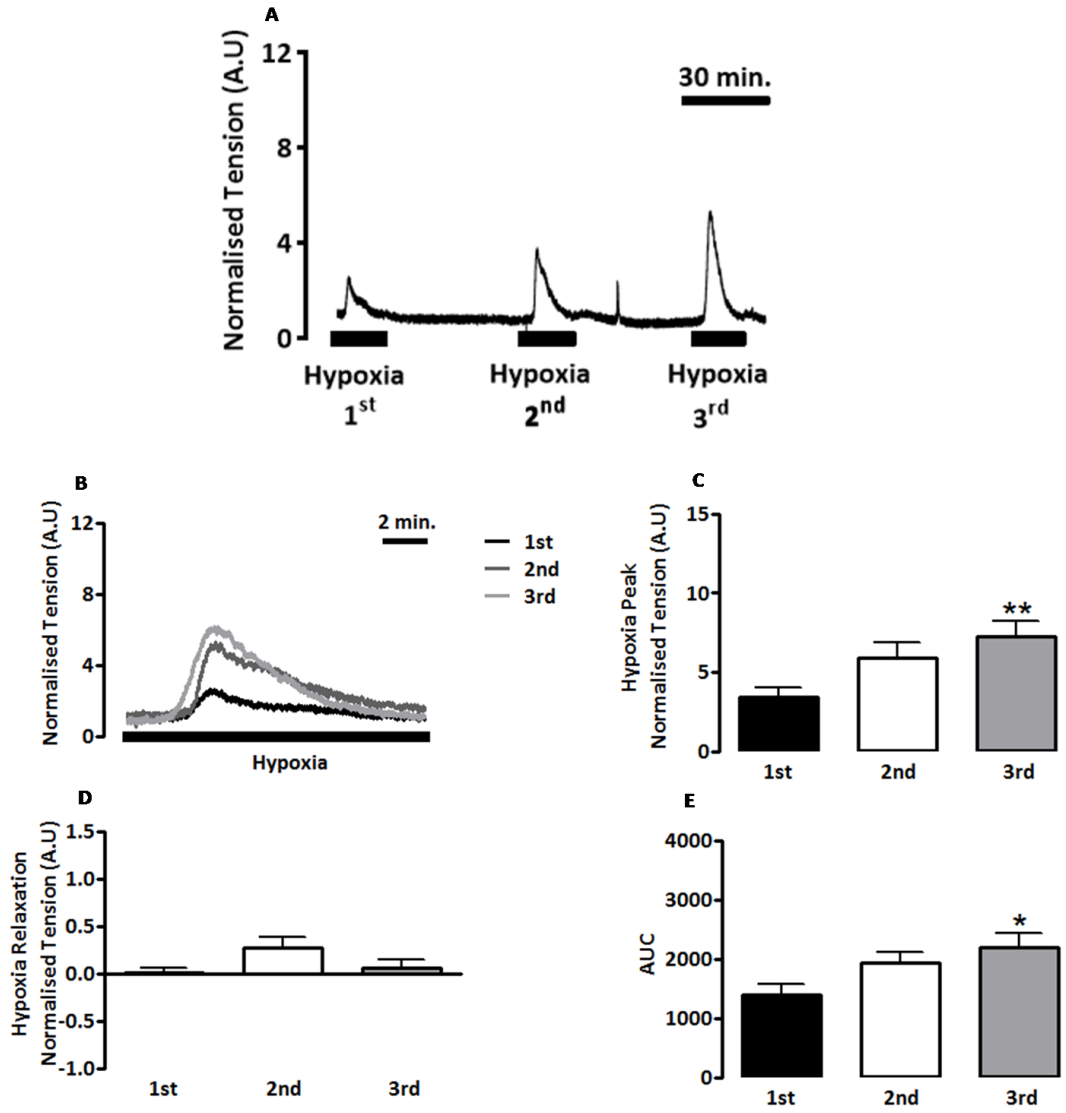

Figure 28. Hypoxic responses in inferior pulmonary veins with repeated exposure. A: representative trace of time course showing increasing contractile response to hypoxia with repeated exposure in inferior pulmonary veins (PVs) in time control vessels, tension values are expressed normalised to initial baseline tension. B: 1st, 2nd and 3rd hypoxic responses in a representative time control plotted on same scale, tension values are expressed normalised to baseline tension. C: magnitude of hypoxic peak and D: magnitude of hypoxic relaxation post-contraction for 1st, 2nd and 3rd exposures in time control vessels; expressed as tension normalised to baseline tension. For the sake of clarity hypoxic relaxation data are expressed with a value of 1 subtracted to more clearly illustrate when relaxation below baseline occurs. E: area under the curve (AUC) for the 1st, 2nd and 3rd hypoxic responses in time controls (traces for AUC were plotted standardised to baseline over a time period of 759 seconds). All data represent mean ± S.E.M, N=18; *P<0.05, ** P<0.01 compared with 1st exposure (analysed using one-way ANOVA with Tukey's post-test).

Impact of K^+ Channel Inhibitors on Inferior PV Basal Tone and Hypoxic Responses

4AP

Initial experiments to investigate the impact of 4AP on inferior PV basal tone and hypoxia-induced responses used Kreb's solution for control (before drug application) and washout (after drug exposure) responses whereas 4AP was dissolved in HEPES buffer. Washout of Kreb's solution with 4AP in HEPES bath led to a transient increase in tension from a baseline of 0.7 ± 0.2g to a peak of 2.4 ± 0.4g (N=8, $P<0.01$); after 30 minutes of exposure, tension had returned to the baseline level of 0.7 ± 0.2g ($P>0.05$ compared to baseline).

For investigation of the impact of 4AP on hypoxic responses of inferior PVs, peak and relaxation data was firstly analysed as tension normalised to baseline tension. The hypoxic peak during exposure to 4AP (in HEPES) was not significantly different from the control hypoxic peak (in Kreb's) before exposure to 4AP (during: 3.2 ± 0.5 A.U, before: 4.3 ± 1.0 A.U; $P>0.05$, N=7). However the hypoxic peak magnitude after washout of 4AP with Kreb's solution (7.3 ± 1.8A.U) was significantly larger than both before ($P<0.05$) and during ($P<0.01$) peaks. Hypoxic relaxation post peak before, during and after exposure to 4AP (Kreb's control and washout) was -0.05 ± 0.1 A.U, -0.2 ± 0.1 A.U and 0.1 ± 0.1 A.U, respectively. Relaxation after washout with Kreb's was significantly greater than relaxation during exposure to 4AP ($P<0.05$, N=7). See Figure 29 for sample traces and mean data.

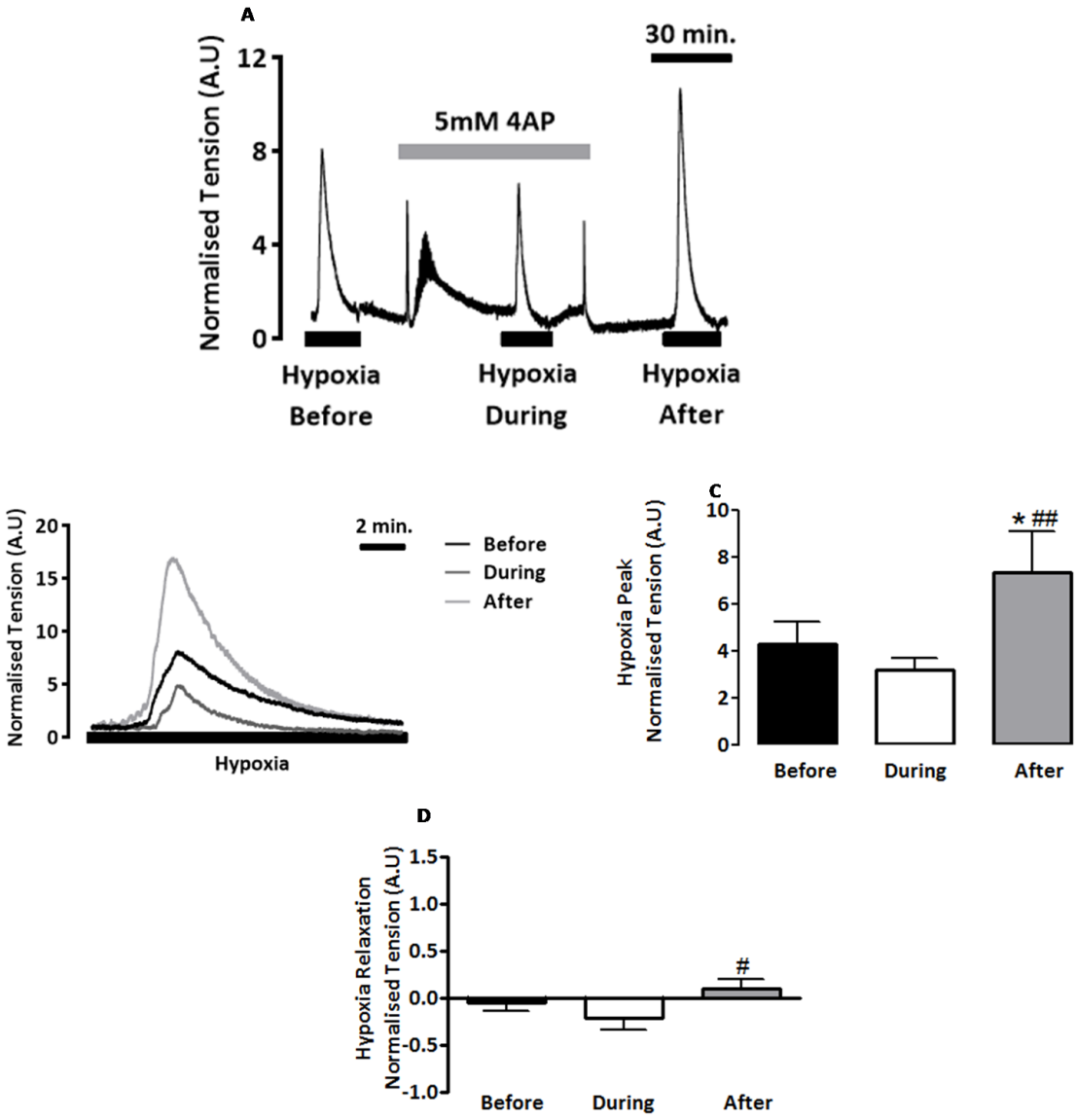

Figure 29. Hypoxic responses in inferior pulmonary veins before, during and after washout of 5mM 4AP (in HEPES buffer), before and after responses in Kreb's solution. A: representative trace of time course showing contractile responses to hypoxia before, during and after 4AP exposure in inferior pulmonary veins (PVs), tension values are expressed normalised to initial baseline tension. B: Representative traces plotted on same scale showing responses to hypoxia in inferior PVs before, during and after 4AP exposure, tension values are expressed normalised to baseline tension. C: magnitude of hypoxic peak and D: magnitude of hypoxic relaxation post-contraction for before (Kreb's), during (4AP in HEPES) and after (Kreb's) exposure to 4AP; expressed as tension normalised to baseline tension. For the sake of clarity hypoxic relaxation data are expressed with a value of 1 subtracted to more clearly illustrate when relaxation below baseline occurs. All data represent mean ± S.E.M, N=7; *P<0.05 compared to "Before", # P<0.05 and ## P<0.01 compared with "During" (analysed using repeated measures one-way ANOVA with Tukey's post-test).

Within these experiments and time control experiments, the peak of hypoxic contraction increases over time. The final (after) response is significantly different from the first (before) response and second (during) response however there is a clear trend for hypoxic peak magnitude to increase over time anyway (see time control data in Figure 28). Considering time control data further, the same trend is evident for AUC data but there is no obvious trend for relaxation data over time. Therefore, to take account of known changes in response over time and to assess the effect of the drug specifically, from this point in the chapter onwards all peak magnitude and AUC data (but not relaxation data) have been further standardised to the corresponding mean time control data. The axis title will remain as "Hypoxia Peak Normalised tension (A.U)" or "Normalised AUC" but will indicate that data has been normalised firstly to baseline tension and then normalised again to mean time control data, as appropriate for 1^{st}, 2^{nd} and 3^{rd} (before, during and after) responses. This will also mean that mean data for peak magnitude will be on a different scale from sample trace data; sample trace data will only be standardised to baseline to allow for ease of comparison of before, during and after traces.

When peak magnitude data was standardised to time control mean data for the above 4AP data, peak before (in Kreb's) was 1.3 ± 0.3 A.U, during (4AP in HEPES) was 0.5 ± 0.1 A.U and after (washout in Kreb's) was 1.0 ± 0.2 A.U . Using the data from this analysis, the peak of hypoxic contraction during exposure to 4AP was significantly reduced compared to the initial control (before) peak ($P<0.01$). Normalising data in this way shows more clearly the effect of the drug exposure by taking account of changing magnitude over time – a comparison of data analysed in this way to data normalised to baseline tension only (same as graph in Figure 29 C) is shown in Figure 30.

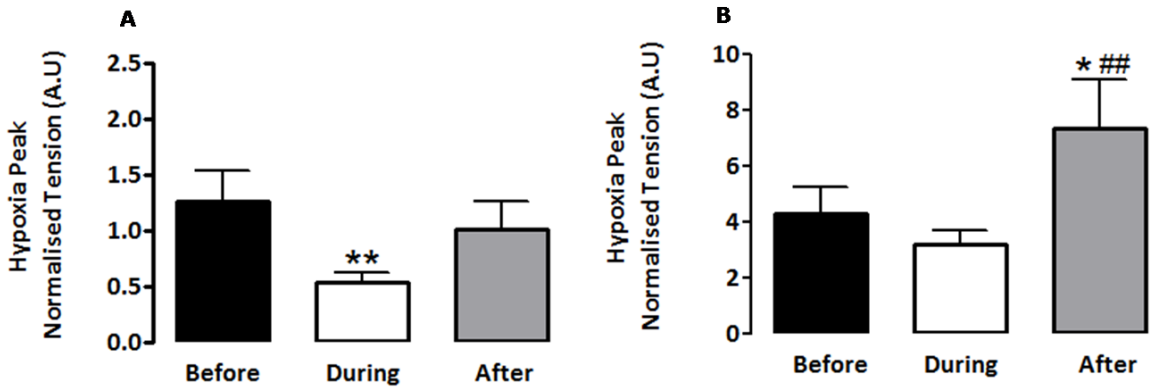

Figure 30. Hypoxic peak magnitude in inferior pulmonary veins before, during and after washout of 5mM 4AP (in HEPES buffer), before and after responses in Kreb's solution: comparison of data analysis methods. A: magnitude of hypoxic peak expressed as tension normalised to baseline tension and then standardised to mean time control data. B: magnitude of hypoxic peak expressed as tension normalised to baseline tension only (same as Figure 29 C). All data represent mean ± S.E.M, N=7; *P<0.05 and **P<0.01 compared to "Before" magnitude of hypoxic peak, ## P<0.01 compared with "During" (analysed using repeated measures one-way ANOVA with Tukey's post-test).

The results above could reflect differences between Kreb's and HEPES buffered solutions and therefore be independent of any 4AP induced effects. Hence specific experiments were undertaken to determine what this effect could be. One group of control experiments (N=6) investigated whether HEPES buffer alone had an impact on baseline tension and/or hypoxic contraction in inferior PVs (with control and washout responses in Kreb's). Another group of experiments (N=6) involved running the control and washout responses in HEPES bath solution as well as during 4AP exposure to investigate the effect of 4AP alone.

Washout of Kreb's solution with HEPES bath, in the control experiment, led to a transient contraction of inferior PVs which was significantly higher than baseline tension (from a baseline of 0.6 ± 0.1g to a peak of 1.8 ± 0.5g (N=7, P<0.05)). After 30 minutes of exposure, tension was not significantly different from baseline (0.7 ± 0.2g, P>0.05).

There was a trend for peak of hypoxic contraction to be smaller when inferior PVs were exposed to HEPEs bath (0.6 ± 0.1 A.U) compared to before (1.4 ± 0.3 A.U) and after washout (1.5 ±0.4 A.U) when vessels were in Kreb's bath solution. However this trend did not reach statistical significance. Relaxation post-hypoxic contraction was significantly inhibited after washout of HEPES with Kreb's

compared to relaxation in the presence of HEPES solution (after: 0.9 ± 0.3 A.U, during: -0.1 ± 0.2 A.U, N=6, *P*<0.05). Relaxation before application of HEPES (in Kreb's) was 0.1 ± 0.1 A.U and was not significantly different from responses during HEPES or after washout in Kreb's. See Figure 31 for sample traces and mean data.

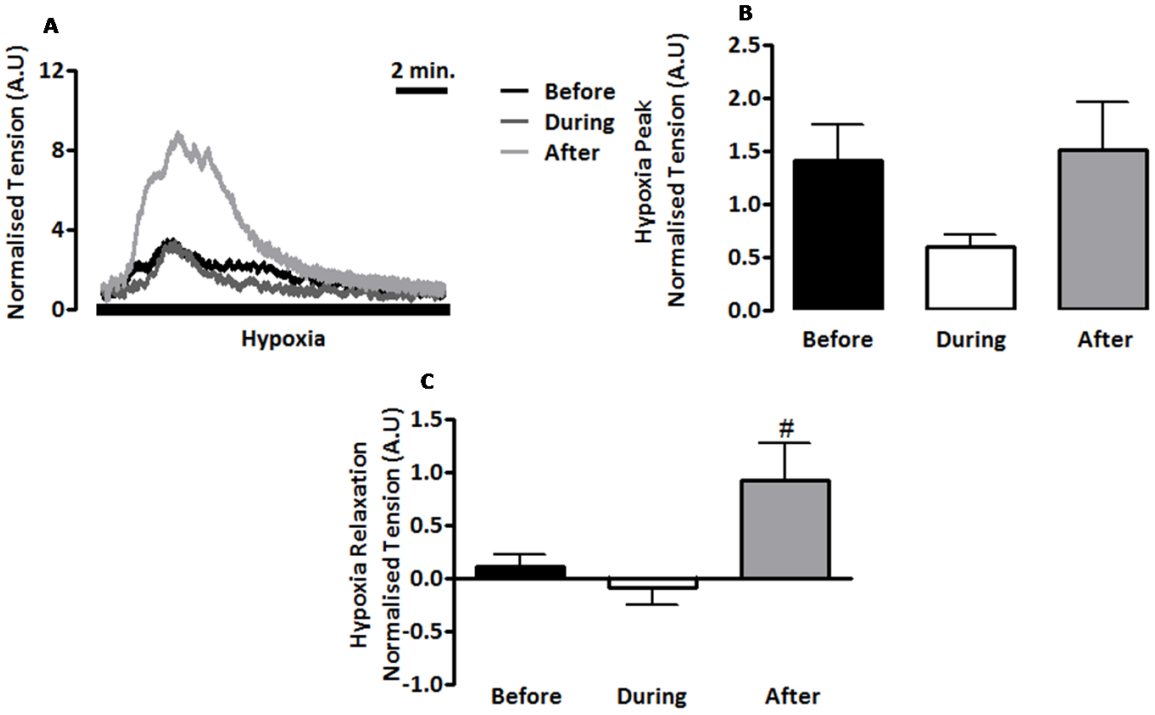

Figure 31. Hypoxic responses in inferior pulmonary veins before, during and after washout of HEPES buffer, before and after responses in Kreb's solution: control experiment. A: Representative traces showing responses to hypoxia in inferior pulmonary veins before (Kreb's), during (HEPES) and after (Kreb's), tension values are expressed normalised to baseline tension. B: magnitude of hypoxic peak (normalised to baseline tension and mean time control for 1st, 2nd and 3rd responses, as appropriate) and C: magnitude of hypoxic relaxation post-contraction (normalised to baseline tension) for before (Kreb's), during (HEPES) and after (Kreb's). For the sake of clarity hypoxic relaxation data are expressed with a value of 1 subtracted to more clearly illustrate when relaxation below baseline occurs. All data represent mean ± S.E.M, N=6; # *P*<0.05 compared with "During" (analysed using repeated measures one-way ANOVA with Tukey's post-test).

In the second experiment investigating 4AP alone (HEPES bath solution present throughout), washout of HEPES bath with HEPES bath containing 4AP also led to a transient contraction in inferior PVs which was significantly larger than baseline tension – 2.3 ± 0.5g (peak) compared to 1.3 ± 0.4g (baseline level, *P*<0.01). After 30 minutes, tension had reduced to 1.5 ± 0.4g (*P*>0.05 compared to baseline, N=7).

The peak hypoxic contraction was not significantly different before (0.7 ± 0.1 A.U), during (0.6 ± 0.2) or after washout (0.5 ± 0.1 A.U) of 4AP (*P*>0.05, N=6). There was also no significant trend for hypoxic relaxation with 4AP exposure (before: -0.01 ± 0.1 A.U, during: 0.1 ± 0.05 A.U, after: 0.3 ±0.1 A.U; *P*>0.05, N=6). In terms of response dynamics, time to 50% hypoxic peak magnitude ($T_{0.5}$ peak) was not significantly different before (258.7 ± 30.5s), during (250.5 ± 20.7s) or after washout (246.0 ± 30.0s) of 4AP (*P*>0.05, N=6). The same applied for time to 75% hypoxic relaxation (before: 487.0 ± 45.2s, during: 470.2 ± 44.3s, after: 447.0 ± 59.7s; *P*>0.05, N=6). AUC (normalised to time control AUC data) after washout of 4AP with HEPES (0.5 ± 0.05 A.U) was significantly smaller than the initial response before exposure to 4AP (0.8 ± 0.1 A.U, *P*<0.01, N=6). However, AUC during 4AP exposure (0.7 ± 0.1 A.U) was not significantly different from responses before or after 4AP exposure (*P*>0.05). See Figure 32 for sample trace and mean data for hypoxic responses with 4AP (control and washout responses in HEPES).

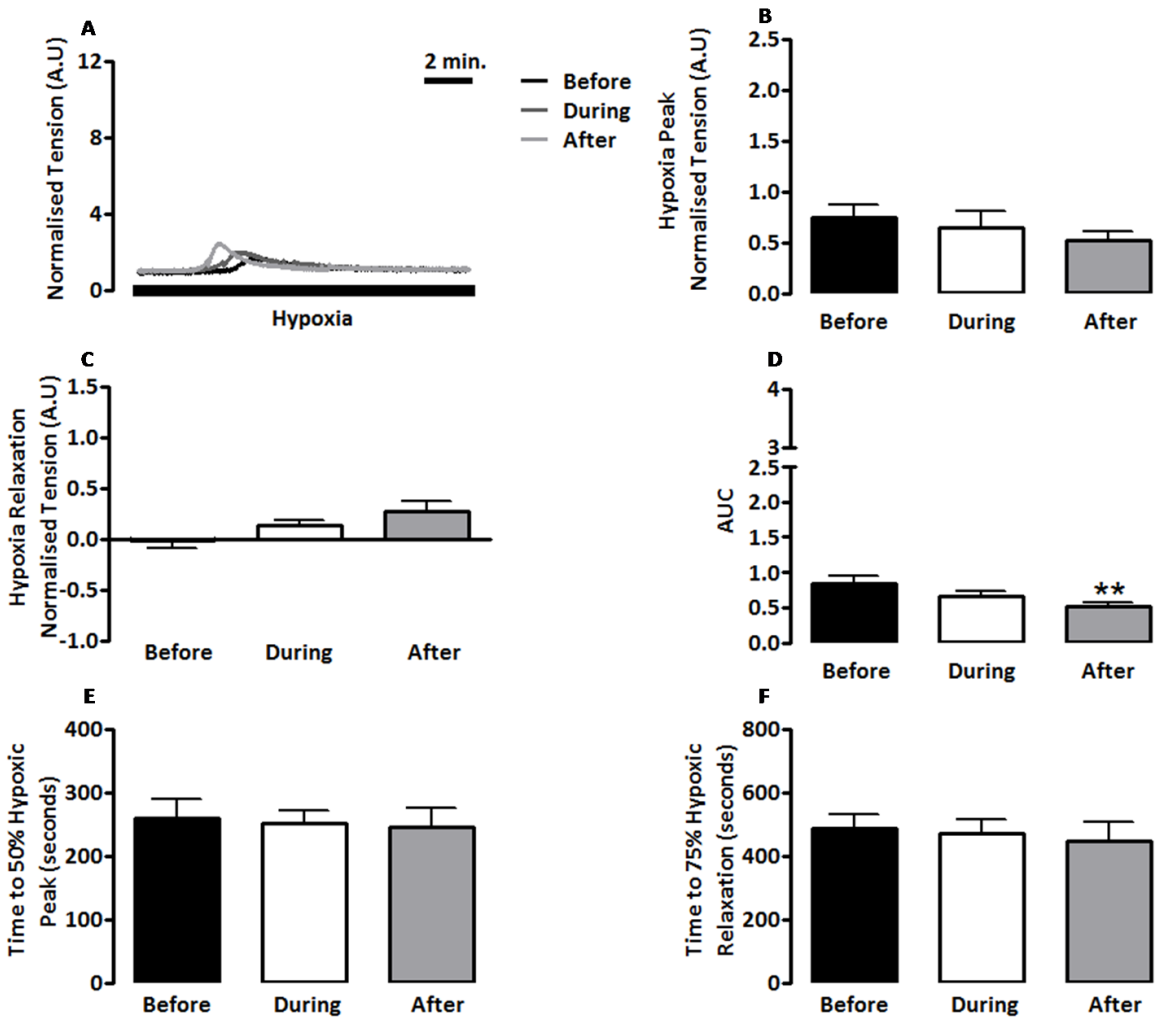

Figure 32. Hypoxic responses in inferior pulmonary veins before, during and after washout of 5mM 4AP, before and after responses in HEPES solution. A: Representative traces showing responses to hypoxia in inferior pulmonary veins before (HEPES), during (5mM 4AP in HEPES) and after (HEPES), tension values are expressed normalised to baseline tension. B: magnitude of hypoxic peak (normalised to baseline tension and mean time control for 1st, 2nd and 3rd responses, as appropriate) and C: magnitude of hypoxic relaxation post-contraction (normalised to baseline tension) before, during and after 4AP exposure. For the sake of clarity hypoxic relaxation data are expressed with a value of 1 subtracted to more clearly illustrate when relaxation below baseline occurs. D: area under the curve (AUC) for the hypoxic response normalised to mean time control data (traces for AUC were plotted standardised to baseline over a time period of 759 seconds); E: time to 50% peak magnitude and F: time to 75% maximal relaxation post-contraction peak before, during and after 4AP exposure. All data represent mean ± S.E.M, N=6; ** $P<0.01$ compared with "Before" (analysed using repeated measures one-way ANOVA with Tukey's post-test).

TEA

Exposure to 5mM TEA increased baseline tension in the PV from 0.7 ± 0.1g to a peak of 2.8 ± 0.5g (*P*<0.01 compared to baseline, N=7). This increase in tension was sustained and remained significantly higher than baseline tension at a level of 1.7 ± 0.3g after 30 minutes of exposure to 5mM TEA (*P*<0.01 compared to baseline).

TEA inhibited hypoxic contraction of PVs by 50% (peak before TEA: 2.0 ± 0.4 A.U; peak during TEA: 1.0 ± 0.1 A.U, *P*<0.05, N=5) although there was no significant recovery after washout (1.3 ± 0.2 A.U, *P*>0.05). Hypoxic relaxation post-peak was inhibited on washout (0.4 ± 0.2 A.U) compared to during TEA exposure (-0.1 ± 0.1 A.U, *P*<0.05, N=5). Hypoxic relaxation in control (before) responses did not differ from during/after responses (0.1 ± 0.05 A.U, *P*>0.05). AUC showed the same trend as hypoxic peak, with inhibition on exposure to 5mM TEA (AUC before: 1.6 ± 0.3 A.U; peak during: 1.0 ± 0.1 A.U, *P*<0.05, N=5) whereas AUC after washout did not recover (1.2 ± 0.1 A.U, *P*>0.05). Time to half maximal contraction was not significantly different comparing all three responses (before: 211.2 ± 20.9s, during: 174.9 ± 13.8s, after: 156.1 ± 15.5s; *P*>0.05). There was also no significant trend for time to 75% relaxation (before: 473.8 ± 40.3s, during: 430.4 ± 11.8s, after: 466.9 ± 45.8s; *P*>0.05). See Figure 33 for sample trace and mean data for 5mM TEA.

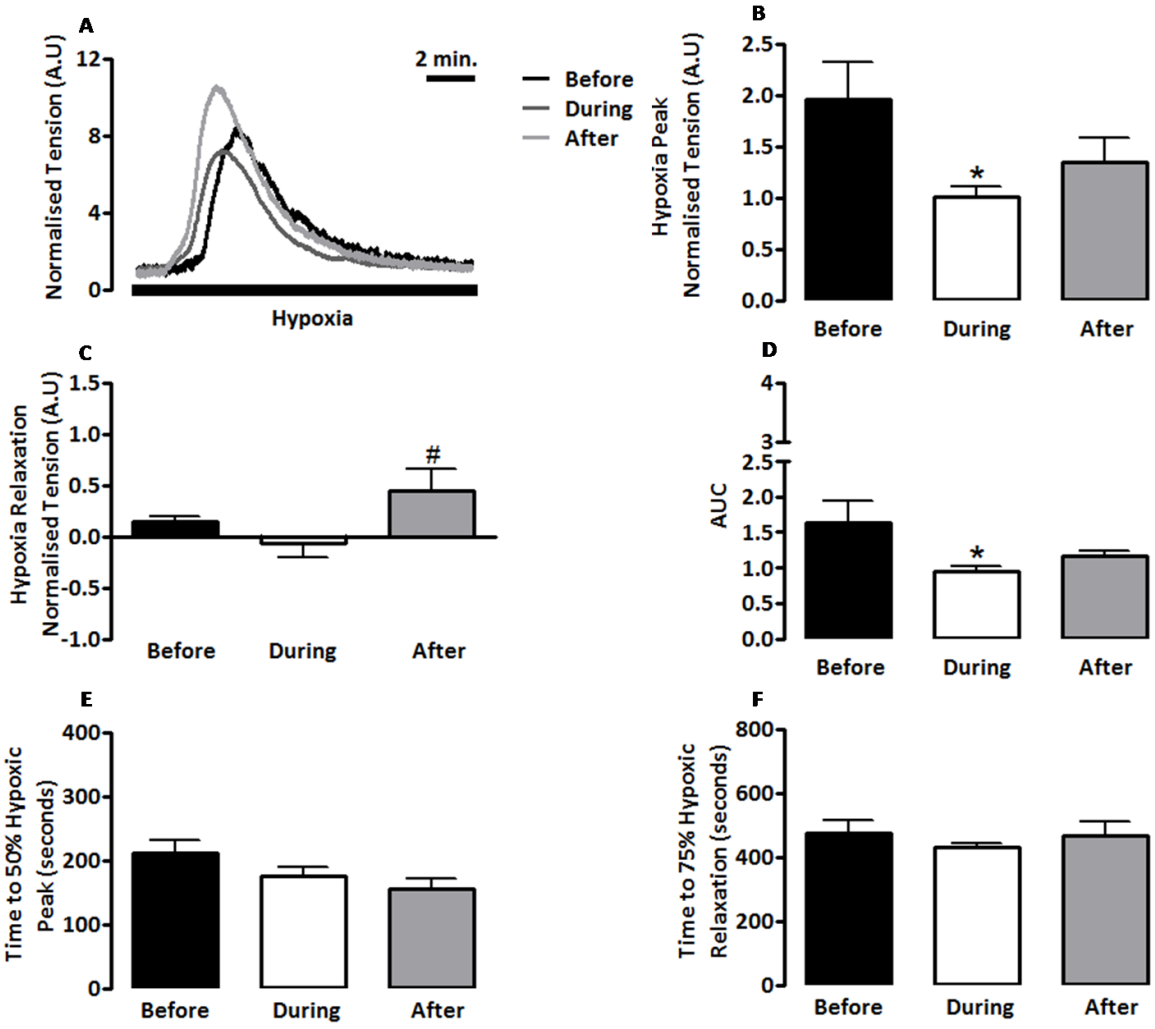

Figure 33. Hypoxic responses in inferior pulmonary veins before, during and after washout of 5mM TEA. A: Representative traces showing responses to hypoxia in inferior pulmonary veins before, during and after application of 5mM TEA, tension values are expressed normalised to baseline tension. B: magnitude of hypoxic peak (normalised to baseline tension and mean time control for 1st, 2nd and 3rd responses, as appropriate) and C: magnitude of hypoxic relaxation post-contraction (normalised to baseline tension) before, during and after 5mM TEA exposure. For the sake of clarity hypoxic relaxation data are expressed with a value of 1 subtracted to more clearly illustrate when relaxation below baseline occurs. D: area under the curve (AUC) for the hypoxic response normalised to mean time control data (traces for AUC were plotted standardised to baseline over a time period of 759 seconds); E: time to 50% peak magnitude and F: time to 75% maximal relaxation post-contraction peak before, during and after TEA exposure. All data represent mean ± S.E.M, N=5; * $P<0.05$ compared with "Before", #$P<0.05$ compared with "During" (analysed using repeated measures one-way ANOVA with Tukey's post-test).

DPO-1

In order to examine any putative role for $K_V1.5$ in baseline tone and hypoxia-induced contractility in the PV, the $K_V1.5$ inhibitor (Lagrutta *et al.,* 2006, Karczewski *et al.*, 2009) was used. Before application of DPO-1 (10μM) application, initial baseline tension was 0.5 ± 0.2g which increased slightly to 0.6 ± 0.1g after exposure (*P*>0.05 compared to baseline, N=7). Ethanol was used as the solvent for DPO-1 at a level of 0.1% and in previous experiments (see Chapter 3), this level of ethanol was found to cause significant relaxation in fresh inferior PVs (from a baseline of 1.4 ± 0.3g down to 1.1 ± 0.2g, N=3) but no relaxation was seen by adding DPO-1 in ethanol. This suggests that DPO-1 inhibits the vehicle effect. A direct comparison of the effects of ethanol and DPO-1 + ethanol on baseline tension is shown in Figure 34.

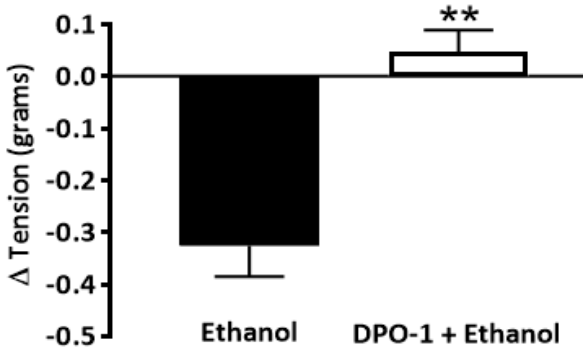

Figure 34. Effect of ethanol alone and DPO-1 (10μM) dissolved in ethanol on baseline tension in inferior pulmonary veins. Absolute change in tension of inferior pulmonary veins on application of either ethanol alone (N=3) or DPO-1 + ethanol (N=7). Please note that 25μL ethanol was added in each case (0.1% final concentration in the bath). ***P*<0.01 compared to ethanol alone (analysed using Students unpaired *t*-test).

Application of 10 μM DPO-1 had no significant effect on the hypoxic response in inferior PVs. There was a trend for an enhanced peak of contraction (before: 1.1 ± 0.3 A.U, during: 1.4 ± 0.2 A.U and after: 1.2 ± 0.2 A.U) and AUC with DPO-1 exposure (before: 1.0 ± 0.2 A.U, during: 1.6 ± 0.3 A.U and after: 1.3 ± 0.2 A.U), however this trend did not reach statistical significance (*P*>0.05, N=5). There was also no significant difference in hypoxic relaxation (before: -0.1 ± 0.1 A.U, during: 0.3 ± 0.2 A.U and after: 0.1 ± 0.1 A.U), time to 50% hypoxic peak (before: 213.4 ± 18.4s, during: 184.1 ± 6.4s and after 174.8 ± 9.8s) or time to 75% relaxation (before: 498.3 ± 25.0s, during: 514.3 ± 24.8s and after

521.3 ± 29.9s) with DPO-1 exposure (*P*>0.05, N=5). Representative traces and mean data are shown in Figure 35.

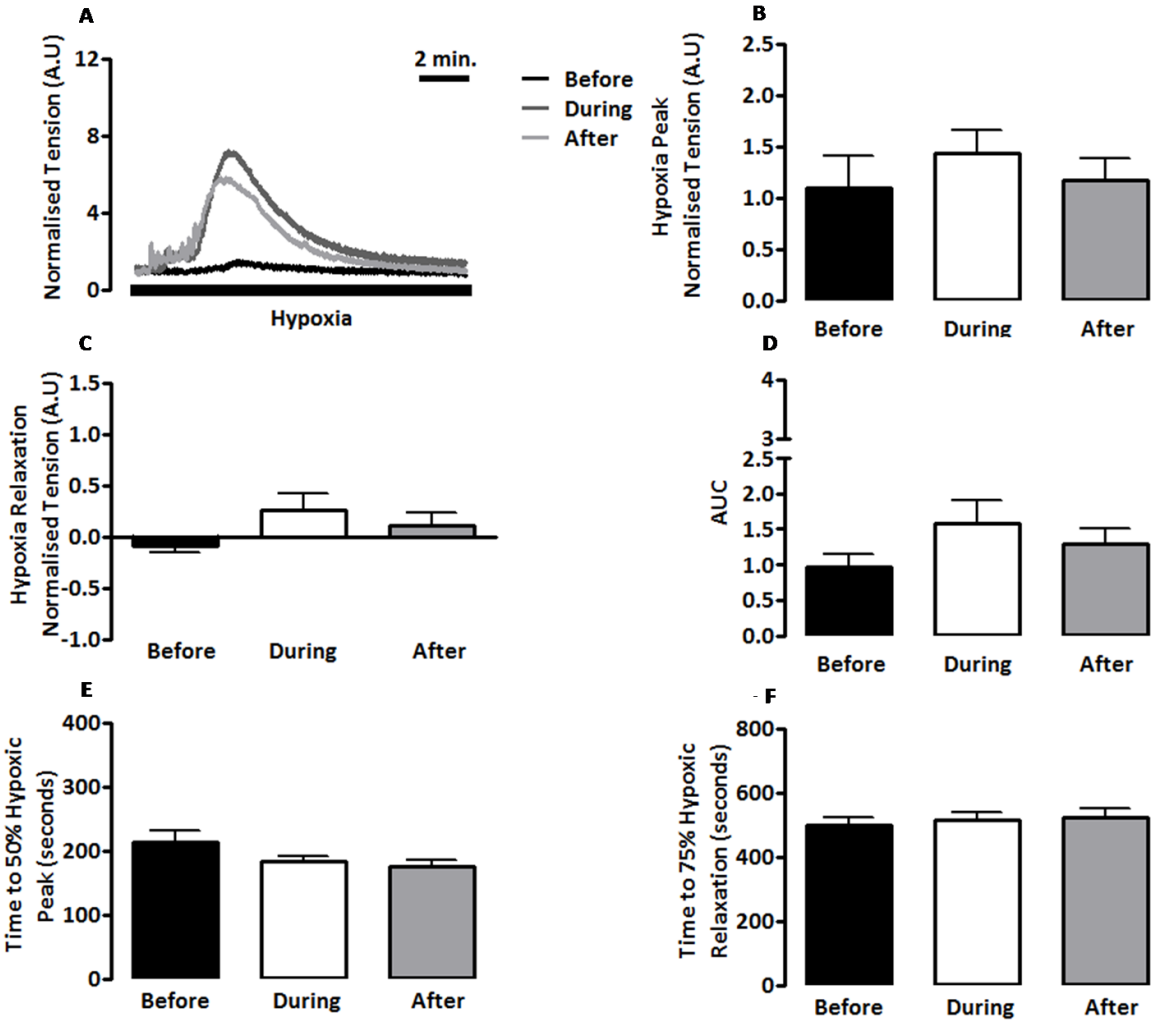

Figure 35. Hypoxic responses in inferior pulmonary veins before, during and after washout of 10µM DPO-1. A: Representative traces showing responses to hypoxia in inferior pulmonary veins before, during and after application of 10µM DPO-1, tension values are expressed normalised to baseline tension. B: magnitude of hypoxic peak (normalised to baseline tension and mean time control for 1st, 2nd and 3rd responses, as appropriate) and C: magnitude of hypoxic relaxation post-contraction (normalised to baseline tension) before, during and after 10µM DPO-1 exposure. For the sake of clarity hypoxic relaxation data are expressed with a value of 1 subtracted to more clearly illustrate when relaxation below baseline occurs. D: area under the curve (AUC) for the hypoxic response normalised to mean time control data (traces for AUC were plotted standardised to baseline over a time period of 759 seconds); E: time to 50% peak magnitude and F: time to 75% maximal relaxation post-contraction peak before, during and after DPO-1 exposure. All data

represent mean ± S.E.M, N=5 (analysed using repeated measures one-way ANOVA with Tukey's post-test).

BDM

In order to examine any putative role for $K_V2.1$ in baseline tone and hypoxia-induced contractility in the PV, the $K_V2.1$ inhibitor BDM (Lopatin and Nichols, 1993) was used. Please note that investigation of the effects of 1, 5 and 10mM BDM on baseline tension and PV hypoxic responses were performed in different pieces of tissue rather than adding cumulatively for a response curve in a single piece of tissue. The effect of BDM on baseline tension of inferior PVs was concentration-dependent. At a concentration of 1mM, BDM had no impact on baseline tension. Initial mean tension was 0.6 ± 0.1g before application of 1mM BDM and after was 0.7 ± 0.3g (P>0.05, N=5). At a higher concentration of 5mM, BDM resulted in a small transient contraction of PVs which was not significantly greater than baseline tension (baseline: 1.0 ± 0.4g, peak: 1.1 ± 0.4g, P>0.05, N=5) followed by relaxation to a level below baseline (0.7 ± 0.5g, P<0.05). Application of 10mM BDM resulted in transient contraction in 4 out of 6 PVs tested. The peak (0.9 ± 0.3g) was significantly greater than baseline in these 4 vessels (0.8 ± 0.2g, P<0.05, N=4). All inferior PVs were significantly relaxed compared to baseline after 30 minutes exposure to 10mM BDM (PVs relaxed from a baseline of 0.7 ± 0.2g to a level of 0.3 ± 0.1g, P<0.05, N=6). The magnitude of relaxation seen with 10mM BDM was not significantly different from that seen with 5mM (10mM: -0.4 ± 0.1g; 5mM: -0.2 ± 0.1g, P>0.05).

Application of 1mM BDM had no significant impact on hypoxic responses in inferior porcine PVs. The peak of hypoxic contraction was no different before (1.0 ± 0.4 A.U), during (1.0 ± 0.3 A.U) or after exposure to 1mM BDM (1.4 ± 0.6 A.U, P>0.05, N=5). Relaxation post-hypoxic contraction also did not change before (-0.1 ± 0.1 A.U), during (0.4 ± 0.2 A.U) or after exposure to 1mM BDM (0.4 ± 0.4 A.U, P>0.05). BDM at a concentration of 1mM had no impact on AUC (before: 0.8 ± 0.2 A.U, during: 0.9 ± 0.2 A.U and after: 2.0 ± 1.3 A.U), time to 50% peak of hypoxic contraction (before: 185.1 ± 15.4s, during: 167.1 ± 17.7s and after: 174.1 ± 17.7s) and time to 75% relaxation (before: 449.5 ± 38.0s, during: 463.6 ± 57.2s and after: 497.6 ± 39.2s) (P>0.05). See Figure 36 for sample traces and mean data for 1mM BDM.

Increasing the concentration of BDM to 5mM abolished the peak of hypoxic contraction compared to control (before) response (before: 0.7 ± 0.2 A.U and during: 0.2 ± 0.004; P<0.05, N=4). There was also significant recovery of the hypoxic contraction after washout of 5mM BDM (0.8 ± 0.1; P<0.01 compared to during and P>0.05 compared to before response). AUC was also significantly reduced

on exposure to 5mM BDM (before: 0.7 ± 0.1 A.U and during: 0.4 ± 0.03; $P<0.05$) and recovered on washout (0.8 ± 0.1 A.U; $P<0.05$ compared to during and $P>0.05$ compared to before response). There was no effect on hypoxic relaxation (before: -0.1 ± 0.05 A.U, during: -0.1 ±0.1 A.U and after: 0.04 ± 0.1 A.U; $P>0.05$) and time to 50% peak and 75% relaxation were not calculated as there was no hypoxic contraction to measure from for the "During" response. Representative traces and mean data for 5mM BDM are shown in Figure 37.

The highest concentration of BDM used (10mM) also abolished the hypoxic contraction in inferior PVs (peak before: 1.4 ± 0.2 A.U, peak during: 0.2 ± 0.001 A.U; $P<0.01$, N=5). However, the peak hypoxic contraction seen after washout of 10mM BDM was not significantly different from before/during responses (0.8 ± 0.1 A.U, $P>0.05$). A similar trend was observed with AUC data; AUC during 10mM BDM exposure (0.4 ± 0.02 A.U) was significantly smaller than before exposure (1.2 ± 0.2 A.U; $P<0.05$). AUC after washout was 1.0 ± 0.1 A.U which was not significantly different from hypoxic responses before or during exposure ($P>0.05$). Similar to 5mM BDM, there was no effect on hypoxic relaxation (before: -0.1 ± 0.1 A.U, during: 0.01 ±0.01 A.U and after: 0.2 ± 0.2 A.U; $P>0.05$) and time to 50% peak and 75% relaxation were not calculated as again there was no hypoxic contraction to measure from for the "During" response. Representative traces and mean data for 10mM BDM are shown in Figure 38.

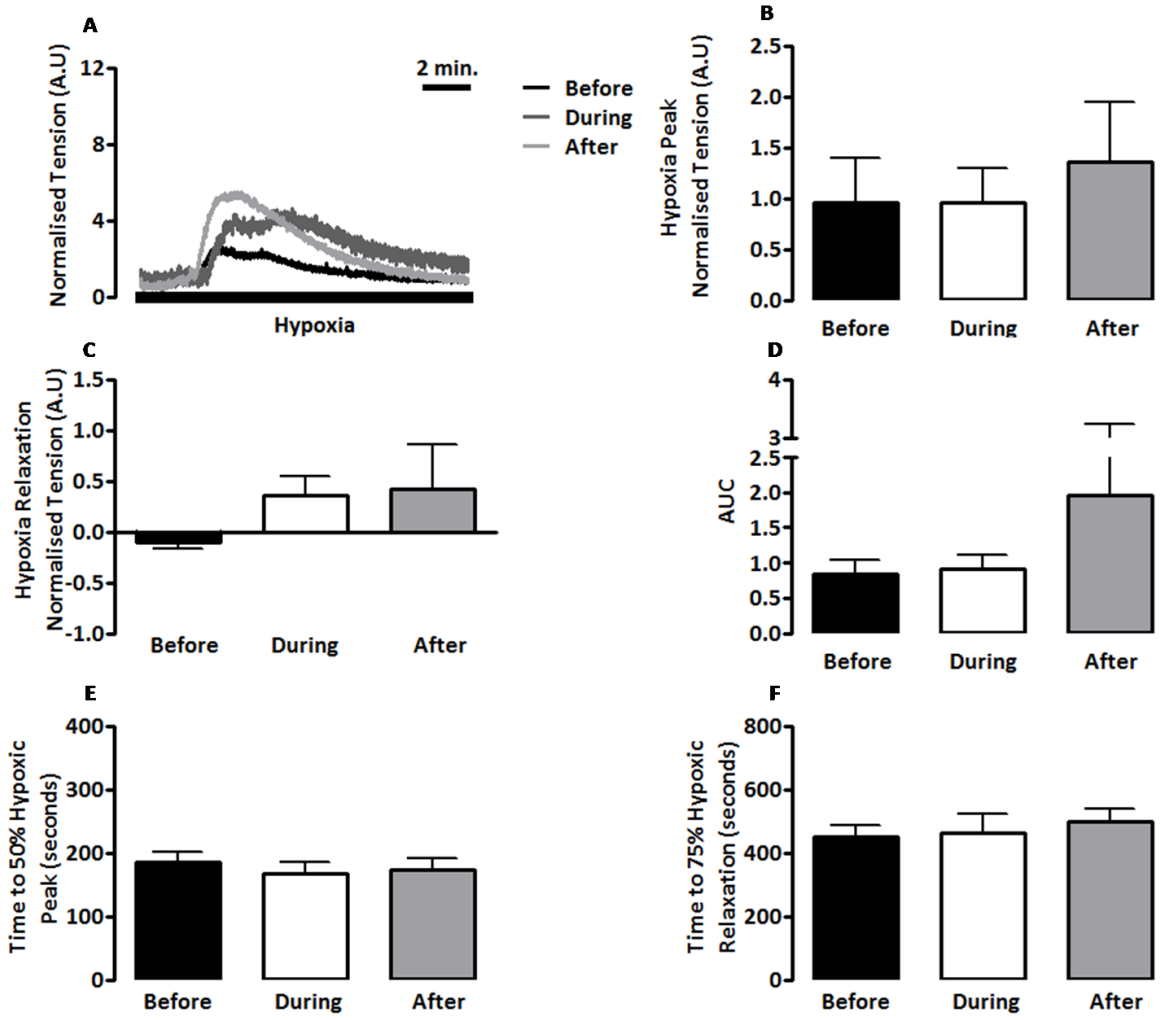

Figure 36. Hypoxic responses in inferior pulmonary veins before, during and after washout of 1mM BDM. A: Representative traces showing responses to hypoxia in inferior pulmonary veins before, during and after application of 1mM BDM, tension values are expressed normalised to baseline tension. B: magnitude of hypoxic peak (normalised to baseline tension and mean time control for 1st, 2nd and 3rd responses, as appropriate) and C: magnitude of hypoxic relaxation post-contraction (normalised to baseline tension) before, during and after 1mM BDM exposure. For the sake of clarity hypoxic relaxation data are expressed with a value of 1 subtracted to more clearly illustrate when relaxation below baseline occurs. D: area under the curve (AUC) for the hypoxic response normalised to mean time control data (traces for AUC were plotted standardised to baseline over a time period of 759 seconds); E: time to 50% peak magnitude and F: time to 75% maximal relaxation post-contraction peak before, during and after 1mM BDM exposure. All data represent mean ± S.E.M, N=5 (analysed using repeated measures one-way ANOVA with Tukey's post-test).

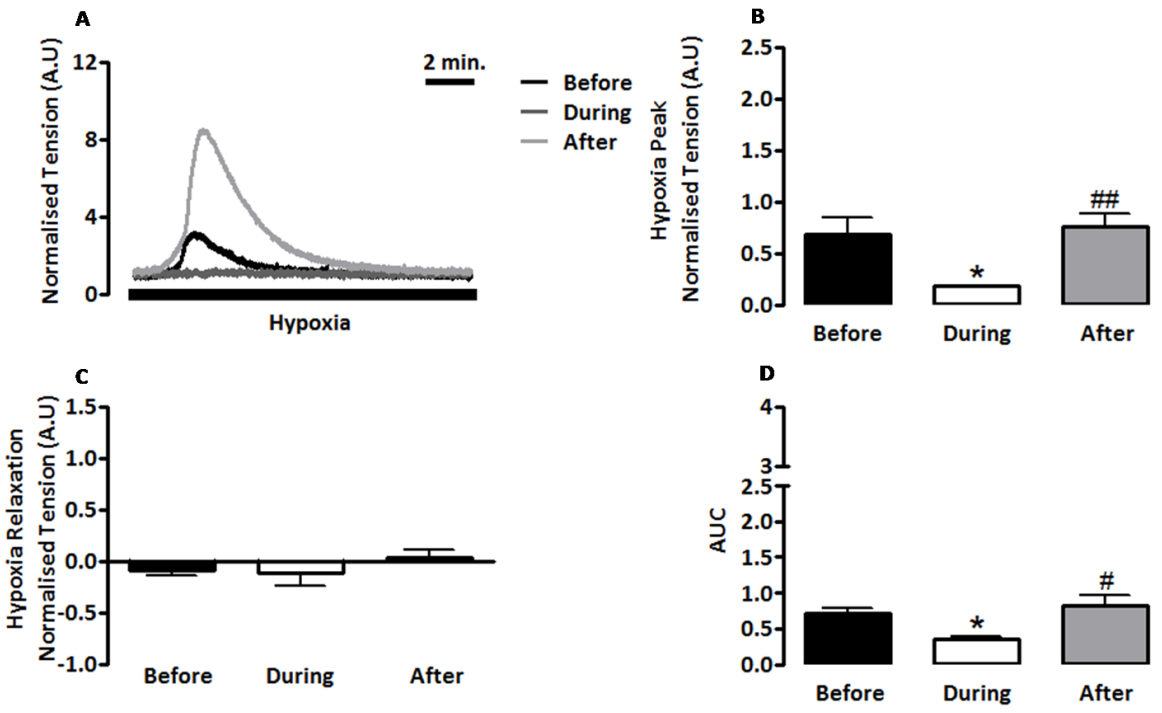

Figure 37. Hypoxic responses in inferior pulmonary veins before, during and after washout of 5mM BDM. A: Representative traces showing responses to hypoxia in inferior pulmonary veins before, during and after application of 5mM BDM, tension values are expressed normalised to baseline tension. B: magnitude of hypoxic peak (normalised to baseline tension and mean time control for 1st, 2nd and 3rd responses, as appropriate) and C: magnitude of hypoxic relaxation post-contraction (normalised to baseline tension) before, during and after 5mM BDM exposure. For the sake of clarity hypoxic relaxation data are expressed with a value of 1 subtracted to more clearly illustrate when relaxation below baseline occurs. D: area under the curve (AUC) for the hypoxic response normalised to mean time control data (traces for AUC were plotted standardised to baseline over a time period of 759 seconds before, during and after 5mM BDM exposure. All data represent mean ± S.E.M, N=4. *P<0.05 compared to "Before", #P<0.05 and ##P<0.01 compared to "During" (analysed using repeated measures one-way ANOVA with Tukey's post-test).

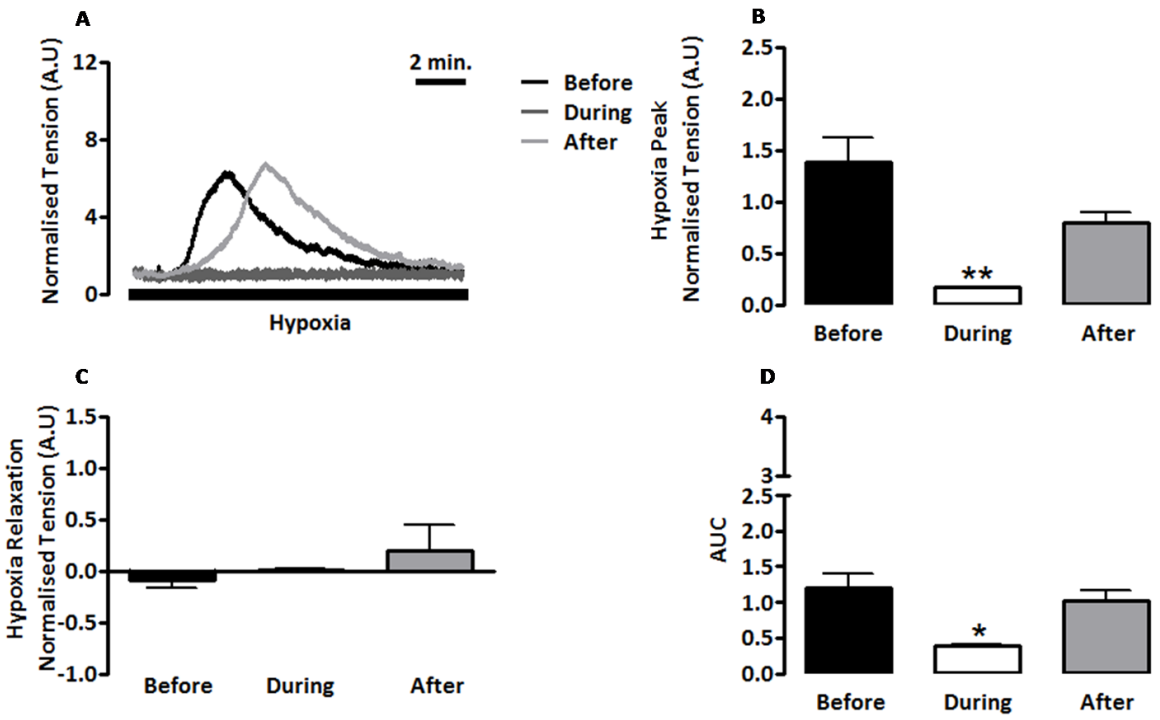

Figure 38. Hypoxic responses in inferior pulmonary veins before, during and after washout of 10mM BDM. A: Representative traces showing responses to hypoxia in inferior pulmonary veins before, during and after application of 10mM BDM, tension values are expressed normalised to baseline tension. B: magnitude of hypoxic peak (normalised to baseline tension and mean time control for 1st, 2nd and 3rd responses, as appropriate) and C: magnitude of hypoxic relaxation post-contraction (normalised to baseline tension) before, during and after 10mM BDM exposure. For the sake of clarity hypoxic relaxation data are expressed with a value of 1 subtracted to more clearly illustrate when relaxation below baseline occurs. D: area under the curve (AUC) for the hypoxic response normalised to mean time control data (traces for AUC were plotted standardised to baseline over a time period of 759 seconds before, during and after 10mM BDM exposure. All data represent mean ± S.E.M, N=5. *P<0.05 and **P<0.01 compared to "Before" (analysed using repeated measures one-way ANOVA with Tukey's post-test).

To investigate the possibility of non-specific effects of BDM at higher concentrations, contractile responses to 80mM KCl were measured before, during and after washout of 1, 5 and 10mM BDM. BDM at the lowest concentration of 1mM had no effect on KCl-induced contraction (before: 13.3 ± 1.9g, during: 13.1 ± 5.3g and after: 12.5 ± 1.6g; P>0.05, N=5). When 5mM BDM was applied, contraction to KCl was significantly reduced (before: 14.2 ± 2.1g, during: 9.5 ± 1.6g; P<0.001, N=5). On washout of 5mM BDM, KCl contraction recovered to the same level as before exposure (13.9 ±

2.0g; *P*<0.001 compared to "During", *P*>0.05 compared to "Before"). The same pattern was observed with 10mM BDM, KCl contraction was inhibited (before: 14.6 ± 1.7g, during: 5.3 ± 0.7g; *P*<0.001, N=7) and responses recovered to a similar level as before exposure when 10mM BDM was washed out (13.2 ± 1.8g, *P*<0.001 compared to "During", *P*>0.05 compared to "Before").

Glyburide

To determine the role of K_{ATP} channels in baseline tone and hypoxia-induced contraction of the PV, the K_{ATP} blocker glyburide (Dospinescu *et al.*, 2012) was used. Glyburide (10µM) did not significantly change baseline tension in inferior PVs during 30 minutes exposure. Initial mean tension was 0.7 ± 0.1g and after glyburide application was 0.5 ± 0.2g (*P*>0.05). DMSO was used as the solvent for glyburide at a level of 0.1%. In previous experiments (see Chapter 3), this level of DMSO was found to have no effect on baseline tension in fresh inferior PVs.

Application of 10µM glyburide had no impact on peak magnitude of the hypoxic response in inferior PVs (before: 1.4 ± 0.4 A.U, during: 1.1 ± 0.3 A.U and after: 1.1 ± 0.2 A.U; *P*>0.05, N=6) and there was also no effect on AUC (before: 1.2 ± 0.2 A.U, during: 1.4 ± 0.6 A.U and after: 1.3 ± 0.2 A.U; *P*>0.05). Relaxation post-hypoxic contraction was significantly inhibited after washout (0.6 ± 0.2 A.U) compared to control responses before glyburide application (-0.03 ± 0.1 A.U, *P*<0.05) however relaxation during glyburide exposure (0.4 ± 0.2 A.U) was not significantly different to before/after responses (*P*>0.05). Time to 50% peak (before: 178.1 ± 10.9s, during: 192.1 ± 19.0s and after: 183.4 ± 11.2s) and time to 75% relaxation (before: 421.3 ± 12.0s, during: 453.8 ± 36.9s and after: 472.3 ± 29.5s) were not significantly different before, during exposure to or after washout of glyburide (*P*>0.05). See Figure 39 for sample traces and mean data from experiments using 10µM glyburide.

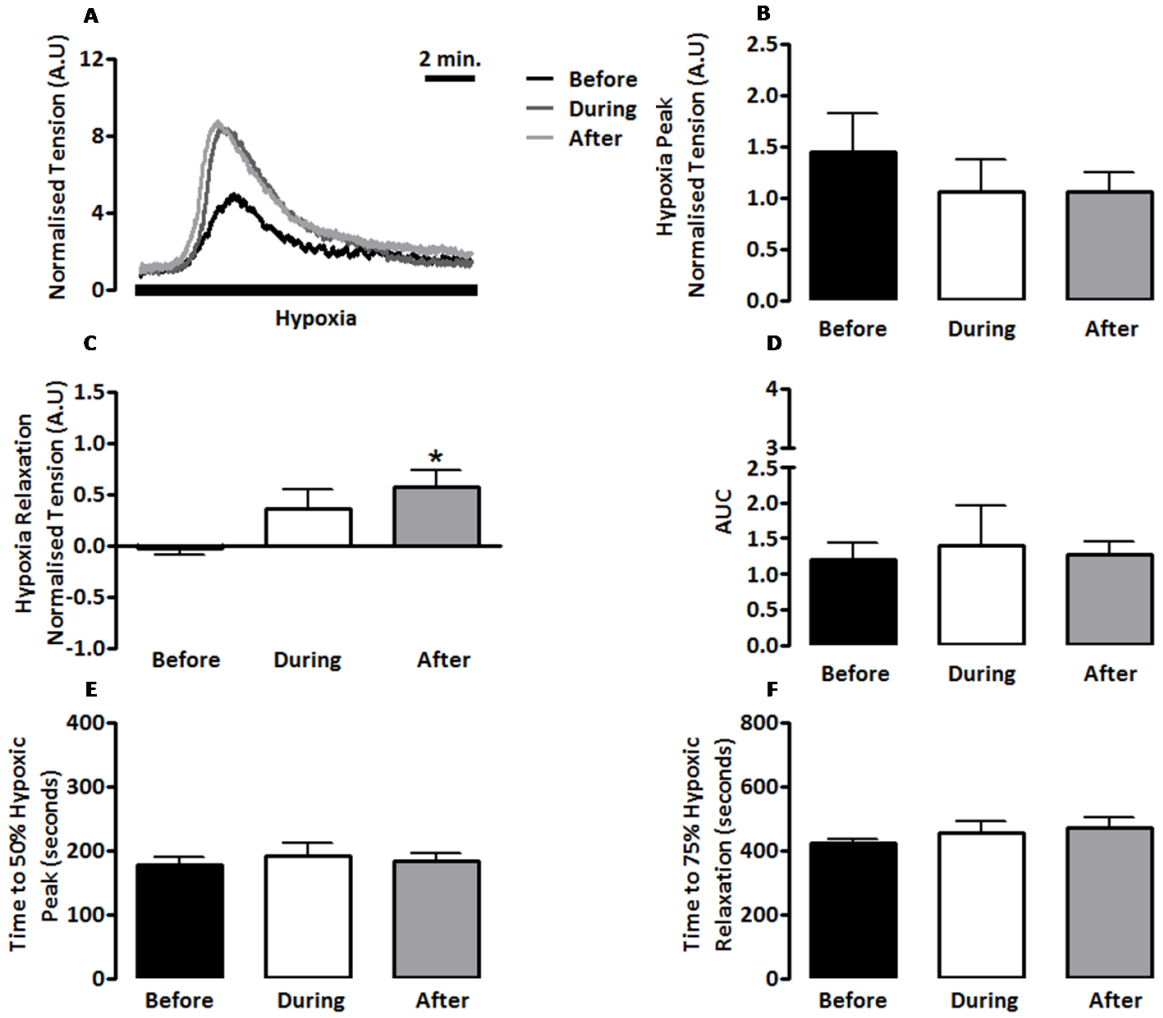

Figure 39. Hypoxic responses in inferior pulmonary veins before, during and after washout of 10µM glyburide. A: Representative traces showing responses to hypoxia in inferior pulmonary veins before, during and after application of 10µM glyburide, tension values are expressed normalised to baseline tension. B: magnitude of hypoxic peak (normalised to baseline tension and mean time control for 1st, 2nd and 3rd responses, as appropriate) and C: magnitude of hypoxic relaxation post-contraction (normalised to baseline tension) before, during and after 10µM glyburide exposure. For the sake of clarity hypoxic relaxation data are expressed with a value of 1 subtracted to more clearly illustrate when relaxation below baseline occurs. D: area under the curve (AUC) for the hypoxic response normalised to mean time control data (traces for AUC were plotted standardised to baseline over a time period of 759 seconds); E: time to 50% peak magnitude and F: time to 75% maximal relaxation post-contraction peak before, during and after 10µM glyburide exposure. All data represent mean ± S.E.M, N=6. *P<0.05 compared to "Before" (analysed using repeated measures one-way ANOVA with Tukey's post-test).

$ZnCl_2$

To determine the role of TASK-1/3 channels in baseline tone and hypoxia-induced contraction of the PV, the TASK-1/3 blocker $ZnCl_2$ (Ali *et al.,* 2014) was used. Baseline tension did not change over the course of a 30 minute application of 1mM $ZnCl_2$ (tension before and after: 0.6 ± 0.1g, *P*>0.05, N=7).

In addition, there was no effect of 1mM $ZnCl_2$ on the hypoxia-induced response of inferior PVs. There was no significant difference in hypoxic peak magnitude (before: 0.7 ± 0.1 A.U, during: 1.0 ± 0.2 A.U and after: 1.0 ± 0.2 A.U) or hypoxic relaxation post-peak (before: -0.02 ± 0.1 A.U, during: 0.04 ± 0.1 A.U and after: 0.2 ± 0.1 A.U) with $ZnCl_2$ exposure (*P*>0.05, N=6). AUC (before: 0.8 ± 0.1 A.U, during: 1.0 ± 0.2 A.U and after: 1.0 ± 0.2 A.U), time to 50% hypoxic peak (before: 241.8 ± 31.5s, during: 259.7 ± 20.1s and after: 235.6 ± 29.1s) and time to 75% relaxation (before: 557.2 ± 56.2s, during: 589.1 ± 46.0s and after: 521.4 ± 50.7s) also did not change on application/washout of $ZnCl_2$. Mean and representative data for $ZnCl_2$ are shown in Figure 40.

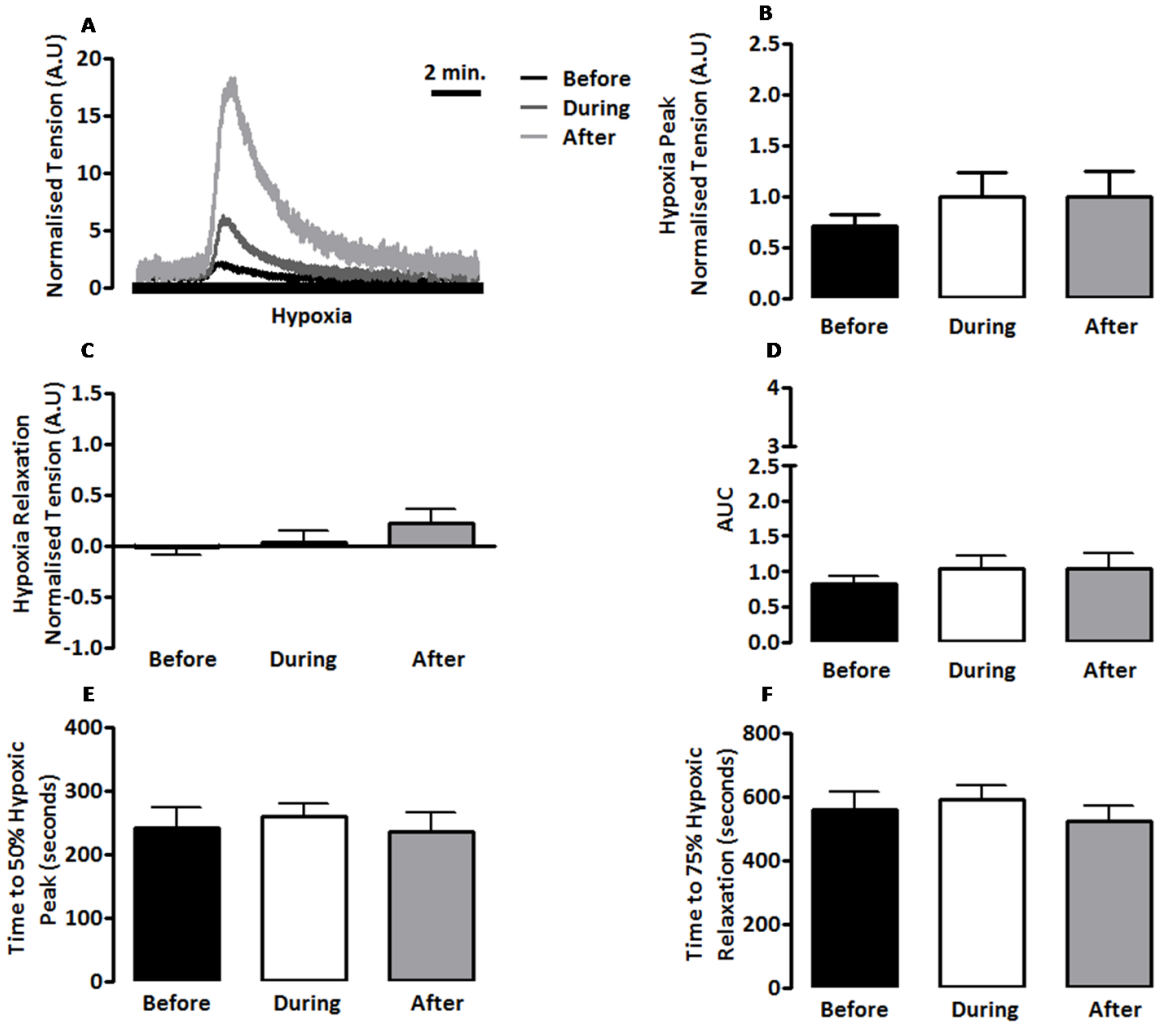

Figure 40. Hypoxic responses in inferior pulmonary veins before, during and after washout of 1mM $ZnCl_2$. A: Representative traces showing responses to hypoxia in inferior pulmonary veins before, during and after application of 1mM $ZnCl_2$, tension values are expressed normalised to baseline tension. B: magnitude of hypoxic peak (normalised to baseline tension and mean time control for 1st, 2nd and 3rd responses, as appropriate) and C: magnitude of hypoxic relaxation post-contraction (normalised to baseline tension) before, during and after 1mM $ZnCl_2$ exposure. For the sake of clarity hypoxic relaxation data are expressed with a value of 1 subtracted to more clearly illustrate when relaxation below baseline occurs. D: area under the curve (AUC) for the hypoxic response normalised to mean time control data (traces for AUC were plotted standardised to baseline over a time period of 759 seconds); E: time to 50% peak magnitude and F: time to 75% maximal relaxation post-contraction peak before, during and after 1mM $ZnCl_2$ exposure. All data represent mean ± S.E.M, N=6 (analysed using repeated measures one-way ANOVA with Tukey's post-test).

Impact of L-NAME on Inferior PV Basal Tone and Hypoxic Responses

For all drugs already discussed, data for baseline tension effects was taken from the point when the drug was added prior to 3rd hypoxia exposure. In some experiments, L-NAME (100µM) was used before any exposure to hypoxia during endothelial function tests (see Results section "Endothelial Function Testing and Impact of L-NAME"). Introduction of 100µM L-NAME at this point caused no significant change in baseline tension of inferior PVs (before: 0.3 ± 0.1g, after: 0.3 ± 0.2g, $P>0.05$, N=5). However, when added to the organ bath before the 3rd hypoxic exposure (with no previous exposure to the drug), L-NAME resulted in a sustained increase in tension in inferior PVs from a baseline of 0.7 ± 0.1g to a significantly higher level of 2.8 ± 0.5g, even after 30 minutes exposure ($P<0.01$ compared to baseline, N=6). As the experimental protocol involved two exposures to hypoxia before drug addition, it was decided to try running a time control where the protocol was run in exactly the same way but without exposure to hypoxia (this included all standard functional tests and resetting the tension to 1.5g at set intervals). In the PVs which acted as time controls, 100µM L-NAME still resulted in a sustained increase in basal tension from 0.4 ± 0.2g to 1.9 ± 0.4g ($P<0.05$ compared to baseline, N=3). The change in tension was significantly larger in both hypoxia (2.1 ± 0.5g) and time control (1.6 ± 0.3g) compared to that seen in earlier endothelial tests (-0.03 ± 0.1g, $P<0.01$). However, the contractile response to L-NAME application in hypoxia and time control tests did not differ ($P>0.05$).

L-NAME (100µM) had a significant impact on the hypoxic response of inferior PVs in terms of both magnitude and response dynamics. The peak magnitude of the hypoxic response was significantly reduced with L-NAME (before: 0.8 ± 0.1 A.U, during: 0.3 ± 0.02 A.U, $P<0.01$, N=6) and the response did not recover on washout (0.3 ± 0.03 A.U, $P<0.01$ compared to "before"). The same trend was observed for AUC (before: 0.8 ± 0.04 A.U, during: 0.4 ± 0.02 A.U and after: 0.4 ± 0.03 A.U, "during" and "after" both $P<0.001$ compared to "before"). Hypoxic relaxation post-peak was enhanced in the presence of 100µM L-NAME (before: -0.1 ± 0.1 A.U and during: -0.6 ± 0.1 A.U, $P<0.001$) and also did not recover on washout of the drug (-0.6 ± 0.1 A.U, $P<0.001$ compared to "before"). Time to 50% peak was significantly shorter in the presence of L-NAME (before: 235.5 ± 23.5s, during: 146.0 ± 14.1s, $P< 0.001$) and washout did not change this (144.5 ± 14.3s, $P<0.001$ compared to "before"). Time to 75% relaxation was the only parameter which was not significantly different with L-NAME (before: 476.9 ± 24.1s, during: 530.3 ± 27.0s and after: 492.3 ± 21.5s, $P>0.05$). Representative traces and mean data for results with 100µM L-NAME are shown in Figure 41.

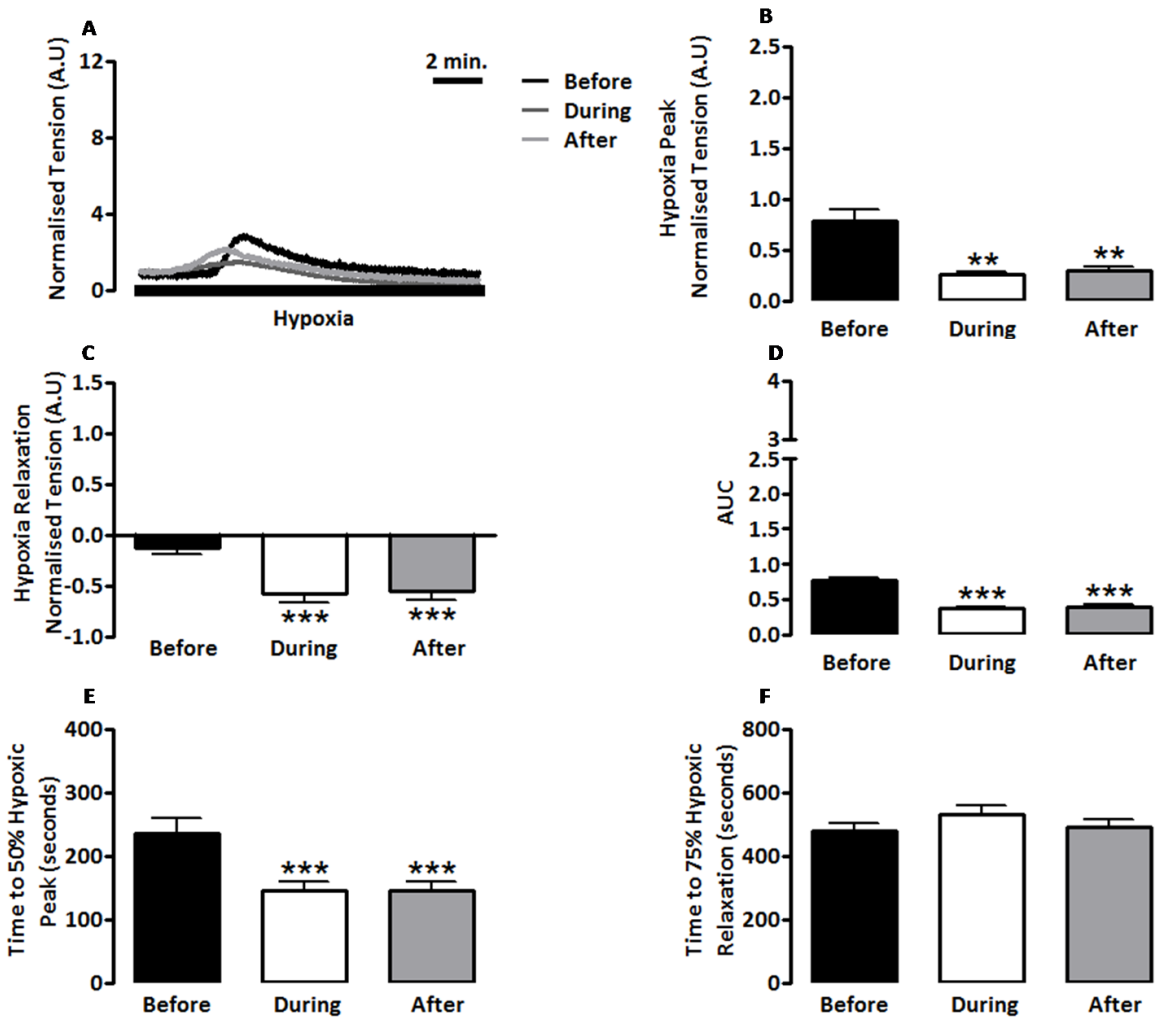

Figure 41. Hypoxic responses in inferior pulmonary veins before, during and after washout of 100µM L-NAME. A: Representative traces showing responses to hypoxia in inferior pulmonary veins before, during and after application of 100µM L-NAME, tension values are expressed normalised to baseline tension. B: magnitude of hypoxic peak (normalised to baseline tension and mean time control for 1st, 2nd and 3rd responses, as appropriate) and C: magnitude of hypoxic relaxation post-contraction (normalised to baseline tension) before, during and after 100µM L-NAME exposure. For the sake of clarity hypoxic relaxation data are expressed with a value of 1 subtracted to more clearly illustrate when relaxation below baseline occurs. D: area under the curve (AUC) for the hypoxic response normalised to mean time control data (traces for AUC were plotted standardised to baseline over a time period of 759 seconds); E: time to 50% peak magnitude and F: time to 75% maximal relaxation post-contraction peak before, during and after 100µM L-NAME exposure. All data represent mean ± S.E.M, N=6. ***P*<0.01 and ****P*<0.001 compared to "Before" (analysed using repeated measures one-way ANOVA with Tukey's post-test).

As L-NAME had a profound impact on the peak and relaxation phase and time course of the hypoxic response, the profile of the L-NAME sensitive component of the response was calculated by subtracting the "during" responses from initial "before" responses. All profiles were then plotted as an averaged tension trace against time. The component of the PV hypoxic response sensitive to L-NAME appeared to be an initial small relaxation followed by a transient contraction then a small sustained contraction component (as seen in Figure 42).

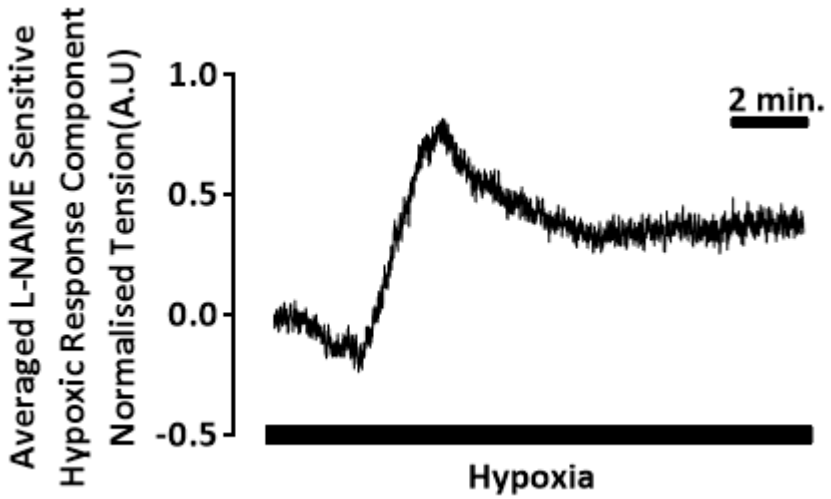

Figure 42. L-NAME sensitive component of the hypoxic response in inferior pulmonary veins. Averaged L-NAME sensitive component calculated by subtracting "during" responses from "before" responses (N=6). Trace represents the mean difference in tension across all pulmonary veins tested. Please note that as both "before" and "during" traces were normalised to baseline and then subtracted from one another any value above 0 represents contraction and below 0 represents relaxation.

Inferior PV Reoxygenation Responses

When two heart and lungs were transported from the abattoir daily, the success rate for reoxygenation contractions was only 2.1% on 1st exposure and 12.5% on 2nd exposure (N=12). Success rates for reoxygenation-induced contraction were still poor when one set of heart and lungs were transported daily: 20.5% (1st exposure) and 51.5% (2nd exposure) compared to previous success rates in fresh PVs in Chapter 3 experiments of 97%. Notably, many of the contractions that did occur were very small and within the range of noise and detection limit of the software (0.1g or less). On this basis, the reoxygenation contraction cannot be considered a stable and consistent functional

response and no in depth analysis of the reoxygenation contraction will be presented for the experiments performed in this chapter.

The only consistent effect worthy of note with regards to reoxygenation contraction was the potentiation seen in the presence of 100µM L-NAME. Exposure to L-NAME significantly increased the peak magnitude of the reoxygenation contraction from 1.3 ± 0.1 A.U to 4.5 ± 0.8 A.U (P<0.05, N=6). After washout of L-NAME from the organ bath, the response increased further to 5.2 ± 1.0 (P<0.05 compared to "before"). (Please note that reoxygenation data is expressed normalised to baseline tension only. This is because reoxygenation peak magnitude data from time controls did not show any significant trend over time (before: 1.6 ± 0.2 A.U, during: 1.7 ± 0.2 A.U and after: 2.2 ± 0.5 A.U, P<0.05, N=17) and hence there was no justification for normalising data to time control data.)

Reoxygenation AUC also increased over time in L-NAME experiments with AUC after washout being significantly larger than control response ("before") L-NAME application (before: 384.9 ± 8.0, during: 1213.2 ± 227.2 and after: 1723.0 ± 495.5, P<0.05 after compared with before, N=4). Time to 50% peak of reoxygenation contraction was significantly longer in the presence of 100µM L-NAME (before: 30.0 ± 15.4s, during: 96.6 ± 2.5s, P<0.01, N=4). The time to 50% peak did not recover on washout of the drug (112.1 ± 3.5s, P<0.001 compared with "before"). Please note there is only an n of 4 for AUC and $T_{0.5}$ peak data because, unfortunately, two raw traces did not have markers present which are used as a starting point for these calculations.

Overall, L-NAME enhanced and prolonged the reoxygenation contraction as is seen in mean data and representative sample traces in Figure 43.

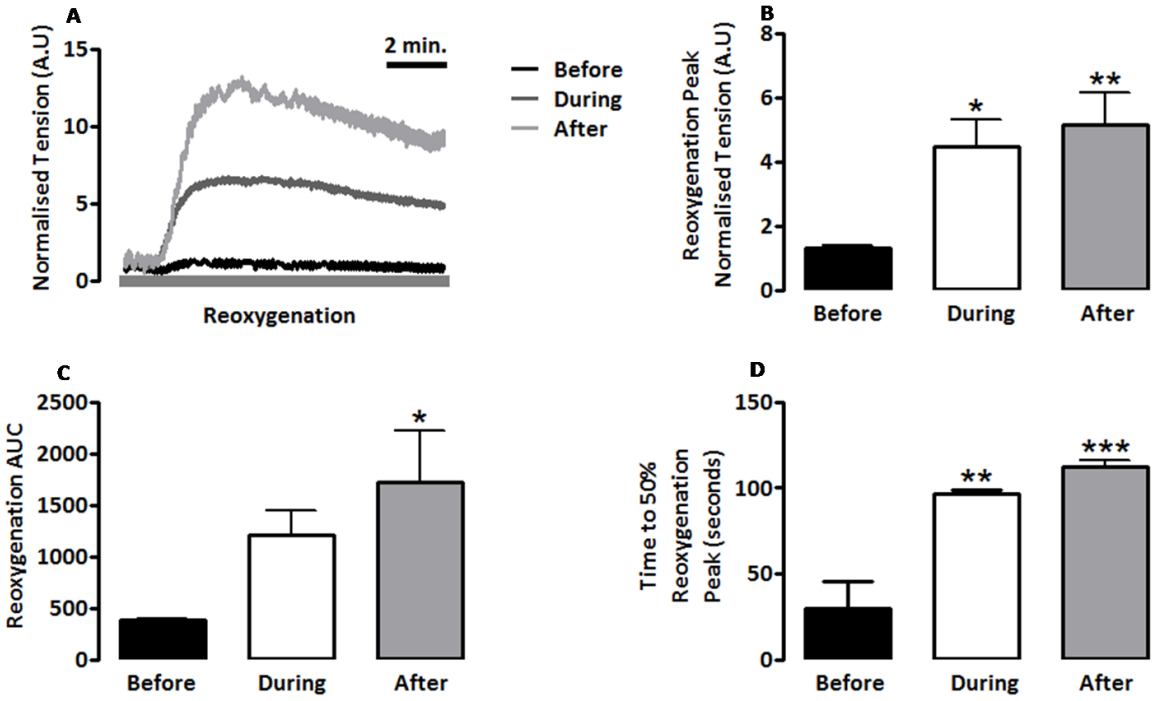

Figure 43. Reoxygenation responses in inferior pulmonary veins before, during and after washout of 100µM L-NAME. A: Representative traces showing responses to reoxygenation after hypoxic exposure in inferior pulmonary veins before, during and after application of 100µM L-NAME, tension values are expressed normalised to baseline tension. B: magnitude of reoxygenation peak, normalised to baseline tension (N=6) and C: area under the curve (AUC) for the reoxygenation response (traces for AUC were plotted standardised to baseline over a time period of 372.25 seconds) and D: time to 50% peak magnitude before, during and after 100µM L-NAME exposure (N=4). All data represent mean ± S.E.M; *P<0.05, **P<0.01 and ***P<0.001 compared to "Before" (analysed using repeated measures one-way ANOVA with Tukey's post-test).

Discussion

Little is currently known about underlying pathways and mechanisms of hypoxia-induced contraction within the PV especially within the inferior PV. Previous studies have investigated hypoxic contraction within superior/middle lobes (Dospinescu *et al.,* 2012) however it cannot be assumed that mechanisms are the same within PVs from inferior lobes since clinical differences exist between superior/inferior PVs (Yamane *et al.*, 2008). This study has set out to identify the underlying pathways and mechanisms of hypoxia-induced responses and regulation of basal tone within fresh porcine inferior PVs.

K_V and TASK channel activity did not appear to affect hypoxia-induced contraction of inferior PVs as 4AP, DPO-1 and $ZnCl_2$ had no effect. TEA inhibited the hypoxic contraction (reduced peak and AUC) whereas 5-10mM BDM completely abolished it. Hypoxic relaxation was significantly inhibited after washout of glyburide: this could be due to incomplete washout and delayed onset of action.

L-NAME reduced peak and AUC of the hypoxic contraction, enhanced hypoxic relaxation and shortened $T_{0.5}$ peak. L-NAME also resulted in a potentiated reoxygenation contraction in inferior PVs after hypoxic exposure. Otherwise, contraction on reoxygenation was poor and inconsistent during the experiments in this chapter.

KCl Viability Tests and Optimisation of Endothelial Function Test

$PGF_{2\alpha}$ (2µM) was not consistent in producing preconstriction before testing the endothelium with carbachol in experiments within this chapter whereas in the previous chapter $PGF_{2\alpha}$ was more reliable. Histamine was chosen as an alternative to $PGF_{2\alpha}$ as it was already established as a stable vasoconstrictor in PVs in previous experiments (Chapter 3) and histamine is specific for PVs compared to PAs (Hasebe *et al*., 1992). As concentration-response curves had also been performed previously (Chapter 3), a concentration for sub-maximal constriction was chosen as 1µM.

Incubation with 100µM L-NAME converted endothelial-mediated relaxation with carbachol (synthetic acetylcholine analogue) to contraction in this study. Reduced acetylcholine-induced endothelial relaxation after NOS inhibition has also been observed in PVs from newborn lambs (Gao *et al.,* 1995) and in human PVs (Norel *et al.*, 2004). Results from studies in culture conditions (see Chapter 3) suggested that endothelial dysfunction may lead to enhanced hypoxic responses in PVs and L-NAME was used as a tool to simulate this dysfunction. Therefore the aim of using L-NAME was achieved in

terms of simulating endothelial dysfunction (by blocking endothelial NOS (eNOS)) as it successfully impaired carbachol-mediated endothelial relaxation.

The traditional classification of NOS as endothelial, neuronal and inducible was based on the cell type from which the isoform was originally isolated (endothelial, neuronal and activated macrophages, respectively). They are now more commonly known as NOS1, NOS2 and NOS3 (neuronal, inducible and endothelial, respectively). Each of these isoforms is also expressed in various other cell types including vascular smooth muscle (Buchwalow *et al.,* 2002) suggesting that L-NAME could be having an effect not only in endothelial cells but in smooth muscle as well. L-NAME is hydrolysed to L-NNA by biological esterases (Griffith and Kilbourn, 1996) and L-NNA (also known as L-NOARG and nitro-L-arginine) has only minor selectivity for NOS1 and 3 (Moore *et al.,* 1996). It also binds to NOS2 although the binding is immediate and can be reversed with arginine; binding to NOS1 and 3 is time-dependent and reverses very slowly (Furfine *et al*., 1994, Klatt *et al.,* 1994). Therefore, despite the fact this experiment shows successful inhibition of endothelial-mediated relaxation with L-NAME, there may be effects on other isoforms and cell types such as smooth muscle.

The effect of L-NAME on histamine contraction helped clarify the site of action of L-NAME. L-NAME enhanced contractions to 1μM histamine compared to the first endothelial test whereas time control vessels which were not exposed to L-NAME showed inhibited histamine-induced contraction compared to the initial endothelial test. Others have also shown enhanced PV constriction to histamine with NOS inhibition (Shi *et al.*, 1998). Histamine may result in NO synthesis (Ignarro *et al.,* 1990) via activation of endothelial H_1 receptors (Toda, 1990) which would act to modulate any constriction via smooth muscle H_1 receptors (Shi *et al.*, 1998, Toda, 1990). The data from time control PVs taken alone could suggest desensitisation of pro-contractile smooth muscle H_1 receptors (Shi *et al.*, 1998, Toda, 1990). However, the increased contraction to histamine seen when NOS was inhibited with L-NAME suggests endothelial H_1 receptor upregulation occurs rather than smooth muscle H_1 receptor desensitisation (Toda, 1990). These results also support the role of L-NAME inhibition of endothelial NOS.

Change in Hypoxic Responses of Inferior PVs with Repeated Exposure

Contractions in response to hypoxia increased over time in this study in terms of peak magnitude and AUC. Many investigators do not directly state their method for isolated vessel hypoxia experiments in terms of whether controls were run side by side on a separate vessel ring or performed in the

same vessel ring before drug exposure. Both time differences and repeated exposure must be considered as a potential confounding factor for experiments yet there are few studies which address the issue. Within rat isolated PAs, experiments have shown that hypoxic contractions either do not change over three separate exposures (Leach *et al.,* 1994) or there is a small non-significant trend for run-down of the response between 2nd and 3rd exposures (Connolly *et al.,* 2013). Hypoxic responses within guinea pig pulmonary venules (~300µM) are repeatable and do not change significantly over 4 exposures (Tracey *et al.,* 1989a, Tracey *et al.,* 1989b). Therefore, inferior porcine PVs (3.5 ± 0.2mm) appear to respond differently to repeated acute hypoxia exposures when compared with PAs and even pulmonary venules (although this may be due to difference in vessel size or species differences).

However, a form of hypoxic preconditioning and upregulation of contractile mechanisms does exist within uterine smooth muscle during full-term pregnancy. Repeated brief exposures to hypoxia gradually increase uterine contractions when the tissue is returned to normoxia. Uterine contraction does not occur under hypoxic conditions *per se* but appears to increase contractile responses associated with labour (Alotaibi *et al.,* 2015).

In terms of data analysis within this chapter, the increase in hypoxic contraction over time justified normalising all further peak magnitude and AUC data to time control data to account for the intrinsic run-up in hypoxic contractions. Other investigators have used a similar approach in PAs to take account of run-down in hypoxic responses over time and to determine the effect of the intervention/drug specifically (Connolly *et al.,* 2013).

Influence of K^+ Channel Blockers on Hypoxic Responses and Baseline Tension of Inferior PVs

4AP

As 4AP is a base which increases extracellular pH when added to solution (Shahid and Rodger, 1989), the drug was made up in HEPES buffered solution and pH adjusted to 7.4 with HCl. In accordance with other preliminary experiments, PVs were in Kreb's solution before application of 4AP and on washout of the drug. Normalising the data to mean time control data reveals the effect of 4AP/HEPES buffer: significant inhibition of the hypoxic contraction compared to hypoxic contraction in Kreb's buffer. Results also showed significant inhibition of hypoxic relaxation on washout (compared to "during"). Experiments with HEPES solution alone also inhibited hypoxic relaxation on washout (compared to "during"). This inhibition of relaxation could be a secondary effect of the

large contraction to hypoxia on replacing HEPES with Kreb's solution meaning the final response was not fully relaxed before reoxygenation began. When HEPES solution was used for "before" and "after" responses in order to look at effects of 4AP only, there was no effect on the hypoxic response of PVs other than AUC being run-down over time.

K_V channels (sensitive to 4AP) regulate resting membrane potential and calcium levels in rat PASMCs and basal tone in rat PAs (Yuan, 1995, Archer *et al.,* 1996). Within superior/middle lobe porcine PVs, 4AP inhibits hypoxic contraction (Dospinescu *et al.,* 2012) and in both porcine and rat PVs 4AP application results in significant contraction above baseline tension (Dospinescu *et al.,* 2012, Michelakis *et al.,* 2001). Both of the studies in PV used 4AP dissolved in bath/aqueous solution with no mention of re-checking pH yet 4AP increases extracellular pH (Shahid and Rodger, 1989). Unfortunately, the main limitation of the method used in this study was that pH adjustment of HEPES was performed at room temperature and then solutions were used at 37°C within organ baths and bubbled with 5% CO_2. The low pH seen in HEPES solutions within the experimental set-up (Chapter 2) could be due to the increase in temperature (Barron *et al.,* 2006) and/or use of high (5% CO_2) which is known to lower pH of HEPES-buffered media within cell incubator set-ups (Elder *et al.,* 2015).

A reduction in pH can cause relaxation of blood vessels from basal tone (Ishizaka and Kuo, 1996) or after precontraction with phenylephrine (Loutzenhiser *et al.,* 1990) and KCl (Austin and Wray, 1993). Therefore it is possible that the effects seen with 5mM 4AP when Kreb's was used for control (Figure 30) and with HEPES buffer alone (Figure 31) were due to the change in pH rather than the drug. The lack of relaxation from baseline tone as a result of reduction in pH on application of 5mM 4AP (in HEPES) or HEPES buffer alone is supported by similar findings in rat aorta (Loutzenhiser *et al.,* 1990) and mesenteric artery (Austin and Wray*,* 1993) where no relaxation occurred unless vessels were preconstricted with a pharmacological agent. All results within this section, including from control experiments with HEPES alone, showed a transient increase in baseline tension which was not sustained. This may suggest a combination of change in pH and 4AP itself contributed to this contraction although pH change is unlikely as a reduction of extracellular pH generally leads to vasodilation (Austin and Wray*,* 1993, Ishizaka and Kuo, 1996, Loutzenhiser *et al.,* 1990). However as the effect of 4AP on baseline tension was not sustained, it is unlikely that K_V channels are involved in long-term control of resting tension within inferior porcine PVs.

Reducing pH to 7.14 in guinea pig pulmonary venules was enough to almost abolish hypoxic contractions (Tracey *et al.,* 1989a). This finding could explain why a reduction in hypoxic contraction was seen with 4AP (with Kreb's control and washout) and HEPES alone (non-significant trend) but not

with 4AP where HEPES was used for control and washout. The reduction in Ca^{2+} concentration by changing from Kreb's solution to HEPES could also impair the hypoxic response as Ca^{2+} influx has been shown to be involved in hypoxic responses of PVs (Dospinescu *et al.,* 2012) and isolated lungs (McMurtry *et al.*, 1976).

The run-down of response over time with 4AP (when HEPES was used for control and washout responses) could be due to reduced pH which is clearly documented to reduce contractile responses (Austin and Wray, 1993, Loutzenhiser *et al.,* 1990) including hypoxia-induced contraction (Tracey *et al.,* 1989a). Maintaining pH between 6.56 and 6.60 (see Chapter 2) may also reduce tissue viability as it is below normal physiological range. A final viability test with 80mM KCl could have helped clarify this but this was not performed as part of the protocol and the low pH alone could reduce force generated with KCl (Austin and Wray*,* 1993).

TEA

TEA (5mM) caused transient followed by sustained constriction of PVs from baseline tension, inhibited hypoxic contraction and inhibited hypoxic relaxation after washout. TEA is as an inhibitor of BK_{Ca} channels (Archer *et al.,* 1996, Moudgil *et al.,* 2005) but is also known to inhibit K_V channels in a concentration dependent manner (Gelband and Hume, 1992, Smirnov *et al.,* 2002). Therefore the inhibition of inferior PV hypoxic contraction with 5mM TEA seen within this study and by Dospinescu *et al.* (2012) may be due to action on K_V channels and/or BK_{Ca} channels. The hypoxia sensitivity of K_V is well documented (Archer *et al.,* 1996, Archer *et al.,* 1998, Archer and Michelakis, 2002, Archer *et al.,* 2004, Moudgil *et al.,* 2005, Platoshyn *et al.,* 2006) and the BK_{Ca} channel is known to have a hypoxia-sensitive splice variant (STREX) (McCartney *et al.,* 2005).

If BK_{Ca} plays a role in attenuating hypoxic constriction as suggested by Peinado *et al.* (2008) and Yan *et al.* (2014) and TEA was inhibiting BK_{Ca} in this study, it would be expected that the hypoxic contraction of inferior PVs would be enhanced in the presence of the drug. However, as TEA inhibited the contraction and had no effect on hypoxic relaxation, this suggests that BK_{Ca} is unlikely to play a role in attenuating hypoxic constriction in the case of inferior PVs. Results from Chapter 3 further support this as they showed no effect of the specific BK_{Ca} blocker Penitrem A (Dospinescu *et al.,* 2012) on the hypoxic response.

Another possibility for the mechanism of TEA is the existence of a specific K_V current in inferior PVs which is sensitive to TEA but insensitive to 4AP. Smirnov *et al.* (2002) identified two different K_V

currents which existed within two separate SMC types identified on isolating cells from rat conduit PAs. One type of K_V current was 4AP-sensitive and TEA-insensitive and proposed to be mediated by K_V channels containing K_V1.5 α subunits (Grissmer *et al.,* 1994). The other was 4AP-insensitive and TEA-sensitive and proposed to involve K_V2.1 α subunits (Patel *et al.,* 1997, Shi *et al.,* 1994). K_V channels containing K_V2.1 α subunits may play a role in hypoxic contraction of the PV hence why inhibition is seen with TEA but not with 4AP or Penitrem A. However, when K_V channels contain only K_V2.1 α subunits, they are rarely activated at membrane potentials more negative than -20mV (Patel *et al.,* 1997). This means that a homomeric K_V2.1 channel is unlikely to be activated at the normal PVSMC RMP of −36 ± 4 mV (Dospinescu *et al.,* 2012) and makes it an unlikely candidate for hypoxia-induced K_V current inhibition. However, when K_V2.1 is co-expressed with K_V9.3, the heteromer channel formed shifts the activation to within the range of RMP of PVSMCs (-50 to -60mV) (Patel *et al.,* 1997). Therefore, a K_V2.1/K_V9.3 channel could play a role in the hypoxic response of inferior PVs. The sustained increase in baseline tension seen with application of 5mM TEA in this study may also indicate a role for K_V2.1/K_V9.3 channels in setting the resting tone of inferior PVs. Notably, K_V2.1 is expressed at the mRNA level within PVs – see Appendix 1 for more details.

Since K_V channels are inhibited by hypoxia (Archer *et al.,* 1996, Archer *et al.,* 1998, Archer and Michelakis, 2002, Archer *et al.,* 2004, Moudgil *et al.,* 2005, Platoshyn *et al.,* 2006), prior block by TEA may mean that the initial K_V trigger is unable to respond to hypoxia and hence the overall response is inhibited. As the response is not completely abolished, there must be other mechanisms which mediate hypoxic contraction of PVs which do not require the involvement of K_V channels.

DPO-1

Building on initial studies using the less selective agents 4AP and TEA, DPO-1 was chosen as a relatively selective inhibitor of K_V1.5 (Lagrutta *et al.,* 2006, Karczewski *et al.*, 2009). However even at 10μM (much higher than the IC_{50} (30 – 266nM)), DPO-1 had no effect on any aspect of the hypoxic response. K_V1.5 channels are characterised as 4AP-sensitive and TEA-insensitive (Grissmer *et al.,* 1994, Smirnov *et al.,* 2002) and the hypoxic response seen in inferior PVs is insensitive to 4AP and sensitive to TEA. Therefore, the results with DPO-1 further support the existing data that K_V1.5 is unlikely to mediate the hypoxic response in inferior PVs. This demonstrates yet another difference between the hypoxic response in PVs and PAs; in the presence of anti-K_V1.5 hypoxic depolarisation of PASMCs is inhibited suggesting K_V1.5 plays a role in the hypoxic response of PASMCs. Unfortunately,

there are no other known publications investigating the effect of DPO-1 specifically on hypoxic contraction within PVs or any other pulmonary vessels.

DPO-1 (10μM) appeared to inhibit the vehicle (ethanol) induced relaxation in inferior PVs observed in previous solvent control experiments (Chapter 3). This may suggest blocking $K_V1.5$ results in contraction which cancels out ethanol-induced relaxation meaning $K_V1.5$ contributes to resting tone in PVs. Experiments earlier in this chapter showed a small, transient contraction of PVs in response to 4AP hence block of $K_V1.5$ could suggest a common mechanism between the two drugs. However, as the contraction with DPO-1 is also likely to be small and transient, if $K_V1.5$ plays a role in controlling resting tone it is probably minor. Despite these findings, $K_V1.5$ is present at the mRNA level within PVs – see Appendix 1 for more details.

BDM

BDM had a concentration dependent effect on both resting tension and hypoxic contraction of inferior PVs. There was no effect on ether baseline tone or hypoxic contraction until the concentration was 5mM. At 5 and 10mM, baseline tension fell to a level significantly below baseline and hypoxic contraction was abolished. The only difference between 5 and 10mM BDM was that the hypoxic response after washout of 5mM recovered fully whereas with 10mM the response did not fully recover. This may suggest that reversibility of BDM is also concentration dependent.

BDM was chosen as a known inhibitor of $K_V2.1$ and this subunit is expressed at the mRNA level within PVs (see Appendix 1) yet the documented IC_{50} for $K_V2.1$ channels expressed in *Xenopus* oocytes is 16.7mM (Lopatin and Nichols, 1993). Hence it may be that the results with BDM are not purely a result of $K_V2.1$ inhibition but also action at another site. BDM is known to be a non-selective agent with multiple sites of action. In terms of outward K^+ currents, BDM can inhibit K_{ATP} currents with an IC_{50} of 15 ± 1mM (Smith *et al.,* 1994) however, as relaxation of basal tone and inhibition of hypoxic contraction occurred at a much lower level of 5mM, this site of action is also unlikely.

Another non-specific effect of BDM is inhibition of L-type Ca^{2+} currents which has been demonstrated in guinea pig ventricular myocytes with an IC_{50} of 5.8 ± 0.4mM (Chapman 1993). Within vascular SMCs (from uterine arteries), 10mM BDM also successfully inhibits voltage gated Ca^{2+} influx (Otun *et al.,* 1993). This may explain the effects of BDM at 5-10mM and the lack of an effect of 1mM BDM on the hypoxic response. Furthermore, this may help explain why 5-10mM BDM inhibits contractile responses to 80mM KCl in inferior PVs as Ca^{2+} entry through voltage-gated L-type Ca^{2+} currents is

essential to the depolarisation-induced contraction produced by KCl (Iino, 1990). The residual contraction could be a result of Ca^{2+} release which is known to occur in other smooth muscle cell types in response to KCl (Iino 1990). L-type Ca^{2+} channel influx is known to contribute to the mechanism of hypoxic contraction in superior/middle PVs as the blocker nifedipine inhibits the contraction (Dospinescu *et al.,* 2012). However, 5-10mM BDM completely abolished hypoxic contraction in this study of inferior PVs whereas with nifedipine in superior/middle lobe PVs, the response was still present although it was significantly inhibited (Dospinescu *et al.,* 2012). Based on this, inhibition of L-type Ca^{2+} currents may only partly explain why BDM abolishes hypoxic responses in inferior PVs.

If the actions of BDM (5-10mM) are related to Ca^{2+} channel inhibition, the relaxation in basal tone seen on drug application may suggest there is an intrinsic influx of Ca^{2+} which maintains tone in inferior PVs. Within rat PAs, relaxation on blockade of L-type Ca^{2+} channel influx was only observed when vessels were maintained in culture for 4 days (Manoury *et al.,* 2009). However, mechanisms regulating resting tone in PVs may be different to those in PAs.

BDM (at a concentration of 10mM) is also known to inhibit myosin light chain (MLC) phosphorylation within PASMCs (Polte *et al.,* 2004) meaning it may have a more intrinsic effect on contraction. MLC phosphorylation in the SMC is required for combination with actin which initiates cross-bridge cycling and contraction (Webb, 2003). This could explain at a more fundamental level why BDM causes relaxation of inferior PVs and abolishes hypoxic contraction.

Therefore, BDM inhibition of the hypoxic response could be as a result of one or a combination of $K_V2.1$ inhibition, K_{ATP} inhibition, L-type Ca^{2+} channel block and inhibition of MLC phosphorylation. The relaxatory effect of BDM on baseline tension may be due to its inhibitory effect on L-type Ca^{2+} channel block and/or inhibition of MLC phosphorylation.

Glyburide

Application of glyburide (10µM) had no significant impact on baseline tension or on the magnitude or dynamics of the hypoxic contraction. Relaxation was increasingly inhibited over time but this was only statistically significant when comparing hypoxic responses after washout to initial responses. The hypoxic contraction also became smaller after washout of the drug although this effect did not reach statistical significance. The inhibition of both hypoxic relaxation and contraction could suggest that glyburide is not fully reversible and has a delayed onset of action. This issue could be addressed

by allowing for a longer incubation time or increasing glyburide concentration in future experiments. Glyburide is a more specific K^+ blocker than some of the others previously discussed, with effects on K_{ATP} (Dospinescu *et al*., 2012). This may indicate that K_{ATP} channels are involved in modulation the hypoxic response of the inferior PV however Dospinescu *et al.* (2012) found that glyburide did not have an effect on hypoxic contraction of superior/middle lobe porcine PVs. This could suggest a possible difference in underlying mechanisms between inferior and superior PVs.

Within foetal and adult rabbit PASMCs, glyburide has no effect on RMP suggesting K_{ATP} does not contribute to membrane potential in these cells (Osipenko *et al.,*1997, Hong *et al.,* 2005) and also does not affect resting tone in rat PVs (Michelakis *et al.,* 2001). This ties in with the results from this study; K_{ATP} channels are unlikely to be involved in regulation of resting tone in inferior PVs.

$ZnCl_2$

Application of $ZnCl_2$ (1mM) had no effect on baseline tension or any aspect of the hypoxic response. $ZnCl_2$ was used to investigate the role of TASK-1/3 (Ali *et al.,* 2014) in resting tone and the hypoxic response of inferior PVs. At a concentration of 1mM, $ZnCl_2$ would be expected to block TASK-3 as the IC_{50} for this channel is ~12 - 20μM (Gruss *et al.,* 2004, Clarke *et al.,* 2004). Previous use of $ZnCl_2$ as a TASK-1/3 blocker in human placental arteries used a concentration of 1mM (Ali *et al.,* 2014). However, at this higher concentration $ZnCl_2$ could also block TREK-1 (another member of the two-pore domain K^+ channel superfamily) as the IC_{50} is 659 ± 94μM (Gruss *et al.,* 2004).

TASK-1 channels are of particular interest because they are known to be inhibited by hypoxia and are involved in control of RMP in human PASMCs, implicating a role in regulation of basal tone in PAs (Olschewski *et al.,* 2006). Interestingly, within a TASK-1/3 knockout mouse model RMP in PASMCs was unchanged and even in wild type mice, hypoxic contraction was poor and inconsistent (Manoury *et al.,* 2011). These findings challenge the use of a mouse model for studying the pulmonary circulation and support the exploration of different models e.g. porcine.

On further investigation of use of $ZnCl_2$ as a TASK-1 blocker, the results of Ali *et al.* (2014) do not provide definitive evidence that $ZnCl_2$ blocks TASK-1 as they examined contractile responses of human placental arteries and did not dissect out the TASK-1 or -3 currents specifically. The inhibitory effect on human TASK-3 is well established (Gruss *et al.,* 2004, Clarke *et al.,* 2004) however human TASK-1 (expressed within *Xenopus* oocytes) current was inhibited by less than 10% by 200μM $ZnCl_2$ (Clarke *et al.,* 2004). In rat TASK-1 (expressed within Xenopus oocytes), $ZnCl_2$ showed an IC_{50} of

175μM (Leonoudakis, 1998). Despite this, the possibility that $ZnCl_2$ was not effectively blocking TASK-1 in these experiments must be considered.

A more suitable alternative to $ZnCl_2$ for investigating TASK-1 contribution specifically may be anandamide. Anandamide has been shown to be a selective inhibitor of TASK-1 at a concentration of 3μM with no effect on other members of the two-pore domain K^+ channel superfamily (including TREK-1 and -2 and TASK-2 and -3) (Maingret *et al.,* 2001). Anandamide increases pulmonary arterial tone at a concentration of 10μM (Wenzel *et al.,* 2013) which could suggest anandamide is acting via TASK-1 inhibition. However, these studies were performed in a mouse model and as earlier described, RMP was unaffected in PASMCs from a TASK-1 knockout mouse model (Manoury *et al.,* 2011) therefore the increased PA tone may be a result of other non-specific effects. As an endocannabinoid, anandamide is likely to have other effects on vascular contractility such as involvement in the fatty acid amide hydrolase pathway (Wenzel *et al.,* 2013).

Further investigation with other pharmacological agents is required before the role of TASK-1 (and other members of the two-pore domain K^+ channel superfamily) in the regulation of basal tone and hypoxic responses in porcine inferior PVs can be established.

Influence of L-NAME on Hypoxic Responses and Baseline Tension of Inferior PVs

When introduced near the beginning of the experimental protocol, L-NAME (100μM) produced no change in tension however when introduced at a later time-point it produced a sustained increase in baseline tone. These results cannot be explained by hypoxia exposure as time controls (where L-NAME was applied at the same time-point but vessels were not exposed to hypoxia) also responded with a sustained contraction. Stretch is documented to result in NO production within pulmonary capillary endothelial cells (Kuebler *et al.,* 2003). Tension was also readjusted to 1.5g in the time controls as part of the standard protocol therefore PVs were under more stretch at the later time point and this may explain the different effects of L-NAME at early and late time-points.

L-NAME (100μM) also had a profound effect on the hypoxia-induced response of inferior PVs: inhibiting and shortening contraction and enhancing relaxation. Plotting the difference between "before" and "during" traces revealed the component of the PV hypoxic response sensitive to L-NAME. This was an initial small relaxation followed by a transient contraction then a small sustained contraction component. Therefore there appears to be a balance of pro-contractile and pro-relaxant

mechanisms during the response to hypoxia in PVs and L-NAME shifts the balance towards pro-relaxant mechanisms particularly during the relaxation phase.

Hypoxic responses showed no recovery after washout of L-NAME indicating the drug is poorly reversible. The purpose for choosing L-NAME was to interfere with endothelial production of NO and therefore mimic the effects of PV maintenance in culture seen in Chapter 3. However the hypoxic responses of inferior PVs seen in the presence of L-NAME did not resemble the hypoxic responses seen in PVs which had been maintained in culture. With L-NAME, peak and AUC were reduced; after maintenance in culture they were increased. Hypoxic relaxation was enhanced with L-NAME yet after maintenance in culture, relaxation was inhibited. Others have also observed partial inhibition of hypoxic contraction in pig PVs with NOS inhibition (Félétou *et al.,* 1995). It is suggested that hypoxia usually results in inhibition of NO production allowing for a contraction to develop, whereas when NOS is already blocked this prevents hypoxic inhibition of the enzyme (Félétou *et al.,* 1995). This could explain why L-NAME caused inhibition of hypoxic contraction of inferior PVs within this study. The results of this study and those of Félétou *et al.* (1995) showed only partial inhibition of hypoxic contraction in PVs yet in PAs NOS inhibition abolishes the contraction (Félétou *et al.,* 1995). Indomethacin (cyclooxygenase inhibitor) has been reported to partially (Félétou *et al.,* 1995) or completely inhibit hypoxic contraction of pig PVs (Miller *et al.,* 1989). Therefore hypoxic inhibition of both NOS and cyclooxygenase may be required in order for development of a contractile response. Only blocking one endothelial vasodilatory pathway may also cause an imbalance and may explain the emergence of a much larger relaxation after hypoxic peak. Inhibition of NOS may lead to increased release or enhanced reactivity to vasodilatory prostaglandins. To investigate this theory further, experiments would need to be conducted in the presence of both L-NAME and indomethacin.

NO can react with superoxide ($O_2^{\cdot-}$) to produce peroxynitrite ($ONOO^-$) which is much less reactive and eventually leads to accumulation of the innocuous by-product NO_3^-(Dweik *et al.,* 2001). If NOS is inhibited and NO levels reduced, less NO is available to "mop up" $O_2^{\cdot-}$. Reactive oxygen species (ROS) including $O_2^{\cdot-}$ are proposed as second messengers during HPV in isolated lung and PASMCs; inhibitors of superoxide dismutase (which converts $O_2^{\cdot-}$ to H_2O_2) inhibit HPV suggesting ROS signalling is important during HPV (Waypa *et al.,* 2001). However, reduced NO and increased $O_2^{\cdot-}$ should lead to increased hypoxic contraction if a similar underlying mechanism is present in PVs. There is another school of thought which suggests hypoxia leads to reduced ROS production followed by K^+ channel inhibition (Archer *et al.,* 1993), membrane depolarisation (Yuan, 1995) and voltage-gated Ca^{2+} influx (McMurtry *et al.,* 1976). Increased $O_2^{\cdot-}$ during NOS inhibition may oppose this mechanism and lead to

reduced contraction. Further investigations using antioxidants and inhibitors of ROS production are required before any of these mechanisms can be consolidated.

Despite the profound impact of L-NAME on the hypoxic response of inferior PVs, there is no clear explanation for its effects as they were different to those anticipated. It is likely to be a complex and multi-factorial process.

Reoxygenation Contractile Responses of Inferior PVs and Impact of L-NAME

Contractile responses to reoxygenation after hypoxic exposure were poor and inconsistent. This was unexpected as reoxygenation contractions within previous experiments (Chapter 3) were consistent and occurred in the majority of PVs. This may be due to the fact that different abattoirs were used to source the tissue and perhaps different sub-species of pig.

A consistent response during reoxygenation was the potentiated contraction in the presence of 100µM L-NAME. The effect of L-NAME was irreversible as reoxygenation contractions were still significantly greater after removal of the drug when compared to initial control ("before") responses.

As discussed previously, if NOS is inhibited by L-NAME and NO levels reduced, less NO will be available to "mop up" $O_2^{\cdot-}$ (Dweik *et al.,* 2001). ROS including $O_2^{\cdot-}$ are proposed as second messengers within hypoxic vasoconstriction within isolated lung and PASMCs (Waypa *et al.,* 2001). Perhaps ROS are involved in mediating the contractile response to reoxygenation which is potentiated after exposure to L-NAME as less NO is available to "mop up" $O_2^{\cdot-}$ resulting in imbalance and increased availability of $O_2^{\cdot-}$ as a second messenger. Others have proposed that ROS may mediate reoxygenation contraction of pig PAs (Liu *et al.*, 2001). Again, further investigation using antioxidants and inhibitors of ROS production would be required before any of these mechanisms can be consolidated.

L-NAME had a consistent effect on both reoxygenation and hypoxic responses of inferior PVs but no definitive conclusions can be drawn as to how exactly it brought about these actions until further studies are performed.

Key Findings

This study set out to investigate mechanisms regulating hypoxia-induced responses within inferior PVs. Inhibition of NOS with L-NAME inhibited hypoxic contraction, enhanced relaxation and potentiated contraction on reoxygenation. The K^+ channel inhibitors TEA and BDM inhibited the hypoxic contraction whereas 4AP, DPO-1, glyburide and $ZnCl_2$ had no effect. Therefore, K_{ATP}, $K_V1.5$ and TASK do not appear to affect hypoxic contraction however a potential candidate for involvement is the $K_V2.1$ α subunit as this is TEA- and BDM-sensitive and 4AP-insensitive (Lopatin and Nichols, 1993, Patel *et al.,* 1997, Shi *et al.,* 1994, Smirnov *et al.,* 2002).

This study has highlighted that both NO and certain K^+ channels contribute to the mechanism underlying hypoxia-induced contraction of porcine inferior PVs. These pathways could provide possible targets for use in the treatment of hypoxia-related disease e.g. high altitude pulmonary oedema where inhomogeneous hypoxic pulmonary venoconstriction causes increased upstream capillary pressure (Bärtsch and Gibbs, 2007, Maggiorini *et al.,* 2001).

Further Work

Regulation of contractile pathways within PVs is likely to be complex and multifactorial. Electrophysiology studies will be used to further investigate the functional contribution of specific K^+ channels to RMP and voltage-activated whole-cell currents and to further explore the hypoxic response at the isolated smooth muscle cell level.

Chapter 5

Impact of Maintenance in Culture Conditions on Morphological and Electrophysiological Characteristics of Inferior Pulmonary Vein Smooth Muscle Cells

Introduction

Isolated porcine PVs have shown marked vasoactive responses to hypoxia, agonists and some K^+ channel inhibitors (Chapters 3 & 4). Exposure of PVs to culture conditions for 24 hours resulted in augmented contractile responses to hypoxia and agonists and endothelial dysfunction/damage was proposed to contribute. However, when L-NAME was used to interfere with endothelial production of NO, hypoxic contraction was inhibited rather than being increased. Therefore it was pertinent to investigate whether maintenance of PV in culture conditions has any direct effect on isolated smooth muscle cells.

Smooth muscle cells (SMCs) are intrinsic to vasoactivity and maintenance of vascular tone in all blood vessels (Dospinescu, 2009). SMC shape and width can both have an impact on contractile force (Tolic-Norrelykke and Wang, 2005) therefore cell morphology is important to characterise and compare between cells isolated from fresh PVs and PVs kept in culture. Furthermore, total area of the cell is directly proportional to membrane capacitance which is a measurement of the phospholipid cell membrane's ability to store electrical charge (Molleman, 2003). Full characterisation of morphological and electrical membrane properties of SMCs isolated from superior/middle PVs has been performed previously (Dospinescu, 2009); the studies within this chapter (as in Chapter 4) will focus on SMCs isolated from inferior PVs.

Further to morphological influences on contraction, resting membrane potential (RMP) and voltage-activated currents of SMCs regulate contractility and resting tension of blood vessels, via the second messenger Ca^{2+}(Dospinescu, 2009, Yuan *et al.,* 1993). SMCs isolated from PAs kept in culture conditions for 4 days had depolarised membrane potentials and reduced K^+ currents compared with

freshly isolated PASMCs (Manoury *et al.,* 2009). The impact of maintaining PVs in culture on the electrophysiological properties of PVSMCs remains to be established.

Potential K^+ channel targets for electrophysiology studies were unfortunately not identified via RT-PCR experiments (Appendix 1) due to persisting problems with tissue homogenisation and extracting RNA of sufficient yield and quality. Due to this, targets and pharmacological agents were selected based on previous findings in isolated inferior PV studies (Chapter 4) and in PVSMCs (Dospinescu *et al.,* 2012, Michelakis *et al*., 2001). Within isolated inferior PVs, 5mM TEA caused a sustained increase in baseline tension and inhibited hypoxic contraction whereas 4AP had no clear effect on either. Voltage-activated outward currents in SMCs from porcine and rodent PVs were sensitive to both TEA and 4AP (Dospinescu *et al.,* 2012, Michelakis *et al*., 2001). Therefore the impact of both 4AP and TEA on RMP and whole-cell voltage-activated currents in inferior PVs was investigated. TASK-1 is another K^+ channel of particular interest as it is inhibited by hypoxia and involved in control of RMP in human PASMCs (Olschewski *et al.,* 2006). $ZnCl_2$ can be used to inhibit TASK-1/3 (Ali *et al.,* 2014, Patel *et al.,* 2013) in order to establish the role of TASK in controlling RMP and the contribution of TASK to whole-cell voltage-activated currents within fresh PVSMCs and SMCs isolated from PVs maintained in culture conditions.

Hypoxic contraction within PVs is a robust and reproducible physiological response augmented by maintenance in culture conditions (Chapters 3 & 4) and hypoxia is known to cause depolarisation of SMCs from PAs (Archer *et al.,* 1996, Archer *et al.,* 2004, Hong *et al.,* 2005, Olschewski *et al.,* 2002, Osipenko *et al.,* 1997, Post *et al.,* 1992, Yuan *et al.,* 1993). Therefore, the impact of hypoxia on RMP of inferior PVSMCs required investigation in order to further explore underlying mechanisms of hypoxic contraction in PVs and the augmentation seen after maintenance in culture conditions.

The aim of this study was to characterise and compare morphological properties and electrophysiological characteristics (RMP and voltage-activated currents) of SMCs isolated from fresh inferior PVs and from inferior PVs maintained in culture conditions for 24 hours.

Methods and Experimental Protocols

Cell Morphology Measurements

After enzymatic cell isolation was complete (see Chapter 2 for details), approximately 80-100µL of cell suspension was pipetted onto a glass slide and cells were allowed to settle for 15-20 minutes. The glass slide was mounted on the stage of a Leica DMI4000 B inverted microscope (Leica Microsystems CMS GmbH, Germany) fitted with a phase-contrast objective (magnification x40, numerical aperture 0.40). The microscope was connected to a Leica DFC300 FX camera (Leica Microsystems Ltd, Heerbrugg, Switzerland) and Leica Application Suite (LAS) software which were used to capture phase-contrast photomicrographs of the PVSMCs.

Image J software, version 1 (US National Institutes of Health, Betheseda, Maryland, USA; available from: http://imagej.net/Downloads) was used to analyse phase-contrast images and make cell measurements. For every PVSMC analysed, the following measurements were made using Image J: perimeter (length of the cell boundary), area (two-dimensional area enclosed within the cell boundary), length and width (at widest point of the cell). Cell length and width were also calculated using the perimeter and area values from Image J by approximation to an ellipse and compared to measured values. Perimeter and area values were also used to calculate circularity of the smooth muscle cell and tri-dimensional membrane surface area was calculated by approximation to an ellipsoid.

Morphological data are presented as mean ± SD, range (minimum – maximum values) and the coefficient of variation (CV). CV is the ratio of SD to the mean and is useful for comparison of dispersion of values between different groups:

$$CV = \frac{SD}{mean}$$

(Equation 4)

In this case, it will be used to compare dispersion of morphological measurements between SMCs isolated from fresh inferior PVs and from PVs maintained in culture. Histograms were plotted side-by-side for fresh/culture PVSMCs for all morphological parameters and fitted with a Gaussian probability density function:

$$f(x) = \frac{1}{\sigma\sqrt{2\pi}} e^{-\frac{(x-\mu)^2}{2\sigma^2}}$$

(Equation 5)

where σ is the standard deviation and μ is the mean. Differences between mean values were assessed using Students unpaired *t*-test.

Membrane Capacitance and Series Resistance

Membrane capacitance (C_m) refers to a measurement of the phospholipid cell membrane's ability to store electrical charge at a given potential and is directly proportional to the total area of the cell membrane (Molleman, 2003). Therefore, C_m is often used to standardise whole cell currents to cell size which converts current values to current densities by dividing the current by the capacitance value measured for the cell in question. C_m was calculated by the WinEDR software using the following equation:

$$C_m = \tau(G_a + G_m)$$

(Equation 6)

τ is the time constant of the exponential decay of the transient capacitive current; this current occurs as a result of a step change in potential (voltage) applied to the cell. During the step change, charge builds up exponentially within the capacitor (cell membrane) before reaching steady state. Visually, the transient capacitive current appears as a spike and then an exponential decay in current. G_a is the access conductance and is the reciprocal of access resistance and G_m is the membrane conductance and is the reciprocal of membrane resistance. G_a was calculated by WinEDR using the equation:

$$G_a = \frac{I_0}{V_{pulse}}$$

(Equation 7)

where I_0 is the initial current at the start of the capacitive transient (estimated from the amplitude of the fitted exponential at the start of the voltage step) and V_{pulse} is the steady state voltage amplitude. G_m was calculated by Win EDR using the equation:

$$G_m = \frac{I_{pulse}}{V_{pulse} - \frac{I_{pulse}}{G_a}}$$

(Equation 8)

where I_{pulse} is the steady state current amplitude. C_m, G_a and G_m were logged via the WinEDR software after approximately 4 minutes of achieving the whole-cell configuration to allow for exchange between cell and pipette solution contents.

During whole-cell patch clamping, series resistance (R_s) is the sum of all resistance encountered by the current before it reaches the cell and can be used as a measure of quality of the cell membrane patch clamp (Molleman, 2003). R_s is made up of membrane resistance and access resistance (which refers to the patch resistance after the whole-cell configuration has been achieved and should be low since the membrane patch is ruptured at this stage). R_s impacts on the voltage which cells are actually exposed to; the greater the series resistance, the greater the reduction in voltage which has adverse effects on voltage clamping and the quality of subsequent cell recordings. R_s should ideally be maintained at less than 20 MΩ (Molleman, 2003) and was calculated using the following equation (knowing G_a and G_m as previously discussed):

$$R_s = \frac{1}{G_a + G_m}$$

(Equation 9)

In order for C_m, G_a and G_m to be calculated correctly, series resistance was not compensated electronically as per WinEDR v3.7.0 instruction manual.

Resting Membrane Potential – Baseline Values, Effect of Flow and Viability Testing

After C_m, G_a and G_m were logged, the amplifier was switched to current clamp mode (at zero current) in order to measure RMP under resting conditions in extracellular bath solution. No adjustment was made for potential differences arising from liquid junction potentials - justification for this is detailed within Chapter 2.

As experimental protocols involving drug application and exposure to hypoxic bath solution were to be performed in the presence of constant flow, RMP was recorded when flow was switched on to investigate whether introduction of flow alone had any impact on RMP. KCl (80mM) was applied via Picospritzer® to test viability in some PVSMCs (in terms of membrane potential depolarisation). RMP was recorded continuously before application (10 seconds), during application (2 seconds) and after washout (10 seconds) of KCl.

Resting Membrane Potential – Effect of K^+ channel Inhibitors and Hypoxia

The contribution of different K^+ channels to the RMP of inferior PVSMCs was investigated by application of K^+ channel blockers via Picospritzer®. RMP was recorded continuously before, during and after application of: the K_V channel inhibitor 4AP (Dospinescu *et al.*, 2012), BK_{Ca} inhibitor TEA (Archer *et al.,* 1996, Moudgil *et al.,* 2005), and TASK-1/3 blocker zinc chloride ($ZnCl_2$) (Ali *et al.,* 2014, Patel *et al.,* 2013). The concentrations used were the same as those used in myography experiments in Chapter 4 – 5mM 4AP, 5mM TEA and 1mM $ZnCl_2$. Baseline RMP ("before") was recorded for 10 seconds followed by a 90 second application of the drug via Picospritzer® and a 10-30 second washout period after application had stopped.

The effect of exposure to hypoxic bath solution on the RMP of PVSMCs was also investigated by continuously recording RMP for 1 minute under baseline normoxic conditions ("before" – solution passively oxygenated with room air), followed by 5 minutes hypoxia (solution bubbled with 100% N_2 for at least 10 minutes) and 5 minutes recovery under normoxic conditions.

Voltage-activated Whole-cell Currents - Effect of K^+ Channel inhibitors

A voltage clamp protocol was used to identify and characterise whole-cell voltage-activated currents within inferior PVSMCs. To create a pharmacological profile of the outward K^+ current, voltage-activated currents were measured before, during and after washout of 5mM 4AP, 5mM TEA and 1mM $ZnCl_2$.

A standard voltage step protocol was applied to identify whole-cell voltage-activated families of outward currents. The resting potential was set at -80mV and 17 separate voltage step pulses were

applied for 400-ms starting at -80mV and increasing incrementally by 10mV up to the final voltage of +80mV (Figure 44 shows a diagram of the protocol used).

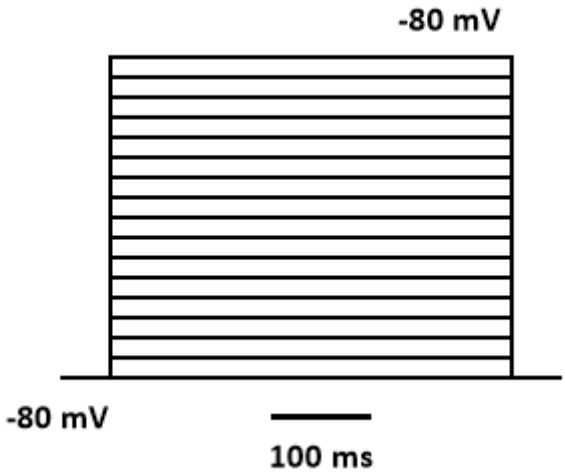

Figure 44. Standard voltage step protocol. Each voltage step was applied for 400-ms and steps went from -80mV to +80mV in 10mV increments.

Voltage step protocols were applied before application of any drug followed by a 60 second rest period then the K^+ channel inhibitor was applied by Picospritzer® for 90 seconds and in the last 30 seconds of application the voltage step protocol was applied. After 60 seconds washout of the K^+ channel inhibitor under constant flow, the voltage step protocol was applied again to assess for recovery of currents.

To calculate the rate of activation of whole-cell voltage-activated currents within inferior PVSMCs, raw traces were fitted with a "one-phase association" curve using GraphPad Prism 7 and the following equation:

$$I = I_0 + \left(I_{plateau} - I_0\right) \times \left(1 - e^{-K_{act}\, x}\right)$$

(Equation 10)

where I_0 is the current at time=0 and $I_{plateau}$ is the current value at steady state. K_{act} is the rate constant of current activation, expressed in the reciprocal of time units and τ_{act} is the time constant of current activation and is computed as the reciprocal of K_{act}. τ_{act} was used to compare activation rates of currents in the presence and absence of K^+ channel inhibitors.

All RMP and whole-cell current protocols were performed using both SMCs isolated from fresh PVs and from PVs maintained in culture for 24 hours. Data for fresh/culture SMCs were analysed separately owing to the differences observed in earlier contractile studies when PVs were exposed to culture conditions for 24 hours (see Chapter 3).

Data Analysis – Electrophysiology

Electrophysiological data (membrane potential and currents) were recorded using WinEDR software and exported to Microsoft Excel and GraphPad Prism 5/7 for analysis. Membrane potential (mV) responses were complex and therefore the most objective method was to measure and average RMP values over the full time periods of "before", "during" and "after" recordings. This was aided by the marker on the recorded trace from the Picospritzer® system which was connected to the Axopatch amplifier. Currents were measured as the average current once steady state was reached. Raw trace data are presented as measured currents (pA) and mean data as current density (in pA/pF) by dividing current by respective capacitance values (pF) to standardise whole cell currents to cell size (as discussed previously) before data were combined. Mean values before, during and after drug application/hypoxia were compared statistically using repeated measures one-way ANOVA with Tukey's post test or repeated measures two-way ANOVA with Bonferroni's post test. Mean values for SMCs isolated from fresh PVs and from PVs maintained in culture were compared statistically using Students unpaired *t*-test or two-way ANOVA with Bonferroni's post test. Statistical significance for all tests was determined at $P<0.05$.

For all cell morphology and electrophysiology, N=number of animals and n=number of cells. For the purposes of all statistical analysis (including calculation of S.E.M.) within this chapter, n (number of cells) will be used.

Results

Cell Morphology

SMC shape and width can both have an impact on contractile force (Tolic-Norrelykke and Wang, 2005) therefore it is important to investigate cell morphology when considering isolated PVSMCs. Furthermore, total cell area is directly proportional to membrane capacitance which is a measurement of the phospholipid cell membrane's ability to store electrical charge (Molleman, 2003).

As described in Chapter 2, the yield and quality of cells produced from each daily isolation procedure were documented. Both yield and quality (in terms of cell membrane and contractile state) varied when the protocol was used on tissue from different animals and on fresh PVs or PVs maintained in culture. Cells which were viable for use in electrophysiology experiments were either relaxed, elongated and spindle-like or partially contracted whilst maintaining an elliptical shape. All cells identified as viable SMCs for patch-clamping had no striations and a single, central nucleus. No other identification of cell phenotype was undertaken beyond morphological and functional responses.

Cell Perimeter and Projected Area

From cell isolation experiments using fresh inferior PVs, measurements were made on 240 cells from 24 different animals (n=240; N=24). From cell isolation experiments using inferior PVs maintained in culture, measurements were made on 131 cells from 19 different animals (n=131; N=19). Only relaxed or partially contracted elliptical cells were measured. All cell membrane qualities were considered for measurements to give a wider cell sample as on some days the protocol only produced poor quality cells. Cells that were fully contracted (spherical in shape) were not included in the analysis.

Using ImageJ, outlines were drawn around each relaxed/partially contracted cell and perimeter (in pixels) and area (in pixels^2) were measured. The values were then converted to µm and µm^2, respectively, using the conversion factor for 40x magnification (0.22 µm/pixel, as calculated from an image of a stage micrometer using ImageJ).

Cells isolated from fresh inferior PVs had a minimum perimeter of 68.8 µm and a maximum of 489.4 µm and cells isolated from PVs maintained in culture had a minimum perimeter of 56.5µm and a

maximum of 560.7 μm. The CV values for cells from fresh PVs and from those maintained in culture were similar (0.37 and 0.44, respectively). However the mean perimeter for cells isolated from PVs maintained in culture (265.7 ± 117.2 μm, n=131) was significantly larger than for fresh PVSMCs (240.7 ± 88.3 μm, $P<0.05$, n=240). See Table 5 for details.

The projected area of cells isolated from fresh PVs ranged from 158.1 to 1836.9 μm^2; for cells from PVs maintained in culture the area ranged from 101.5 to 1946.5 μm^2. The CV for cells from fresh PVS was smaller (0.45) than the CV for cells from PVs maintained in culture (0.53) indicating a wider distribution of values in the latter. Mean projected area values were not significantly different (Fresh: 785.3 ± 353.6 μm^2 and Culture: 848.8 ± 446.4 μm^2, mean ± SD, $P>0.05$). See Table 5 for details. Histograms comparing the distribution of values for perimeter and projected area for SMCs isolated from fresh PVs and from PVs maintained in culture are shown in Figure 45.

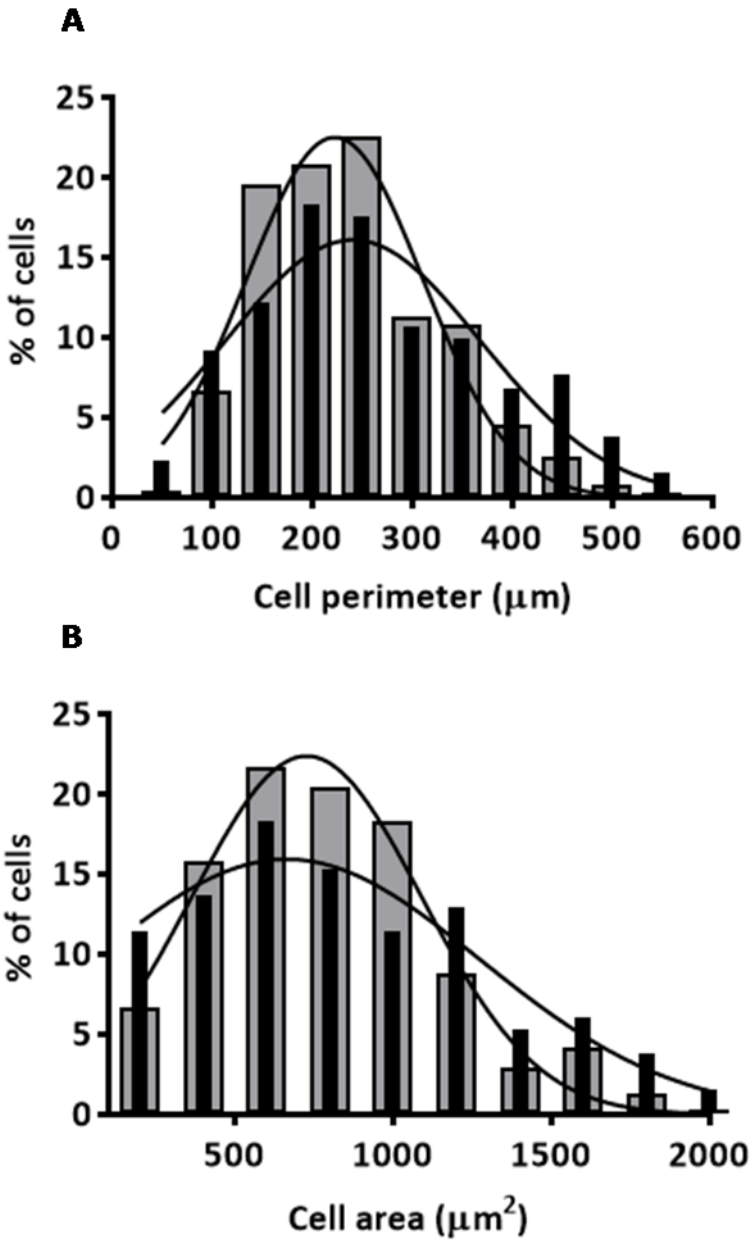

Figure 45. Perimeter and projected area of smooth muscle cells isolated from fresh pulmonary veins (PVs) and from PVs maintained in culture. Histograms show the distribution of (A) perimeter and (B) projected area of smooth muscle cells (SMCs) isolated from fresh PVs (wide, grey bars (n=240; N=24)) and PVs maintained in culture (narrow, black bars (n=131; N=19)), as measured on photomicrographs. Data values were fitted with Gaussian distributions (black curves).

Cell Length and Width

Cell length and width were measured (in pixels) by drawing lines of length and width (at widest point) using ImageJ and converted to µm using the conversion factor 0.22 µm/pixel. Cell length and width were also calculated by approximating PVSMC shape to an ellipse using the perimeter and projected area values measured for the cell using ImageJ software. The length and width of the PVSMC were approximated as the major and minor axis, respectively, of the corresponding ellipse (see Figure 46).

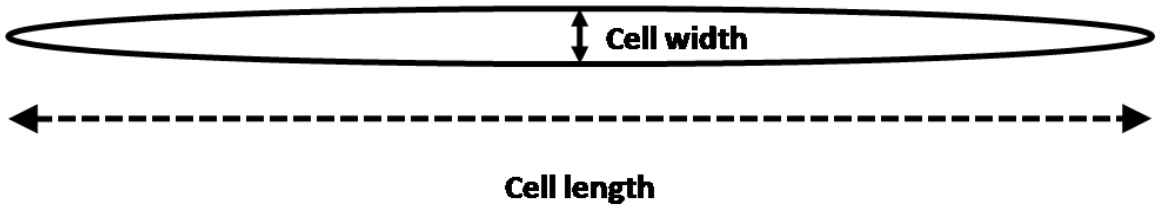

Figure 46. Estimation of cell shape for length and width calculations. The shape of each measured PVSMC was approximated to an ellipse of the same area and perimeter as the measured cell in order to calculate cell length (major ellipse axis in figure) and width (minor ellipse axis in figure).

The size of the major and minor ellipse axes were calculated from the standard equation for the area of an ellipse:

$$A = \pi ab$$

(Equation 11)

along with another equation by Euler which approximates the perimeter of an ellipse (Almkvist and Berndt, 1988):

$$P = \pi\sqrt{2(a^2 + b^2)}$$

(Equation 12)

where *a* is the semi-major axis and *b* is the semi-minor axis of the ellipse. From the two equations above considering area (*A*) and perimeter (*P*) were known, a biquadratic equation was produced:

$$x^4 - \frac{P^2}{2\pi^2}x^2 + \frac{A^2}{\pi^2} = 0$$

(Equation 13)

with the two positive solutions to Equation 13 being the semi-major axis (half length) and semi-minor axis (half width) of the approximated ellipse and corresponding PVSMC.

Values from measurements directly from photomicrographs and those calculated from approximation to an ellipse were compared to investigate the reliability of each method. For cells isolated from fresh inferior PVs, the mean measured length (± SD) was 112 ± 43.5 μm (range 27.3 – 231.2 μm) whereas the mean length calculated from approximation to an ellipse was 107.8 ± 39.9 μm (range 30.0 – 220.1 μm). Coefficients of variation were similar indicating a similar dispersion of values – 0.39 and 0.37, respectively. See Table 5 for details. Calculated length values were significantly shorter than their corresponding measured values (P<0.001). There was a strong and significant correlation between measured and calculated cell length (Pearson's r coefficient = 0.9974, P<0.001), as shown in Figure 47.

For cells isolated from PVs maintained in culture, the mean measured length (± SD) was 124.4 ± 57.3 μm (range 25.2 –270 μm) whereas the mean length calculated from approximation to an ellipse was 119.2 ± 52.9μm (range 25.0 – 252.2 μm). Coefficients of variation were similar: 0.46 and 0.44, respectively. See Table 5 for details. Length values calculated by approximation to an ellipse were significantly shorter than their corresponding measured values (P<0.001). For cells isolated from PVs maintained in culture, there was also a significant correlation between measured and calculated length values (Pearson's r coefficient = 0.9979, P<0.001), as shown in Figure 47. Cells isolated from PVs maintained in culture were significantly longer than those isolated from fresh PVs when considering either measured or calculated values (P<0.05).

The measured width of cells isolated from fresh PVs ranged from 2.5 to 19.3 μm with a mean of 9.3 ± 3.0 μm; width values calculated from approximation to an ellipse ranged from 3.4 to 18.9 μm with a mean of 9.3 ± 2.7 μm. CVs were similar – 0.32 and 0.29, respectively and there was no significant difference between measured and calculated width values (P<0.05). See Table 5 for details. There was a significant correlation between measured and calculated cell width (Pearson's r coefficient = 0.7959, P<0.001), see Figure 47.

The measured width of cells isolated from PVs maintained in culture ranged from 3.0 to 19.9 μm with a mean of 8.8 ± 3.3 μm; width values calculated from approximation to an ellipse ranged from 4.4 to 19.2 μm with a mean of 8.9 ± 2.7 μm. CV for measured widths was larger (0.37) to CV for calculated widths (0.30) indicating more dispersion within the measured values. See Table 5 for details. There was no significant difference between measured and corresponding calculated width values (P<0.05). There was a significant correlation between measured and calculated cell width (Pearson's r

coefficient = 0.7892, *P*<0.001), see Figure 47. There was no significant difference between measured or calculated width values when comparing cells isolated from fresh PVs to those maintained in culture (*P*>0.05). Histograms for measured and calculated lengths and widths are shown in Figure 48.

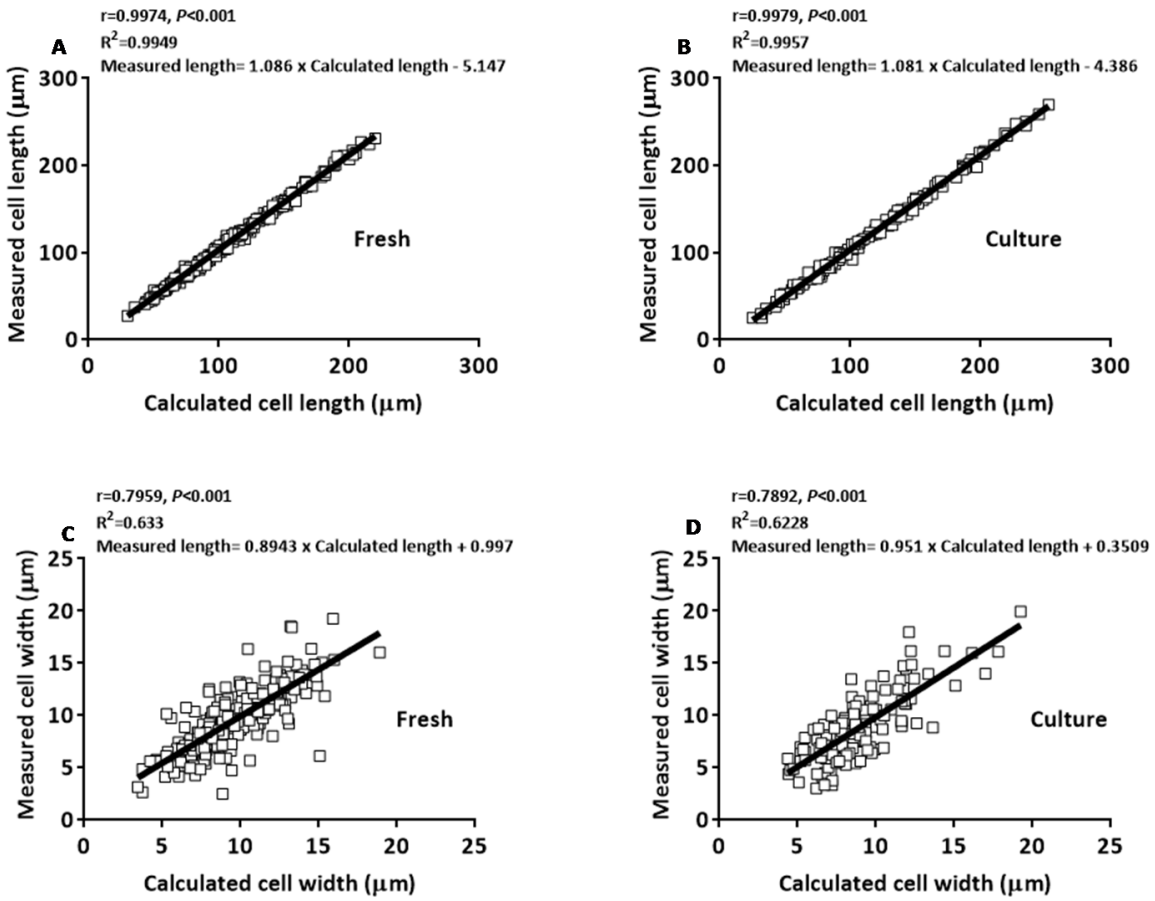

Figure 47. Correlation of cell length and width values measured and calculated by approximation to an ellipse. Measured values were plotted against calculated values for A: cell length in SMCs isolated from fresh inferior PVs; B: cell length in SMCs isolated from inferior PVs maintained in culture; C: cell width in SMCs isolated from fresh inferior PVs and D: cell width in SMCs isolated from inferior PVs maintained in culture. Black lines represent the slopes calculated by linear regression analysis; r is Pearson's correlation coefficient; R^2 represents goodness of fit (calculated by linear regression). Fresh PVSMCs: n=240; N=24; SMCs from PVs maintained in culture: n=131; N=19.

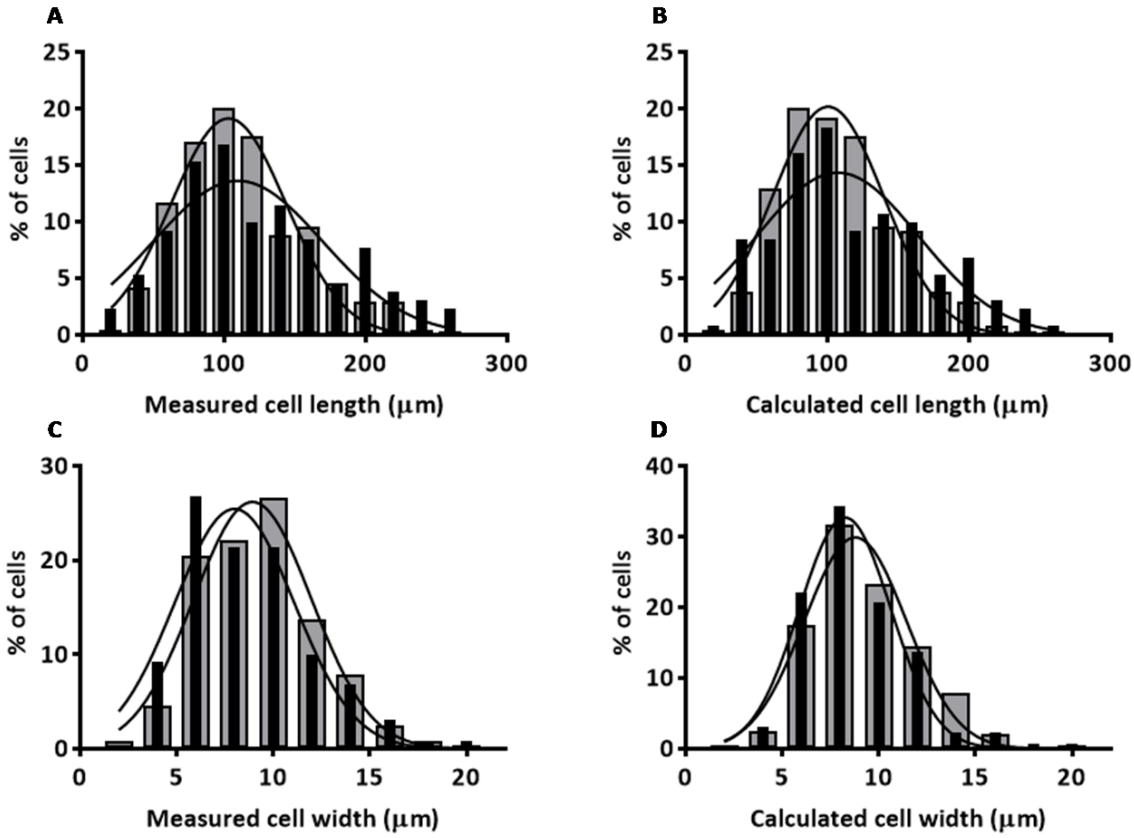

Figure 48. Cell length and width – measured and calculated from approximation to an ellipse. Histograms show the distribution of A: measured length; B: length calculated by approximation to an equivalent ellipse; C: measured width and D: width calculated by approximation to an equivalent ellipse in smooth muscle cells (SMCs). SMCs were either isolated from fresh pulmonary veins (PVs) (wide, grey bars (n=240; N=24)) or PVs maintained in culture (narrow, black bars (n=131; N=19)). Data values were fitted with Gaussian distributions (black curves).

Circularity

Smooth muscle cell shape has an impact on contractile force (Tolic-Norrelykke and Wang, 2005) hence this was taken into account when undertaking morphological characterisation of inferior PVSMCs. Circularity was calculated as a quantitative measure of SMC elongation (Auman *et al.,* 2007) using known projected area (A) and perimeter (P) measurements from ImageJ and the following equation:

$$Circularity = 4\pi A/P^2$$

(Equation 14)

Circularity is a unit-less ratio which can range from 0 to 1; a value of 1 represents a perfect circle and values approaching 0 indicate increasing elongation of the cell. Circularity in SMCs isolated from fresh inferior PVs had a mean value of 0.19 ± 0.09 and ranged from 0.06 to 0.58 (n=240). In SMCs isolated from inferior PVs maintained in culture for 24 hours, mean circularity was 0.18 ± 0.09 and ranged from 0.05 to 0.51 (n=131, *P*>0.05 compared to fresh PVSMCs). CV values for circularity were similar for SMCs isolated from fresh PVs (0.49) and from PVs maintained in culture conditions (0.52) indicating similar dispersion of values for both. See Table 5 for details. A histogram comparing the distribution of values for circularity for SMCs isolated from fresh PVs and from PVs maintained in culture is shown in Figure 50.

Tri-dimensional Surface Area

Measurements of projected area made from photomicrographs using ImageJ software (see Figure 45) represent only a bi-dimensional projection of SMC area and therefore do not precisely quantify total membrane surface area. For this reason, a more representative, tri-dimensional cell surface area was calculated by approximation to an ellipsoid. The type of ellipsoid used for approximation was a prolate spheroid (where the polar axis is longer than the equatorial diameter) (see Figure 49). The long axis corresponds to cell length (l) and the two short axes correspond to cell width (w).

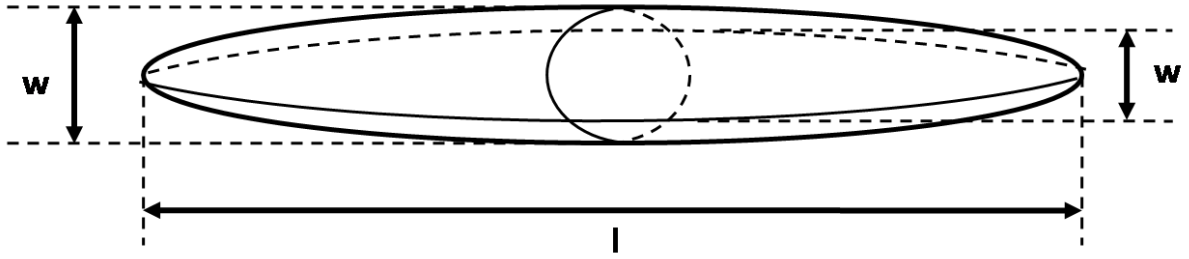

Figure 49. Approximation of pulmonary vein smooth muscle cell to a prolate spheroid. Tri-dimensional cell surface area was calculated using the length and width values calculated previously as the prolate axes.

The ellipsoid surface area (S) was calculated using an equation by Knud Thomsen (Michon, 2004, McGahon *et al.,* 2007):

$$S \approx 4\pi \left(\frac{a^p b^p + a^p c^p + b^p c^p}{3} \right)^{1/p}$$

(Equation 15)

where p = lg(3) = ln(3)/ln(2) ≈ 1.6075 and a is equal to half the length and b and c are both equal to half the width. Please note that length and width values calculated from approximation to an ellipse were used in all calculations of tri-dimensional surface area rather than measured values.

For SMCs isolated from fresh inferior PVs, mean (± SD) tri-dimensional surface area was 2459.5 ± 1102.9 μm^2 and ranged from 494.5 to 5734.5 μm^2. For SMCs isolated from PVs maintained in culture for 24 hours the mean tri-dimensional surface area was 2654.4 ± 1391.6 μm^2 and ranged from 323.4 to 6060.5 μm^2 (P>0.05 compared to fresh PVSMCs). CV values for circularity were larger in SMCs isolated from PVs maintained in culture conditions (0.52) compared to SMCs from fresh PVs (0.45) indicating a wider dispersion of values for cells isolated from PVs maintained in culture. See Table 5 for details. A histogram comparing the distribution of values for tri-dimensional surface area for cells from fresh PVs and from PVs maintained in culture is shown in Figure 50.

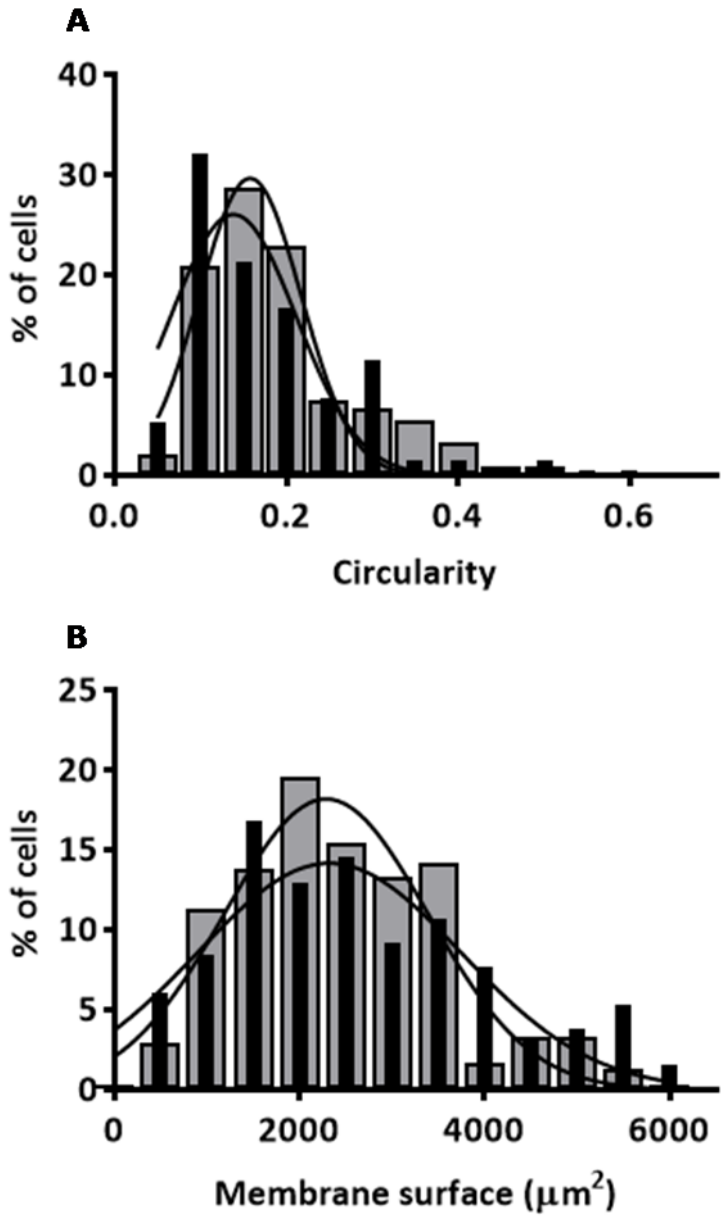

Figure 50. Circularity and tri-dimensional membrane surface area of smooth muscle cells isolated from fresh pulmonary veins (PVs) and from PVs maintained in culture. Histograms show the distribution of (A) circularity, an indicator of cell shape (calculated using projected area and perimeter measurements from photomicrographs) and (B) tri-dimensional membrane surface area (calculated by approximation to an ellipsoid) of smooth muscle cells isolated from fresh PVs (wide, grey bars (n=240; N=24)) and PVs maintained in culture (narrow, black bars (n=131; N=19)). Data values were fitted with Gaussian distributions (black curves).

Table 5. Morphometric measurements of smooth muscle cells isolated from either freshly dissected inferior PVs (fresh) or inferior PVs maintained in culture conditions for 24 hours (culture). Area, perimeter, length and width were measured using ImageJ on photomicrographs; length and width were also separately calculated by approximation of cell shape to an ellipse; circularity was calculated using area and perimeter values; tri-dimensional surface area was calculated by approximation of cells to a prolate spheroid. Fresh: N=24, n=240; culture: N=19, n=131. **P*<0.05 compared to fresh (analysis using Students unpaired *t*-tests).

Cell measurement	Mean value ± SD		(Minimum value – Maximum value)		CV	
	Fresh	Culture	Fresh	Culture	Fresh	Culture
Projected area (μm^2)	785.3 ± 353.6	848.8 ± 446.4	158.1 – 1836.9	101.5 – 1946.5	0.45	0.53
Perimeter (μm)	240.7 ± 88.3	265.7 ± 117.2*	68.8 – 489.4	56.5 – 560.7	0.37	0.44
Measured Length (μm)	112 ± 43.5	124.4 ± 57.3*	27.3 – 231.2	25.2 – 270	0.39	0.46
Calculated Length (μm)	107.8 ± 39.9	119.2 ± 52.9*	30.0 – 220.1	25.0 – 252.2	0.37	0.44
Measured Width (μm)	9.3 ± 3.0	8.8 ± 3.3	2.5 – 19.3	3.0 – 19.9	0.32	0.37
Calculated Width (μm)	9.3 ± 2.7	8.9 ± 2.79*	3.4 – 18.9	4.4 – 19.2	0.29	0.30
Circularity	0.19 ± 0.09	0.18 ± 0.09	0.06 – 0.58	0.05 – 0.51	0.49	0.52
Tridimensional surface area (μm^2)	2459.5 ± 1102.9	2654.4 ± 1391.6	494.5 – 5734.5	323.4 – 6060.5	0.45	0.52

Membrane Capacitance and Series Resistance

C_m was calculated and logged using WinEDR software from 91 cells isolated from fresh inferior PVs from 22 different animals (n=91; N=22). C_m was also calculated for 72 cells isolated from inferior PVs maintained in culture for 24 hours and from 17 different animals (n=72; N=17). C_m of SMCs isolated

from fresh PVs was 38.9 ± 20.6 pF (range: 12.0 – 133.5 pF). C_m of SMCs isolated from PVs maintained in culture conditions was 39.7 ± 16.6 (range: 11.5 – 135 pF) and was not significantly different from the C_m of fresh PVSMCs (*P*>0.05). See Table 6 for details. A histogram comparing the distribution of values for C_m for cells from fresh PVs and from PVs maintained in culture is shown in Figure 51.

Specific membrane capacitance can be calculated by dividing the mean C_m value by the mean value for cell surface area (Firth *et al.,* 2011). For SMCs isolated from fresh PVs the specific membrane capacitance had a value of 1.6 $\mu F/cm^2$ (38.9 pF/2459.5 μm^2). For SMCs isolated from fresh PVs the specific membrane capacitance was similar to fresh PVSMCs at 1.5 $\mu F/cm^2$ (39.7 pF/2654.4 μm^2).

R_S had a mean value of 25.7 ± 1.3 MΩ (mean ± S.E.M, n=155) when considering data from cells where G_a and G_m values had been logged via WinEDR. A total of 7 cells were excluded from the mean data as they were considered to be significant positive outliers; any recordings made from these 7 cells were also excluded from further analysis.

Resting Membrane Potential – Baseline Values

RMP was measured under resting conditions (before experimental protocols were run) in 82 cells isolated from fresh inferior PVs (22 different animals: n=82; N=22) and 70 cells isolated from inferior PVs maintained in culture for 24 hours (18 different animals: n=70; N= 18). SMCs isolated from fresh PVs had a mean RMP of -39.7 ± 14.2 mV with a range of -9.1 to -68.3 mV. RMP in SMCs isolated from PVs kept in culture was less negative with a mean RMP of -36.6 ± 12.8 mV and a range of -7.9 to -63.8 mV. The difference between fresh/culture PVSMCs was not statistically significant (*P*>0.05). See Table 6 for details. A histogram comparing the distribution of values for baseline RMP for cells from fresh PVs and from PVs maintained in culture is shown in Figure 51.

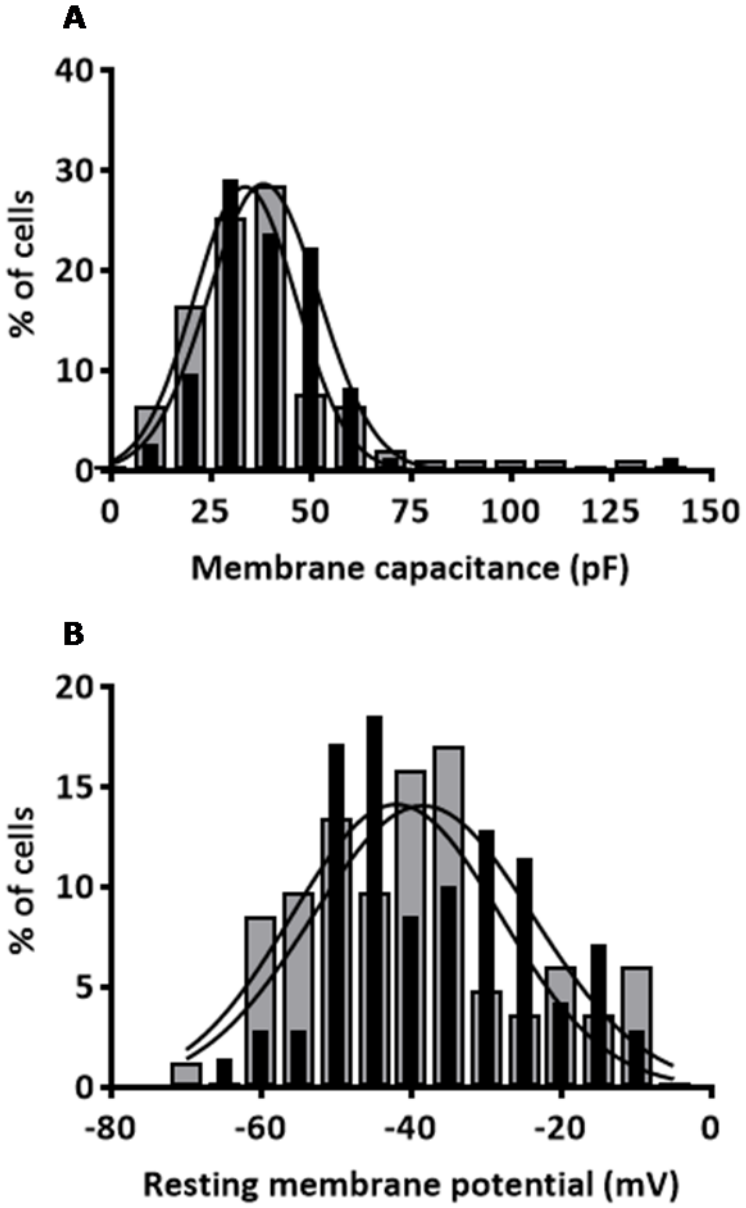

Figure 51. Membrane capacitance and resting membrane potential of smooth muscle cells isolated from fresh pulmonary veins (PVs) and from PVs maintained in culture. Histograms show the distribution of (A) membrane capacitance (calculated by WinEDR software) and (B) resting membrane potential (measured at baseline under current clamp (I=0)) of smooth muscle cells isolated from fresh PVs (wide, grey bars) and PVs maintained in culture (narrow, black bars). Data values were fitted with Gaussian distributions (black curves). For (A): n=91, N=22 for fresh PVSMCs and n=72, N=17 for SMCs isolated from PVs maintained in culture. For (B): n=82, N=22 for fresh PVSMCs and n=70, N=18 for SMCs isolated from PVs maintained in culture.

Table 6. Passive electrical membrane properties of smooth muscle cells isolated from either freshly dissected inferior PVs (fresh) or from PVs maintained in culture conditions for 24 hours (culture). For resting membrane potential: n=82, N=22 for fresh PVSMCs and n=70, N=18 for SMCs isolated from PVs maintained in culture. For membrane capacitance: n=91, N=22 for fresh PVSMCs and n=72, N=17 for SMCs isolated from PVs maintained in culture. Analysis performed using Students unpaired t-tests.

Cell measurement	Mean value ± SD		(Minimum value–Maximum value)		N (n)	
	Fresh	Culture	Fresh	Culture	Fresh	Culture
Resting membrane potential, mV	-39.7 ± 14.2	-36.6 ± 12.8	-68.3 – -9.1	-63.8 – -7.9	22 (82)	18 (70)
Membrane capacitance, pF	38.9 ± 20.6	39.7 ± 16.6	12.0 – 133.5	11.5 – 135	22 (90)	17 (72)

Resting Membrane Potential – Effect of Flow and Viability Testing

Effect of Flow

As experimental protocols were to be performed in the presence of constant flow, RMP was measured at the time when flow was started in order to investigate whether introduction of flow alone had any impact on RMP. In cells isolated from fresh PVs, RMP did not change when flow was commenced (before: -39.9 ± 13.9 mV; after: -39.6 ± 14.9 mV; $P>0.05$, n=52, N=18). In cells isolated from PVs kept in culture conditions, RMP was also unchanged on introduction of flow (before: -36.7 ± 12.5 mV; after: -36.5 ± 12.9 mV; $P>0.05$, n=53, N=16).

Viability Testing with 80mM KCl

Of cells tested for viability by applying 80mM KCl, 94% of those isolated from fresh PVs and 90% from PVs maintained in culture responded with depolarisation of RMP; of those cells which depolarised, 97% responded with repolarisation on washout. Cells which did not depolarise in response to KCl and/or repolarise on washout were excluded from further analysis. Fresh PVSMCs had a starting

RMP of -37.1 ± 4.1 mV (mean ± S.E.M) which depolarised to -17.5 ± 3.3 mV (*P*<0.001 compared to baseline) on exposure to 80mM KCl. After washout, RMP recovered to -33.9 ± 4.6 mV (*P*<0.001 compared to during exposure, n=12; N=8). SMCs isolated from PVs maintained in culture depolarised to KCl from an initial RMP of -32.4 ± 2.8 mV to -19.0 ± 2.4 mV (*P*<0.001 compared to baseline). RMP then recovered to -29.6 ± 2.0 mV after washout of the drug (*P*<0.001 compared to during exposure, n=17; N=8). The magnitude of depolarisation to KCl in cells isolated from PVs kept in culture was smaller (+13.4 ± 3.2 mV) than in fresh PVSMCs (+19.6 ± 3.6 mV), however this difference was not statistically significant (*P*>0.05). See Figure 52 for raw traces and mean data for SMCs isolated from fresh PVs and from PVs maintained in culture which were exposed to 80mM KCl.

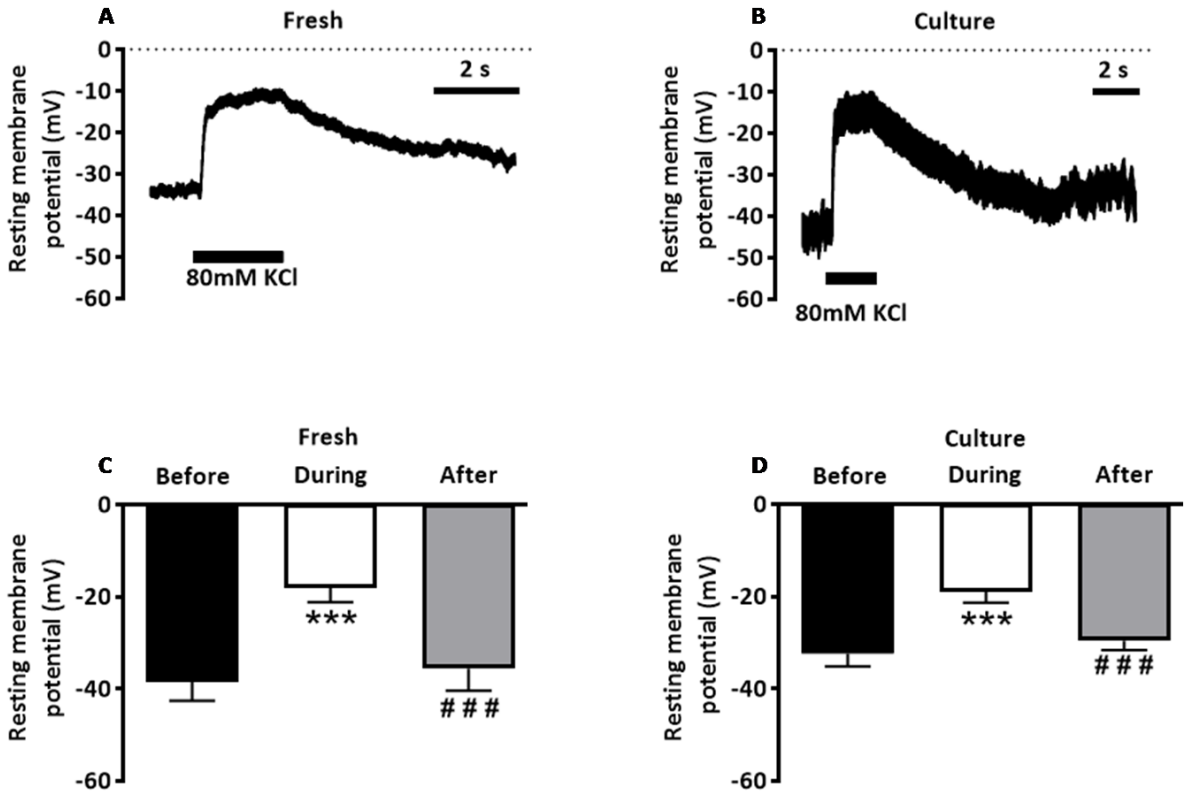

Figure 52. Effect of 80mM KCl on resting membrane potential of smooth muscle cells isolated from fresh pulmonary veins (PVs) and from PVs maintained in culture. Raw traces showing KCl application to A: cell isolated from fresh inferior PV and B: cell isolated from inferior PV maintained in culture for 24 hours. Black bars represent 80mM KCl application by Picospritzer®. Mean data (± S.E.M) showing resting membrane potential before, during and after application of 80mM KCl to smooth muscle cells C: isolated from fresh inferior PV (n=12; N=8) and D: isolated from inferior PV maintained in culture for 24 hours (n=17; N=8). ****P*<0.001 compared to "Before"; ###*P*<0.001 compared to "During" (analysis using repeated measures one-way ANOVA with Tukey's post-test)..

Resting Membrane Potential – Effect of K^+ channel Inhibitors and Hypoxia

4AP

In order to examine any putative role for K_V channels in control of RMP in PVSMCs, the K_V inhibitor 4AP (Dospinescu *et al.,* 2012) was used. There was no clear and definitive effect of 5mM 4AP application on RMP in PVSMCs. In cells isolated from fresh inferior PVs, RMP became progressively more depolarised over the experimental protocol from -36.5 ± 2.0 mV (before application) to -33.6 ± 2.6 mV (during application) to -32.3 ± 2.7 mV (after application) (n=8; N=8). The only significant difference was between baseline RMP and RMP after washout of 4AP ($P<0.05$). Cells isolated from PVs maintained in culture became progressively more hyperpolarised during the protocol from -43.8 ± 1.6 mV (before application) to -46.1 ± 1.1 mV (during application) to -48.3 ± 3.2 mV (after application) (n=5; N=5). However, RMP values before, during and after were not significantly different from one another ($P>0.05$). There was also no significant difference in the magnitude of the change in RMP with 4AP application in fresh PVSMCs (+3.0 ± 1.5 mV) and SMCs isolated from PVs kept in culture (-2.3 ± 1.9 mV)(($P>0.05$). Figure 53 shows raw traces showing application of 5mM 4AP and mean data for SMCs isolated from fresh PVs and from PVs maintained in culture.

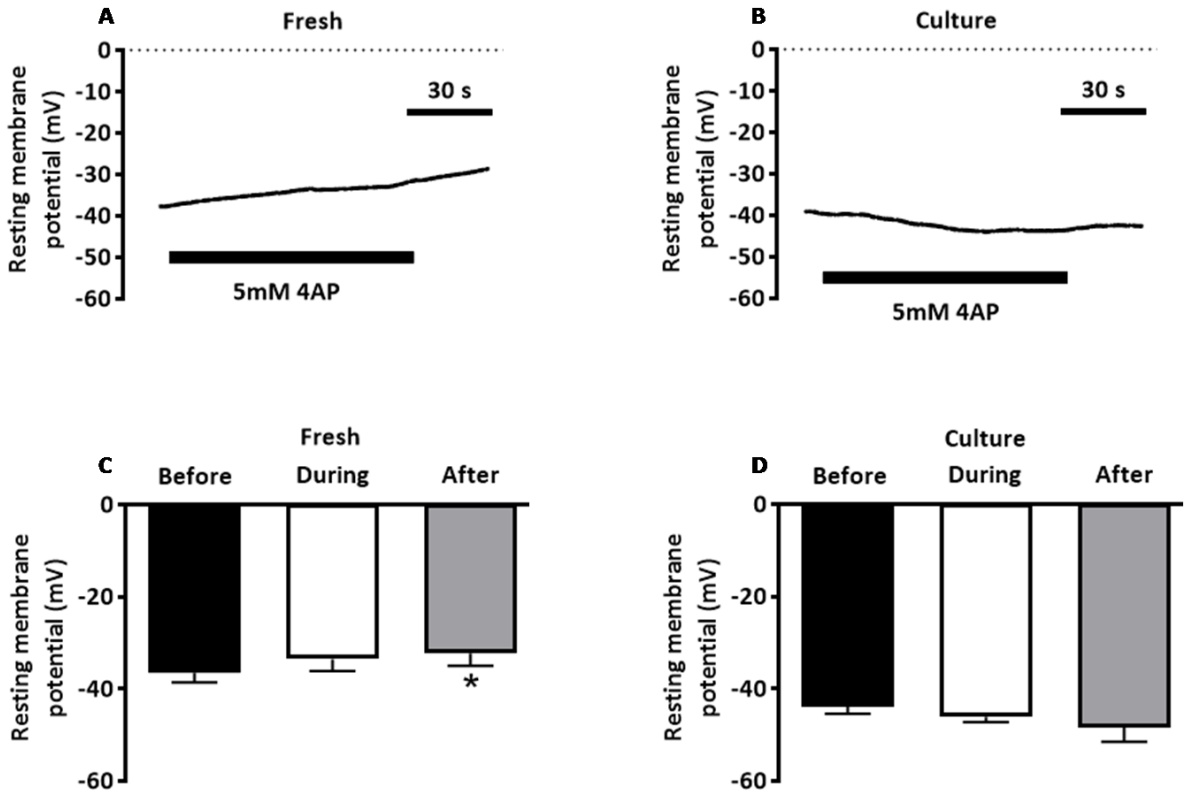

Figure 53. Effect of 5mM 4AP on resting membrane potential of smooth muscle cells isolated from fresh pulmonary veins (PVs) and from PVs maintained in culture. Raw traces showing 4AP application to A: a cell isolated from fresh inferior PV and B: a cell isolated from inferior PV maintained in culture for 24 hours. Black bars represent 5mM 4AP application by Picospritzer®. Mean data (± S.E.M) showing resting membrane potential before, during and after application of 5mM 4AP to smooth muscle cells C: isolated from fresh inferior PV (n=8; N=8) and D: isolated from inferior PV maintained in culture for 24 hours (n=5; N=5). **P*<0.05 compared to "Before" (analysis using repeated measures one-way ANOVA with Tukey's post-test).

TEA

To determine whether BK_{Ca} played a role in setting RMP in PVSMCs, the blocker TEA (Archer *et al.,* 1996, Moudgil *et al.,* 2005) was used. Application of TEA (5mM) caused significant depolarisation in all SMCs isolated from fresh inferior PVs from -45.4 ± 5.0 mV at baseline to -38.4 ± 4.1 mV (P<0.01). On washout of the drug, RMP recovered to -43.1 ± 5.2 mV (P<0.05 compared to "during" exposure, n=6; N=6). TEA caused depolarisation in five out of six SMCs isolated from PVs maintained in culture, the one cell which hyperpolarised on TEA application was excluded from further analysis. Of the cells which depolarised, RMP increased from -40.3 ± 5.3 mV to -25.6 ± 56 mV (P<0.05). Only three out of the five cells repolarised on washout of the drug, two cells depolarised further. Hence the mean RMP on recovery was not significantly different from the RMP during exposure (-32.7 ± 5.4 mV, P>0.05, n=5; N=5). Notably, the mean depolarisation induced by TEA was significantly larger in SMCs isolated from PVs maintained in culture (+14.7 ± 3.5 mV) than the depolarisation seen in fresh PVSMCs (+7.0 ± 1.2 mV, P<0.05). Figure 54 shows raw traces showing depolarisation on application of 5mM TEA and mean data for SMCs isolated from fresh PVs and from PVs maintained in culture.

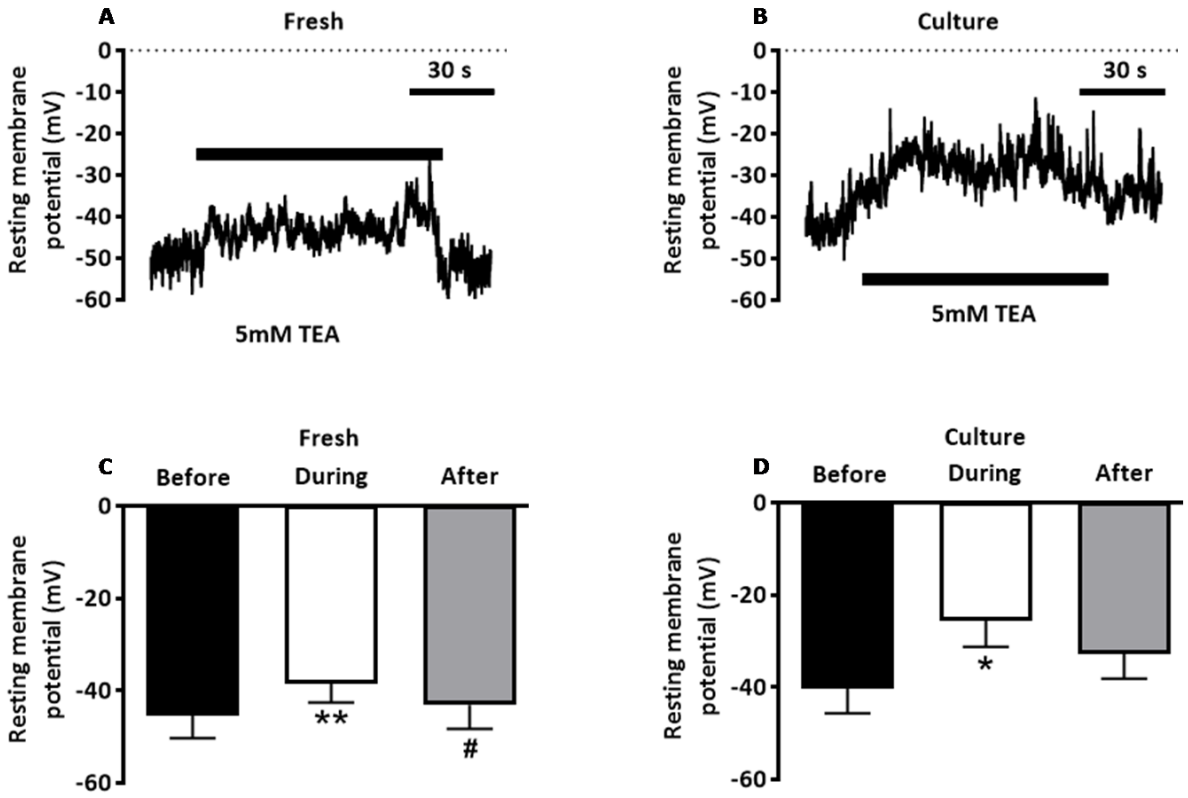

Figure 54. Effect of 5mM TEA on resting membrane potential of smooth muscle cells isolated from fresh pulmonary veins (PVs) and from PVs maintained in culture. Raw traces showing TEA application to A: a cell isolated from fresh inferior PV and B: a cell isolated from inferior PV maintained in culture for 24 hours. Black bars represent 5mM TEA application by Picospritzer®. Mean data (± S.E.M) showing resting membrane potential before, during and after application of 5mM TEA to smooth muscle cells C: isolated from fresh inferior PV (n=6; N=6) and D: isolated from inferior PV maintained in culture for 24 hours (n=5; N=5). *P<0.05 and ** P<0.01 compared to "Before". # P<0.05 compared to "During" (analysis using repeated measures one-way ANOVA with Tukey's post-test).

$ZnCl_2$

To evaluate whether TASK-1/3 channels were involved in controlling RMP of PVSMCs, the TASK-1/3 blocker $ZnCl_2$ was used (Ali *et al.,* 2014, Patel *et al.,* 2013). Application of 1mM $ZnCl_2$ had no significant effect on RMP of PVSMCs. In fresh PVSMCs, 50% of cells tested depolarised on application of $ZnCl_2$ and 50% hyperpolarised. On washout, 70% became depolarised and 30% became hyperpolarised relative to during application. Therefore, mean RMP in fresh PVSMCs did not change significantly over the course of experiments (before: -49.7 ± 2.9 mV, during: -50.1 ± 4.1 mV and after: -47.7 ± 4.1 mV; P>0.05, n=10; N=7).

In SMCs isolated from PVs maintained in culture, application of 1mM $ZnCl_2$ caused depolarisation in 43% of cells tested; all other cells hyperpolarised in response to $ZnCl_2$. When $ZnCl_2$ was washed out 43% of cells became depolarised and the others hyperpolarised relative to during application. Mean RMP in SMCs isolated from PVs kept in culture did not change significantly throughout the experimental protocol (before: -41.0 ± 4.3 mV, during: -43.6 ± 5.9 mV and after: -42.5 ± 4.2 mV; P>0.05, n=7; N=4). The mean effect in cells isolated from fresh PVs and from PVs maintained in culture was a slight non-significant hyperpolarisation relative to baseline (-0.3 ± 3.8 mV and -2.6 ± 2.7 mV, respectively). The effect magnitudes were not significantly different from one another (P>0.05). Figure 55 shows raw traces demonstrating hyperpolarisation on application of 1mM $ZnCl_2$ and mean data for SMCs isolated from fresh PVs and from PVs maintained in culture.

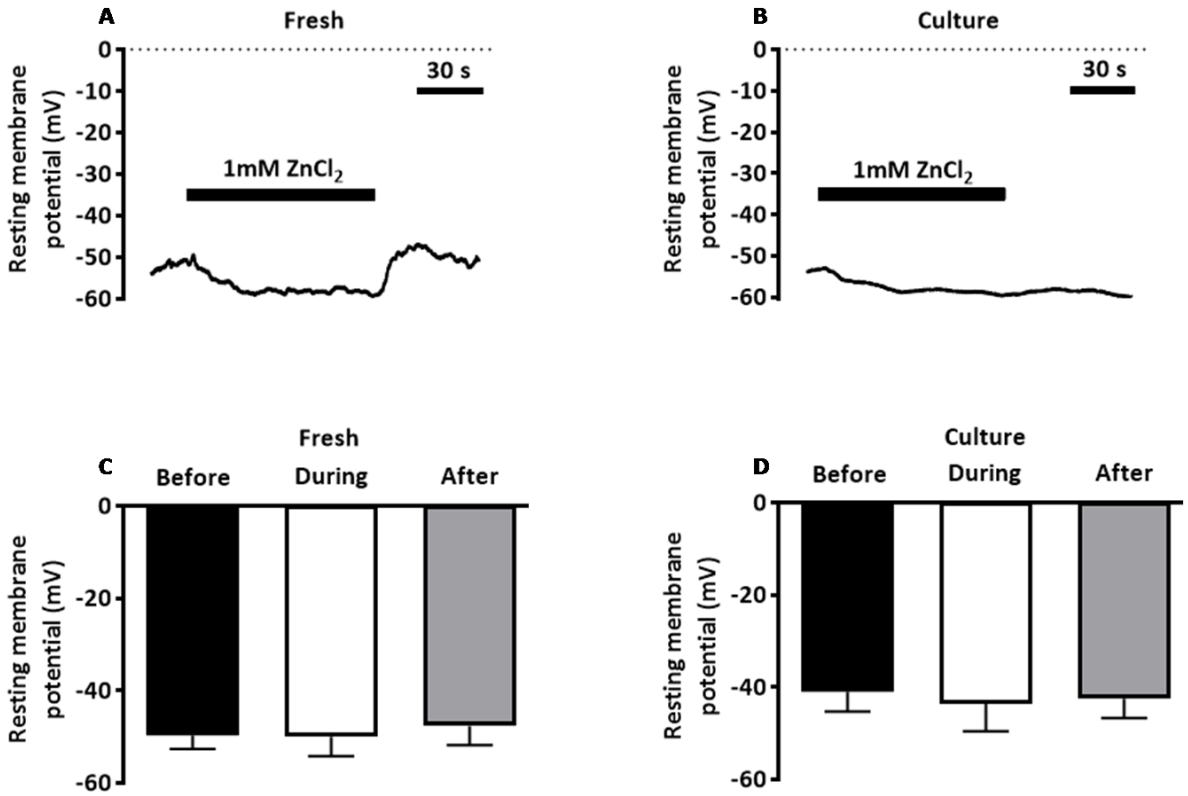

Figure 55. Effect of 1mM $ZnCl_2$ on resting membrane potential of smooth muscle cells isolated from fresh pulmonary veins (PVs) and from PVs maintained in culture. Raw traces showing $ZnCl_2$ application to A: a cell isolated from fresh inferior PV and B: a cell isolated from inferior PV maintained in culture for 24 hours. Black bars represent 1mM $ZnCl_2$ application by Picospritzer®. Mean data (± S.E.M) showing resting membrane potential before, during and after application of 1mM $ZnCl_2$to smooth muscle cells C: isolated from fresh inferior PV (n=10; N=7) and D: isolated from inferior PV maintained in culture for 24 hours (n=7; N=4) (analysis using repeated measures one-way ANOVA with Tukey's post-test).

Hypoxia

In fresh PVSMCs, exposure to hypoxic bath solution resulted in depolarisation of the RMP in all but one cell (which was then excluded from further analysis). On removing hypoxic flow and reinstating normoxic bath solution, one cell hyperpolarised and all others continued to depolarise. RMP started at an initial mean level of -39.9 ± 4.8 mV which increased to -34.9 ± 4.9 mV during hypoxic flow (P<0.001, n=8; N=5). RMP then further depolarised on reoxygenation to -31.5 ± 5.2 mV (P<0.01 compared to "before", n=8; N=5).

In SMCs isolated from PVs kept in culture conditions, exposure to hypoxic flow resulted in depolarisation of the RMP in all but one cell (which was then excluded from further analysis). On reoxygenation, 2 cells hyperpolarised and all others continued to depolarise. RMP increased from -36.6 ± 5.8 mV to -29.4 ± 5.2 mV although the difference was not statistically significant (P>0.05, n=6; N=4). RMP then further depolarised on reoxygenation to a level significantly higher than baseline RMP (-27.5 ± 5.9 mV, P<0.05, n=6; N=4).

The magnitude of depolarisation in fresh PVSMCs (+5.0 ± 0.6 mV) was not significantly different from the depolarisation seen in SMCs from PVs maintained in culture (+7.2 ± 2.1 mV, P>0.05). Similarly, there was no significant difference in the magnitude of depolarisation on reoxygenation (fresh: +3.4 ± 1.2 mV; culture: +1.8 ± 2.8 mV; P>0.05). Figure 56 shows raw traces demonstrating depolarisation of RMP on hypoxic flow and reoxygenation and mean data for SMCs isolated from fresh PVs and from PVs maintained in culture.

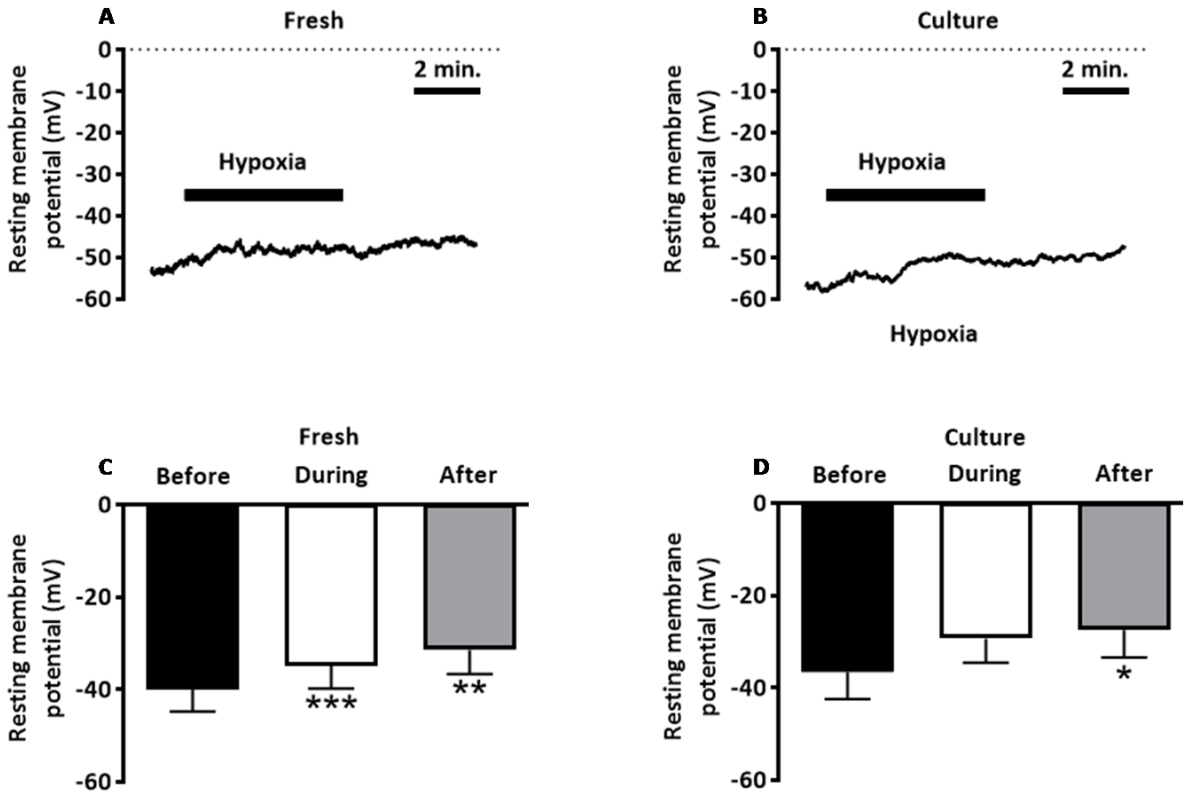

Figure 56. Effect of hypoxia and reoxygenation on resting membrane potential of smooth muscle cells isolated from fresh pulmonary veins (PVs) and from PVs maintained in culture. Raw traces showing hypoxic exposure to A: a cell isolated from fresh inferior PV and B: a cell isolated from inferior PV maintained in culture for 24 hours. Black bars represent duration of hypoxic flow. Mean data (± S.E.M) showing resting membrane potential before (normoxia), during (hypoxia) and after (reoxygenation) for smooth muscle cells C: isolated from fresh inferior PV (n=8; N=5) and D: isolated from inferior PV maintained in culture for 24 hours (n=6; N=4). **P*<0.05, ** *P*<0.01 and ****P*<0.001 compared to "Before" normoxic resting membrane potential (analysed using repeated measures one-way ANOVA with Tukey's post-test).

Voltage-activated Whole-cell Currents - Effect of K^+ Channel inhibitors

To help further identify K^+ channels which may contribute to RMP in PVSMCS and therefore be potential candidates for involvement in the hypoxic response, voltage-activated whole cell currents were studied in the presence of 4AP, TEA or $ZnCl_2$.

In order to characterise voltage-activated whole cell currents present in PVSMCs, a protocol involving 400-ms depolarising voltage steps in 10mV increments was applied from a holding voltage of -80mV. In the absence of drugs ("before" traces), the voltage-activated whole-cell currents were large, rapidly activating, non-inactivating outward currents (I_{out}) with superimposed spontaneous transient outward currents (STOCs). The presence of STOCs, particularly at the higher voltage steps suggested a complex current with multiple components. In an attempt to identify the types of K^+ channels contributing to the multi-component currents elicited, the protocol was run before, during and after application of 5mM 4AP, 5mM TEA and 1mM $ZnCl_2$. These drugs were chosen to investigate the role of K_V, BK_{Ca} and TASK-1/3 channels, respectively, in the voltage-activated I_{out} of PVSMCs.

4AP

To evaluate the contribution of K_V channels to the voltage-activated outward current in PVSMCs, the K_V blocker 4AP (Dospinescu *et al.*, 2012) was used. In fresh PVSMCs, application of 5mM 4AP by Picospritzer® had no significant effect on the mean steady-state current density across the voltage step protocol. Mean steady-state outward current density at +80mV was not significantly different before, during and after washout of 4AP: 45.4 ± 14.2 pA/pF, 39.5 ± 11.7 pA/pF and 42.0 ± 13.1 pA/pF, respectively (P>0.05, n=7; N=6). Raw traces of currents before, during and after 4AP application and mean current density-voltage relationship for fresh PVSMCs are shown in Figure 57.

In SMCs isolated from PVs maintained in culture conditions, 5mM 4AP application did not significantly alter the mean steady-state current density across the voltage step protocol. Mean steady-state current at +80mV was not significantly different before, during and after washout of 4AP: 78.2 ± 21.6 pA/pF, 66.6 ± 15.5 pA/pF and 78.1 ± 17.5 pA/pF, respectively (P>0.05, n=6; N=6). Raw traces of currents before, during and after 4AP application and mean current density-voltage relationship for SMCs isolated from PVs maintained in culture conditions are shown in Figure 58.

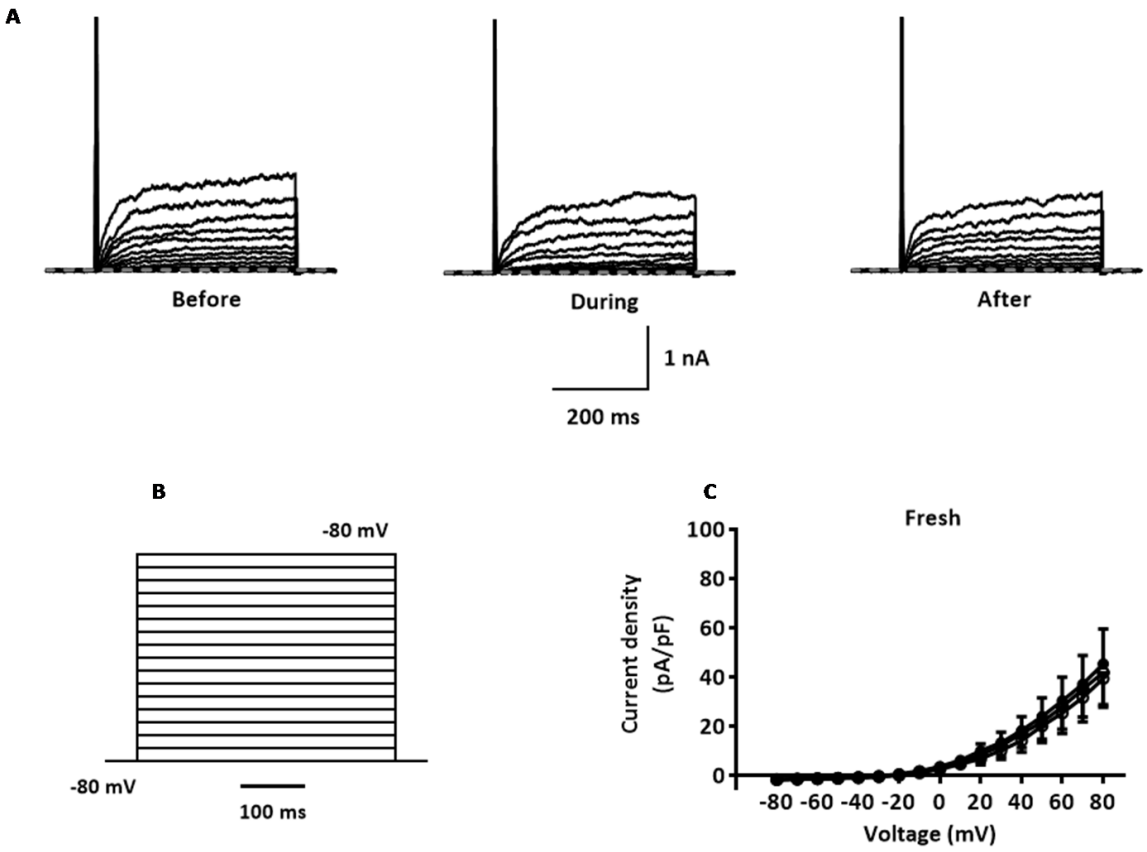

Figure 57. The effect of 5mM 4AP on voltage-activated outward currents in fresh pulmonary vein smooth muscle cells. A: representative raw current traces recorded in response to application of voltage step protocol (B) before, during and after 4AP application; grey dashed line marks zero current level, capacitance transients have been truncated for clarity. C: Mean (± S.E.M) current density values for 7 cells before (filled circles), during (open circled) and after (half-filled circles) 4AP application plotted against test potential to give current-voltage relationship (n=7; N=6); analysis using repeated measures two-way ANOVA with Bonferroni's post test. Note that one cell was excluded from this data set as a positive outlier.

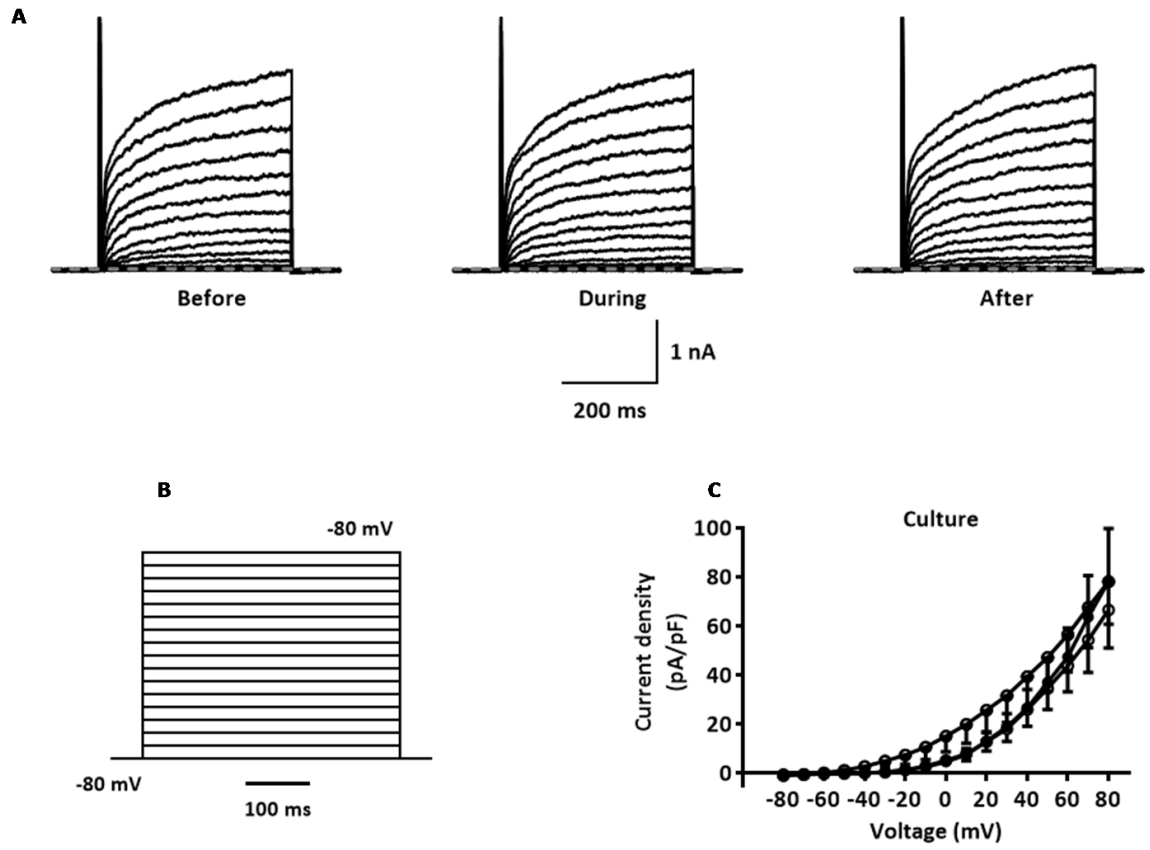

Figure 58. The effect of 5mM 4AP on voltage-activated outward currents in smooth muscle cells isolated from pulmonary veins maintained in culture conditions for 24 hours. A: representative raw current traces recorded in response to application of voltage step protocol (B) before, during and after 4AP application; grey dashed line marks zero current level, capacitance transients have been truncated for clarity. C: Mean (± S.E.M) current density values for 6 cells before (filled circles), during (open circled) and after (half-filled circles) 4AP application plotted against test potential to give current-voltage relationship (n=6; N=6); analysis using repeated measures two-way ANOVA with Bonferroni's post test.

TEA

To determine whether BK_{Ca} channels contribute to the voltage-activated outward current in PVSMCs, the blocker TEA (Archer *et al.,* 1996, Moudgil *et al.,* 2005) was used. In fresh PVSMCs, application of 5mM TEA resulted in significant inhibition of the mean steady-state current density at voltage steps between +30 and +80mV. At +80mV TEA produced a 49% inhibition of current density (from 40.5 ± 8.5 pA/pF (before) to 20.6 ± 7.8 pA/pF (during), *P*<0.001, n=4; N=4). One minute after washout of the drug, the current density at +80mV recovered to 97% of the original baseline (39.2 ± 10.1 pA/pF, *P*<0.001 compared to "during" TEA exposure). Representative current traces and current density-voltage relationships for fresh PVSMCs are shown in Figure 59.

In SMCs isolated from PVs kept in culture, application of TEA also significantly reduced the mean steady-state current density starting from a higher test potential of +40mV (*P*<0.05). At +80mV, TEA produced a marked 70% inhibition of the current density (from 101.6 ± 28.2 pA/pF (before) to 30.5 ± 9.7 pA/pF (after), *P*<0.001, n=5; N=5). After one minute of drug washout, current density at +80mV returned to 105% of the original baseline value (106.8 ± 58.1 pA/pF), *P*<0.001 compared to "during" TEA exposure). Representative raw traces and current-voltage relationships are shown in Figure 60.

As TEA had a marked effect on outward current magnitude in PVSMCs, the impact of TEA exposure was analysed in more detail by investigating the impact on outward current activation kinetics. "One-phase association" curves were fitted (using GraphPad Prism 7) for currents recorded at-10mV to +80mV. At voltage steps between -80mV and -20mV, curve fitting was often ambiguous and values for τ_{act} could not be calculated. In fresh PVSMCs, no change in activation kinetics (assessed by τ_{act} values) was observed across all test potentials applied (P>0.05, n=4; N=4). Figure 61 shows raw traces with curve fitting and mean τ_{act} values plotted against test potential for fresh PVSMCs. In SMCs isolated from PVs kept in culture conditions, the only significant change in activation kinetics was observed at -10mV where currents "after" washout of TEA were significantly slower to activate (mean τ_{act}= 162.2 ± 75.4 ms) than "during" TEA exposure (mean τ_{act}= 55.2 ± 29.7 ms, *P*<0.05, n=5; N=5). There was no significant difference between mean τ_{act} for "during"/"after" and "before" TEA exposure at -10mV (80.4 ± 13.2 ms, *P*>0.05). There was also no significant difference between τ_{act} values at any other test potential. Raw traces showing curve fitting and mean τ_{act} values plotted against test potential for SMCs isolated from PVs kept in culture are shown in Figure 62.

Overall, TEA reduced current magnitude at +80mV by approximately 50% in fresh PVSMCs and by 70% in SMCs isolated from PVs maintained in culture conditions for 24 hours and significant inhibition began at test potentials between +30 and +40 mV. There was no clear effect on the rate of

activation of voltage-activated outward currents in SMCs. Therefore, it could be implied that the TEA-sensitive current in fresh inferior PVSMCs would have a steady-state I_{out} of approximately 50% of control "before" currents and in SMCs isolated from PVs kept in culture would have a steady-state I_{out} of approximately 70% of control "before" currents. It could also be implied that activation kinetics would be similar to control currents. In order to fully characterise the TEA-sensitive component of I_{out} in inferior PVSMCs in terms of shape and kinetics, current values recorded "during" TEA exposure were subtracted from values from "before" exposure to reveal the TEA-sensitive difference current (see Figure 63).

The TEA-sensitive difference current was significantly larger in SMCs isolated from PVs maintained in culture compared to fresh PVSMCs at test potentials of +70 and +80 mV (P<0.01). At +80mV the mean TEA-sensitive difference current in SMCs isolated from PVs kept in culture (expressed in current density) was 71.2 ± 22.3 pA/pF (n=5; N=5) whereas in fresh PVSMCs the current was 19.8 ± 3.9 pA/pF (n=4; N=4). The current was rapidly activating and non-inactivating as previously suspected owing to the lack of an effect of TEA on τ_{act} values. Mean (±S.E.M) difference current density values were plotted against test potential in order to illustrate and compare the difference current-voltage relationships for fresh and culture PVSMCs (shown in Figure 63).

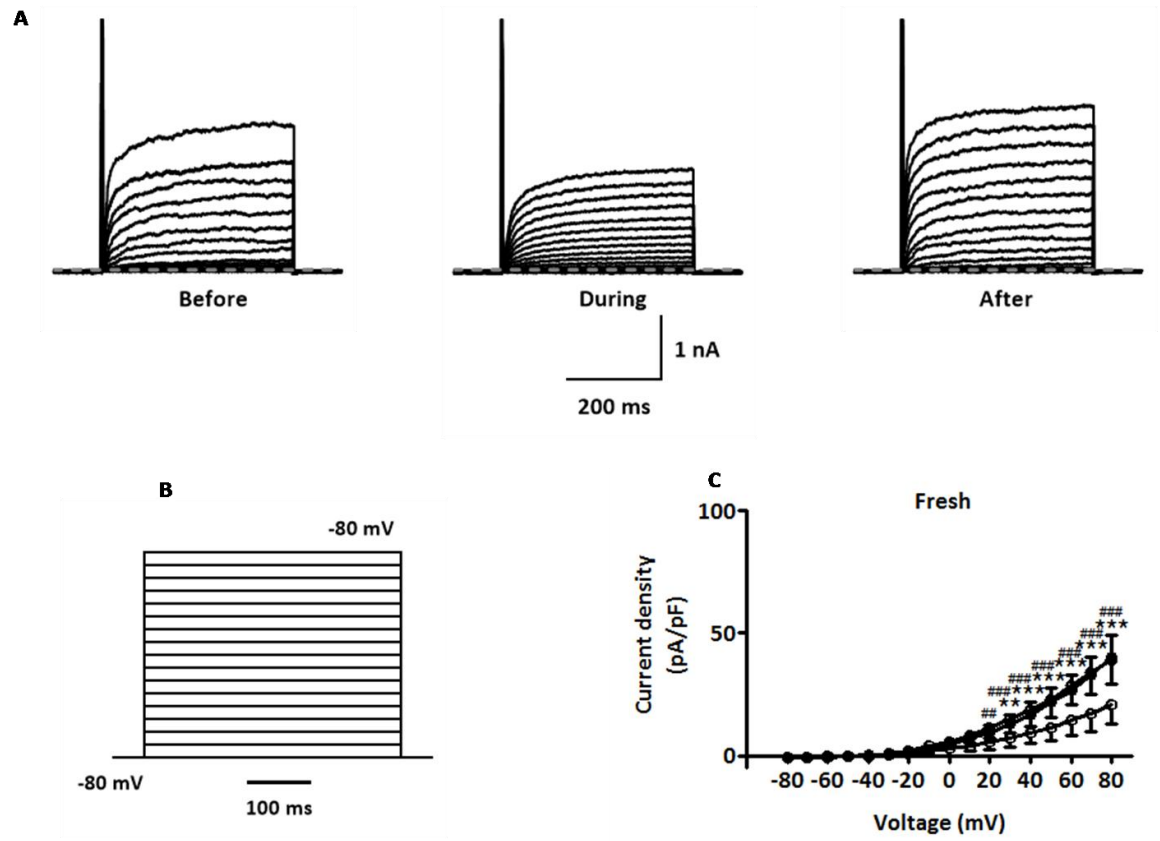

Figure 59. The effect of 5mM TEA on voltage-activated outward currents in fresh pulmonary vein smooth muscle cells. A: representative raw current traces recorded in response to application of voltage step protocol (B) before, during and after TEA application; grey dashed line marks zero current level, capacitance transients have been truncated for clarity. C: Mean (± S.E.M) current density values for 4 cells before (filled circles), during (open circles) and after (half-filled circles) TEA application plotted against test potential to give current-voltage relationship. ***P*<0.01 and ****P*<0.001 "during" compared to "before". ##*P*<0.01 and ### *P*<0.001 "after" compared to "during" (n=4; N=4); analysis using repeated measures two-way ANOVA with Bonferroni's post test. Note that one cell was excluded from this data set as a positive outlier.

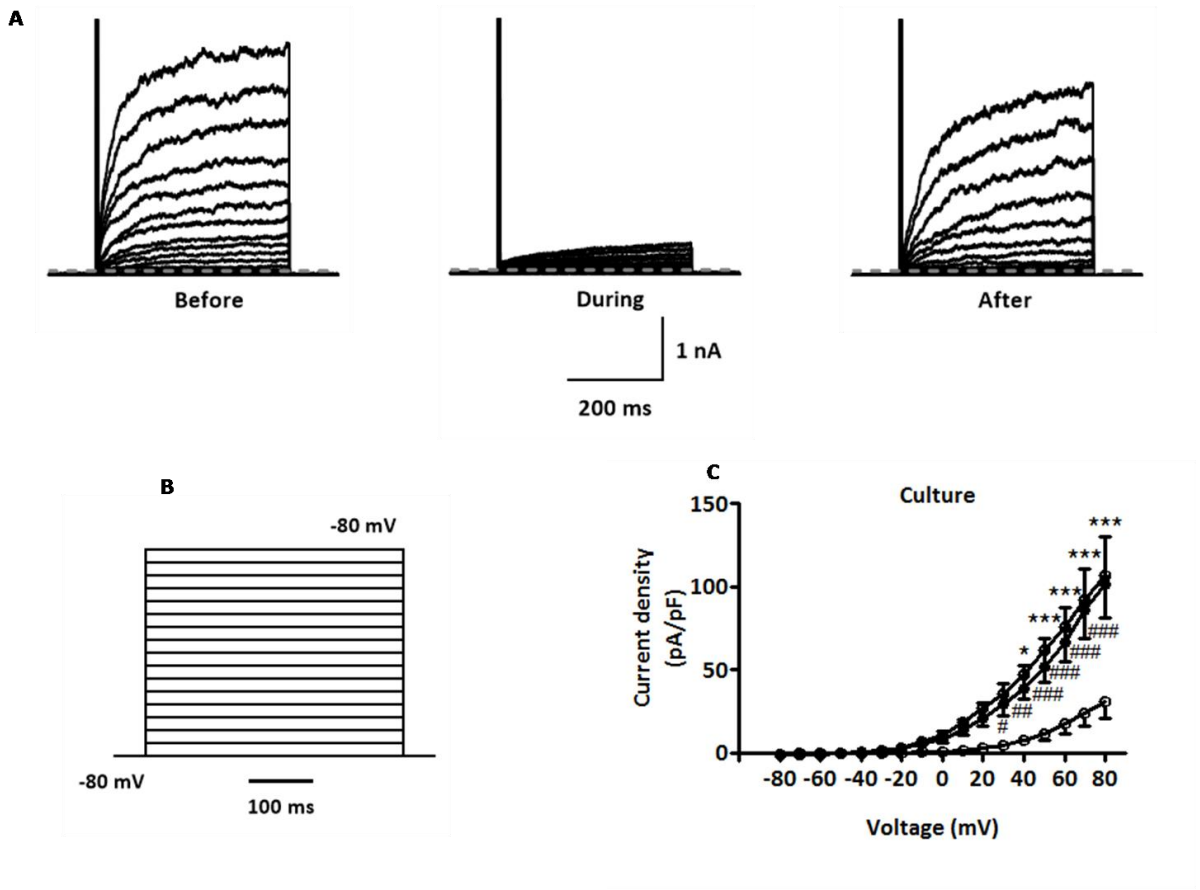

Figure 60. The effect of 5mM TEA on voltage-activated outward currents in smooth muscle cells isolated from pulmonary veins maintained in culture conditions for 24 hours. A: representative raw current traces recorded in response to application of voltage step protocol (B) before, during and after TEA application; grey dashed line marks zero current level, capacitance transients have been truncated for clarity. C: Mean (± S.E.M) current density values for 5 cells before (filled circles), during (open circles) and after (half-filled circles) TEA application plotted against test potential to give current-voltage relationship. **P*<0.05 and ****P*<0.001 "during" compared to "before". #*P*<0.05, ##*P*<0.01 and ###*P*<0.001 "after" compared to "during" (n=5; N=5); analysis using repeated measures two-way ANOVA with Bonferroni's post test.

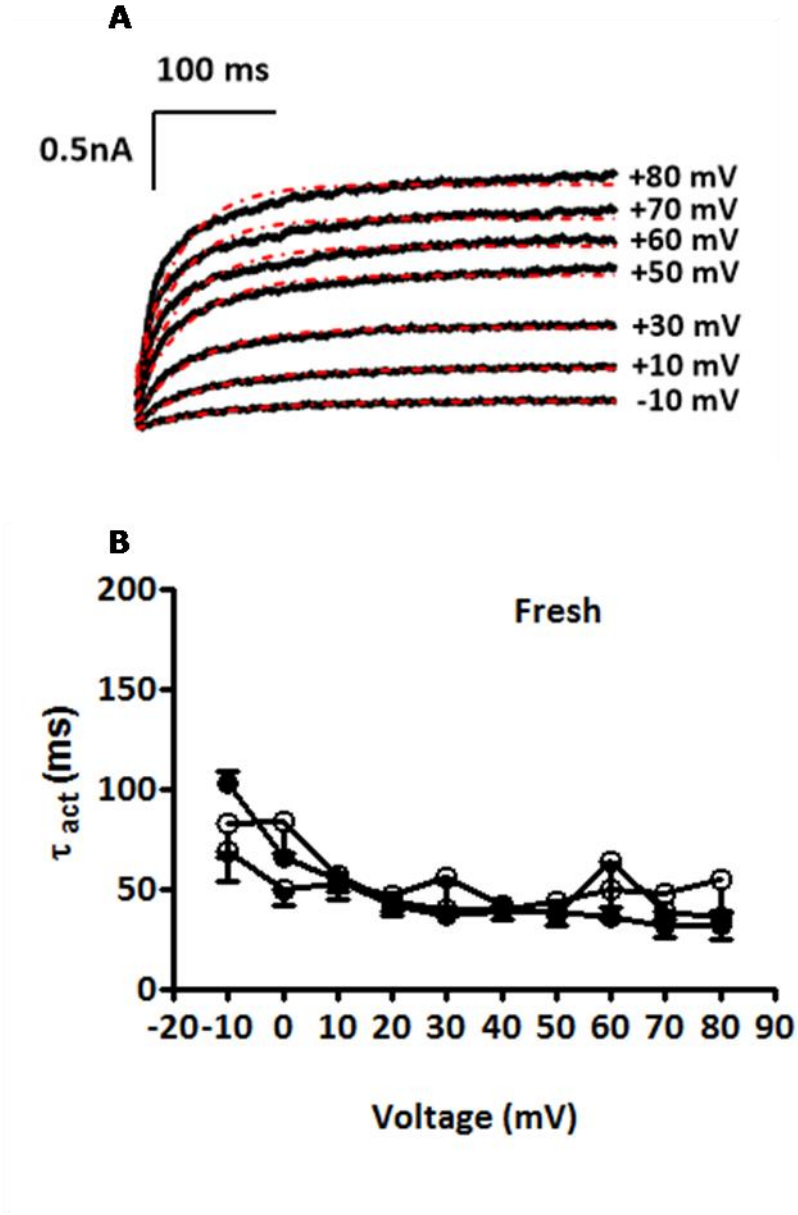

Figure 61. The effect of 5mM TEA on activation of outward currents in fresh pulmonary vein smooth muscle cells. A: raw traces showing activation of currents across different voltages in the presence of 5mM TEA. Black solid lines represent currents recorded and red dashed lines are curves fitted using "one-phase association" (GraphPad Prism 7); for clarity, not all traces are shown. B: Mean τ_{act} plotted against test potential "before" (filled circles), "during" (open circles) and "after" (half-filled circles) TEA exposure by Picospritzer®. (n=4; N=4); analysis using repeated measures two-way ANOVA with Bonferroni's post test. Note that one cell was excluded from this data set as a positive outlier.

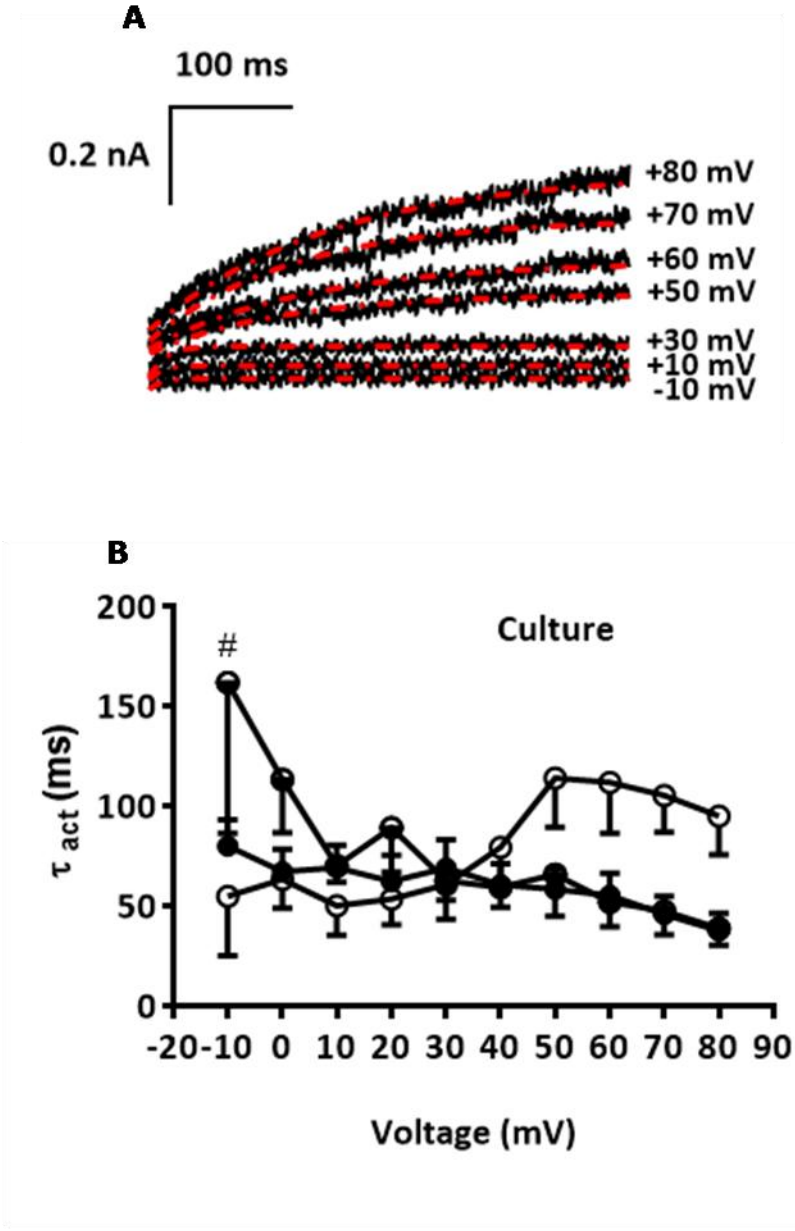

Figure 62. The effect of 5mM TEA on activation of outward currents in smooth muscle cells isolated from pulmonary veins maintained in culture for 24 hours. A: raw traces showing activation of currents across different voltages in the presence of 5mM TEA. Black solid lines represent currents recorded and red dashed lines are curves fitted using "one-phase association" (GraphPad Prism 7); for clarity, not all traces are shown. B: Mean τ_{act} plotted against test potential "before" (filled circles), "during" (open circles) and "after" (half-filled circles) TEA exposure by Picospritzer®. #P<0.05 "after" compared to "during" (n=5; N=5); analysis using repeated measures two-way ANOVA with Bonferroni's post test.

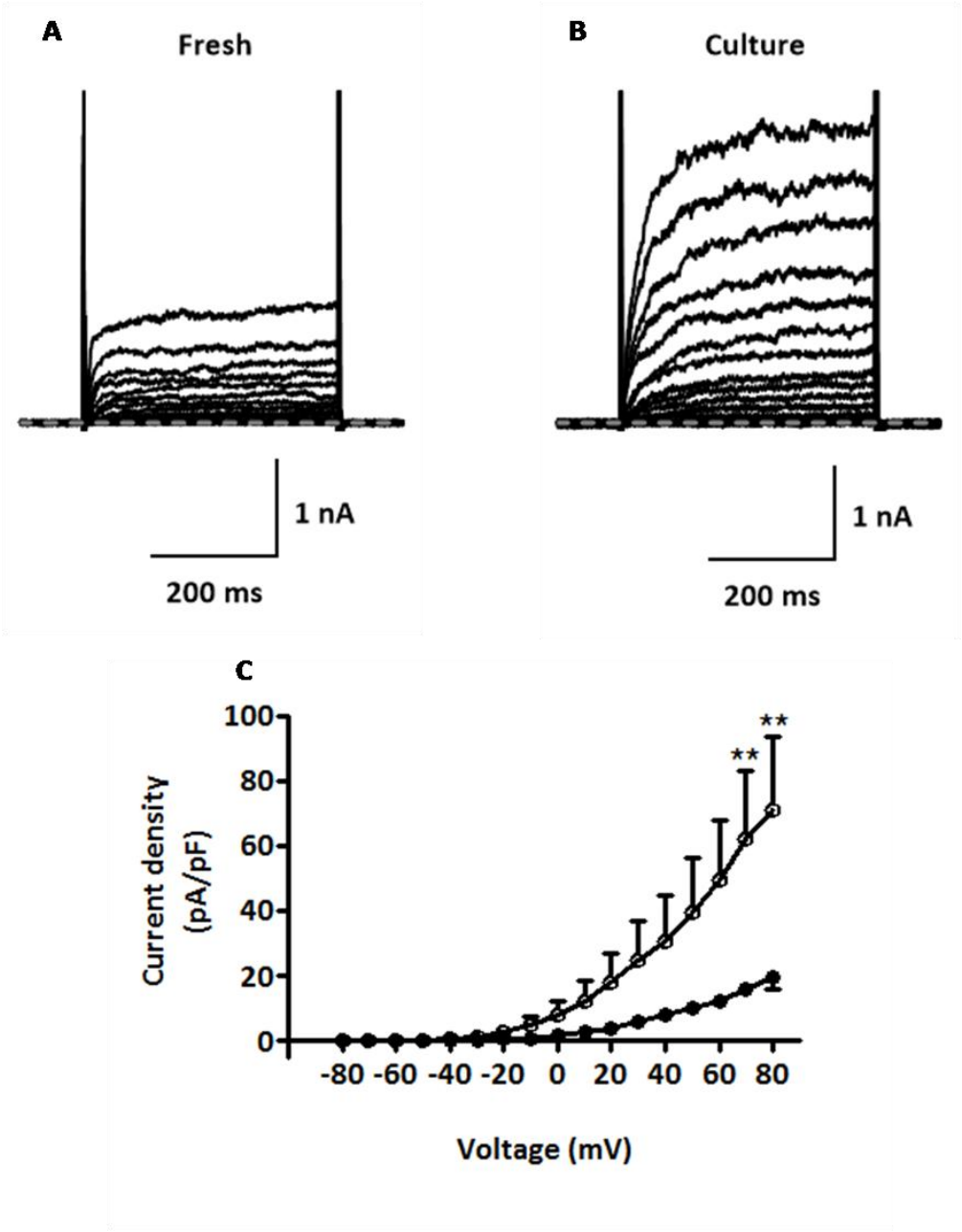

Figure 63. TEA-sensitive difference current in smooth muscle cells from fresh pulmonary veins (PVs) and from PVs maintained in culture for 24 hours. A: representative family of TEA sensitive difference currents obtained by subtracting current values "during" 5mM TEA exposure from "before" current values. Currents were elicited by depolarising voltage steps from -80mV to +80mV in 10mV increments starting from a holding potential of -80mV; grey dashed line marks zero current level, capacitance transients have been truncated for clarity. B: Mean (± S.E.M) current density values for 4 cells isolated from fresh inferior PVs (filled circles) and 5 cells isolated from PVs maintained in culture conditions (open circles) (fresh: n=4; N=4, culture: n=5; N=5). ***P*<0.01 fresh compared to culture (analysis using repeated measures two-way ANOVA with Bonferroni's post test). Note that one cell was excluded for the "fresh" group as a positive outlier.

$ZnCl_2$

To investigate the contribution of TASK channels to the voltage-activated whole cell currents in PVSMCs, the TASK-1/3 channel inhibitor $ZnCl_2$ was used (Ali *et al.,* 2014, Patel *et al.,* 2013). Application of 1mM $ZnCl_2$ significantly inhibited steady-state I_{out} at +60mV, +70mV and +80mV in fresh PVSMCs. At a test potential of +80mV, $ZnCl_2$ reduced voltage-activated currents by 32% from 67.7 ± 17.8 pA/pF to 45.8 ± 9.2 pA/pF (*P*<0.001, n=6; N=4). After one minute of washout of the drug, steady-state I_{out} at +80mV did not recover fully but returned to 82% of the original current elicited before application (55.8 ± 16.1 pA/pF, *P*>0.05 compared to "before" and "during"). Representative current traces and current density-voltage relationships for fresh PVSMCs are shown in Figure 64.

In PVSMCs isolated from vessels maintained in culture for 24 hours, $ZnCl_2$ also reduced the mean steady-state outward current density however significant inhibition was present at a lower test potential of +30mV (*P*<0.05). At +80mV, mean currents were reduced by 26% from 42.2 ± 7.2 pA/pF to 31.1 ± 4.0 pA/pF (*P*<0.001, n=6; N=5). On washout for one minute, steady state I_{out} +80mV recovered to 104% of original baseline values (43.7 ± 9.1 pA/pF, *P*<0.001). Significant recovery of the current was also seen for test potentials between +40mV and +70mV. Representative current traces and current density-voltage relationships for PVSMCs isolated from vessels maintained in culture are shown in Figure 65.

The impact of $ZnCl_2$ exposure on PVSMC outward current activation kinetics was also analysed. In fresh PVSMCs, the only significant difference in activation kinetics when comparing currents "before", "during" and "after" $ZnCl_2$ was at a test potential of 0mV. Outward currents at 0mV became more rapidly activating over time reflected by decreasing values for time constant of activation (τ_{act}) – before $ZnCl_2$ exposure: 108.4 ± 21.5 ms, during $ZnCl_2$ exposure: 80.7 ± 11.5 ms and after $ZnCl_2$ washout: 60.9 ± 11.1 ms. The only difference which reached significance was by comparing "before" to "after" activation (*P*<0.05, n=6; N=4). In PVSMCs isolated from vessels maintained in culture no significant difference was seen across all test potentials when "before", "during" and "after" current activation kinetics were compared (*P*>0.05, n=6; N=5). Raw traces showing curve fitting and mean τ_{act} plotted against test potential for fresh PVSMCs and PVSMCs isolated from vessels maintained in culture are shown in Figure 66 and 67, respectively.

Overall, $ZnCl_2$ reduced current magnitude by 32% at test potentials of between +60 and +80mV for fresh PVSMCs and by 26% between +30 and +80mV for SMCs isolated from PVs maintained in culture conditions for 24 hours. However there was no clear effect on the rate of activation of voltage-activated outward currents in SMCs. Therefore, it could be suggested that the $ZnCl_2$-sensitive current

in inferior PVSMCs would have a steady-state I_{out} of approximately 30% of control "before" currents and similar activation kinetics. In order to fully characterise the $ZnCl_2$-sensitive component of I_{out} in inferior PVSMCs, difference currents were calculated as described previously for TEA.

In the majority of PVSMCs, the $ZnCl_2$-sensitive difference current was rapidly activating and non-inactivating (see representative current traces in Figure 68). However in one cell from fresh PV and one cell from PV maintained in culture revealed that $ZnCl_2$ appeared to activate an outward current at test potentials between +60 and +80 mV since the difference current was negative. These two cells were excluded from further data analysis for the $ZnCl_2$-sensitive difference current.

Mean (±S.E.M) difference current density values were plotted against test potential in order to illustrate the difference current-voltage relationship. Current-voltage plots for fresh and culture PVSMCs were compared to identify any differences (shown in Figure 68). At a test potential of +80mV the $ZnCl_2$-sensitive difference current was significantly larger in fresh PVSMCs than SMCs isolated from PVs maintained in culture for 24 hours (P<0.01; n=5 and N=4 for both).

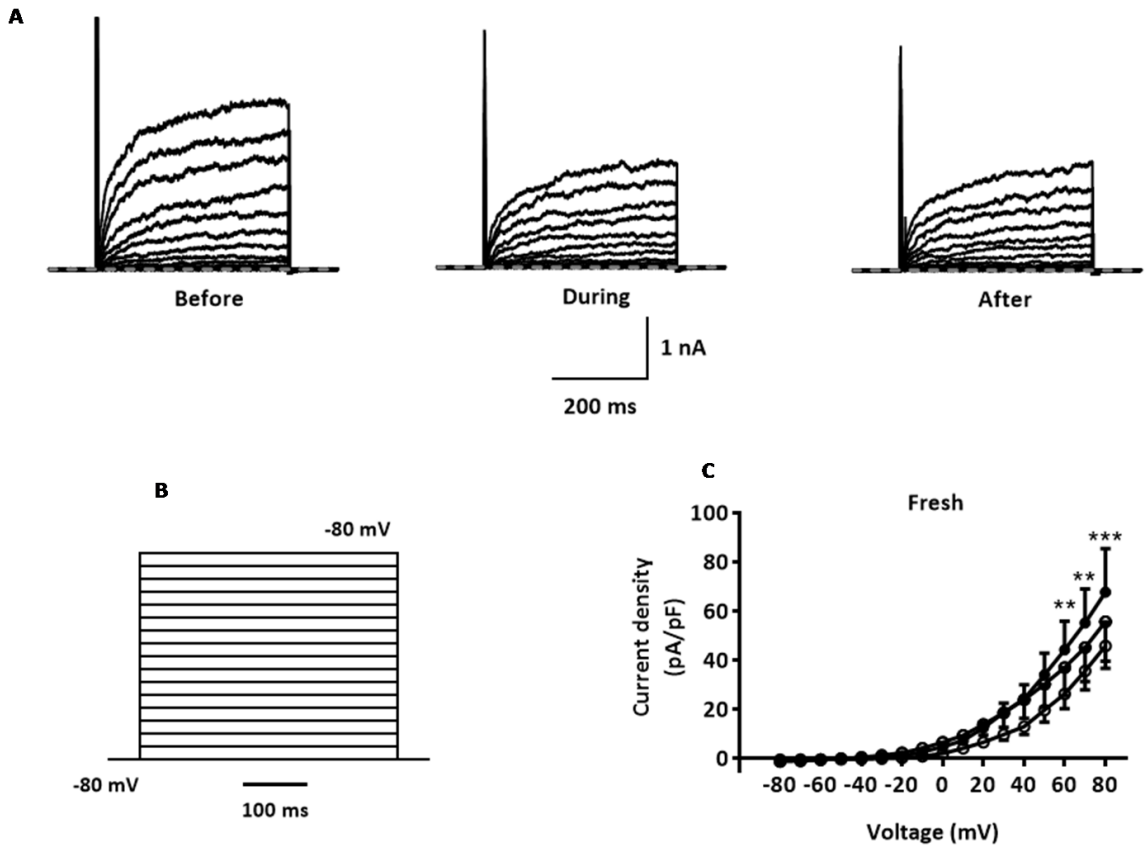

Figure 64. The effect of 1mM $ZnCl_2$ on voltage-activated outward currents in fresh pulmonary vein smooth muscle cells. A: representative raw current traces recorded in response to application of voltage step protocol (B) before, during and after $ZnCl_2$ application; grey dashed line marks zero current level, capacitance transients have been truncated for clarity. C: Mean (± S.E.M) current density values for 6 cells before (filled circles), during (open circles) and after (half-filled circles) $ZnCl_2$ application plotted against test potential to give current-voltage relationship. ***P*<0.01 and ****P*<0.001 "during" compared to "before" (n=6; N=4); analysis using repeated measures two-way ANOVA with Bonferroni's post test.

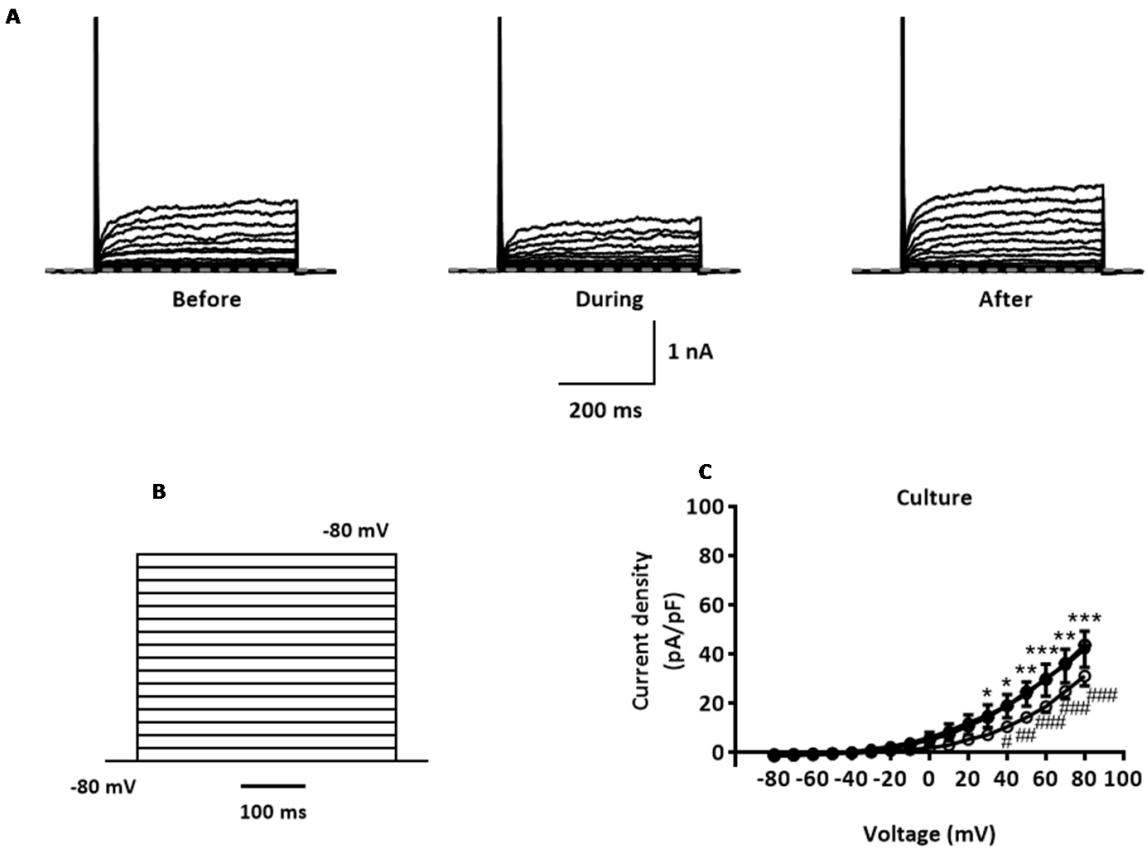

Figure 65. The effect of 1mM $ZnCl_2$ on voltage-activated outward currents in smooth muscle cells isolated from pulmonary veins maintained in culture conditions for 24 hours. A: representative raw current traces recorded in response to application of voltage step protocol (B) before, during and after $ZnCl_2$ application; grey dashed line marks zero current level, capacitance transients have been truncated for clarity. C: Mean (± S.E.M) current density values for 6 cells before (filled circles), during (open circles) and after (half-filled circles) $ZnCl_2$ application plotted against test potential to give current-voltage relationship. **P*<0.05, ***P*<0.01 and ****P*<0.001 "during" compared to "before". #*P*<0.05, ##*P*<0.01 and ###*P*<0.001 "after" compared to "during" (n=6; N=5); analysis using repeated measures two-way ANOVA with Bonferroni's post test.

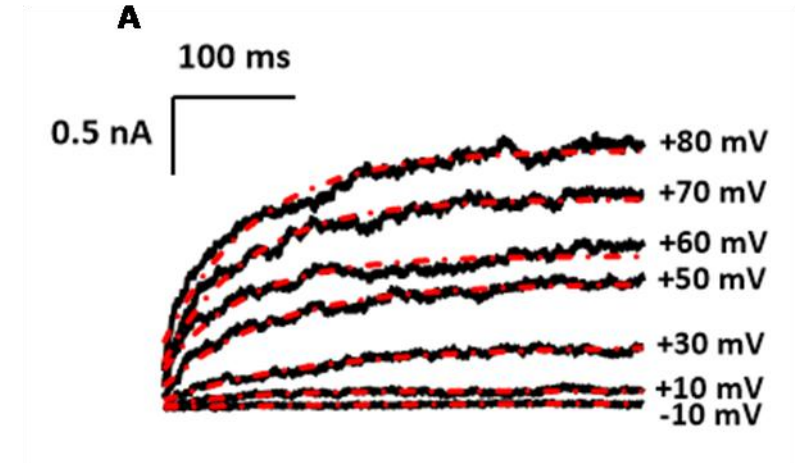

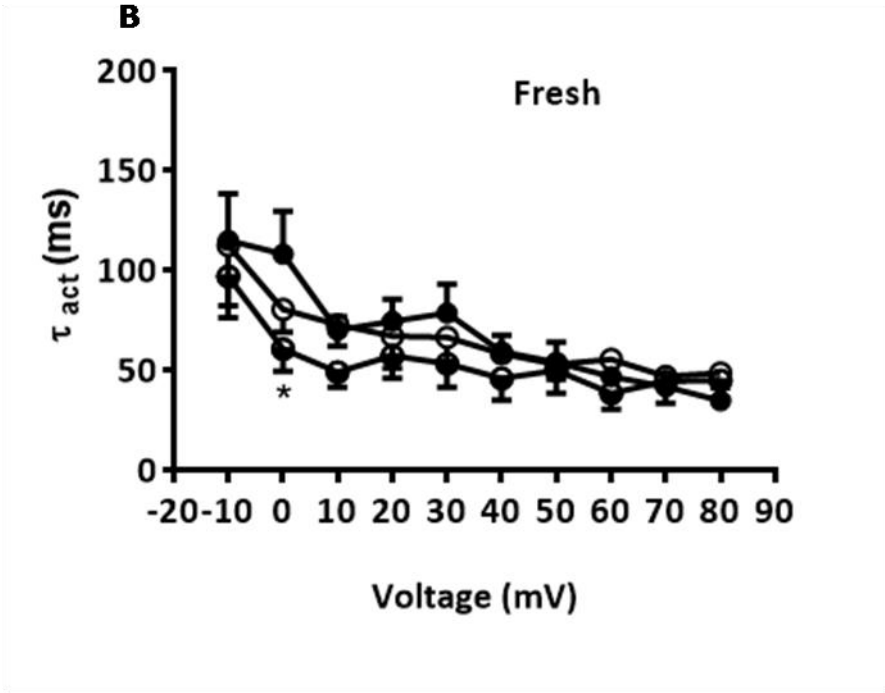

Figure 66. The effect of 1mM $ZnCl_2$ on activation of outward currents in fresh pulmonary vein smooth muscle cells. A: raw traces showing activation of currents across different voltages in the presence of 1mM $ZnCl_2$. Black solid lines represent currents recorded and red dashed lines are curves fitted using "one-phase association" (GraphPad Prism 7); for clarity, not all traces are shown. B: Mean τ_{act} plotted against test potential "before" (filled circles), "during" (open circles) and "after" (half-filled circles) $ZnCl_2$exposure by Picospritzer®. **P*<0.05 "after" compared to "before" (n=6; N=4); analysis using repeated measures two-way ANOVA with Bonferroni's post test.

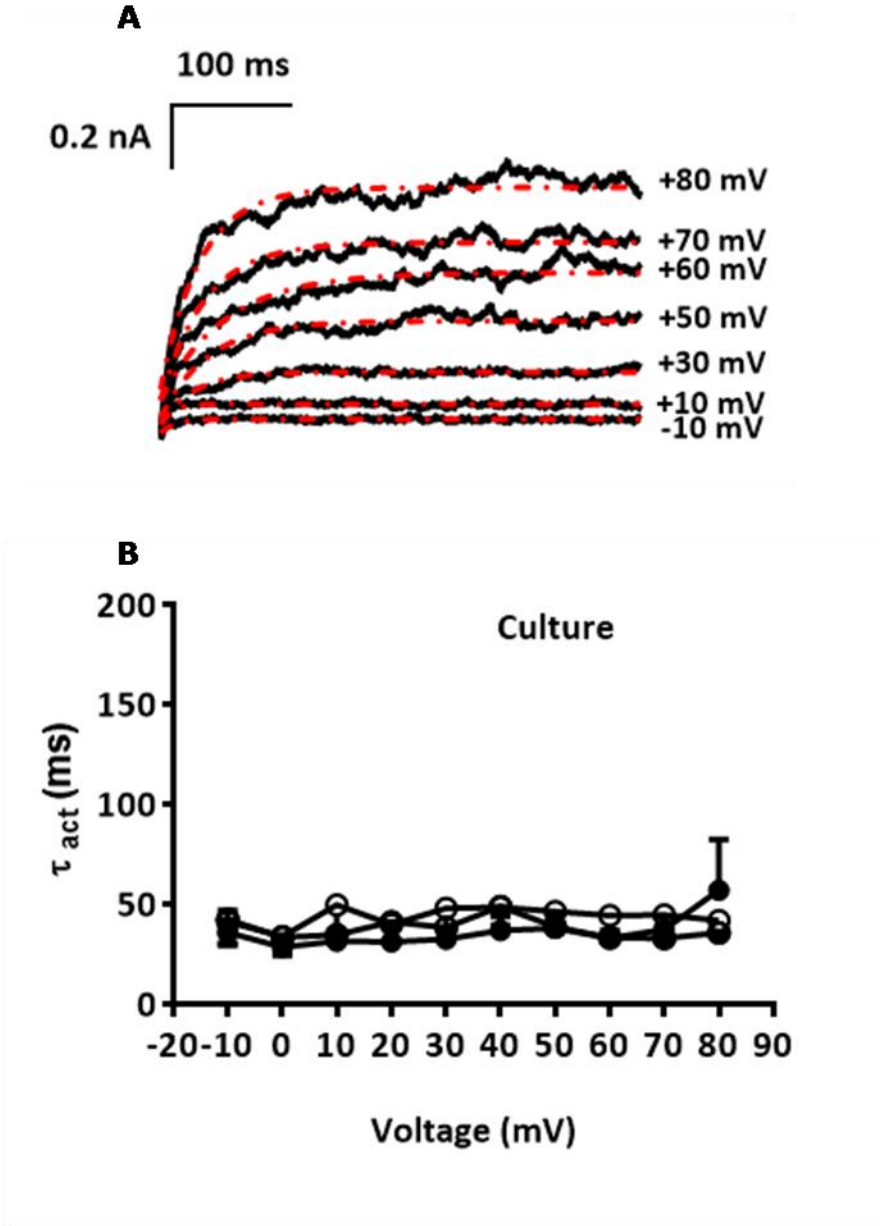

Figure 67. The effect of 1mM $ZnCl_2$ on activation of outward currents in smooth muscle cells isolated from pulmonary veins maintained in culture for 24 hours. A: raw traces showing activation of currents across different voltages in the presence of 1mM $ZnCl_2$. Black solid lines represent currents recorded and red dashed lines are curves fitted using "one-phase association" (GraphPad Prism 7); for clarity, not all traces are shown. B: Mean τ_{act} plotted against test potential "before" (filled circles), "during" (open circles) and "after" (half-filled circles) $ZnCl_2$ exposure by Picospritzer® (n=6; N=5); analysis using repeated measures two-way ANOVA with Bonferroni's post test.

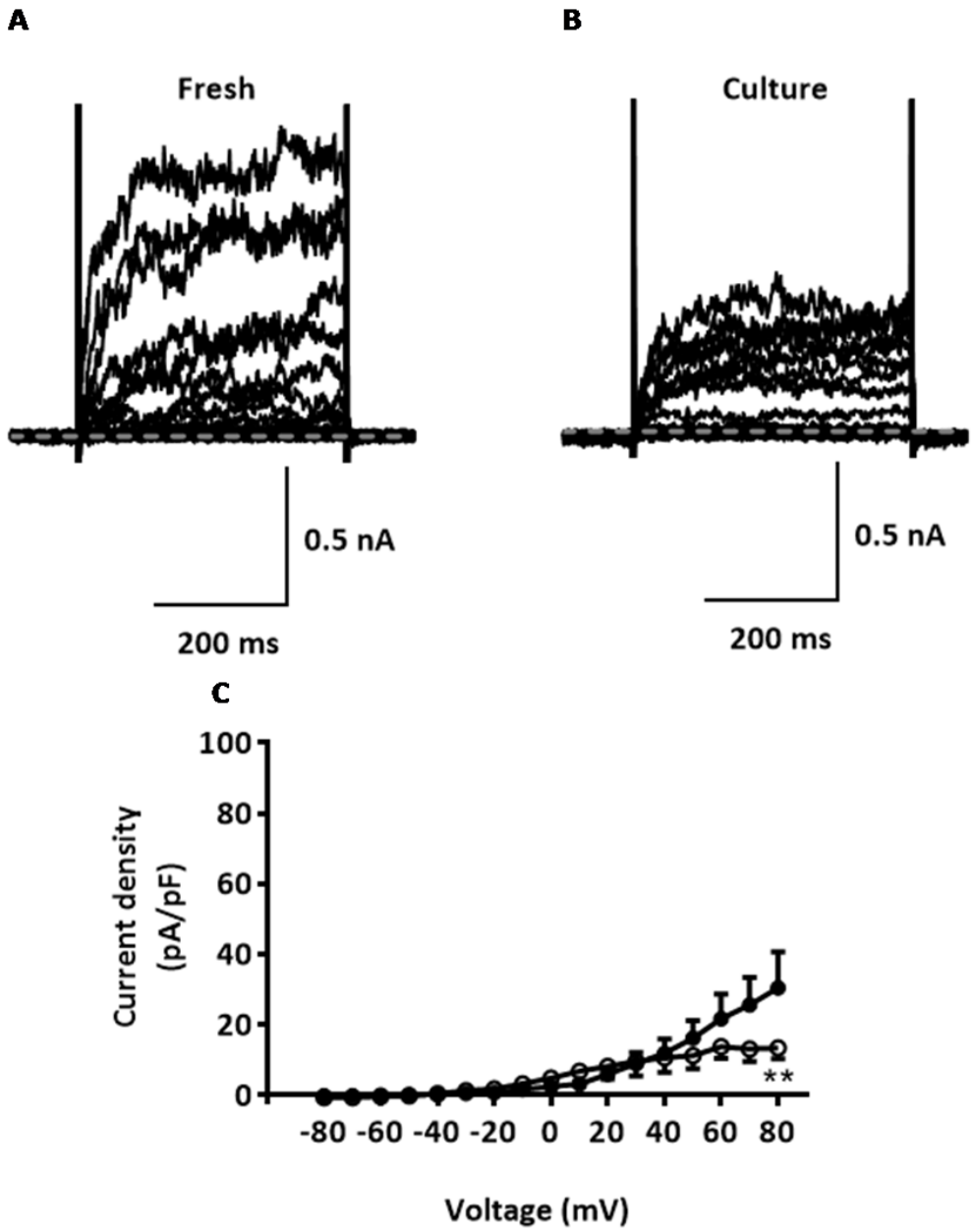

Figure 68. $ZnCl_2$-sensitive difference current in smooth muscle cells from fresh pulmonary veins (PVs) and from PVs maintained in culture for 24 hours. A: representative family of $ZnCl_2$-sensitive difference currents obtained by subtracting current values "during" 1mM $ZnCl_2$ exposure from "before" current values. Currents were elicited by depolarising voltage steps from -80mV to +80mV in 10mV increments starting from a holding potential of -80mV; grey dashed line marks zero current level, capacitance transients have been truncated for clarity. B: Mean (± S.E.M) current density values for 5 cells isolated from fresh PVs (filled circles) and 5 cells isolated from PVs maintained in culture (open circles) (n=5; N=4). ***P*<0.01 fresh vs. culture (analysis using repeated measures two-way ANOVA with Bonferroni's post test).

Voltage-activated Whole-cell Currents - Effect of Maintaining PVs in Culture

The identification of an enhanced TEA-sensitive current and a reduced $ZnCl_2$-sensitive current in SMCs isolated from PVs maintained in culture highlighted the need to characterise other potential differences in the voltage-activated outward currents in SMCs when PVs are exposed to culture conditions. To directly compare the current-voltage relationship for SMCs isolated from fresh PVs and those isolated from PVs maintained in culture conditions in the absence of any drug treatment, all baseline "before" currents were averaged and compared. Current density was significantly increased in SMCs from PVs maintained in culture conditions at a test potential of +80mV compared with fresh PVSMCs ($P>0.05$). Mean current density (±S.E.M) at +80mV for fresh PVSMCs was 52.1 ± 8.8 pA/pF (n=17, N=11) and for SMCs isolated from PVs kept in culture was 72.4 ± 12.3 pA/pF (n=17, N=10). Current-voltage relationships for fresh/culture PVSMCs are shown in Figure 69 A.

Time constants for current activation (τ_{act}) were compared for SMCs isolated from fresh PVs and those isolated from PVs maintained in culture at test potentials between -10 and +80mV for a total of 21 cells. Currents were more rapidly activating in SMCs isolated from PVs maintained in culture at -10mV ($P>0.001$) and 0mV ($P>0.01$, fresh: n=10, N=7; culture: n=11, N=9), reflected in smaller τ_{act} values. At -10mV τ_{act} was 56.3 ± 10.7 ms for SMCs isolated from PVs kept in culture and 110.3 ± 13.9 ms for fresh PVSMCs. At 0mV τ_{act} was 46.5 ± 8.4 ms for SMCs isolated from PVs kept in culture and 91.4 ± 14.3 ms for fresh PVSMCs. τ_{act} values are plotted against voltage for fresh/culture PVSMCs in Figure 69 B.

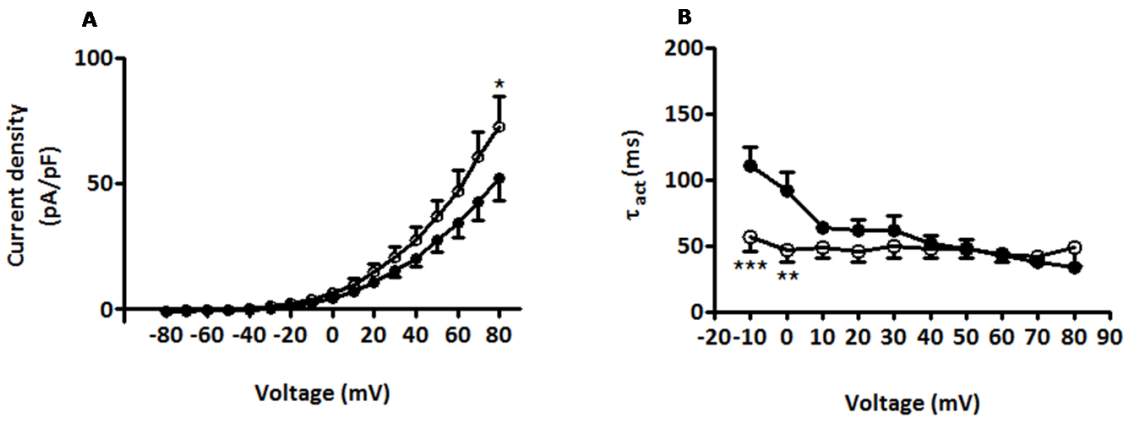

Figure 69. The effect of maintenance in culture conditions on magnitude and activation kinetics of voltage-activated outward currents in pulmonary vein smooth muscle cells. A: Mean (± S.E.M) baseline "before" current density values for cells isolated from fresh pulmonary veins (PVs) (filled circles, n=17; N=11, two cells excluded from data set as positive outliers) and those isolated from PVs maintained in culture (open circles, n=17; N=10) plotted against test potential to give current-voltage relationship. B: Mean (± S.E.M) τ_{act} for baseline "before" currents plotted against test potential for fresh PVs (filled circles, n=10; N=7, one cell excluded as a positive outlier) and those isolated from PVs maintained in culture (open circles, n=11; N=9). **P*<0.01, ***P*<0.01 and ****P*<0.001 fresh compared to culture (analysis using repeated measures two-way ANOVA with Bonferroni's post test).

Discussion

Exposure of PVs to culture conditions has a marked effect on contractility including enhanced hypoxic contraction which was hypothesised to be a result of endothelial damage (Chapter 3). However results of experiments using L-NAME to interfere with endothelial production of NO and mimic the effects of PV maintenance in culture produced unexpected results (Chapter 4). In order to investigate differences at the smooth muscle cell level, cells were isolated from fresh PVs and from PVs maintained in culture conditions for 24 hours and morphological and electrophysiological characteristics were compared.

Previous morphological/electrophysiological characterisation studies in PVSMCs were performed with cells isolated from superior/middle pulmonary lobes (Dospinescu, 2009) however it cannot be assumed that characteristics are the same in PVSMCs from different lung locations. This study has focused on SMCs isolated from inferior PVs and morphological data and characterisation of electrophysiology in terms of RMP and voltage-activated whole cell currents are presented within this chapter. RMP responses to hypoxia were investigated to explore whether exposure of PVs to culture conditions affects hypoxic responses in the isolated smooth muscle cell level as well as the isolated vessel level. The K_V channel inhibitor 4AP (Dospinescu *et al.*, 2012), BK_{Ca} inhibitor TEA (Archer *et al.,* 1996, Moudgil *et al.,* 2005), and TASK-1/3 blocker zinc chloride ($ZnCl_2$) (Ali *et al.,* 2014, Patel *et al.,* 2013) were used to provide a basic characterisation of K^+ channels involved in setting RMP in order to highlight potential candidates for involvement in the hypoxic response of inferior PV/PVSMCs.

Morphologically, SMCs isolated from fresh PVs and those isolated from PVs maintained in culture were similar in terms of area (bi- and tri-dimensional), width and circularity. However, on average PVSMCs from vessels maintained in culture were longer and had a larger perimeter. Passive electrical membrane properties – membrane capacitance, specific membrane capacitance and baseline RMP - were all comparable between fresh PVSMCs and SMCs from PVs maintained in culture conditions.

Hypoxia resulted in depolarisation of the RMP in both fresh PVSMCs and SMCs isolated from PVs maintained in culture (in the latter this did not reach statistical significance); the magnitude of hypoxic depolarisation was not significantly different between fresh/culture. In both groups of SMCs, RMP continued to depolarise on reoxygenation to a level significantly less negative than baseline. TEA caused depolarisation of RMP and inhibited voltage-activated outward currents in SMCs from fresh PVs and from PVs maintained in culture and TEA-induced depolarisation was larger

in SMCs from PVs maintained in culture. K_V channels do not appear to contribute to maintenance of the RMP or voltage-activated outward currents in PVSMCs owing to the lack of effect of 4AP. TASK-1/3 channels do not appear to be involved in controlling RMP of PVSMCs however they do appear to contribute to voltage-activated outward currents.

Maintenance of PVs in culture conditions resulted in an increased TEA-sensitive current and reduced $ZnCl_2$-sensitive current along with more rapid activation and increased magnitude of outward currents in PVSMCs at higher test potentials.

Cell Morphology

Morphological analysis within this study found that SMCs isolated from fresh PVs and those isolated from PVs maintained in culture were similar in terms of cell area, width and circularity. However, SMCs from PVs maintained in culture were longer and had a larger perimeter.

Smooth muscle cells within blood vessels are involved in controlling vascular tone and blood flow; their width and shape can influence contractility (Tolic-Norrelykke and Wang, 2005). In-depth quantitative morphological analysis has previously been performed in SMCs from 5^{th} to 7^{th} order superior/middle PVs (Dospinescu, 2009). However, the focus of this study was on 4^{th} to 5^{th} order inferior PVs which were more than three times larger in terms of outer diameter (3.0 ± 0.7 mm compared with 0.91 ± 0.11 mm). It was therefore important to characterise the morphology of cells from a different location in both the lung and the vascular tree. Little else is known about PVSMCs in terms of morphology. Michelakis *et al.* (2001) worked with SMCs isolated from rat PVs and measured average cell length but no further analysis was performed. Another research group working with primary cultures of rat distal PVSMCs did not provide measurements of cell morphology but instead gave a qualitative description of cell division, shape and arrangement (Peng *et al.,* 2010).

SMCs isolated using the optimised protocol from both fresh inferior PVs and PVs maintained in culture were normally suitable for whole cell recordings during electrophysiology studies. The PVSMCs isolated from fresh PVs and from PVs kept in culture were visually similar to each other and were comparable to those isolated by previous investigators (Dospinescu, 2009, Michelakis *et al.,* 2001). SMCs isolated from superior/middle PVs by Dospinescu (2009) were spindle-like and relaxed and those types of cell were also identified in this study in inferior PVs. Partially contracted cells (which remained elliptical in shaped) were also isolated and used in electrophysiology studies as this was considered to be another marker of viability. Partially contracted cells were visually similar to

the PVSMC in the photomicrograph presented by Michelakis *et al.* (2001) and some cells in photomicrographs presented by Peng *et al.* (2010). In general, a sufficient number of viable spindle-like relaxed cells or partially contracted cells with intact membranes were present in order to attempt a range of current-clamp/voltage-clamp protocols on any given experimental day.

A summary of cell size parameters are presented in Table 5. SMCs isolated from porcine inferior PVs were comparably larger than PVSMCs isolated from rats (average cell length 8 ± 2 μM, Michelakis *et al.,* 2001) but were smaller than SMCs isolated from more distally located porcine superior/middle PVs (average cell length 159.1 ± 36.8 μM, Dospinescu, 2009). These differences may be explained by the size difference between species and PV location in the lung/vascular tree, respectively. The smaller size of porcine PVSMCs from proximal (4^{th}-5^{th} order) compared with distal (5^{th}-7^{th} order) PVs is in keeping with studies of porcine PASMCs. PASMCs from proximal vessels were shorter than those from distal vessels (55.8 ± 1.2 μM compared with 77.8 ± 2μM, Sham *et al.,* 2000). The length and perimeter of cells differed between cells isolated from fresh PVs and those from PVs maintained in culture with the latter being significantly longer. However, this does not necessarily suggest a difference in contractility of smooth muscle cells as studies of human airway smooth muscle cells showed that contractility was not dependent on cell length but on projected area and cell width (Tolic-Norrelykke and Wang, 2005). Projected area and width were not significantly different between SMCs from fresh PVs and those from PVs kept in culture conditions.

Cell lengths and widths were measured directly from photomicrographs and also calculated from approximation to an ellipse using area and perimeter values for the cell. Calculated length values were significantly shorter than their corresponding measured values however calculated width values were not significantly different from measured values. Calculated values were considered to be more reliable as this excluded the error introduced by measurement identified by the significant difference between the two values for cell length. Calculated values were therefore used for all other morphometric calculations.

Morphological parameters for SMCs isolated from fresh inferior PVs could be directly compared to those of Dospinescu (2009) however information regarding the effect of maintenance of PVs in culture on SMC morphology was not readily available in the literature. Most morphological parameters measured/calculated demonstrated that fresh PVSMCs from 4^{th}-5^{th} order inferior PVs were smaller than PVSMCs from 5^{th}-7^{th} order superior/middle PVs. Projected cell area (785.3 ± 353.6 compared with 1070.2 ± 267.6 μm^2), cell perimeter (240.7 ± 88.3 compared with 354 ± 81.6 μm) and tri-dimensional surface area (2459.5 ± 1102.9 compared with 3336.7 ± 832 μm^2). On average, cells from inferior PVs were also slightly wider (9.3 ± 2.7 cf 8.6 ± 1.2 μm) and had higher circularity values

indicating they were less elongated (0.19 ± 0.09 cf 0.11 ± 0.03). This makes sense however, owing to the wider inclusion criteria for cells measured in this study which included cells identified as "partially contracted". Dospinescu (2009) only measured cells which were fully relaxed and spindle-like. This wider sample population also helps explain the larger CV values seen across all morphometric parameters in this study compared to CV values documented by Dospinescu (2009) indicating a wider dispersion of values.

Other than the extensive analysis performed by Dospinescu (2009), there is no data readily available in the literature documenting area, perimeter, width and circularity of PVSMCs.

Membrane Capacitance and Series Resistance

The membrane capacitance for freshly isolated inferior PVSMC was 38.9 ± 20.6 pF and membrane capacitance was not significantly different in SMCs isolated from PVs maintained in culture (39.7 ± 16.6 pF). In PVSMCs isolated from superior/middle PVs, capacitance was much higher at 108 ± 42 pF however as capacitance is directly proportional to the total area of the cell membrane (Molleman, 2003) and cells in this study had a smaller area, this was to be expected. The values observed in this study are closer to values reported for cultured human PASMC (35.27 ± 5.9 pF (Peng *et al.,* 1996) and 34.5 ± 5 pF (Firth *et al.,* 2011) and freshly isolated rabbit PASMC (31 ± 7 pF, Franco-Obregon and Lopez-Barneo, 1996).

SMCs isolated from rat PAs maintained under culture conditions for 4 days also showed no change in C_m when compared to freshly isolated PASMCs (12 ± 1 pF for both, Manoury *et al.,* 2009). C_m for these cells was considerably lower than seen in this study but as cell surface area was not documented, it cannot be concluded as to why this was the case. C_m values for human PASMC kept in culture conditions did not change significantly over an 8 day period (Firth *et al.,* 2011). These results cannot be directly compared to the results within this chapter as the isolated PASMCs were kept in culture as opposed to intact vessels however they help provide further evidence that culture conditions do not appear to affect C_m directly.

The average specific membrane capacitance for inferior PVSMCs was 1.5-1.6 $\mu F/cm^2$ which is slightly higher than the standard proposed value of 1 $\mu F/cm^2$ in SMCs (Toro *et al.,* 1986). The specific membrane capacitance for rat PASMCs is comparable to inferior PVSMCs at 1.25 $\mu F/cm^2$ (Firth *et al.,* 2011). Rat caudal artery SMCs kept in culture conditions and freshly isolated rat uterine SMCs also

have similar values of specific membrane capacitance: 1.3 µF/cm^2 (Toro *et al.,* 1986) and 1.42 µF/cm^2 (Yoshino *et al.,* 1997), respectively.

On the other hand, Dospinescu (2009) calculated a specific membrane capacitance for porcine PVSMCs which was double the value calculated in this study (3.2 µF/cm^2). The high value was proposed to be due to intrinsic membrane properties specific to the cell type and/or an underestimation of cell surface area. However, this does provide an explanation for the discrepancy between specific membrane capacitance in this study for inferior PVSMCs and the value for superior PVSMCs.

R_S in these experiments had an average value of 25.7 ± 1.3 MΩ. Ideally, R_s should be maintained below 20 MΩ; high R_s is detrimental to voltage clamping of the membrane. R_s is less of a problem in current clamp mode therefore membrane potential recordings are less of a concern (Molleman, 2003). During voltage clamp however, high R_s can mean that the full magnitude of command potentials (in a voltage step) are not reached resulting in a degree of voltage error. This high resistance may mean that cells are not exposed to the command potential expected and recorded currents are less than expected (Barbour, 2014). Series resistance can be compensated electronically however this can impair the ability of WinEDR software to calculate C_m, G_a and G_m, as previously discussed. Series resistance compensation can also increase high frequency noise in the recording leading to the need for filtering (Barbour, 2014) which can be problematic as cell-generated data may also be removed by the filter. As the purpose of voltage-clamp protocols within this study was to provide a basic pharmacological characterisation of whole-cell currents in PVSMCs and not a detailed biophysical characterisation, R_s was not considered a major problem and hence was not compensated.

Resting Membrane Potential – Baseline Values

RMP values for SMCs isolated from fresh inferior PVs and those isolated from inferior PVs kept in culture were -39.7 ± 14.2 mV and -36.6 ± 12.8 mV, respectively. Despite PVSMCs from vessels kept in culture being on average more depolarised than freshly isolated PVSMCs, this trend was not statistically significant (P>0.05). Baseline RMP values in inferior PVSMCs are comparable to those seen for porcine superior/middle PVSMCs (-35.8 ± 5.9 mV, Dospinescu, 2009) and freshly isolated PASMC in mouse (-27.9 ± 0.9 mV, Ko *et al.,* 2007), rat (-40 ± 1 mV, Hogg *et al.,* 2002) and rabbit (-50.4

± 4mV, Osipenko *et al.,* 1997). RMP was also within the range seen in cultured human PASMC (-45.5 ± 5mV, Firth *et al.,* 2011).

SMCs isolated from PAs exposed to culture conditions for 4 days showed a small but significant depolarisation (+4mV) in RMP compared with freshly isolated PASMCs (Manoury *et al.,* 2009). The +3.1mV depolarisation in RMP of SMCs seen after 24 hours of PV maintenance in culture conditions in this study was comparable to the change seen in PASMCs yet statistical significance was not reached. Perhaps a longer maintenance in culture conditions could have resulted in further depolarisation of baseline RMP in PVSMCs; further experiments would be required to test this theory.

Resting Membrane Potential – Effect of Flow and Viability Testing

Introduction of flow to the bath chamber caused no significant change to RMP in PVSMCs. This was reassuring as all experimental protocols were run in the presence of flow and hypoxia experiments required flow changeover from normoxic to hypoxic bath solution. Therefore, responses observed in PVSMCs can be considered to be a direct effect of the pharmacological agents or hypoxia rather than flow conditions.

Examples of continuous RMP recordings from PVSMCs are not readily available in the literature. There are also a limited number of high quality RMP recordings presented in the literature in response to drugs/hypoxia in isolated smooth muscle cells in general, even in response to simple depolarising stimuli like high KCl solution.

Exposure to 80mM KCl in this study caused a +19.6mV depolarisation in fresh PVSMCs and a +13.4 mV depolarisation in SMCs isolated from PVs maintained in culture for 24 hours. One report in freshly dissociated PASMCs which documented averaged responses (no raw traces) showed that exposure to high concentration KCl solution (concentration not stated) resulted in a depolarisation of 11mV (from approximately -38 to -27mV) (Archer *et al.,* 1996). This is much smaller than the response seen in freshly dissociated PVSMC but similar to the depolarisation seen in PVSMCs isolated from vessels kept in culture conditions. However results cannot be directly compared because the concentration of KCl used by Archer *et al.* (1996) was not documented.

The reduction in depolarisation in cells isolated from PVs maintained in culture observed (non-significant trend) is at odds with the data from contractile studies in isolated PV showing significantly

increased contraction in response to 80mM KCl after maintenance in culture (Chapter 3). This increased contraction with no associated increase in depolarisation may be explained by increased Ca^{2+}-sensitisation in response to KCl (Ratz *et al.*, 2005) in PVs after maintenance in culture conditions. In isolated PAs, contraction in response to 50mM KCl was diminished after 3 days maintenance in culture conditions however RMP responses at the cellular level were not recorded (Manoury *et al.,* 2009).

Depolarisation in response to 80mM KCl was used as a measure of viability of PVSMCs in this study. KCl was applied via Picospritzer® and change of Picospritzer® pipette was not possible once a cell was in whole-cell recording mode as this could have resulted in a seal break since both pipettes were in close proximity (see Chapter 2, Figure 11). Therefore, a KCl viability test could not be performed for every cell which could be considered a study limitation. The main indicators of viability in other cells were based on visual inspection (bright halo, intact membrane) and the ability to record stable RMP/currents.

Resting Membrane Potential – Effect of K^+ channel Inhibitors and Hypoxia

4AP

There was no clear or significant effect of 5mM 4AP application on the RMP of inferior porcine PVSMCs in this study. The only significant effect was observed in fresh PVSMCs where RMP progressively depolarised and RMP recorded after washout was significantly less negative than baseline RMP. This may indicate a delayed onset of action and poor reversibility of 4AP however this is unlikely as 4AP is well known for being readily reversible and onset of action is rapid (Osipenko *et al.,* 1997, Yuan, 1995) and would usually occur within the exposure time used in these experiments. Osipenko *et al.* (1997) also used a 4AP exposure time of 90 seconds in rabbit PASMCs and saw membrane potential depolarise and reach a plateau within this time.

In earlier experiments (Chapter 3), 4AP caused a transient increase in baseline tension of freshly isolated inferior PVs but this was not sustained. Taken together with the lack of effect of 4AP on membrane potential, this suggests that K_V channels sensitive to 4AP are unlikely to play a role in long-term control of resting membrane potential/tone in porcine inferior PVSMCs/PVs. Previous research in PVs showed a significant increase in tension to 5mM 4AP in both porcine superior/middle PV (Dospinescu *et al.,* 2012) and rat PV (Michelakis *et al.,* 2001). This discrepancy may be due to species differences or difference in location in the lung/vascular tree (Dospinescu *et al.* (2012) used

5^{th}-7^{th} order porcine PVs as opposed to 4^{th}-5^{th} order PVs used in this study). Data investigating the effect of 5mM 4AP on RMP in PVSMCs is not readily available in the literature. The general consensus within PASMCs is that 4AP (1-10mM) causes depolarisation of the membrane potential: this has been demonstrated within freshly dissociated PASMCs from rat (Archer *et al.,* 1996, Archer *et al.,* 1998) and rabbit (Hong *et al.,* 2005, Osipenko *et al.,* 1997) and primary cultured PASMCs from rat (Yuan, 1995). However freshly dissociated PASMCs from mouse did not depolarise after exposure to 1mM 4AP (Manoury *et al.,* 2011). This may suggest that mechanisms underlying control of RMP differ between PVSMCs and PASMCs and between species.

An increased contractile response to 1mM 4AP was observed in PAs after 3-4 days of exposure to culture conditions compared to freshly dissected PAs (Manoury *et al.,* 2009). As was the case for KCl experiments, no membrane potential responses were recorded by Manoury *et al.* (2009). After 24 hours of blood vessel maintenance in culture conditions in this study, isolated PVSMCs showed no sign of increased sensitisation to 4AP. In fact, SMCs became progressively more hyperpolarised over the course of the experimental protocol, a trend which did not reach statistical significance. Overall, it is unlikely that K_V channels sensitive to 4AP contribute to RMP within inferior porcine PVSMCs.

TEA

TEA (5mM) caused significant membrane depolarisation in SMCs isolated from both fresh PVs and PVs maintained in culture conditions for 24 hours. In earlier experiments (Chapter 4), TEA (5mM) caused a sustained increased in baseline tension of freshly isolated inferior PVs. This suggests that K^+ channels sensitive to block by TEA contribute to control of RMP and resting tone in inferior porcine PVMSCs/PVs. Previous research in rat PVs suggested that 5mM TEA only caused minimal constriction perhaps suggesting a difference in PVs between different species (Michelakis *et al.,* 2001).

There is no previous known research investigating the effect of TEA on RMP in PVSMCs specifically. Studies investigating the effect of TEA on membrane potential in PASMCs showed variable results. Unlike the consistent effect of TEA seen in this study, in mouse PASMCs, 10mM TEA resulted in depolarisation of only 29% of cells tested yet when all data was averaged there was a significant difference between RMP in the presence and absence of the drug (Manoury *et al.,* 2011). In PASMCs from rat, 5mM TEA had no effect on RMP (Archer *et al.,* 1996). The difference between the two studies could be accounted for in terms of species differences however Manoury *et al.* (2011) isolated cells from 1^{st}-3^{rd} order PAs and Archer *et al.* (1996) from 4^{th}-5^{th} order PAs which could be an alternative explanation. Archer *et al.* (1996) proposed that different cell types and K^+ currents

predominate in rat conduit and resistance PASMCs with Ca^{2+}-activated K^+ channels being more abundant in conduit PAs (1^{st}-2^{nd} order) and K_V channels being more abundant in resistance PAs (4^{th}-5^{th} order). However, TEA (10mM) had no effect on RMP in rabbit conduit PASMCs (Osipenko *et al.,* 1997) hence this points more towards potential species differences. TEA appears to have a more clear and consistent effect on RMP in PVSMCs than PASMCs.

TEA was used in these experiments primarily to determine the potential role of BK_{Ca} channels to the RMP of PVSMCs because at concentrations of 5mM and lower, TEA is reportedly selective for BK_{Ca} channels (Archer *et al.,* 1996, Moudgil *et al.,* 2005). Hence results observed may indicate that BK_{Ca} plays a role in regulation of RMP within porcine inferior PVSMCs. Other BK_{Ca} channel inhibitors have similarly variable effects on RMP to TEA within PASMCs with charybdotoxin having no effect on membrane potential on PASMCs from rat (Yuan, 1995) and adult rabbit (Osipenko *et al.,* 1997) and iberiotoxin causing depolarisation in foetal rabbit PASMCs (Hong *et al.,* 2005).

As discussed in Chapter 4, TEA may also inhibit K_V channels and specifically those with $K_V2.1$ α subunits (Smirnov *et al.,* 2002). A current which was 4AP-insensitive and TEA-sensitive was identified in some PASMCs from rat conduit PAs (Smirnov *et al.,* 2002) and was proposed to be mediated by $K_V2.1$ α subunits (Patel *et al.,* 1997, Shi *et al.,* 1994). The depolarisation seen with TEA in this study could suggest that K^+ channels expressing $K_V2.1$ α subunits play a role in controlling RMP of PVSMCs. When K_V channels contain only $K_V2.1$ α subunits, they are rarely activated at membrane potentials more negative than -20mV (Patel *et al.,* 1997). This means that a homomeric $K_V2.1$ channel is unlikely to be activated at the RMP of inferior porcine PVSMCs measured in this study (-39.7 ± 14.2 mV (fresh); -36.6 ± 12.8 mV (culture)). Activation is shifted to within the range of RMP of PVSMCs (-50 to -60mV) when $K_V2.1$ subunits form a heteromer with $K_V9.3$ (Patel *et al.,* 1997). Therefore, a $K_V2.1/K_V9.3$ heteromeric channel could play a role in setting the RMP of inferior PVSMCs.

The mean TEA-induced depolarisation in SMCs isolated from PVs maintained in culture was more than double the depolarisation seen in fresh PVSMCs (culture: +14.7 ± 3.5 mV; fresh: +7.0 ± 1.2 mV). This finding was particularly interesting as it was the first real suggestion that maintaining PVs in culture had a direct effect on isolated smooth muscle cells. It also ties in with results from PAs whereby an increased contractile response to 10mM TEA was observed after 3-4 days maintenance in culture conditions compared to fresh PAs (Manoury *et al.,* 2009) although the effect on membrane potential was not investigated.

Maintenance in culture conditions appears to sensitise PVSMCs to the effects of TEA which could be due to upregulation or increased expression of BK_{Ca} channels or K_V channels expressing $K_V2.1$ α

subunits. Baseline RMP was also slightly higher in culture (-36.6 ± 12.8 mV compared with fresh: 39.7 ± 14.2 mV; *P*>0.05), which could lead to increased activation of K^+ channels hence why TEA had a more profound effect.

$ZnCl_2$

Application of $ZnCl_2$ had no consistent effect on the RMP of PVSMCs, some cells depolarised and some hyperpolarised with the mean effect of the drug remaining unclear. If TASK-1/3 channels were involved in controlling RMP in PVSMCs then blocking these channels with $ZnCl_2$ would result in depolarisation (Ali *et al.,* 2014) which was not observed consistently. In Chapter 4, the role of $ZnCl_2$ as a TASK-1 blocker was challenged and it was highlighted that $ZnCl_2$ could block TREK-1 at the concentration used in this experiment (Gruss *et al.,* 2004). Therefore, the action of $ZnCl_2$ as a selective blocker of TASK-1/3 channels should be viewed with caution.

The hyperpolarisation observed on application of $ZnCl_2$ in approximately 50-57% of cells could be a result of a repolarisation mechanism (e.g. BK_{Ca} channel activation) which results in negative-feedback regulation after initial depolarisation due to TASK/TREK blockade. This repolarisation mechanism has been identified with 4AP whereby activation of BK_{Ca} occurs after 4AP-induced depolarisation and influx of Ca^{2+} (Yuan, 1995). In order to further investigate this possible mechanism, responses to $ZnCl_2$ would need to be recorded in the presence of a BK_{Ca} blocker (e.g. TEA or Penitrem A). In order to record $ZnCl_2$-sensitive currents, previous investigators have used 10mM TEA and 5mM 4AP during whole-cell recordings (Patel *et al.,* 2013). This may be a useful approach to use in future studies to ascertain the effect of $ZnCl_2$ in the absence of any repolarisation mechanisms which may exist.

As well as blocking TASK/TREK channels, $ZnCl_2$ can cause inhibition of Ca^{2+} channel currents (Ali *et al.,* 2014) which could provide an alternative explanation for the hyperpolarisation seen in some cells if basal Ca^{2+}influx is present in PVSMCs. In PAs, maintenance in culture conditions for 3-4 days resulted in the emergence of an uncharacteristic relaxation in response to the block of Ca^{2+} channels with nifedipine indicating that Ca^{2+} influx was contributing to basal tone (Manoury *et al.,* 2009) and perhaps RMP of PASMCs. However a similar proportion of cells isolated from fresh PVs (50%) and those isolated from vessels maintained in culture conditions (57%) became hyperpolarised on $ZnCl_2$ application. As the effects of 1mM $ZnCl_2$ on RMP are unclear and it is also unclear which channel(s) $ZnCl_2$ is inhibiting, no real conclusions can be drawn as to the mechanism of action or contribution of $ZnCl_2$-sensitive channels to RMP in PVSMCs.

Hypoxia

Exposure to hypoxic bath solution lead to depolarisation in SMCs isolated from both fresh PVs and PVs maintained in culture however the hypoxic depolarisation only reached statistical significance in SMCs isolated from fresh PVs (when initial baseline RMP was compared to RMP during hypoxia). The size of depolarisations seen in fresh/culture PVSMCs were not significantly different from one another. On reoxygenation, SMCs continued to depolarise; RMP on reoxygenation was significantly more depolarised than baseline RMP in both fresh and culture PVSMCs. Data from experiments investigating the effect of hypoxia on the RMP of PVSMCs are not readily available in the literature. Previous study of hypoxia in PVSMCs during whole-cell electrophysiology focussed on hypoxia-sensitive whole cell currents as opposed to RMP under current-clamp conditions (Dospinescu *et al.,* 2012).

Hypoxia is known to cause depolarisation in freshly dissociated PASMC from rat (Archer *et al.,* 1996, Archer *et al.,* 2004, Olschewski *et al.,* 2002), dog (Post *et al.,* 1992) and rabbit (Hong *et al.,* 2005, Osipenko *et al.,* 1997) and in primary cultured PASMCs from rat (Yuan *et al.,* 1993). When PASMCs were exposed to bath solution bubbled with gas containing 0% O_2 (N_2 with or without CO_2), depolarisation magnitudes ranged from values similar to those seen in PVSMCs: approximately +7 to +10mV (Hong *et al.,* 2005, Osipenko *et al.,* 1997) up to much larger values of +22 to +30mV (Archer *et al.,* 1996, Archer *et al.,* 2004, Olschewski *et al.,* 2002). Yuan *et al.* (1993) used sodium dithionite as an oxygen scavenger and PASMCs depolarised by approximately +15mV. In this study of inferior PVSMCs, exposure time to hypoxic bath solution was 5 minutes as there were problems with holding the cell long enough to record baseline, hypoxia and recovery and recovery of the RMP to baseline levels was not achieved. This challenge was also encountered by Osipenko *et al.* (1997) who found that the time course of the depolarisation and recovery was slow and RMP only partially recovered on re-equilibration with room air. In contrast, others found that depolarisation of PASMCs in response to hypoxia was rapid (Archer *et al.,* 1996, Archer *et al.,* 2004) and RMP fully recovered on reoxygenation (Archer *et al.,* 2004, Yuan *et al.,* 1993). Interestingly, one study found that when the solution was bubbled with 3% O_2 PASMCs became depolarised and this was reversible on returning to normoxia however at 0% O_2 depolarisation was irreversible (Olschewski *et al.,* 2002), similar to the results observed in PVSMCs.

A notable difference between these hypoxia studies in PASMCs was that some researchers conducted experiments at room temperature (22-25°C) (Osipenko *et al.,* 1997, Yuan *et al.,* 1993) similar to temperature used in this study (21-22°C) and others used temperatures of 30-35°C (Archer *et al.,* 1996, Archer *et al.,* 2004, Hong *et al.,* 2005, Olschewski *et al.,* 2002, Post *et al.,* 1992). The

reason for using this higher temperature was that the "O_2-sensitive channel" within PASMCs is not active at room temperature (Archer *et al.,* 1996). This could help provide some explanation as to the variation in the size of depolarisations observed in PASMCs however the mechanism of hypoxic depolarisation in PVSMCs may be different; temperature may be a factor worth taking into consideration in future experiments.

Voltage-activated Whole-cell Currents - Effect of K^+ Channel inhibitors

General characteristics of Voltage-activated Whole-cell Currents in PVSMCs

Voltage-activated whole cell currents in inferior PVSMCs were outward, rapidly activating and non-inactivating with spiky STOC components at more depolarised potentials and no inward rectification. These characteristics have all been observed previously within superior/middle PVSMCs and rat PVSMCs with the STOC components suggested to involve BK_{Ca} channels (Dospinescu, 2009, Michelakis *et al.,* 2001).

4AP

Extracellular application of 4AP (5mM) had no effect on voltage-activated outward currents in SMCs isolated from either fresh PVs or PVs maintained in culture conditions. In previous studies in porcine and rat PVSMCs, 5mM 4AP inhibited outward K^+ currents (Dospinescu, 2009, Michelakis *et al.,* 2001). Notably, Dospinescu (2009) performed experiments in the presence of Penitrem A to block contribution of BK_{Ca} currents to the overall whole cell K^+ current and saw ~25% inhibition with 4AP at a single depolarisation step of -80mV to +80mV. On the other hand, Michelakis *et al.* (2001) saw partial inhibition of K^+ currents with 4AP in the absence of BK_{Ca} blockade. Repolarisation mechanisms can occur whereby BK_{Ca} channels are activated after K_V inhibition with 4AP (Yuan, 1995) which can overshadow the current inhibition. To further ascertain whether K_V channels contribute to outward K^+ currents in PVSMCs, future experiments could be performed in conditions which inhibit the contribution of BK_{Ca}. Pharmacological inhibition of BK_{Ca} is only one of the ways in which K_V currents can be isolated; bath and pipette solutions can also be manipulated in favour of K_V currents. Optimal conditions for K_V currents are Ca^{2+} free bath solution (plus 1mM EGTA) and Ca^{2+} free intracellular pipette solution (plus 10mM EGTA) (Firth *et al.,* 2011) to eliminate the BK_{Ca} current (Yuan, 1995). The

experimental conditions used in this study were more in favour of BK_{Ca}; therefore solid conclusions about 4AP sensitive K_V currents cannot be made from the results of this study.

A possible alternative explanation for the differences seen with 4AP between this study and the study by Dospinescu (2009), as previously discussed, would be the order of PVs used for SMC isolation (5^{th}-7^{th} order superior/middle PVs (Dospinescu, 2009) and 4^{th}-5^{th} order inferior PVs). Clear differences between K^+ currents from SMCs isolated from larger conduit PAs and those from smaller resistance PAs have been identified with the former having a larger contribution from BK_{Ca} channels and the latter from K_V (Archer *et al.,* 1996, Archer *et al.,* 2004, Smirnov *et al.,* 2002). The same relationship could exist between smaller and larger PVs however, without manipulation of experimental solutions/conditions, the reason for the differences observed cannot be inferred.

TEA

Applying TEA (5mM) to SMCs caused significant but reversible inhibition of the average steady state current over the depolarising steps of +30 to +80 mV for cells from fresh PVs and +40 to +80 mV for cells from PVs kept in culture. A larger proportion of the current (70%) was inhibited in SMCs isolated from PVs kept in culture than in fresh PVSMCs (50%) at a test potential of +80mV. It was therefore not surprising that the magnitude of the TEA-sensitive difference current was significantly increased in cells isolated from PVs maintained in culture (at +70 and +80mV voltage steps). TEA (5mM) also inhibited voltage-activated outward currents in SMCs isolated from freshly dissected superior/middle PVs (Dospinescu, 2009) however the inhibition was greater (77.5%) than the inhibition seen in fresh inferior PVSMCs. In rat PVSMCs, TEA inhibited outward currents by ~75% and to a greater extent than 5mM 4AP (~30% inhibition compared with control) (Michelakis *et al.,* 2001). This suggests that in SMCs isolated from fresh inferior 4^{th}-5^{th} order porcine PVs, there is a larger proportion of the outward K^+ current which is TEA-insensitive than for other PV locations/other species.

TEA is likely to inhibit both BK_{Ca} and K_V to some extent, as discussed in detail earlier in this chapter. Studies of voltage-activated currents within rabbit PASMCs provide further evidence to support this with TEA (10mM) causing 33% inhibition in contrast to iberiotoxin/charybdotoxin (more selective BK_{Ca} blockers) which inhibited only 14% of the current (Osipenko *et al.,* 1997). At a lower concentration of 1mM TEA, however, there is a negligible effect on K_V currents (Firth *et al.,* 2011). Bearing in mind that these experiments inadvertently provided experimental conditions favourable for recording BK_{Ca} currents (Firth *et al.,* 2011), it may be more likely that TEA is blocking BK_{Ca}. In

order to fully understand the role of BK_{Ca} currents within inferior PVSMCs, a more selective blocker of BK_{Ca} would be required, for example Penitrem A. Another finding which warrants further investigation is the TEA-insensitive proportion of the current (particularly in fresh PVSMCs where 50% of the outward current remained) although results from experiments with $ZnCl_2$ helped shed some light on this residual current.

$ZnCl_2$

$ZnCl_2$ (1mM) inhibited 32% and 26% of the whole-cell voltage-activated currents in SMCs isolated from fresh PVs and from PVs maintained in culture, respectively, at a test potential of +80mV. Interestingly this is within the range of the proportion of current remaining after TEA-inhibition (50% and 30% TEA-insensitive current remaining in fresh/culture, respectively) and TEA is not known to inhibit currents sensitive to $ZnCl_2$ (TASK/TREK) (Patel *et al.,* 2013).

The $ZnCl_2$-sensitive difference current was significantly reduced at a voltage step of +80mV in SMCs isolated from culture conditions; this is opposite to the results seen with TEA where TEA-sensitive currents increased. It can therefore be proposed that K^+ currents within inferior PVSMCs are a balance of TEA-sensitive BK_{Ca}/K_V channel currents and $ZnCl_2$-sensitive TASK/TREK currents and that this balance shifts when inferior PVs are exposed to culture conditions for 24 hours. To confirm this theory, experiments would need to be performed in the presence of both agents and in this case, near complete inhibition would be expected.

$ZnCl_2$ was initially chosen as an inhibitor of TASK-1 because this channel controls RMP and is hypoxia-sensitive, however results within this chapter show $ZnCl_2$ has no significant effect on RMP and there was no significant effect on hypoxic pulmonary venoconstriction (Chapter 4). There was no definitive evidence from Ali *et al.* (2014) that $ZnCl_2$ at the concentration used in this study (1mM) would block TASK-1 however evidence of TASK-3 and TREK-1 blockade has been reported (Gruss *et al.,* 2004). Results within this chapter and Chapter 4 could suggest that although TASK-3 and TREK-1 currents appear to be present within PVSMCs, they are not active at RMP and are not involved in the hypoxic contraction of PVs. In order to investigate the role of TASK-1, a more selective pharmacological inhibitor would be required such as anandamide (Maingret *et al.,* 2001) however as an endocannabinoid it is likely to have other non-specific effects. Alternatively, the experimental solutions/conditions could be manipulated. Previous studies of TASK channels in freshly dissociated endometrial epithelial cells investigated TASK in the presence of 4AP and TEA (due to known lack of sensitivity towards several K2P channels) and by reducing extracellular pH from 7.4 to 6.6 (Patel *et*

al., 2013). As TASK channels are the only members of the two-pore domain K^+ channel superfamily inhibited by extracellular pH, any reduction in the whole-cell outward current could be attributed to TASK channel contribution (Patel *et al.,* 2013). This would not isolate TASK-1 from other TASK channels (TASK-2/3) however it may be the best approach to take given the lack of potent and specific blockers available.

Voltage-activated Whole-cell Currents - Effect of Maintaining PVs in Culture

Maintenance of PVs in culture conditions had a significant impact on both magnitude and activation kinetics of whole cell outward currents in PVSMCs. Current density in SMCs isolated from PVs maintained in culture conditions was significantly greater at the +80mV voltage step and τ_{act} values suggest currents were more rapidly activating at -10 and 0mV voltage steps compared with fresh PVSMCs. There is no known previous work evaluating the effect of maintenance of PVs in culture on voltage activated currents in PVSMCs. In contrast to the results observed in this study, SMCs isolated from PAs kept under culture conditions for 4 days had significantly reduced voltage-activated K^+ currents compared with freshly isolated PASMCs (Manoury *et al.,* 2009).

Taken together with the results seen in PV contractile studies (Chapter 3), these results suggest that maintenance in culture condition not only has a significant impact on isolated PV function but also has minor effects on PVSMC function in terms of magnitude and kinetics of outward K^+ currents and their sensitivity to TEA and $ZnCl_2$. Maintenance in culture conditions may have an impact on both endothelium and smooth muscle cells or even on the electrical coupling between the two (Emerson and Segal, 2000).

Key Findings

This study set out to characterise inferior PVSMCs in terms of morphology and electrophysiology (RMP and whole-cell outward K^+ currents) and to determine whether maintenance in culture had any impact on those characteristics. Key findings within this chapter suggest that maintaining PVs in culture has minimal effect on isolated SMCs in terms of morphology, membrane capacitance, RMP and notably, RMP responses to hypoxia. This implies that the increased contractions of intact PVs to hypoxia after maintenance in culture (Chapter 3) were not due to enhanced activity/altered RMP at the SMC level.

TEA caused a larger depolarisation of RMP in SMCs isolated from PVs maintained in culture and a larger TEA-sensitive current was present in SMCs isolated from PVs kept in culture. $ZnCl_2$-sensitive currents were reduced in SMCs isolated from PVs kept in culture. As the effects on TEA- and $ZnCl_2$-sensitive currents were only observed at the highest test potentials (+70 to +80 mV), it is questionable whether these results are physiologically relevant since SMCs would not be exposed to these voltages under normal conditions (Moudgil *et al.,* 2005). $ZnCl_2$ and 4AP had no impact on RMP and 4AP had no impact on whole-cell currents in PVSMCs.

This study has provided a detailed morphological characterisation and basic electrophysiological characterisation of SMCs isolated from porcine inferior PVs. It has highlighted that, although differences in function after PV maintenance in culture exist at the isolated vessel level, there is less of an impact on SMCs in terms of morphology and electrical membrane properties.

Chapter 6

Conclusions and Further Work

The studies presented within this thesis aimed to characterise and identify underlying mechanisms of hypoxic responses of porcine PVs and to evaluate the impact of maintenance in culture conditions. Myography studies successfully characterised the PV hypoxic response and identified likely regulatory pathways and also helped demonstrate the profound impact of culture conditions alone on PV contractility. Studies using isolated PVSMCs aimed to characterise morphological and electrical membrane properties including the impact of PV maintenance in culture and responses to hypoxia. A full morphological and basic electrophysiological characterisation was achieved which identified minimal impact on isolated SMCs when PVs were kept in culture conditions for 24 hours. The effect of K^+ channel inhibitors on RMP and voltage-activated currents was studied along with the effect of hypoxia on RMP however underlying mechanisms of hypoxic responses in PVSMCs were not characterised.

Initial myography studies identified a robust and reproducible hypoxic contraction in porcine PVs and revealed a novel contractile response on reoxygenation after hypoxic exposure. The effects of maintenance of PVs in culture conditions were also investigated using myography with a view to using the technique for future studies whereby environmental conditions could be manipulated in order to assess their impact on PV function. Maintenance of PVs in culture conditions for 24 hours had a profound effect on PV contractile function, particularly in inferior PVs where contractions to histamine, KCl, U46619 and hypoxia were increased and hypoxic relaxation and reoxygenation contraction were inhibited. These altered contractile and relaxant responses were suggested to result from endothelial dysfunction/damage as endothelium-dependent relaxations to carbachol were inhibited in PVs maintained in culture for 24 hours compared to fresh PVs.

The contribution of endothelial-mediated pathways to hypoxic and reoxygenation responses was further investigated in fresh inferior PVs. L-NAME, an inhibitor of NOS (Bardou *et al.,* 2001, Félétou *et al.,* 1995) was used in an attempt to simulate the effects of PV maintenance in culture. The effect of L-NAME was unexpected and opposed the results seen after PV exposure to culture conditions (where hypoxic contraction was increased and hypoxic relaxation and reoxygenation contraction

were inhibited). In terms of the hypoxic response, L-NAME inhibited the transient hypoxic contraction, enhanced relaxation and significantly altered dynamics of the response in fresh PVs. The NOS inhibitor also potentiated the reoxygenation contraction. Relatively simple experiments investigating the impact of L-NAME on endothelial function tests confirmed the drug was having an effect on NOS in the endothelium rather than in smooth muscle within PVs. L-NAME inhibited endothelial-mediated relaxations to carbachol and enhanced contractions to histamine whereas time control PVs showed reduced histamine contraction on re-exposure. Taken alone, the data from time control PVs suggest possible desensitisation of pro-contractile smooth muscle H_1 receptors (Shi *et al.*, 1998, Toda, 1990). However, the increased contraction to histamine seen when NOS was inhibited with L-NAME suggests endothelial H_1 receptor upregulation occurs rather than smooth muscle H_1 receptor desensitisation (Toda, 1990). These results also support the role of L-NAME inhibition of endothelial NOS.

Results of hypoxia studies using L-NAME were not in keeping with results seen after PV maintenance in culture and indicated that data from contractile studies were not explained fully by endothelial function/dysfunction. Hence, the impact of PV maintenance in culture was explored at the single smooth muscle cell level. Morphologically, SMCs isolated from PVs maintained in culture were longer and had a larger perimeter than freshly isolated PVSMCs but were otherwise similar. A difference in cell length and perimeter does not necessarily suggest a difference in contractility of SMCs as previous studies have found that contractility was not dependent on cell length but on area and width (Tolic-Norrelykke and Wang, 2005). Furthermore, passive electrical properties (C_m and RMP) were not significantly different between SMCs isolated from PVs maintained in culture and those isolated from fresh PVs. Hypoxia caused depolarisation of RMP in both fresh and culture PVSMCs but the effect only reached significance in fresh PVSMCs and the size of the depolarisation was comparable in fresh/culture PVSMCs. Hence, initial results in SMCs suggested that maintenance of PVs in culture had no obvious effect on their morphology or function.

PV K^+ channel function and expression were explored as K^+ channels were known to play a key role in hypoxic responses of both resistance PAs (Archer *et al.,* 1996, Archer *et al.,* 1998, Archer and Michelakis, 2002, Archer *et al.,* 2004, Moudgil *et al.,* 2005, Platoshyn *et al.,* 2006) and 5^{th}-7^{th} order superior/middle PVs (Dospinescu *et al.,* 2012). K^+ channel inhibitors were used to explore underlying mechanisms and pathways of hypoxic contraction in inferior PVs. Penitrem A, 4AP, DPO-1, $ZnCl_2$ and glyburide all failed to have an effect on hypoxic contraction however TEA and BDM both inhibited the hypoxic response. This suggested that TASK, $K_V1.5$, BK_{Ca} and K_{ATP} do not play a role in the mechanism of hypoxia-induced contraction of inferior PVs however K_V channels containing $K_V2.1$ α subunits could

modulate the response. K^+ channels appear to tell only part of the story regarding the hypoxic response in PVs. This is notable because it highlights a fundamental difference between the hypoxic response of the PV and the PA. In the latter, K^+ channels play a pivotal role in the mechanism of HPV whereby inhibition of K_V channels leads to PASMC depolarisation, VGCC influx and PA constriction (Archer *et al.,* 1996, Archer *et al.,* 1998, Archer and Michelakis, 2002, Archer *et al.,* 2004, Leach *et al.,* 1994, McMurtry *et al.,* 1976, Moudgil *et al.,* 2005, Platoshyn *et al.,* 2006). This is in keeping with clinical findings where treatments for PAH (prostacyclin, bosentan, calcium channel blockers) may cause pulmonary oedema in patients with pulmonary venous involvement (Creagh-Brown *et al.,* 2008, Montani *et al.,* 2008 and Palmer *et al.,* 1998) suggesting mechanisms of dysregulation and disease may differ between PAs and PVs.

Based on the in-depth functional characterisation performed and presented within this thesis, the underlying mechanism of the PV hypoxic reponse is now better understood at the isolated vessel level. This could have implications physiologically, whereby hypoxic pulmonary venoconstriction is hypothesised to recruit upstream capillaries and optimise gas exchange in healthy humans (Taylor *et al.,* 2011). The experiments performed emphasise the importance of PV hypoxic constriction as a robust and reproducible physiological response which increases in magnitude with repeated exposure. This research may also suggest mechanisms which play a role in hypoxia-related disease such as high altitude pulmonary oedema, where inhomogeneous hypoxic pulmonary venoconstriction is suggested to cause regional overperfusion and subsequent oedema in the lungs (Bärtsch and Gibbs, 2007). Figure 70 summarises the proposed role of hypoxic pulmonary venoconstriction in normal physiology and disease.

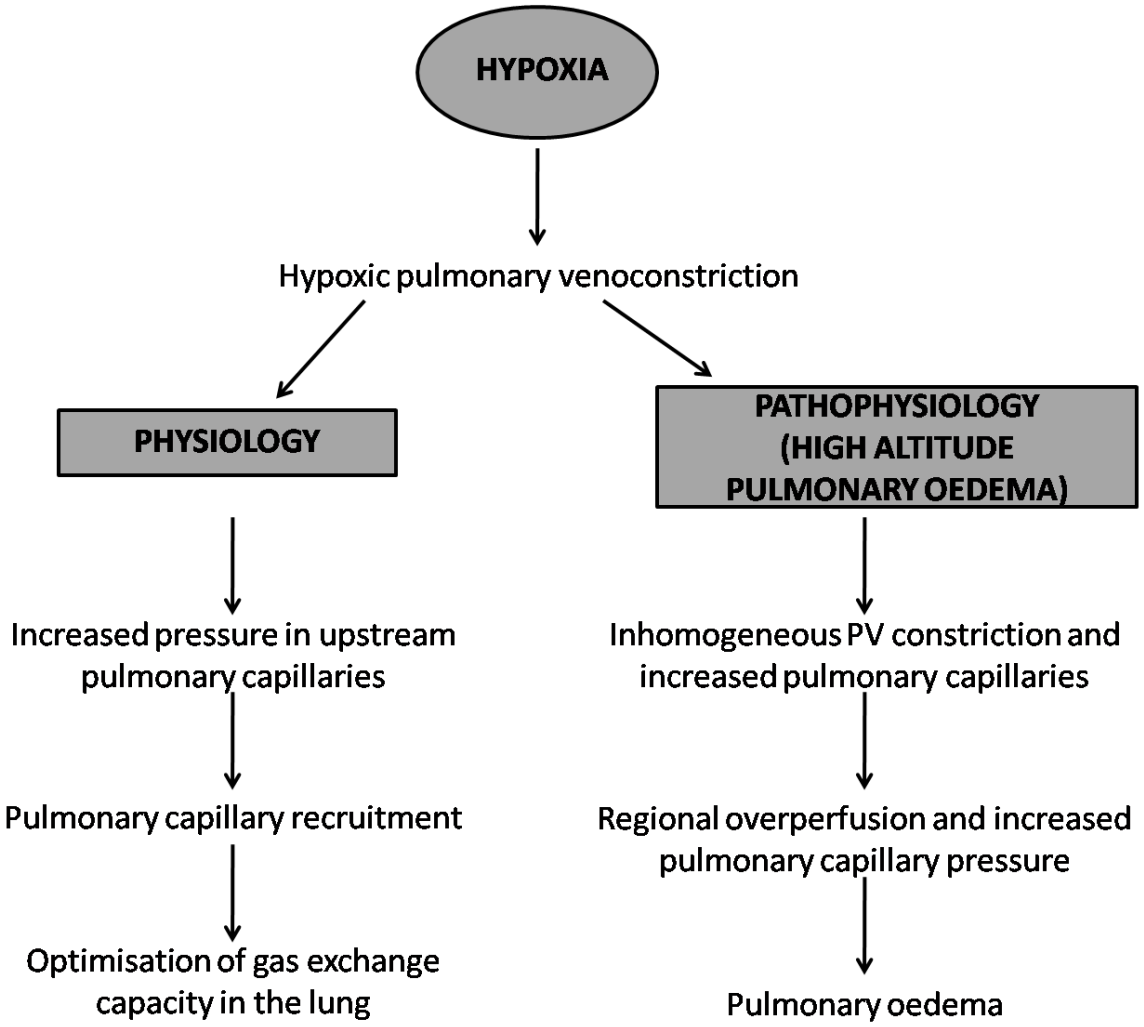

Figure 70. Diagram showing the proposed role of hypoxic pulmonary venoconstriction under normal physiological condtions and in disease (in the context of high altitude pulmonary oedema). Physiologically, hypoxic PV constriction is proposed to increase upstream pressure and recruit pulmonary capillaries leading to optimisation of gas exchange (Taylor *et al.,* 2011). Hypoxic PV constriction during high altitude pulmonary oedema is proposed to be inhomogeneous and lead to regional overperfusion (Bärtsch and Gibbs, 2007), increased pulmonary capillary pressure (Maggiorini *et al.,* 2001) and ultimately, pulmonary oedema.

K^+ channel inhibitors for electrophysiology were selected based on previous findings in inferior PV contractile studies (Chapter 4) and isolated PVSMCs (Dospinescu *et al.,* 2012, Michelakis *et al*., 2001). K^+ channel blockers were used in attempt to identify any impact of maintaining PVs in culture conditions on K^+ currents and their contribution to RMP in SMCs. The BK_{Ca}/K_V blocker TEA caused a significantly larger depolarisation in SMCs isolated from PVs kept in culture; this was the first suggestion that maintaining PVs in culture had any direct effect on electrical properties of SMCs. In

terms of voltage-activated outward K^+ currents, PVSMCs from vessels kept in culture had a larger TEA-sensitive current, smaller $ZnCl_2$-(TASK/TREK blocker) sensitive current and larger overall current. These effects were only observed at the highest test potentials (+70 to +80 mV) therefore it is questionable whether these results are physiologically relevant since SMCs would not be exposed to such high voltages under normal conditions (Moudgil *et al.,* 2005). Therefore, maintaining PVs in culture conditions had minor effects on the K^+ currents studied and their contribution to RMP and current effects occurred at voltages which cells may not be exposed to physiologically.

K^+ channels appear to play only a minor modulatory role in hypoxic contraction in inferior PVs and K^+ currents in SMCs are only minimally affected after PV maintenance in culture. Hypoxic responses with L-NAME and in PVs exposed to culture conditions suggest that endothelial regulation is a more important focus for research going forward in terms of hypoxia studies and for the development of PV culture as a disease model for investigation of a range of environmental conditions.

The difference observed in hypoxic responses after exposure to culture and with L-NAME may be more related to the underlying balance between NO and other endothelial relaxing factors e.g. prostaglandins and endothelial contracting factors e.g. endothelin-1. Exposure to culture conditions resulted in endothelial dysfunction/damage as demonstrated by the inhibition of endothelial-mediated relaxation to carbachol. Dysfunction of or damage to the endothelium in response to maintenance in culture conditions may result in altered release of any combination of endothelial relaxing/contracting factors and further research is warranted in this area.

Endothelial cells within pulmonary capillaries are important for the detection of hypoxia and propagation of the HPV signal via connexin-40 gap junctions to the endothelium of pulmonary arterioles in mice (Wang *et al.,* 2012). It would be interesting to investigate whether this same signal propagation occurs on the venous side of the pulmonary circulation. Endothelial cells not only communicate with one another but are electrically coupled to smooth muscle cells as demonstrated in hamster feed arteries (Emerson and Segal, 2000). Hyperpolarisation and depolarisation of endothelial cells was directly linked to SMC hyperpolarisation/relaxation and depolarisation/contraction, respectively. RMP measurements were made in isolated hamster feed arteries which were cannulated, pressurised and exposed to continuous flow; two microelectrodes were used to impale one endothelial and one smooth muscle cell for simultaneous recordings. This approach could be used in future studies of pulmonary veins/venules. It may be more physiologically relevant than electrophysiology studies of isolated SMCs since intercellular communication between endothelial and smooth muscle cells seems vital to vasoactivity.

Cannulated and pressurised blood vessels could be applied in studies where maintenance in culture conditions is used as a tool to manipulate environmental conditions and simulate disease states. Maintenance of PVs in an unpressurised state under conditions of no flow whilst exposed to culture conditions may have contributed to the impaired relaxation and enhanced contractility observed in studies presented here. In addition to considering pressurisation and flow, the model would require appropriate controls, for example, if glucose was manipulated, PVs exposed to isosmotic culture conditions should act as control vessels rather than freshly isolated PVs or PVs exposed to standard culture medium.

There is a distinct lack of research investigating the role of PVs in disease, as acknowledged by Tuder *et al.* (2013). Research presented here demonstrates development and evaluation of a potential tool for use a disease model for manipulation of environmental conditions. This is important because there is an established link between metabolic syndrome and pulmonary venous hypertension (Robbins *et al.,* 2009) yet the direct impact of conditions associated with metabolic syndrome on PV function remains unknown. Results also demonstrate the significant vasoactivity of PVs in response to hypoxia and agonists and sensitivity of PV function to short term exposure to culture conditions. Results from contractile studies are particularly intriguing because the large 4^{th}-5^{th} order inferior PVs studied would have historically been regarded as passive conduit vessels. The considerable vasoactivity of PVs suggests that dysfunction may result in harmful physiological consequences including raised pulmonary vascular resistance (Gao and Raj, 2005, Her *et al.,* 2010) and pulmonary oedema (Bärtsch and Gibbs, 2007, Maggiorini *et al.,* 2001). The findings presented within this thesis help begin to clarify mechanisms underlying physiological and pathophysiological responses of PVs and suggests potential therapeutic targets for diseases originating in the PV.

Chapter 7

References

ALI, T.Y., PIPKIN, F.B. and KHAN, R.N., 2014. The effect of pH and ion channel modulators on human placental arteries. *PloS One,* 9(12), e114405.

ALM, R., EDVINSSON, L. and MALMSJÖ, M., 2002. Organ culture: a new model for vascular endothelium dysfunction. *BMC Cardiovascular Disorders.* [online] 2(8). Available from: http://www.biomedcentral.com/1471-2261/2/8%20?iframe=true&width=100%&height=100% [Accessed 20 September 2016].

ALMKVIST, G. and BERNDT, B., 1988. Gauss, Landen, Ramanujan, the arithmetic-geometric mean, ellipses, π, and the Ladies Diary. *American Mathematical Monthly,* 95(7), pp. 585-608.

ALOTAIBI, M., ARROWSMITH, S. and WRAY, S., 2015. Hypoxia-induced force increase (HIFI) is a novel mechanism underlying the strengthening of labor contractions, produced by hypoxic stresses. *Proceedings of the National Academy of Sciences of the United States of America,* 112(31), pp. 9763-9768.

ANGUS, J.A., COCKS, T.M. and SATOH, K., 1986. α_2-adrenoceptors and endothelium-dependent relaxation in canine large arteries. *British Journal of Pharmacology,* 88(4), pp. 767-777.

ARCHER, S. and MICHELAKIS, E., 2002. The mechanism(s) of hypoxic pulmonary vasoconstriction: potassium channels, redox O_2 sensors, and controversies. *News in Physiological Sciences,* 17(4), pp. 131-137.

ARCHER, S.L., HUANG, J., HENRY, T., PETERSON, D. and WEIR, E.K., 1993. A redox-based O_2 sensor in rat pulmonary vasculature. *Circulation Research,* 73(6), pp. 1100-1112.

ARCHER, S.L., HUANG, J.M.C., REEVE, H.L., HAMPL, V., TOLAROVÁ, S., MICHELAKIS, E. and WEIR, E.K., 1996. Differential distribution of electrophysiologically distinct myocytes in conduit and resistance arteries determines their response to nitric oxide and hypoxia. *Circulation Research,* 78(3), pp. 431-442.

ARCHER, S.L., SOUIL, E., DINH-XUAN, A.T., SCHREMMER, B., MERCIER, J.C., EL YAAGOUBI, A., NGUYEN-HUU, L., REEVE, H.L. and HAMPL, V., 1998. Molecular identification of the role of voltage-gated K channels, K_V1.5 and K_V2.1, in hypoxic pulmonary vasoconstriction and control of resting membrane potential in rat pulmonary artery myocytes. *Journal of Clinical Investigation,* 101(11), pp. 2319-2330.

ARCHER, S.L., LONDON, B., HAMPL, V., WU, X., NSAIR, A., PUTTAGUNTA, L., HASHIMOTO, K., WAITE, R.E. and MICHELAKIS, E.D., 2001. Impairment of hypoxic pulmonary vasoconstriction in mice lacking the voltage-gated potassium channel K_V1.5. *The FASEB Journal,* 15(10), pp. 1801-1803.

ARCHER, S.L., WU, X.C., THÉBAUD, B., NSAIR, A., BONNET, S., TYRRELL, B., MCMURTRY, M.S., HASHIMOTO, K., HARRY, G. and MICHELAKIS, E.D., 2004. Preferential expression and function of voltage-gated, O_2-sensitive K^+ channels in resistance pulmonary arteries explains regional heterogeneity in hypoxic pulmonary vasoconstriction ionic diversity in smooth muscle cells. *Circulation Research,* 95(3), pp. 308-318.

ARDAILLOU, R., 1999. Angiotensin II receptors. *Journal of the American Society of Nephrology,* 10, pp.S30-9.

ARIYARATNAM, P., LOUBANI, M., BENNETT, R., GRIFFIN, S., CHAUDHRY, M.A., COWEN, M.E., GUVENDIK, L., CALE, A.R.J., and MORICE, A.H., 2013. Hyperoxic vasoconstriction of human pulmonary arteries: a novel insight into acute ventricular septal defects. *ISRN Cardiology.* [online] 2013. Available from: http://www.hindawi.com/isrn/cardiology/2013/685735/ [Accessed 20 September 2016].

ARRIGONI, F., HISLOP, A., HAWORTH, S. and MITCHELL, J., 1999. Newborn intrapulmonary veins are more reactive than arteries in normal and hypertensive piglets. *American Journal of Physiology-Lung Cellular and Molecular Physiology,* 277(5), pp. L887-L892.

ASANO, S., BRATZ, I.N., BERWICK, Z.C., FANCHER, I.S., TUNE, J.D. AND DICK, G.M., 2012. Penitrem A as a tool for understanding the role of large conductance Ca^{2+}/voltage-sensitive K^+ channels in vascular function. *The Journal of Pharmacology and Experimental Therapeutics*, 342(2), pp. 453-460.

ASIMAKOPOULOS, G., SMITH, P.L.C., RATNATUNGA, C.P. and TAYLOR, K.M., 1999. Lung injury and acute respiratory distress syndrome after cardiopulmonary bypass. *The Annals of Thoracic Surgery,* 68(3), pp. 1107-1115.

AUDI, S.H., DAWSON, C.A., RICKABY, D.A. and LINEHAN, J.H., 1991. Localization of the sites of pulmonary vasomotion by use of arterial and venous occlusion. *Journal of Applied Physiology,* 70(5), pp. 2126-2136.

AUMAN, H.J., COLEMAN, H., RILEY, H.E., OLALE, F., TSAI, H. and YELON, D., 2007. Functional modulation of cardiac form through regionally confined cell shape changes. *PLoS Biology,* 5(3), e53.

AUSTIN, C. and WRAY, S., 1993. Extracellular pH signals affect rat vascular tone by rapid transduction into intracellular pH changes. *The Journal of Physiology,* 466(1), pp. 1-8.

BARBOUR, B., 2014. *Electronics for electrophysiologists.* [online]. Paris, France: IBENS. Available from: http://www.biologie.ens.fr/~barbour/ [Accessed 20 September 2016].

BARDOU, M., GOIRAND, F., MARCHAND, S., ROUGET, C., DEVILLIER, P., DUMAS, J., MORCILLO, E.J., ROCHETTE, L. and DUMAS, M., 2001. Hypoxic vasoconstriction of rat main pulmonary artery: role of endogenous nitric oxide, potassium channels, and phosphodiesterase inhibition. *Journal of Cardiovascular Pharmacology,* 38(2), pp. 325-334.

BARNES, P.J. and LIU, S.F., 1995. Regulation of pulmonary vascular tone. *Pharmacological Reviews,* 47(1), pp. 87-131.

BARRON, J.J., ASHTON, C. and GEARY, L., 2006. *The effects of temperature on pH measurement.* [online]. County Clare, Ireland: Reagecon. Available from: http://reagecon.com/pdf/technicalpapers/Effects_of_Temperature_on_pH_v4-_TSP-01-2.pdf [Accessed 20 September 2016].

BÄRTSCH, P. and GIBBS, J.S.R., 2007. Effect of altitude on the heart and the lungs. *Circulation,* 116(19), pp. 2191-2202.

BAS, A., FORSBERG, G., HAMMARSTRÖM, S. and HAMMARSTRÖM, M., 2004. Utility of the housekeeping genes 18S rRNA, β-Actin and glyceraldehyde-3-phosphate-dehydrogenase for normalization in real-time quantitative reverse transcriptase-polymerase chain reaction analysis of gene expression in human T lymphocytes. *Scandinavian Journal of Immunology,* 59(6), pp. 566-573.

BINA, S., HART, J.L., SEI, Y. and MULDOON, S.M., 1998. Factors contributing to differences in the regulation of cGMP in isolated porcine pulmonary vessels. *European Journal of Pharmacology,* 351(2), pp. 253-260.

BINKO, J., MEACHEM, S. and MAJEWSKI, H., 1999. Endothelium removal induces iNOS in rat aorta in organ culture, leading to tissue damage. *American Journal of Physiology-Endocrinology and Metabolism,* 276(1), pp. E125-E134.

BLAND, R.D., DEMLING, R.H., SELINGER, S.L. and STAUB, N.C., 1977. Effects of alveolar hypoxia on lung fluid and protein transport in unanesthetized sheep. *Circulation Research,* 40(3), pp. 269-274.

BLATZ, A.L. and MAGLEBY, K.L., 1984. Ion conductance and selectivity of single calcium-activated potassium channels in cultured rat muscle. *The Journal of General Physiology,* 84(1), pp. 1-23.

BONNET, S., HYVELIN, J.M., BONNET, P., MARTHAN, R. and SAVINEAU, J.P., 2001. Chronic hypoxia-induced spontaneous and rhythmic contractions in the rat main pulmonary artery. *American Journal of Physiology-Lung Cellular and Molecular Physiology,* 281(1), pp. L183-L192.

BONNET, S., MICHELAKIS, E.D., PORTER, C.J., ANDRADE-NAVARRO, M.A., THEBAUD, B., BONNET, S., HAROMY, A., HARRY, G., MOUDGIL, R., MCMURTRY, S., WEIR, E.K. and ARCHER, S.L., 2006. An abnormal mitochondrial-hypoxia inducible factor-1α-K_V channel pathway disrupts oxygen sensing and triggers pulmonary arterial hypertension in fawn hooded rats: similarities to human pulmonary arterial hypertension. *Circulation,* 113(22), pp. 2630-2641.

BONNET, S. and ARCHER, S.L., 2007. Potassium channel diversity in the pulmonary arteries and pulmonary veins: implications for regulation of the pulmonary vasculature in health and during pulmonary hypertension. *Pharmacology & Therapeutics,* 115(1), pp. 56-69.

BORON, W.F. and BOULPAEP, E.L., 2005. *Medical Physiology.* Updated ed. Philadelphia, PA: Elsevier Inc.

BRESSACK, M.A. and BLAND, R.D., 1980. Alveolar hypoxia increases lung fluid filtration in unanesthetized newborn lambs. *Circulation Research,* 46(1), pp. 111-116.

BRINK, C., GILLARD, V., ROUBERT, P., MENCIA-HUERTA, J., CHABRIER, P., BRAQUET, P. and VERLEY, J., 1991. Effects and specific binding sites of endothelin in human lung preparations. *Pulmonary Pharmacology,* 4(1), pp. 54-59.

BUCHWALOW, I.B., PODZUWEIT, T., BOCKER, W., SAMOILOVA, V.E., THOMAS, S., WELLNER, M., BABA, H.A., ROBENEK, H., SCHNEKENBURGER, J. and LERCH, M.M., 2002. Vascular smooth muscle and nitric oxide synthase. *The FASEB Journal,* 16(6), pp. 500-508.

CAO, Y.X., HE, L.C., XU, C.B., LUO, G.G. and EDVINSSON, L., 2005. Enhanced transcription of contractile 5-hydroxytryptamine 2A receptors via extracellular signal-regulated kinase 1/2 after

organ culture of rat mesenteric artery. *Basic & Clinical Pharmacology & Toxicology,* 96(4), pp. 282-288.

CHALIKI, H.P., HURRELL, D.G., NISHIMURA, R.A., REINKE, R.A. and APPLETON, C.P., 2002. Pulmonary venous pressure: relationship to pulmonary artery, pulmonary wedge, and left atrial pressure in normal, lightly sedated dogs. *Catheterization and Cardiovascular Interventions,* 56(3), pp. 432-438.

CHAND, N., 1981. 5-hydroxytryptamine induces relaxation of goat pulmonary veins: evidence for the non-involvement of M and D-tryptamine receptors. *British Journal of Pharmacology,* 72(2), pp. 233-237.

CHAPMAN, R.A., 1993. The effect of oximes on the dihydropyridine-sensitive Ca^{2+} current of isolated guinea-pig ventricular myocytes. *Pflügers Archiv,* 422(4), pp. 325-331.

CHEN, L., TIAN, L., MACDONALD, S.H., MCCLAFFERTY, H., HAMMOND, M.S., HUIBANT, J.M., RUTH, P., KNAUS, H.G. and SHIPSTON, M.J., 2005. Functionally diverse complement of large conductance calcium- and voltage-activated potassium channel (BK) alpha-subunits generated from a single site of splicing. *The Journal of Biological Chemistry,* 280(39), pp. 33599-33609.

CLARKE, C.E., VEALE, E.L., GREEN, P.J., MEADOWS, H.J. and MATHIE, A., 2004. Selective block of the human 2-P domain potassium channel, TASK-3, and the native leak potassium current, IK_{SO}, by zinc. *The Journal of Physiology,* 560(1), pp. 51-62.

CLOUGH, A.V., HAWORTH, S.T., MA, W. and DAWSON, C.A., 2000. Effects of hypoxia on pulmonary microvascular volume. *American Journal of Physiology-Heart and Circulatory Physiology,* 279(3), pp. H1274-H1282.

COLEMAN, R.A., SMITH, W.L. and NARUMIYA, S., 1994. International Union of Pharmacology classification of prostanoid receptors: properties, distribution, and structure of the receptors and their subtypes. *Pharmacological Reviews,* 46(2), pp. 205-229.

CONFORTI, L. and MILLHORN, D.E., 2000. Regulation of Shaker-type potassium channels by hypoxia: oxygen-sensitive K^+ channels in PC12 cells. *Advances in Experimental Medicine and Biology,* 475, pp. 265-274.

CONNOLLY, M.J., PRIET-LLORET, J., BECKER, S. WARD, J.P. and AARONSON, P.I., 2013. Hypoxic pulmonary vasoconstriction in the absence of pretone: essential role for intracellular Ca^{2+} release. *The Journal of Physiology,* 591(18), pp. 4473-4498.

COSENTINO, F., HISHIKAWA, K., KATUSIC, Z.S. and LUSCHER, T.F., 1997. High glucose increases nitric oxide synthase expression and superoxide anion generation in human aortic endothelial cells. *Circulation,* 96(1), pp. 25-28.

COULANGE, M., ROSSI, P., GARGNE, O., GOLE, Y., BESSEREAU, J., REGNARD, J., JAMMES, Y., BARTHELEMY, A., AUFFRAY, J.P. and BOUSSUGES, A., 2010. Pulmonary oedema in healthy SCUBA divers: new physiopathological pathways. *Clinical Physiology and Functional Imaging,* 30(3), pp. 181-186.

CREAGH-BROWN, B.C., NICHOLSON, A.G., SHOWKATHALI, R., GIBBS, J.S. and HOWARD, L.S., 2008. Pulmonary veno-occlusive disease presenting with recurrent pulmonary oedema and the use of nitric oxide to predict response to sildenafil. *Thorax,* 63(10), pp. 933-934.

DAWSON, C.A., 1984. Role of pulmonary vasomotion in physiology of the lung. *Physiological Reviews,* 64(2), pp. 544-616.

DE MEY, J.G., UITENDAAL, M.P., BOONEN, H.C., VRIJDAG, M.J., DAEMEN, M.J. and STRUYKER-BOUDIER, H.A., 1989. Acute and long-term effects of tissue culture on contractile reactivity in renal arteries of the rat. *Circulation Research,* 65(4), pp. 1125-1135.

DEHNERT, C., RISSE, F., LEY, S., KUDER, T.A., BUHMANN, R., PUDERBACH, M., MENOLD, E., MERELES, D., KAUCZOR, H.U. and BÄRTSCH, P., 2006. Magnetic resonance imaging of uneven pulmonary perfusion in hypoxia in humans. *American Journal of Respiratory and Critical Care Medicine,* 174(10), pp. 1132-1138.

DEMBINSKI, R., HENZLER, D. and ROSSAINT, R., 2004. Modulating the pulmonary circulation: an update. *Minerva Anestesiologica,* 70(4), pp. 239-243.

DEN HENGST, W.A., GIELIS, J.F., LIN, J.Y., VAN SCHIL, P.E., DE WINDT, L.J. and MOENS, A.L., 2010. Lung ischemia-reperfusion injury: a molecular and clinical view on a complex pathophysiological process. *American Journal of Physiology-Heart and Circulatory Physiology,* 299(5), pp. H1283-H1299

DING, X. and MURRAY, P.A., 2005. Cellular mechanisms of thromboxane A_2-mediated contraction in pulmonary veins. *American Journal of Physiology-Lung Cellular and Molecular Physiology,* 289(5), pp. L825-L833.

DINGEMANS, K. and WAGENVOORT, C., 1978. Pulmonary arteries and veins in experimental hypoxia. An ultrastructural study. *The American Journal of Pathology,* 93(2), pp. 353-361.

DIPP, M. and EVANS, A.M., 2001. Cyclic ADP-ribose is the primary trigger for hypoxic pulmonary vasoconstriction in the rat lung *in situ*. *Circulation Research,* 89(1), pp. 77-83.

DIPP, M., NYE, P.C.G. and EVANS, A.M., 2001. Hypoxic release of calcium from the sarcoplasmic reticulum of pulmonary artery smooth muscle. *American Journal of Physiology-Lung Cellular and Molecular Physiology,* 281(2), pp. L318-L325.

DOSPINESCU, C., 2009. *Cellular mechanisms of acute hypoxic pulmonary vasoconstriction in intrapulmonary veins.* [online]. PhD thesis, Robert Gordon University. Available from: https://openair.rgu.ac.uk/handle/10059/380 [Accessed 20 September 2016].

DOSPINESCU, C., WIDMER, H., ROWE, I., WAINWRIGHT, C. and CRUICKSHANK, S.F., 2012. Hypoxia sensitivity of a voltage-gated potassium current in porcine intrapulmonary vein smooth muscle cells. *American Journal of Physiology-Lung Cellular and Molecular Physiology,* 303(5), pp. L476-L486.

DWEIK, R.A., COMHAIR, S.A., GASTON, B., THUNNISSEN, F.B., FARVER, C., THOMASSEN, M.J., KAVURU, M., HAMMEL, J., ABU-SOUD, H.M. and ERZURUM, S.C., 2001. NO chemical events in the human airway during the immediate and late antigen-induced asthmatic response. *Proceedings of the National Academy of Sciences of the United States of America,* 98(5), pp. 2622-2627.

ELDER, K., VAN DEN BERG, M. and WOODWARD, B., 2015. *Trouble-shooting and problem-solving in the IVF laboratory.* Cambridge, UK: Cambridge University Press.

EMERSON, G.G. and SEGAL, S.S., 2000. Endothelial cell pathway for conduction of hyperpolarization and vasodilation along hamster feed artery. *Circulation Research,* 86(1), pp. 94-100.

EVANS, A.M., MUSTARD, K.J.W, WYATT, C.N., PEERS, C., DIPP, M., KUMAR, P., KINNEAR, N.P. and HARDIE, D.G., 2005. Does AMP-activated protein kinase couple inhibition of mitochondrial oxidative phosphorylation by hypoxia to calcium signalling in O_2-sensing cells? *The Journal of Biological Chemistry,* 280(50), pp. 41504-41511.

EVANS, A.M., 2006. AMP-activated protein kinase and the regulation of Ca^{2+} signalling in O_2 sensing cells. *The Journal of Physiology,* 574(1), pp. 113-123.

FANCHER, I.S., BUTCHER, J.T., BROOKS, S.D., ROTTGEN, T.S., SKAFF, P.R., FRISBEE, J.C. and DICK, G.M., 2015. Diphenyl phosphine oxide-1-sensitive K^+ channels contribute to the vascular tone and reactivity of resistance arteries from brain and skeletal muscle. *Microcirculation,* 22(4), pp. 315-325.

FÉLÉTOU, M., GIRARD, V. and CANET, E., 1995. Different involvement of nitric oxide in endothelium-dependent relaxation of porcine pulmonary artery and vein: influence of hypoxia. *Journal of Cardiovascular Pharmacology,* 25(4), pp. 665.

FIGL, T., LEWIS, T.M. and BARRY, P.H., 2004. Liquid junction potential corrections. *AxoBits,* 39, pp. 1-10.

FIRTH, A.L., GORDIENKO, D.V., YUILL, K.H. and SMIRNOV, S.V., 2009. Cellular localization of mitochondria contributes to K_V channel-mediated regulation of cellular excitability in pulmonary but not mesenteric circulation. *American Journal of Physiology – Lung Cellular and Molecular Physiology,* 296(3), pp. L347-L360.

FIRTH, A.L., REMILLARD, C.V., PLATOSHYN, O., FANTOZZI, I., KO, E.A. and YUAN, J.X., 2011. Functional ion channels in human pulmonary artery smooth muscle cells: voltage-dependent cation channels. *Pulmonary Circulation,* 1(1), pp. 48-71.

FRANCO-OBREGON, A. and LOPEZ-BARNEO, J., 1996. Low PO_2 inhibits calcium channel activity in arterial smooth muscle cells. *American Journal of Physiology-Heart and Circulatory Physiology,* 271(6), pp. H2290-H2299.

FUNG, Y.C. and HUANG, W., 2004. The physics of hypoxic pulmonary hypertension and its connection with gene actions. In: X.J. YUAN, ed. *Hypoxic pulmonary vasoconstriction: cellular and molecular mechanisms.* Boston, MA: Kluwer Academic Publishers.

FURCHGOTT, R.F. and ZAWADZKI, J.V., 1980. The obligatory role of endothelial cells in the relaxation of arterial smooth muscle by acetylcholine. *Nature,* 288(5789), pp. 373-376.

FURFINE, E.S., HARMON, M.F., PAITH, J.E., KNOWLES, R.G., SALTER, M., KIFF, R.J., DUFFY, C., HAZELWOOD, R., OPLINGER, J.A. and GARVEY, E.P., 1994. Potent and selective inhibition of human nitric oxide synthases. Selective inhibition of neuronal nitric oxide synthase by S-methyl-L-thiocitrulline and S-ethyl-L-thiocitrulline. *The Journal of Biological Chemistry,* 269(43), pp. 26677-26683.

FYNN, S.P. and KALMAN, J.M., 2004. Pulmonary veins: anatomy, electrophysiology, tachycardia, and fibrillation. *Pacing and Clinical Electrophysiology,* 27(11), pp. 1547-1559.

GAO, Y., ZHOU, H. and RAJ, J.U., 1995. Endothelium-derived nitric oxide plays a larger role in pulmonary veins than in arteries of newborn lambs. *Circulation Research,* 76(4), pp. 559-565.

GAO, Y. and RAJ, J.U., 2005. Role of veins in regulation of pulmonary circulation. *American Journal of Physiology-Lung Cellular and Molecular Physiology,* 288(2), pp. L213-L226.

GAO, Y., PORTUGAL, A.D., LIU, J., NEGASH, S., ZHOU, W., TIAN, J., XIANG, R., LONGO, L.D. and RAJ, J.U., 2008. Preservation of cGMP-induced relaxation of pulmonary veins of fetal lambs exposed to chronic high altitude hypoxia: role of PKG and Rho kinase. *American Journal of Physiology-Lung Cellular and Molecular Physiology,* 295(5), pp. L889-L896.

GELBAND, C.H. and HUME, J.R., 1992. Ionic currents in single smooth muscle cells of the canine renal artery. *Circulation Research,* 71(4), pp. 745-758.

GLAZIER, J.B. and MURRAY, J.F., 1971. Sites of pulmonary vasomotor reactivity in the dog during alveolar hypoxia and serotonin and histamine infusion. *The Journal of Clinical Investigation,* 50(12), pp. 2550-2558.

GRIFFITH, O.W. and KILBOURN, R.G., 1996. Nitric oxide synthase inhibitors: amino acids. *Methods in Enzymology,* 268, pp. 375-392.

GRISSMER, S., NGUYEN, A.N., AIYAR, J., HANSON, D.C., MATHER, R.J., GUTMAN, G.A., KARMILOWICZ, M.J., AUPERIN, D.D. and CHANDY, K.G., 1994. Pharmacological characterization of five cloned voltage-gated K^+ channels, types K_V1.1, 1.2, 1.3, 1.5, and 3.1, stably expressed in mammalian cell lines. *Molecular Pharmacology,* 45(6), pp. 1227-1234.

GRUSS, M., MATHIE, A., LIEB, W.R. and FRANKS, N.P., 2004. The two-pore-domain K^+ channels TREK-1 and TASK-3 are differentially modulated by copper and zinc. *Molecular Pharmacology,* 66(3), pp. 530-537.

GUIBERT, C., SAVINEAU, J.P., CREVEL, H., MARTHAN, R. and ROUSSEAU, E., 2005. Effect of short-term organoid culture on the pharmaco-mechanical properties of rat extra-and intrapulmonary arteries. *British Journal of Pharmacology,* 146(5), pp. 692-701.

HAISSAGUERRE, M., JAÏS, P., SHAH, D.C., TAKAHASHI, A., HOCINI, M., QUINIOU, G., GARRIGUE, S., LE MOUROUX, A., LE METAYER., P. and CLEMENTY, J., 1998. Spontaneous initiation of atrial fibrillation by ectopic beats originating in the pulmonary veins. *New England Journal of Medicine,* 339(10), pp. 659-666.

HAMPL, V., BÍBOVÁ, J., STRAŇÁK, Z., WU, X., MICHELAKIS, E.D., HASHIMOTO, K. and ARCHER, S.L., 2002. Hypoxic fetoplacental vasoconstriction in humans is mediated by potassium channel inhibition. *American Journal of Physiology-Heart and Circulatory Physiology,* 283(6), pp. H2440-H2449.

HARDIE, D.G. and HAWLEY, S.A., 2001. AMP-activated protein kinase: the energy charge hypothesis revisited. *Bioessays,* 23(12), pp. 1112-1119.

HASEBE, N., ONODERA, S., YAMASHITA, H., KAWAMURA, Y., HANEDA, T. and TOBISE, K., 1992. Site of hypoxic pulmonary vasoconstriction in pulsatile perfused canine lung lobes. *Japanese Circulation Journal,* 56(8), pp. 837-846.

HER, C., MANDY, S. and BAIRAMIAN, M., 2005. Increased pulmonary venous resistance contributes to increased pulmonary artery diastolic–pulmonary wedge pressure gradient in acute respiratory distress syndrome. *Anesthesiology,* 102(3), pp. 574-580.

HER, C., CERABONA, T., BAEK, S.H. and SHIN, S.W., 2010. Increased pulmonary venous resistance in morbidly obese patients without daytime hypoxia: clinical utility of the pulmonary artery catheter. *Anesthesiology,* 113(3), pp. 552-559.

HILLIER, S.C., GRAHAM, J.A., HANGER, C.C., GODBEY, P.S., GLENNY, R.W. and WAGNER, W.W., 1997. Hypoxic vasoconstriction in pulmonary arterioles and venules. *Journal of Applied Physiology,* 82(4), pp. 1084-1090.

HISLOP, A. and REID, L., 1973. Fetal and childhood development of the intrapulmonary veins in man--branching pattern and structure. *Thorax,* 28(3), pp. 313-319.

HLASTALA, M.P., LAMM, W.J.E., KARP, A., POLISSAR, N.L., STARR, I.R. and GLENNY, R.W., 2004. Spatial distribution of hypoxic pulmonary vasoconstriction in the supine pig. *Journal of Applied Physiology,* 96(5), pp. 1589-1599.

HOGG, D.S., DAVIES, A.R., MCMURRAY, G. and KOZLOWSKI, R.Z., 2002. $K_V2.1$ channels mediate hypoxic inhibition of I_{Kv} in native pulmonary arterial smooth muscle cells of the rat. *Cardiovascular Research,* 55(2), pp. 349-360.

HONG, Z., WEIR, E.K., VARGHESE, A. and OLSCHEWSKI, A., 2005. Effect of normoxia and hypoxia on K^+ current and resting membrane potential of fetal rabbit pulmonary artery smooth muscle. *Physiological Research,* 54(2), pp. 175-184.

HOPKINS, S.R., KLEINSASSER, A., BERNARD, S., LOECKINGER, A., FALOR, E., NERADILEK, B., POLISSAR, N.L. and HLASTALA, M.P., 2007. Hypoxia has a greater effect than exercise on the redistribution of pulmonary blood flow in swine. *Journal of Applied Physiology,* 103(6), pp. 2112-2119.

HU, L.M. and JONES, R., 1989. Injury and remodeling of pulmonary veins by high oxygen. A morphometric study. *The American Journal of Pathology,* 134(2), pp. 253-262.

HUGHES, J.M.B. and MORELL, N.W., 2001. *Vascular Structure and Function. Pulmonary Circulation: From Basic Mechanisms to Clinical Practice.* London, UK: Imperial College Press.

HURTADO DEL POZO, C., CALVO, R.M., VESPERINAS-GARCÍA, G., GÓMEZ-AMBROSI, J., FRÜHBECK, G., CORRIPIO-SÁNCHEZ, R., RUBIO, M.A. and OBREGON, M., 2010. *IPO8* and *FBXL10*: new reference genes for gene expression studies in human adipose tissue. *Obesity,* 18(5), pp. 897-903.

HYMAN, A.L., MATHE, A.A., LESLIE, C.A., MATTHEWS, C.C., BENNETT, J.T., SPANNHAKE, E.W. and KADOWITZ, P.J., 1978. Modification of pulmonary vascular responses to arachidonic acid by alterations in physiological state. *The Journal of Pharmacology and Experimental Therapeutics,* 207(2), pp. 388-401.

IGNARRO, L.J., 1990. Haem-dependent activation of guanylate cyclase and cyclic GMP formation by endogenous nitric oxide: a unique transduction mechanism for transcellular signaling. *Pharmacology & Toxicology,* 67(1), pp. 1-7.

IINO, M., 1990. Calcium release mechanisms in smooth muscle. *The Japanese Journal of Pharmacology,* 54(4), pp. 345-354.

ISHIZAKA, H. and KUO, L., 1996. Acidosis-induced coronary arteriolar dilation is mediated by ATP-sensitive potassium channels in vascular smooth muscle. *Circulation Research,* 78(1), pp. 50-57

IWAKI, M., IMAIZUMI, K., YOKOI, T., KONDO, M., KAWAGUCHI, K. and HASEGAWA, Y., 2009. Idiopathic pulmonary veno-occlusive disease. *Internal Medicine,* 48(15), pp. 1289-1292.

JABR, R.I., TOLAND, H., GELBAND, C.H., XIA WANG, X. and HUME, J.R., 1997. Prominent role of intracellular Ca^{2+} release in hypoxic vasoconstriction of canine pulmonary artery. *British Journal of Pharmacology,* 122(1), pp. 21-30.

JAKOUBEK, V., BÍBOVÁ, J. and HAMPL, V., 2006. Voltage-gated calcium channels mediate hypoxic vasoconstriction in the human placenta. *Placenta,* 27(9), pp. 1030-1033.

KADOWITZ, P.J., JOINER, P.D., HYMAN, A.L. and GEORGE, W.J., 1975. Influence of prostaglandins E_1 and $F_{2\alpha}$ on pulmonary vascular resistance, isolated lobar vessels ad cyclic nucleotide levels. *The Journal of Pharmacology and Experimental Therapeutics,* 192(3), pp. 677-687.

KARCZEWSKI, J., KISS, L., KOBLAN, K.S., LYNCH, R.J. and SPENCER, R.H., 2009. High-throughput analysis of drug binding interactions for the human cardiac channel, $K_V1.5$. *Biochemical Pharmacology,* 77(2), pp. 177-185.

KAY, J.M., 1983. Comparative morphologic features of the pulmonary vasculature in mammals. *American Review of Respiratory Disease,* 128(2P2), pp. S53-S57.

KEMP, B.K., SMOLICH, J.J. and COCKS, T.M., 1997. Evidence for specific regional patterns of responses to different vasoconstrictors and vasodilators in sheep isolated pulmonary arteries and veins. *British Journal of Pharmacology,* 121(3), pp. 441-450.

KHAN, R., 2004. Identifying and understanding the role of pulmonary vein activity in atrial fibrillation. *Cardiovascular Research,* 64(3), pp. 387-394.

KLATT, P., SCHMIDT, K., BRUNNER, F. and MAYER, B., 1994. Inhibitors of brain nitric oxide synthase. Binding kinetics, metabolism, and enzyme inactivation. *The Journal of Biological Chemistry,* 269(3), pp. 1674-1680.

KO, E.A., BURG, E.D., PLATOSHYN, O., MSEFYA, J., FIRTH, A.L. and YUAN, J.X., 2007. Functional characterization of voltage-gated K^+ channels in mouse pulmonary artery smooth muscle cells. *American Journal of Physiology-Cell Physiology,* 293(3), pp. C928-C937.

KUEBLER, W.M., UHLIG, U., GOLDMANN, T., SCHAEL, G., KEREM, A., EXNER, K., MARTIN, C., VOLLMER, E. and UHLIG, S., 2003. Stretch activates nitric oxide production in pulmonary vascular endothelial cells in situ. *American Journal of Respiratory and Critical Care Medicine,* 168(11), pp. 1391-1398.

LAGRUTTA, A., WANG, J., FERMINI, B. and SALATA, J.J., 2006. Novel, potent inhibitors of human $K_v1.5$ K^+ channels and ultrarapidly activating delayed rectifier potassium current. *The Journal of Pharmacology and Experimental Therapeutics,* 317(3), pp. 1054-1063.

LAHM, T., ALBRECHT, M., FISHER, A.J., SELEJ, M., PATEL, N.G., BROWN, J.A., JUSTICE, M.J., BROWN, M.B., VAN DEMARK, M., TRULOCK, K.M., DIEUDONNE, D., REDDY, J.G., PRESSON, R.G. and PETRACHE, I., 2012. 17β-estradiol attenuates hypoxic pulmonary hypertension via estrogen receptor-mediated effects. *American Journal of Respiratory and Critical Care Medicine*, 185(9), pp.965-980.

LAL, H., WILLIAMS, K.I. and WOODWARD, B., 1999. Chronic hypoxia differentially alters the responses of pulmonary arteries and veins to endothelin-1 and other agents. *European Journal of Pharmacology,* 371(1), pp. 11-21.

LEACH, R.M., ROBERTSON, T.P., TWORT, C.H.C. and WARD, J.P.T., 1994. Hypoxic vasoconstriction in rat pulmonary and mesenteric arteries. *American Journal of Physiology-Lung Cellular and Molecular Physiology,* 266(3), pp. L223-L231.

LEACH, R.M., HILL, H.M., SNETKOV, V.A., ROBERTSON, T.P., WARD, J., 2001. Divergent roles of glycolysis and the mitochondrial electron transport chain in hypoxic pulmonary vasoconstriction of the rat: identity of the hypoxic sensor. *The Journal of Physiology,* 536(1), pp. 211-224.

LEONOUDAKIS, D., GRAY, A.T., WINEGAR, B.D., KINDLER, C.H., HARADA, M., TAYLOR, D.M., CHAVEZ, R.A., FORSAYETH, J.R. and YOST, C.S., 1998. An open rectifier potassium channel with two pore domains in tandem cloned from rat cerebellum. *The Journal of Neuroscience,* 18(3), pp. 868-877.

LEVITZKY, M.G., 2002. *Blood flow to the lung. Pulmonary physiology.* 6th Ed. New York, NY: McGraw-Hill Professional.

LIU, Q., SHAM, J.S., SHIMODA, L.A. and SYLVESTER, J.T., 2001. Hypoxic constriction of porcine distal pulmonary arteries: endothelium and endothelin dependence. *American Journal of Physiology-Lung Cellular and Molecular Physiology,* 280(5), pp. L856-L865.

LOPATIN, A.N. and NICHOLS, C.G., 1993. 2,3-Butanedione monoxime (BDM) inhibition of delayed rectifier DRK1 (K_V2.1) potassium channels expressed in Xenopus oocytes. *The Journal of Pharmacology and Experimental Therapeutics,* 265(2), pp. 1011-1016.

LOPEZ-VALVERDE, V., ANDERSEN, C.U., LAURSEN, B.E., MULVANY, M.J. and SIMONSEN, U., 2005. Glibenclamide reveals role for endothelin in hypoxia-induced vasoconstriction in rat intrapulmonary arteries. *Journal of Cardiovascular Pharmacology,* 46(4), pp. 422-429.

LOUTZENHISER, R., MATSUMOTO, Y., OKAWA, W. and EPSTEIN, M., 1990. H^+-induced vasodilation of rat aorta is mediated by alterations in intracellular calcium sequestration. *Circulation Research,* 67(2), pp. 426-439.

LU, X., GUO, X., KARATHANASIS, S.K., ZIMMERMAN, K.M., ONYIA, J.E., PETERSON, R.G. and KASSAB, G.S., 2010. Rosiglitazone reverses endothelial dysfunction but not remodeling of femoral artery in Zucker diabetic fatty rats. *Cardiovascular Diabetology.* [online] 9(19). Available from: http://cardiab.biomedcentral.com/articles/10.1186/1475-2840-9-19 [Accessed 20 September 2016].

MACKENZIE, A., COOPER, E.J. and DOWELL, F.J., 2008. Differential effects of glucose on agonist-induced relaxations in human mesenteric and subcutaneous arteries. *British Journal of Pharmacology,* 153(3), pp. 480-487.

MACLEAN, M.R. and MORECROFT, I., 2001. Increased contractile response to 5-hydroxytryptamine$_1$-receptor stimulation in pulmonary arteries from chronic hypoxic rats: role of pharmacological synergy. *British Journal of Pharmacology,* 134(3), pp. 614-620.

MAGGIORINI, M., MÉLOT, C., PIERRE, S., PFEIFFER, F., GREVE, I., SARTORI, C., LEPORI, M., HAUSER, M., SCHERRER, U. and NAEIJE, R., 2001. High-altitude pulmonary edema is initially caused by an increase in capillary pressure. *Circulation,* 103(16), pp. 2078-2083.

MAINGRET, F., PATEL, A.J., LAZDUNSKI, M. and HONORE, E., 2001. The endocannabinoid anandamide is a direct and selective blocker of the background K^+ channel TASK-1. *The EMBO Journal,* 20(1-2), pp. 47-54.

MANOURY, B., ETHERIDGE, S.L., REID, J. and GURNEY, A.M., 2009. Organ culture mimics the effects of hypoxia on membrane potential, K^+ channels and vessel tone in pulmonary artery. *British Journal of Pharmacology,* 158(3), pp. 848-861.

MANOURY, B., LAMALLE, C., OLIVEIRA, R., REID, J. and GURNEY, A.M., 2011. Contractile and electrophysiological properties of pulmonary artery smooth muscle are not altered in TASK-1 knockout mice. *The Journal of Physiology,* 589(13), pp. 3231-3246.

MARTIN, Y.N. and PABELICK, C.M., 2014. Sex differences in the pulmonary circulation: implications for pulmonary hypertension. *American Journal of Physiology - Heart and Circulatory Physiology,* 306(9), pp. H1253-H1264.

MCCARTNEY, C.E., MCCLAFFERTY, H., HUIBANT, J.M., ROWAN, E.G., SHIPSTON, M.J. and ROWE, I., 2005. A cysteine-rich motif confers hypoxia sensitivity to mammalian large conductance voltage-and Ca-activated K (BK) channel α-subunits. *Proceedings of the National Academy of Sciences of the United States of America,* 102(49), pp. 17870-17876.

MCGAHON, M.K., DAWICKI, J.M., ARORA, A., SIMPSON, D.A., GARDINER, T.A., STITT, A.W., SCHOLFIELD, C.N., MCGEOWN, J.G. and CURTIS, T.M., 2007. $K_V1.5$ is a major component underlying the A-type potassium current in retinal arteriolar smooth muscle. *American Journal of Physiology-Heart and Circulatory Physiology,* 292(2), pp. H1001-H1008.

MCMURTRY, I.F., DAVIDSON, A.B., REEVES, J.T. and GROVER, R.F., 1976. Inhibition of hypoxic pulmonary vasoconstriction by calcium antagonists in isolated rat lungs. *Circulation Research,* 38(2), pp. 99-104.

MCMURTRY, I.F., PETRUN, M.D. and REEVES, J.T., 1978. Lungs from chronically hypoxic rats have decreased pressor response to acute hypoxia. *American Journal of Physiology-Heart and Circulation Physiology,* 235(1), pp. H104-H109.

MERKUS, D., DE BEER, V.J., HOUWELING, B. and DUNCKER, D.J., 2008. Control of pulmonary vascular tone during exercise in health and pulmonary hypertension. *Pharmacology & Therapeutics,* 119(3), pp. 242-263.

MICHELAKIS, E.D., WEIR, E.K., WU, X., NSAIR, A., WAITE, R., HASHIMOTO, K., PUTTAGUNTA, L., KNAUS, H.G. and ARCHER, S.L., 2001. Potassium channels regulate tone in rat pulmonary veins. *American Journal of Physiology-Lung Cellular and Molecular Physiology,* 280(6), pp. L1138-L1147.

MICHON, G.P., 2004. *Surface area of an ellipsoid.* [online]. Los Angeles, CA: Numericana.com. Available from: http://www.numericana.com/answer/ellipsoid.htm [Accessed 20 September 2016]

MILLER, D., YAGHI, A., HAMILTON, J. and PATERSON, N., 1989. Role of arachidonic acid metabolites in hypoxic contractions of isolated porcine pulmonary artery and vein. *Experimental Lung Research,* 15(2), pp. 213-222.

MOLLEMAN, A., 2003. *Patch clamping. An introductory guide to patch clamp electrophysiology.* Chichester, UK: John Wiley & Sons Ltd.

MONTANI, D., ACHOUH, L., DORFMULLER, P., ACHOUH, L., JAÏS, X., YAÏCI, A., SITBON, O., MUSSET, D., SIMONNEAU, G. and HUMBERT, M., 2008. Pulmonary veno-occlusive disease: Clinical, functional, radiologic, hemodynamic characteristics and outcome of 24 cases confirmed by histology. *Medicine (Baltimore),* 87(4), pp. 220-233.

MONTANI, D., PRICE, L.C., DORFMULLER, P., ACHOUH, L., JAÏS, X., YAÏCI, A., SITBON, O., MUSSET, D., SIMONNEAU, G. and HUMBERT, M., 2009. Pulmonary veno-occlusive disease. *European Respiratory Journal,* 33(1), pp. 189-200.

MOORE, P.K., BABBEDGE, R.C., WALLACE, P., GAFFEN, Z.A., and HART, S.L., 1993. 7-Nitro indazole, an inhibitor of nitric oxide synthase, exhibits anti-nociceptive activity in the mouse without increasing blood pressure. *British Journal of Pharmacology,* 108(2), pp.296-297.

MOORE, W.M., WEBBER, R.K., FOK, K.F., JEROME, G.M., KORNMEIER, C.M., TJOENG, F.S. and CURRIE, M.G., 1996. Inhibitors of human nitric oxide synthase isoforms with the carbamidine moiety as a common structural element. *Bioorganic & Medicinal Chemistry,* 4(9), pp. 1559-1564.

MORITA, T., YAMAWAKI, H., OKADA, M. and HARA, Y., 2010. Contractile characteristics of rat mesenteric artery after organ culture. *Journal of Veterinary Medical Science,* 72(12), pp. 1621-1627.

MORITA, T., OKADA, M., HARA, Y. and YAMAWAKI, H., 2013. Addition of adult serum improves endothelium-dependent relaxation of organ-cultured rat mesenteric artery via inhibiting mitochondrial reactive oxygen species. *Vascular Pharmacology,* 58(1), pp. 105-111.

MOUDGIL, R., MICHELAKIS, E.D. and ARCHER, S.L., 2005. Hypoxic pulmonary vasoconstriction. *Journal of Applied Physiology,* 98(1), pp. 390-403.

MURALIDHAR, K., 2002. Central venous pressure and pulmonary capillary wedge pressure monitoring. *Indian Journal of Anaesthesiology,* 46(4), pp. 298-303.

MURRAY, F., INSEL, P.A., and YUAN, J.X.J, 2006. Role of O_2-sensitive K^+ and Ca^{2+} channels in the regulation of the pulmonary circulation: Potential role of caveolae and implications for high altitude pulmonary edema. *Respiratory Physiology & Neurobiology*, 151(2-3), pp. 192-208.

NAEYE, R.L., 1965. Pulmonary vascular changes with chronic unilateral pulmonary hypoxia. *Circulation Research,* 17(2), pp. 160-167.

NAGASAKA, Y., BHATTACHARYA, J., NANJO, S., GROPPER, M. and STAUB, N., 1984. Micropuncture measurement of lung microvascular pressure profile during hypoxia in cats. *Circulation Research,* 54(1), pp. 90-95.

NATHAN, H. and GLOOBE, H., 1970. Myocardial atrio-venous junctions and extensions (sleeves) over the pulmonary and caval veins. Anatomical observations in various mammals. *Thorax,* 25(3), pp. 317-324.

NG, L.C., WILSON, S.M. and HUME, J.R., 2005. Mobilization of sarcoplasmic reticulum stores by hypoxia leads to consequent activation of capacitative Ca^{2+} entry in isolated canine pulmonary arterial smooth muscle cells. *The Journal of Physiology,* 563(2), pp. 409-419.

NOBE, K., NEZU, Y., TSUMITA, N., HASHIMOTO, T. and HONDA, K., 2008. Intra-and extrarenal arteries exhibit different profiles of contractile responses in high glucose conditions. *British Journal of Pharmacology,* 155(8), pp. 1204-1213.

NOREL, X., WALCH, L., GASCARD, J., DE MONTPREVILLE, V. and BRINK, C., 2004. Prostacyclin release and receptor activation: differential control of human pulmonary venous and arterial tone. *British Journal of Pharmacology,* 142(4), pp. 788-796.

OLSCHEWSKI, A., HONG, Z., NELSON, D.P. and WEIR, E.K., 2002. Graded response of K^+ current, membrane potential, and $[Ca^{2+}]_i$ to hypoxia in pulmonary arterial smooth muscle. *American Journal of Physiology-Lung Cellular and Molecular Physiology,* 283(5), pp. L1143-L1150.

OLSCHEWSKI, A., LI, Y., TANG, B., HANZE, J., EUL, B., BOHLE, R.M., WILHELM, J., MORTY, R.E., BRAU, M.E., WEIR, E.K., KWAPISZEWSKA, G., KLEPETKO, W., SEEGER, W. and OLSCHEWSKI, H., 2006. Impact of TASK-1 in human pulmonary artery smooth muscle cells. *Circulation Research,* 98(8), pp. 1072-1080.

OSIPENKO, O.N., EVANS, A.M. and GURNEY, A.M., 1997. Regulation of the resting potential of rabbit pulmonary artery myocytes by a low threshold, O_2-sensing potassium current. *British Journal of Pharmacology,* 120(8), pp. 1461-1470.

OSIPENKO, O.N., ALEXANDER, D., MACLEAN, M.R. and GURNEY, A.M., 1998. Influence of chronic hypoxia on the contributions of non-inactivating and delayed rectifier K currents to the resting potential and tone of rat pulmonary artery smooth muscle. *British Journal of Pharmacology,* 124(7), pp. 1335-1337.

OTUN, H., GILLESPIE, J.I., GREENWELL, J.R. and DUNLOP, W., 1993. The actions of caffeine and 2,3-butanedione monoxime on calcium transients in human vascular smooth muscle. *Experimental Physiology,* 78, pp. 255-258.

PALMER, S.M., ROBINSON, L.J. WANG, A., GOSSAGE, J.R., BASHORE, T. and TAPSON, V.F., 1998. Massive pulmonary edema and death after prostacyclin infusion in a patient with pulmonary veno-occlusive disease. *Chest,* 113(1), pp. 237-240.

PATEL, A.J., LAZDUNSKI, M. and HONORE, E., 1997. Kv2.1/Kv9.3, a novel ATP-dependent delayed-rectifier K^+ channel in oxygen-sensitive pulmonary artery myocytes. *The EMBO journal,* 16(22), pp. 6615-6625.

PATEL, S.K., JACKSON, L., WARREN, A.Y., ARYA, P., SHAW, R.W. and KHAN, R.N., 2013. A role for two-pore potassium (K2P) channels in endometrial epithelial function. *Journal of Cellular and Molecular Medicine,* 17(1), pp. 134-146.

PEINADO, V.I., PARÍS, R., RAMÍREZ, J., ROCA, J., RODRIGUEZ-ROISIN, R. and BARBERÀ, J.A., 2008. Expression of BK_{Ca} channels in human pulmonary arteries: relationship with remodeling and hypoxic pulmonary vasoconstriction. *Vascular Pharmacology,* 49(4), pp. 178-184.

PENG, G., WANG, J., LU, W. and RAN, P., 2010. Isolation and primary culture of rat distal pulmonary venous smooth muscle cells. *Hypertension Research,* 33(4), pp. 308-313.

PENG, G., RAN, P., LU, W., ZHONG, N. and WANG, J., 2013. Acute hypoxia activates store-operated Ca^{2+} entry and increases intracellular Ca^{2+} concentration in rat distal pulmonary venous smooth muscle cells. *Journal of Thoracic Disease,* 5(5), pp. 605-612.

PENG, W., KARWANDE, S.V., HOIDAL, J.R. and FARRUKH, I.S., 1996. Potassium currents in cultured human pulmonary arterial smooth muscle cells. *Journal of Applied Physiology,* 80(4), pp. 1187-1196.

PIETRA, G.G., CAPRON, F., STEWART, S., LEONE, O., HUMBERT, M., ROBBINS, I.M., REID, L.M. and TUDER, R.M., 2004. Pathologic assessment of vasculopathies in pulmonary hypertension. *Journal of the American College of Cardiology,* 43(12), pp. S25-S32.

PLATOSHYN, O., YU, Y., GOLOVINA, V.A., MCDANIEL, S.S., KRICK, S., LI, L., WANG, J.Y., RUBIN, L.J. and YUAN, J.X., 2001. Chronic hypoxia decreases K_V channel expression and function in pulmonary artery myocytes. *American Journal of Physiology-Lung Cellular and Molecular Physiology,* 280(4), pp. L801-L812.

PLATOSHYN, O., BREVNOVA, E.E., BURG, E.D., YU, Y., REMILLARD, C.V. and YUAN, J.X.J., 2006. Acute hypoxia selectively inhibits KCNA5 channels in pulmonary artery smooth muscle cells. *American Journal of Physiology-Cell Physiology,* 290(3), pp. C907-C916.

POLTE, T.R., EICHLER, G.S., WANG, N. and INGBER, D.E., 2004. Extracellular matrix controls myosin light chain phosphorylation and cell contractility through modulation of cell shape and cytoskeletal prestress. *American Journal of Physiology-Cell Physiology,* 286(3), pp. C518-C528.

PORRES, D.V., MORENZA, Ó.P., PALLISA, E., ROQUE, A., ANDREU, J. and MARTÍNEZ, M., 2013. Learning from the pulmonary veins. *Radiographics,* 33(4), pp. 999-1022.

POST, J.M., HUME, J.R., ARCHER, S.L. and WEIR, E.K., 1992. Direct role for potassium channel inhibition in hypoxic pulmonary vasoconstriction. *American Journal of Physiology-Cell Physiology,* 262(4), pp. C882-C890.

POST, J.M., GELBAND, C.H. and HUME, J.R., 1995. $[Ca^{2+}]_i$ inhibition of K^+ channels in canine pulmonary artery: novel mechanism for hypoxia-induced membrane depolarisation. *Circulation Research,* 77(1), pp.131-139.

RABINOVITCH, M., GAMBLE, W.J., MIETTINEN, O.S. and REID, L., 1981. Age and sex influence on pulmonary hypertension of chronic hypoxia and on recovery. *American Journal of Physiology – Heart and Circulatory Physiology*, 240(1), pp. H62-H72.

RAJ, J. and CHEN, P., 1986. Micropuncture measurement of microvascular pressures in isolated lamb lungs during hypoxia. *Circulation Research,* 59(4), pp. 398-404.

RAJ, J.U., CHEN, P. and NAVAZO, L., 1986. Micropuncture measurement of lung microvascular pressure profile in 3-to 4-week-old rabbits. *Pediatric Research,* 20(11), pp. 1107-1111.

RAJ, J.U., HILLYARD, R., KAAPA, P., GROPPER, M. and ANDERSON, J., 1990. Pulmonary arterial and venous constriction during hypoxia in 3-to 5-wk-old and adult ferrets. *Journal of Applied Physiology,* 69(6), pp. 2183-2189.

RATZ, P.H., BERG, K.M., URBAN, N.H. and MINER, A.S., 2005. Regulation of smooth muscle calcium sensitivity: KCl as a calcium-sensitizing stimulus. *American Journal of Physiology-Cell Physiology,* 288(4), pp. C769-C783.

REYER, E., 2013. *The hemodynamic and physiological relevance of continuous central venous oxygenation monitoring: it's not just for sepsis.* [online]. San Clemente, CA: ICU Medical Inc. Available from: http://www.icumed.com/media/402627/M1-1430%20Reyer%20%20-%20SCVO2%20Oximetry%20White%20Paper%20Rev.01-Web.pdf [Accessed 20 September 2016]

RISSO, A., COMERMA-STEFFENSEN, S., ROJAS, J., ASCANIO, E., HAHN, M., REGGIO, M. and ZERPA, H., 2012. Effect of hypoxia/reoxygenation on the contractility of the isolated bovine digital vein. *Research in Veterinary Science,* 92(2), pp. 299-305.

RIVERA-ESTRADA, C., SALTZMAN, P.W., SINGER, D. and KATZ, L.N., 1958. Action of hypoxia on the pulmonary vasculature. *Circulation Research,* 6(1), pp. 10-14.

ROBBINS, I.M., NEWMAN, J.H., JOHNSON, R.F., HEMNES, A.R., FREMONT, R.D., PIANA, R.N., ZHAO, D.X. and BYRNE, D.W., 2009. Association of the metabolic syndrome with pulmonary venous hypertension. *CHEST Journal,* 136(1), pp. 31-36.

ROBERTSON, T., HAGUE, D., AARONSON, P. and WARD, J., 2004. Voltage-independent calcium entry in hypoxic pulmonary vasoconstriction of intrapulmonary arteries of the rat. *The Journal of Physiology,* 525(3), pp. 669-680.

ROBERTSON, T.P., MUSTARD, K.J.W, LEWIS, T.H., CLARK, J.H., WYATT, C.N., BLANCO, E.A., PEERS, C., HARDIE, D.G. and EVANS, A.M., 2008. AMP-activated protein kinase and hypoxic pulmonary vasoconstriction. *European Journal of Pharmacology,* 595(1), pp.39-43.

RODMAN, D.M., STELZNER, T.J., ZAMORA, M.R., BONVALLET, S.T., OKA, M., SATO, K., O'BRIEN, R.F. and MCMURTRY, I.F., 1992. Endothelin-1 increases the pulmonary microvascular pressure and causes

pulmonary edema in salt solution but not blood-perfused rat lungs. *Journal of Cardiovascular Pharmacology,* 20(4), pp. 658-663.

ROUNDS, S. and MCMURTRY, I.F., 1981. Inhibitors of oxidative ATP production cause transient vasoconstriction and block subsequent pressor responses in rat lungs. *Circulation Research*, 48(3), pp. 393-400.

ROUX, N., HAVET, E. and MERTL, P., 2004. The myocardial sleeves of the pulmonary veins: potential implications for atrial fibrillation. *Surgical and Radiologic Anatomy,* 26(4), pp. 285-289.

RUSS, U., METZGER, F., KICKENWEIZ, E., HAMBROCK, A., KRIPPEIT-DREWS, P. and QUAST, U., 1997. Binding and effects of K_{ATP} channel openers in the vascular smooth muscle cell line, A10. *British Journal of Pharmacology,* 122(6), pp. 1119-1126

SAKAI, T., TERADA, K., KITAMURA, K. and KURIYAMA, H., 1988. Ryanodine inhibits the Ca-dependent K current after depletion of Ca stored in smooth muscle cells of the rabbit ileal longitudinal muscle. *British Journal of Pharmacology*, 95(4), pp.1089-1100.

SELYANKO, A.A., ROBBINS, J. and BROWN, D.A., 1995. Putative M-type potassium channels in neuroblastoma-glioma hybrid cells: inhibition by muscarine and bradykinin. *Receptors & Channels,* 3(2), pp. 147-159.

SELYANKO, A.A., HADLEY, J.K., WOOD, I.C., ABOGADIE, F.C., JENTSCH, T.J. and BROWN, D.A., 2000. Inhibition of KCNQ1-4 potassium channels expressed in mammalian cells via M1 muscarinic acetylcholine receptors. *The Journal of Physiology,* 522(3), pp. 349-355.

SHAHID, M. and RODGER, I., 1989. The inotropic effect of 4−aminopyridine and pH changes in rabbit papillary muscle. *Journal of Pharmacy and Pharmacology,* 41(9), pp. 601-606.

SHAM, J.S.K., CRENSHAW JR., B.R., DENG, L.H., SHIMODA, L.A. and SYLVESTER, J.T., 2000. Effects of hypoxia in porcine pulmonary arterial myocytes: roles of K_V channel and endothelin-1. *American Journal of Physiology-Lung Cellular and Molecular Physiology,* 279(2), pp. L262-L272.

SHEEHAN, D.W., FARHI, L.E. and RUSSELL, J.A., 1992. Prolonged lobar hypoxia in vivo enhances the responsivity of isolated pulmonary veins to hypoxia. *American Journal of Respiratory and Critical Care Medicine,* 145(3), pp. 640-645.

SHI, G., KLEINKLAUS, A.K., MARRION, N.V. and TRIMMER, J.S., 1994. Properties of $K_V2.1$ K^+ channels expressed in transfected mammalian cells. *The Journal of Biological Chemistry,* 269(37), pp. 23204-23211.

SHI, W., WANG, C.G., DANDURAND, R.J., EIDELMAN, D.H. and MICHEL, R.P., 1998. Differential responses of pulmonary arteries and veins to histamine and 5-HT in lung explants of guinea-pigs. *British Journal of Pharmacology,* 123(8), pp. 1525-1532.

SIMONNEAU, G., GALIÉ, N., RUBIN, L.J., LANGLEBEN, D., SEEGER, W., DOMENIGHETTI, G., GIBBS, S., LEBREC, D., SPEICH, R., BEGHETTI, M., RICH, S. and FISHMAN, A., 2004. Clinical classification of pulmonary hypertension. *Journal of the American College of Cardiology,* 43(12), pp. 5S-12S.

SMIRNOV, S.V., BECK, R., TAMMARO, P., ISHII, T. and AARONSON, P.I., 2002. Electrophysiologically distinct smooth muscle cell subtypes in rat conduit and resistance pulmonary arteries. *The Journal of Physiology,* 538(3), pp. 867-878.

SMITH, P.A., WILLIAMS, B.A. and ASHCROFT, F.M., 1994. Block of ATP-sensitive K^+ channels in isolated mouse pancreatic β-cells by 2, 3-butanedione monoxime. *British Journal of Pharmacology,* 112(1), pp. 143-149.

SREBNIK, H.H., 2002. *Concepts in Anatomy.* New York, NY: Springer US.

STARR, I., LAMM, W., NERADILEK, B., POLISSAR, N., GLENNY, R. and HLASTALA, M., 2005. Regional hypoxic pulmonary vasoconstriction in prone pigs. *Journal of Applied Physiology,* 99(1), pp. 363-370.

STAUB, N.C., 1985. Site of hypoxic pulmonary vasoconstriction. *CHEST Journal,* 88(4), pp. 240S-245S.

SYLVESTER, J., SHIMODA, L.A., AARONSON, P.O. and WARD, J.P.T., 2012. Hypoxic pulmonary vasoconstriction. *Physiological Reviews,* 92(1), pp. 367-520.

TAGAWA, H., TOMOIKE, H. and NAKAMURA, M., 1991. Putative mechanisms of the impairment of endothelium-dependent relaxation of the aorta with atheromatous plaque in heritable hyperlipidemic rabbits. *Circulation Research,* 68(2), pp. 330-337.

TAKAHASHI, H., SOMA, S., MURAMATSU, M., OKA, M. and FUKUCHI, Y., 2001. Upregulation of ET-1 and its receptors and remodeling in small pulmonary veins under hypoxic conditions. *American Journal of Physiology-Lung Cellular and Molecular Physiology,* 280(6), pp. L1104-L1114.

TAYLOR, B.J., KJAERGAARD, J., SNYDER, E.M., OLSON, T.P. and JOHNSON, B.D., 2011. Pulmonary capillary recruitment in response to hypoxia in healthy humans: a possible role for hypoxic pulmonary venoconstriction? *Respiratory Physiology & Neurobiology,* 177(2), pp. 98-107.

THELLIN, O., ZORZI, W., LAKAYE, B., DE BORMAN, B., COUMANS, B., HENNEN, G., GRISAR, T., IGOUT, A. and HEINEN, E., 1999. Housekeeping genes as internal standards: use and limits. *Journal of Biotechnology,* 75(2), pp. 291-295.

THOMAS, S., 2003. The use of the Laplace equation in the calculation of sub-bandage pressure. *EWMA Journal*, 3(1), pp. 21-23.

THORNE, G.D., SHIMIZU, S. and PAUL, R.J., 2001. Hypoxic vasodilation in porcine coronary artery is preferentially inhibited by organ culture. *American Journal of Physiology-Cell Physiology,* 281(1), pp. C24-C32.

THORNE, G.D., CONFORTI, L. and PAUL, R.J., 2002. Hypoxic vasorelaxation inhibition by organ culture correlates with loss of K_V channels but not Ca^{2+} channels. *American Journal of Physiology-Heart and Circulatory Physiology,* 283(1), pp. H247-H253.

THORNE, G.D. and PAUL, R.J., 2003. Effects of organ culture on arterial gene expression and hypoxic relaxation: role of the ryanodine receptor. *American Journal of Physiology-Cell Physiology,* 284(4), pp. C999-C1005.

TIAN, X.Y., WONG, W.T., XU, A., LU, Y., ZHANG, Y., WANG, L., CHEANG, W.S., WANG, Y., YAO, X. and HUANG, Y., 2012. Uncoupling protein-2 protects endothelial function in diet-induced obese mice. *Circulation Research,* 110(9), pp. 1211-1216.

TODA, N., 1990. Mechanism underlying responses to histamine of isolated monkey and human cerebral arteries. *The American Journal of Physiology,* 258(2), pp. H311-H317.

TOGA, H., IBE, B.O. and RAJ, J.U., 1992. In vitro responses of ovine intrapulmonary arteries and veins to endothelin-1. *American Journal of Physiology-Lung Cellular and Molecular Physiology,* 263(1), pp. L15-21.

TOLIC-NORRELYKKE, I.M. and WANG, N., 2005. Traction in smooth muscle cells varies with cell spreading. *Journal of Biomechanics,* 38(7), pp. 1405-1412.

TORO, L., GONZALEZ-ROBLES, A. and STEFANI, E., 1986. Electrical properties and morphology of single vascular smooth muscle cells in culture. *American Journal of Physiology-Cell Physiology,* 251(5), pp. C763-C773.

TORTORA, G.J. and DERRICKSON, B., 2006. *Principles of Anatomy and Physiology.* 11th ed. Hoboken, NJ: John Wiley & Sons, Inc.

TOWNSLEY, M.I., 2012. Structure and composition of pulmonary arteries, capillaries, and veins. *Comprehensive Physiology,* 2, pp. 675-709.

TRACEY, W.R., HAMILTON, J.T., CRAIG, I.D. and PATERSON, N.A., 1989a. Responses of isolated guinea pig pulmonary venules to hypoxia and anoxia. *Journal of Applied Physiology,* 67(5), pp. 2147-2153.

TRACEY, W.R., BEND, J.R., HAMILTON, J. and PATERSON, N., 1989b. Role of lipoxygenase, cyclooxygenase and cytochrome P-450 metabolites in contractions of isolated guinea pig pulmonary venules induced by hypoxia and anoxia. *The Journal of Pharmacology and Experimental Therapeutics,* 250(3), pp. 1097-1104.

TUDER, R.M., ARCHER, S.L., DORFMÃTLLER, P., ERZURUM, S.C., GUIGNABERT, C., MICHELAKIS, E., RABINOVITCH, M., SCHERMULY, R., STENMARK, K.R. and MORRELL, N.W., 2013. Relevant issues in the pathology and pathobiology of pulmonary hypertension. *Journal of the American College of Cardiology,* 62(25), pp. D4-D12.

UZUN, O. and DEMIRYÜREK, A.T., 2003. Involvement of tyrosine kinase pathway in acute hypoxic vasoconstriction in sheep isolated pulmonary vein. *Vascular Pharmacology,* 40(3), pp. 175-181.

VIERA, A.J., 2007. The new "normal" blood pressure: what are the implications for family medicine? *Journal of the American Board of Family Medicine,* 20(1), pp. 45-51.

WAGENVOORT, C. and WAGENVOORT, N., 1976. Pulmonary venous changes in chronic hypoxia. *Virchows Archiv,* 372(1), pp. 51-56.

WAGENVOORT, C. and WAGENVOORT, N., 1982. Pulmonary veins in high-altitude residents: a morphometric study. *Thorax,* 37(12), pp. 931-935.

WALCH, L., DE MONTPREVILLE, V., BRINK, C. and NOREL, X., 2001. Prostanoid EP_1- and TP-receptors involved in the contraction of human pulmonary veins. *British Journal of Pharmacology*, 134(8), pp. 1671-1678.

WANG, L., YIN, J., NICKLES, H.T., RANKE, H., TABUCHI, A., HOFFMANN, J., TABELING, C., BARBOSA-SICARD, E., CHANSON, M., KWAK, B.R., SHIN, H., WU, S., ISAKSON, B.E., WITZENRATH, M., DE WIT, C., FLEMING, I., KUPPE, H. and KUEBLER, W.M., 2012. Hypoxic pulmonary vasoconstriction requires connexin 40–mediated endothelial signal conduction. *The Journal of Clinical Investigation,* 122(11), pp. 4218-4230.

WAYPA, G.B., CHANDEL, N.S. and SCHUMACKER, P.T., 2001. Model for hypoxic pulmonary vasoconstriction involving mitochondrial oxygen sensing. *Circulation Research,* 88(12), pp. 1259-1266.

WAYPA, G.B., MARKS, J.D., MACK, M.M., BORIBOUN, C., MUNGAI, P.T. and SCHUMACKER, P.T., 2002. Mitochondrial reactive oxygen species trigger calcium increases during hypoxia in pulmonary arterial myocytes. *Circulation Research,* 91(8), pp. 719-726.

WEAVER, L.K. and CHURCHILL, S., 2001. Pulmonary edema associated with hyperbaric oxygen therapy. *CHEST Journal,* 120(4), pp. 1407-1409.

WEBB, R.C., 2003. Smooth muscle contraction and relaxation. *Advances in Physiology Education,* 27(4), pp. 201-206.

WEISSMAN, N., EBERT, N., AHRENS, M., GHOFRANI, H.A., SCHERMULY, R.T., HÄNZE, J., LUDGER, F., ROSE, F., CONZEN, J., SEEGER, W. and GRIMMINGER, F., 2003. Effects of mitochondrial inhibitors and uncouplers on hypoxic vasoconstriction in rabbit lungs. *American Journal of Respiratory Cell and Molecular Biology,* 29(6), pp. 721-732.

WENZEL, D., MATTHEY, M., BINDILA, L., LERNER, R., LUTZ, B., ZIMMER, A. and FLEISCHMANN, B.K., 2013. Endocannabinoid anandamide mediates hypoxic pulmonary vasoconstriction. *Proceedings of the National Academy of Sciences of the United States of America,* 110(46), pp. 18710-18715.

WIDMAIER, E.P., RAFF, D. and STRANG, K.T., 2006. *Vander's Human Physiology.* 10th ed. New York, NY: McGraw-Hill Education.

WIECZOREK, D., DELAURIERE, L. and SCHAGAT, T., 2012. *Methods of RNA quality assessment.* [online]. Madison, WI: Promega Corporation. Available from: https://www.promega.co.uk/resources/pubhub/methods-of-rna-quality-assessment/?activeTab=0 [Accessed 20 September 2016]

WILKINSON, J.M., SARGENT, C.A., GALINA-PANTOJA, L. and TUCKER, A.W., 2010. Gene expression profiling in the lungs of pigs with different susceptibilities to Glässer's disease. *BMC Genomics.* [online] 11(1). Available from: http://bmcgenomics.biomedcentral.com/articles/10.1186/1471-2164-11-455 [Accessed 20 September 2016]

YAMANE, T., DATE, T., TOKUDA, M., ARAMAKI, Y., INADA, K., MATSUO, S., SHIBAYAMA, K., MIYANAGA, S., MIYAZAKI, H., SUGIMOTO, K. and YOSHIMURA, M., 2008. Hypoxemia in inferior

pulmonary veins in supine position is dependent on obesity. *American Journal of Respiratory and Critical Care Medicine,* 178(3), pp. 295-299.

YAN, J., CHEN, R., LIU, P. and GU, Y., 2014. Docosahexaenoic acid attenuates hypoxic pulmonary vasoconstriction by activating the large conductance Ca^{2+}-activated K^{+} currents in pulmonary artery smooth muscle cells. *Pulmonary Pharmacology & Therapeutics,* 28(1), pp. 9-16.

YOSHINO, M., WANG, S.Y. and KAO, C.Y., 1997. Sodium and calcium inward currents in freshly dissociated smooth myocytes of rat uterus. *The Journal of General Physiology,* 110(5), pp. 565-577

YUAN, X.J., GOLDMAN, W.F., TOD, M.L., RUBIN, L.J. and BLAUSTEIN, M.P., 1993. Hypoxia reduces potassium currents in cultured rat pulmonary but not mesenteric arterial myocytes. *American Journal of Physiology-Lung Cellular and Molecular Physiology,* 264(2), pp. L116-L123.

YUAN, X.J., 1995. Voltage-gated K^{+} currents regulate resting membrane potential and $[Ca^{2+}]_i$ in pulmonary arterial myocytes. *Circulation Research,* 77(2), pp. 370-378.

ZELLERS, T.M., MCCORMICK, J. and WU, Y., 1994. Interaction among ET-1, endothelium-derived nitric oxide, and prostacyclin in pulmonary arteries and veins. *American Journal of Physiology-Heart and Circulatory Physiology,* 267(1), pp. H139-H147.

ZHAO, Y., PACKER, C.S. and RHOADES, R.A., 1993. Pulmonary vein contracts in response to hypoxia. *American Journal of Physiology-Lung Cellular and Molecular Physiology,* 265(1), pp. L87-L92.

ZHAO, Y., PACKER, C.S. and RHOADES, R.A., 1995. Chronic hypoxia impairs pulmonary venous smooth muscle contraction. *Respiration Physiology,* 100(1), pp. 75-82.

ZHAO, Y., PACKER, S. and RHOADES, R.A., 1996. The vein utilizes different sources of energy than the artery during pulmonary hypoxic vasoconstriction. *Experimental Lung Research,* 22(1), pp. 51-63.

ZHUANG, F.Y., FUNG, Y.C. and YEN, R.T., 1983. Analysis of blood flow in cat's lung with detailed anatomical and elasticity data. *Journal of Applied Physiology,* 55(4), pp. 1341-1348.

Appendix 1

Molecular Profiling of K^+ Channel Expression in Porcine Pulmonary Veins

Introduction

The aim of studies within this appendix was to investigate the molecular basis of K^+ channels in PVs identified in myography experiments (Chapter 4) and to identify potential targets for electrophysiological experiments (Chapter 5). To that aim, RNA was extracted from PVs before amplifying transcripts using a suite of molecular biology techniques called reverse transcription polymerase chain reaction (RT-PCR).

Despite previous successful RNA extraction and RT-PCR from blood vessels by both this research group (Dospinescu *et al.*, 2012) and others (Archer *et al.*, 2004, Michelakis *et al.,* 2001), data were disappointing. The exact reason for this could not be pinpointed although achieving proper homogenisation of blood vessels (due to thick vessel walls and high content of connective tissue) was suspected as a major contributing factor to the large variations observed in RNA yield and quality. The findings within this appendix reflect attempts to optimise RNA extraction and RT-PCR from abattoir-derived porcine PVs and other blood vessels.

RNA Extraction

RNA of good quality and yield is required for transcripts (mRNAs) to get reliably amplified for molecular profiling. Extraction results are summarised in Table 1. The data illustrate the wide range of RNA yields and concentrations observed when extracting RNA from porcine blood vessels (including PVs). Note that a significant proportion of extractions (18.6%) produced undetectable RNA. However, in extractions which yielded enough RNA to use for reverse transcription (RT) this was often not successful either which may have been due to poor RNA quality. The issue of RNA quality will be discussed later in this appendix.

Table 1. Results of RNA extractions from porcine blood vessels. RNA data were obtained with the fluorescent Qubit™ 2.0 kit (Life Technologies, UK); lower detection limit 4ng/μL. Data represent RNA extraction from porcine pulmonary veins, pulmonary arteries, coronary artery and vena cava and exclude data from freshly dissociated cells.

	Porcine blood vessels
Number of extractions (n)	43
Number of animals (N)	14
Sample weight (mg)	22.5 ± 2.6 (mean ± S.E.M); range: 4.8 – 42
RNA yield (ng/mg tissue)	72.7 ± 22.2 (mean ± S.E.M); range: 3.3 – 326.5
RNA concentration (ng/μL)	65.2 ± 35.2 (mean ± S.E.M); range: 5.0 – 760.7
Volume of eluate (μL)	10 – 50
% of samples with undetectable RNA (<4μg/mL)	18.6

In contrast to the variable results seen with blood vessels, RNA extractions from a variety of other tissues (liver, retina, adrenal gland and brain tissue) proved more reliable (Table 2). Indeed, extractions from all tissues apart from diaphragm produced detectable RNA concentrations and resulting yields/concentrations were more reproducible. Interestingly, diaphragm (where RNA levels were undetectable) is composed mainly of smooth muscle, similar to blood vessels, whereas the other tissues used contain little connective tissue.

Table 2. Results of RNA extractions from tissues other than blood vessels. RNA data were obtained with the fluorescent Qubit™ 2.0 kit (Life Technologies, UK); lower detection limit 4ng/µL. Diaphragm, liver and retina were obtained from pig; adrenal gland and brain tissue were obtained from mouse.

Tissue	Diaphragm	Liver	Retina	Adrenal gland	Brain tissue
Number of extractions	1	3	1	1	2
Sample weight (mg)	21	[16 – 43]	22	7	[9 – 10]
RNA yield (ng/mg tissue)	N/A	[37.1 – 82.5]	49.4	71.1	[23.3 – 103.1]
RNA concentration (ng/µL)	<4	[35 – 63.8]	43.5	19.9	[9.3 – 37.1]
Volume of eluate (µL)	25	25	25	25	25
% of samples with undetectable RNA (<4µg/mL)	100	0	0	0	0

Therefore it appears the difficulties experienced with RNA extraction in these experiments are likely to be intrinsic to blood vessels. Within the next section, selected examples were chosen which best illustrate the findings of this study.

Assessing RNA Quality

Obtaining good quality, intact RNA is crucial when profiling gene expression. A good test of RNA quality is to look at quality and intensity of 28S and 18S ribosomal RNA bands on an agarose gel. For mammalian RNA, two bands are observed, the longer corresponding to the 28S and the shorter corresponding to the 18S. A 28S:18S intensity ratio of 2:1 is generally indicative of good quality RNA. If genomic DNA is present this appears as another higher molecular weight band which has not run as far as the 28S and 18S. Low quality RNA appears as a smear on the gel corresponding to degraded, small RNA fragments (Wieczorek *et al.*, 2012).

By the criteria above, RNA extracted from blood vessels appeared fairly degraded in terms of low band intensity and smearing on the gel (Figure 1A). RNA extracted from liver is shown for comparison (Figure 1B).

RNA samples were combined with loading buffer (Promega, UK) and made up to a final volume of 14µL with nuclease-free water. Of this, 12µL was loaded on a 1.5% agarose gel in 1x TBE (Tris base, Boric Acid, EDTA, Life Technologies, UK) buffer containing 0.005% GelRed nucleic acid gel stain (Cambridge Bioscience, UK). The gel was run in an electrophoretic gel tank (Thermo Fisher Scientific, UK) at 80V for 80 minutes.

Figure 1 compares RNA samples obtained from blood vessels and liver. Please note that, for the sake of clarity, these and all other gel images within the appendix have had contrast inverted using Image J software.

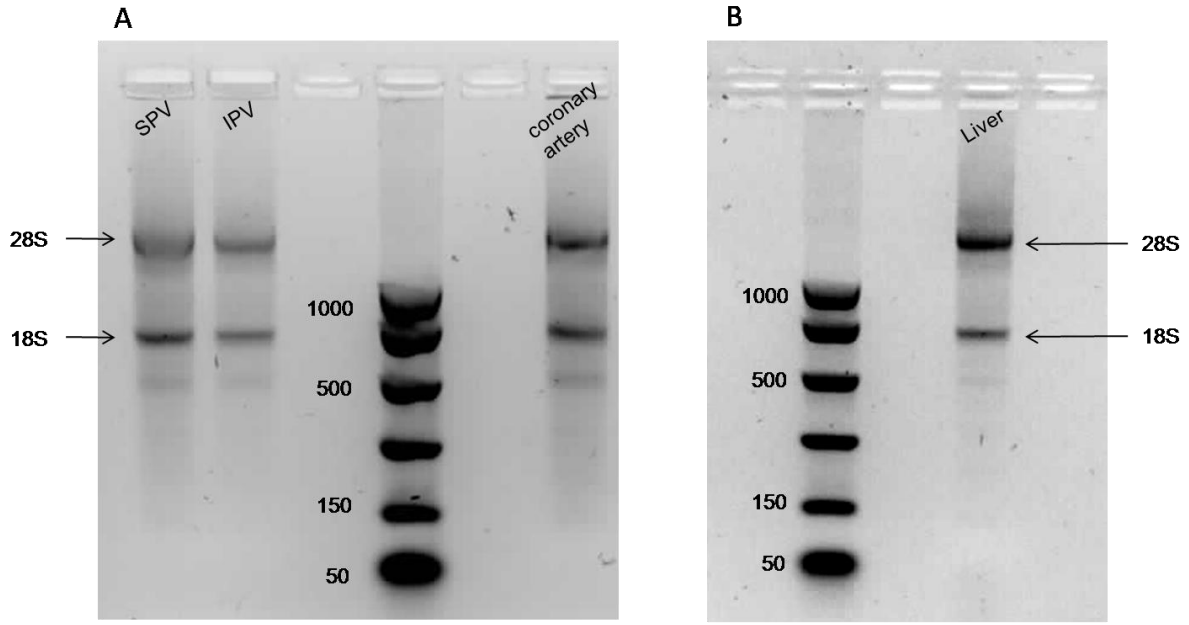

Figure 1. RNA gel showing samples extracted from porcine blood vessels (A) and liver (B). RNA amounts respectively loaded on gel – SPV (superior pulmonary vein): 418.5ng; IPV (inferior pulmonary vein): 307.7ng; coronary artery: 610ng and liver: 264ng. Ladder: PCR Markers Ladder 50-1000 bp (Promega, UK).

As shown in Figure 1, 28S and 18S bands were present for all samples however there was some smearing for the RNA from blood vessels (Figure 1A) whereas RNA from liver shows less smearing with clearer 28S and 18S bands (Figure 1B). This suggests RNA extracted from porcine blood vessels

was not of optimal quality due to lower molecular weight products suggesting RNA degradation. Note that the RNA amount loaded for the liver sample was less (264ng) than for the blood vessels (307-610ng) yet the 28S and 18S bands for liver appear more intense. The extract from liver also appears to show an approximately 2:1 ratio of 28S:18S however RNA extracted from blood vessels was of similar intensity at both bands. Taken together these data suggest that RNA extracted from liver was of better quality and less degraded than RNA from blood vessels. Each band of the PCR markers ladder represents approximately 41 – 55ng product and the fact that all bands of the ladder appear saturated is a reflection of RNA band weakness in the samples.

Crushing and homogenisation of liver tissue was noticeably easier than for blood vessels. Note that in this particular instance different RNA extraction kits were used (for blood vessels: RNeasy mini kit + DNAse (Qiagen) and for liver: High Pure RNA Tissue kit (Roche)). To assess whether the difference in RNA quality was due to the extraction kit or tissue, the same kit (High Pure RNA Tissue kit (Roche)) was used to extract from porcine superior PV and murine pituitary gland.

Homogenisation of murine pituitary gland was much easier than homogenisation of superior PV and was carried out by passing the tissue sample through an 18G then 21G needle whereas the superior PV sample required to be crushed using a mortar and pestle in preparation for needle work. Results are shown in Figure 2.

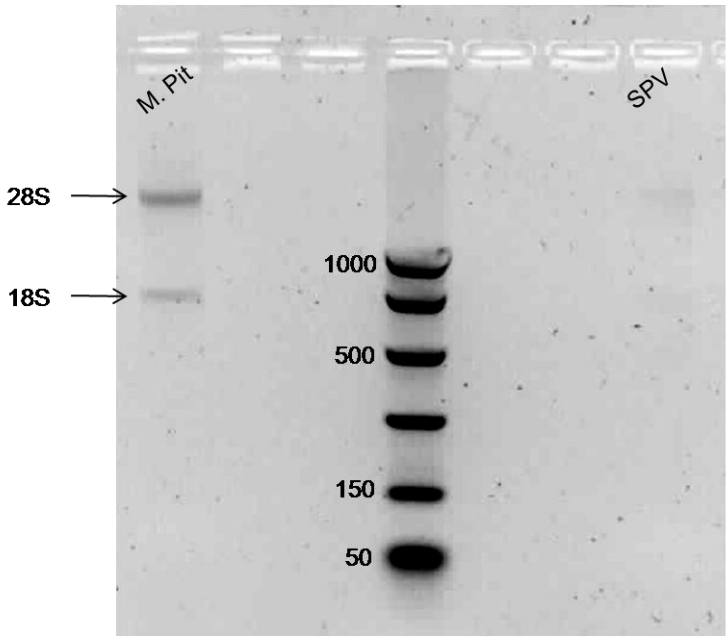

Figure 2. Gel image showing RNA extracted from pituitary gland and superior pulmonary vein. M. Pit: murine pituitary gland (185.5ng) and SPV: porcine superior PV (70.5ng). Ladder: PCR Markers Ladder 50-1000 bp (Promega, UK).

As shown in Figure 2, RNA extracted from porcine superior PV showed smearing on the gel while 28S/18S bands were barely visible, both of which suggest degraded RNA. On the other hand RNA extracted from murine pituitary gland showed two clear and distinct bands with an approximately 2:1 ratio of 28S:18S. This again suggests that RNA extracted from tissues "softer" than blood vessels was of better quality and less degraded. Nonetheless, the ladder bands all appear saturated reflecting the overall weak intensity of bands in samples loaded (similar to Figure 1). Note however the difference in RNA amounts loaded.

Taken together, the data above show that the difference in RNA yield and quality between tissues could not be attributed to the RNA extraction kit but instead confirm the issue probably lies with intrinsic difficulties in homogenising blood vessels.

Reverse Transcription/cDNA Synthesis

After assessment of quality and concentration, RNA was reverse transcribed into complementary DNA (cDNA) prior to amplification because DNA is more stable by its nature than RNA. Transcriptor High Fidelity cDNA Synthesis kit (Roche, UK) was used for reverse transcription (RT) according to manufacturer's instructions and the cDNA produced was then used to investigate gene expression within the samples.

Controls are crucial in the RT process in order to identify any potential genomic contamination within the sample. Any genomic DNA which may be present within the sample will be amplified (alongside cDNA) and can act as a template during PCR producing false positive results. In order to minimise the risk of such contamination, the High Pure RNA Tissue kit (Roche, UK) routinely includes a DNAse incubation step. The RNeasy mini kit (Qiagen, UK) did not contain a specific DNAse step however this was introduced as a separate step of the protocol whereby DNAse was added directly to the column membrane for 15 minutes at room temperature according to manufacturer's instructions. RT controls were carried out as a further precautionary step towards identifying genomic DNA and any false positive results. RT controls here were set up and run in the absence of RT enzyme in parallel with reverse transcribed RNA samples. In such controls, any amplicons could only result from genomic DNA contamination.

PCR

Synthesised cDNA was then used as a template to amplify transcripts of a range of genes by PCR using GoTaq DNA Polymerase (Promega, UK). Primer sequences for each of the transcripts studied are shown in Table 3. Primers were designed to amplify all known variants of a single gene. The primers for BK_{Ca} used here were designed in such a way that they straddle the splice variant STREX, therefore two products may be expected here, depending on cell expression: a shorter band, corresponding to no insert (ZERO) and a longer band corresponding to the STREX insert (Chen *et al.,* 2005, Dospinescu *et al.,* 2012).

Murine primers for Ipo8, Fbxl10 and 18S RNA came as part of QuantiTect Primer Assay kits (Qiagen, UK).

Table 3. Primer sequences for polymerase chain reaction experiments.

Gene	Species	Forward Primer (5' to 3')	Reverse Primer (5' to 3')	Expected Product Length (bp)
K_v1.5 (Kcna5)	Porcine *Sus scrofa*	ccttgtcatcctcatctccatca	aggatctgcagccccttggagt	505
K_v2.1 (Kcnb1)	Porcine *Sus scrofa*	tcctcgccataatttccatca	ttgtcatggtaatggtggccc	560
BK_{Ca} (Kcnma1)	Porcine *Sus scrofa*	gtccttccctactgtttg	gtgcttgagctcatggtagt	670 (zero) 845 (STREX)
β-actin (ACTB)	Porcine *Sus scrofa*	tccctggagaagagctacga	tgttggcgtagaggtccttc	182 (cDNA) 280 (gDNA)
Ipo8	Porcine *Sus scrofa*	ctctttgaacgatatggaagcc	gccatcatttttggcaacacc	427
Fbxl10	Porcine *Sus scrofa*	acgccatggagggcaaagattt	ttctctgaaacatgggccaagg	235
BK_{Ca} (Kcnma1)	Murine *Mus musculus*	gtttgtgagctgtgttttgtg	gtgtttgagctcatgatagtg	611 (zero) 791 (STREX)
β-actin (ACTB)	Murine *Mus musculus*	tcctccctgagaaagagcta	accagacagcactgtgttgg	203

DNA amplification via PCR was carried out along the parameters shown in Figure 3 with a T3000 Biometra thermocycler (T3000, Biometra, Göttingen, Germany). The steps of PCR include denaturation, annealing and elongation. Denaturation involves breaking the hydrogen bonds between the two strands of cDNA allowing it to unwind and separate into single-strands. Annealing involves the primers attaching to the complementary part of cDNA template. Elongation requires DNA Polymerase enzyme and involves synthesis of a new strand of DNA complementary to the

starting cDNA template by addition of dNTPs starting from the annealed primer and moving in a 5'to 3' direction.

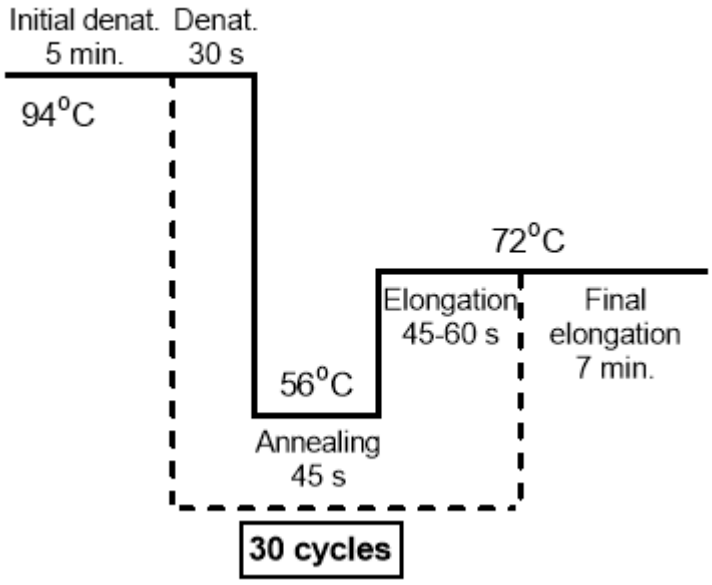

Figure 3. Diagram showing DNA amplification parameters for polymerase chain reaction. Note denat. = denaturation.

End products were run on an agarose gel in a gel tank (Bio-Rad, UK) at 100V for 40 – 90 minutes depending on tank size.

Optimising Reverse Transcription

In view of the often low RNA yields, it was thought worthwhile to spend some time optimising RT conditions. This optimisation was carried out using murine pituitary RNA and concentrated on annealing temperatures and the type of RT primers. The effects of varying these parameters were examined for the following amplicons: BK_{Ca}, IPO_8 and Fbxl10 (see also section - "Choosing the most appropriate housekeeping gene"). Note that the same amount of RNA (50ng) was used in each reverse transcription reaction to facilitate comparison. Results are shown in Figure 4.

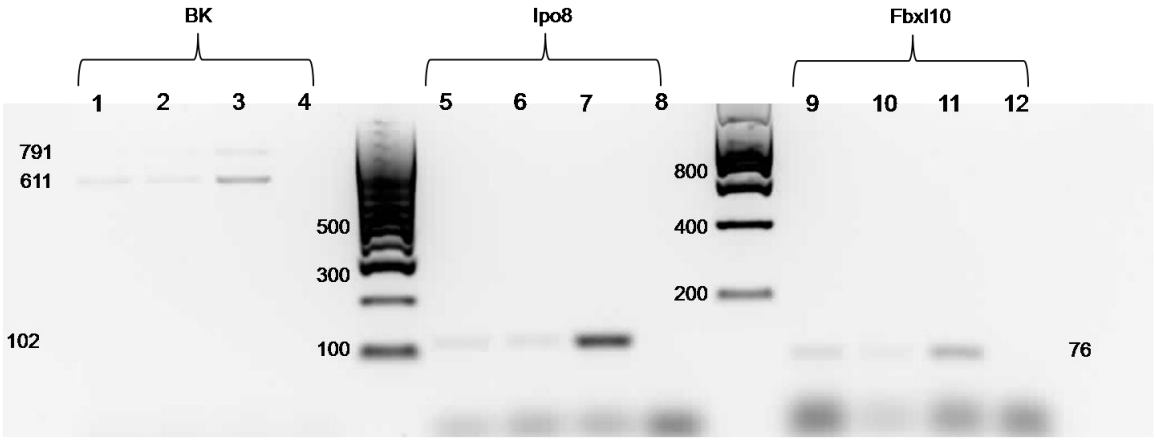

Figure 4. Reverse transcription optimisation: effect of annealing temperature and primer types on amplicons intensity. DNA gel showing amplified transcripts of BK_{Ca}, IPO_8 and Fbxl10 from mouse pituitary. The gel was loaded in groups of four lanes for each transcript. In each group, the four lanes from left to right represent: RT temperature 45°C with oligodT, RT temperature 55°C with oligodT, RT temperature 45°C with random hexamers and PCR control. HyperLadder™ 100bp (left ladder) and HyperLadder™ 1kb (right ladder; both Bioline, UK).

When RT was performed with oligodT primers at either 45°C or 55°C, all bands were very faint; by contrast bands were present and clear for all genes with random hexamers,. Therefore using random hexamers in the RT (as opposed to oligodT) produced the most noticeable improvement in amplicon intensity. This might be expected considering priming with oligodT means only RNA fragments with an intact poly-A tail (i.e. mRNA) will be reverse transcribed while random hexamers randomly prime any RNA fragments including RNA which is degraded and has subsequently lost the poly-A tail. On the downside, DNA fragments may also get reverse transcribed hence increasing the risk of genomic contamination. In light of the improved amplicon intensity with random hexamers, all further experiments were performed in the presence of random hexamers as well as oligodT. The effect of temperature could not be assessed because bands were too weak in these instances.

The bands for the ladders used in this experiment represent varying amounts of product (weight ladders) thus allowing a measure of amplicon intensity. The 100 bp band, which was of comparable intensity to IPO_8 in lane 7 (random hexamers), represents 40ng of product. All other amplicon band intensities were lower than the least intense band of the ladder (200 bp) which represents only 20ng product suggesting a very low amount of transcript was produced in these reactions.

To rule out contamination, PCR controls were run on the gel beside samples. PCR controls were performed by omitting cDNA template in the reaction, replacing it with H_2O. RT controls were not performed in this particular case as DNA levels were undetectable using Qubit™ (<2ng/µL DNA).

Choosing the Most Appropriate Housekeeping Gene

The rationale for using housekeeping genes during PCR is that they provide an internal control as they are expressed at stable levels in a given cell type (Thellin *et al.,* 1999).

β-actin

β-actin is widely used as a housekeeping gene because of its essential function in all cells in the structure and kinetics of the cytoskeleton (Thellin *et al.,* 1999). Initial experiments with porcine RNA were performed with β-actin as the housekeeping gene however the intensity of the β-actin band was much stronger than for the K^+ channels (see Figure 5).

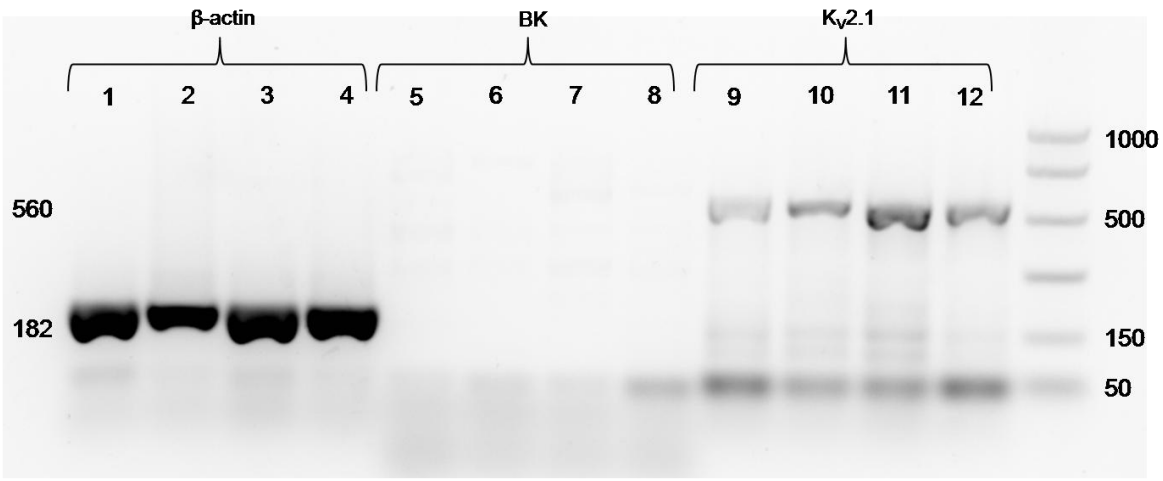

Figure 5. DNA gel image showing K+ channel amplicons alongside β-actin as a housekeeping gene in porcine pulmonary veins. Gel showing amplicons of K_V2.1, BK_{Ca} and β-actin from porcine superior and inferior pulmonary veins (PVs). The gel was loaded in groups of four lanes for each gene. In each group, the first two lanes represent superior PV (2 separate PCR reactions with the same cDNA) while the third and fourth lanes represent inferior PV (2 separate PCR reactions with the same cDNA). RNA amounts used in the RT, respectively – superior PV: 248ng; inferior PV: 537ng. cDNA was diluted 1 in 5 for all reactions. Ladder: PCR Markers Ladder 50-1000bp. Each band of the ladder represents approximately 41-55ng of product.

In Figure 5, there were no bands for BK_{Ca}, weak bands for K_V2.1 and very strong bands for β-actin. The β-actin bands were saturated and of much higher intensity than both the K^+ channels (BK_{Ca} and K_V2.1). The bands for K_V2.1 were similar to the intensity of the ladder (41-55ng) however bands for BK_{Ca} were not visible. The primers for β-actin were designed specifically by Wilkinson *et al.* (2010) to span an intron-exon boundary (intron 4) therefore when genomic DNA is used as a template the amplicon contains the intron (280 bp) and is larger than when cDNA acts as a template (182 bp). Hence in the presence of genomic DNA contamination two distinct bands would be visible on the gel. The bands for β-actin in Figure 5 represent cDNA as they appear at 182 bp.

In an attempt to better match band intensity between β-actin and K^+ channels, the cDNA was diluted 10 times in the β-actin reaction tube (Figure 6). In this experiment, 50ng RNA was used in the RT for both brainstem and adrenal gland. RT controls were also performed as a double check as DNA levels were undetectable (<2ng/μL DNA) with Qubit™.

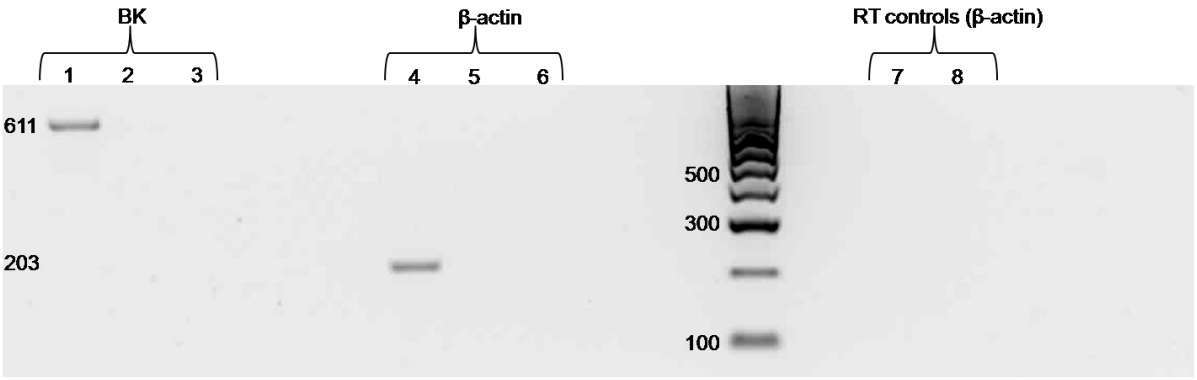

Figure 6. DNA gel image showing BKCa channel amplicons alongside β-actin. Gel showing amplicons of BK_{Ca} and β-actin from mouse brainstem and adrenal gland RNA, respectively. Note that cDNA was diluted 1 in 10 for β-actin. Gels were loaded in groups of three lanes for BK_{Ca} and β-actin. In each group from left to right: brainstem, adrenal gland and PCR control. RT controls (with β-actin primers) were loaded on right of the ladder: mouse brainstem (7) and adrenal gland (8). Ladder: HyperLadder™ 100bp.

As can be seen in Figure 6, bands for BK_{Ca} and β-actin, respectively, were obvious in brainstem but not in adrenal gland. As β-actin was missing this points to a failure in the RT reaction for adrenal gland. This suspicion was later confirmed when a second RT was performed with the same adrenal gland RNA which produced a band for β-actin.

When cDNA was diluted 1 in 10 for β-actin, the band intensity in mouse brainstem was similar to that for BK_{Ca} which allows for direct comparison of expression levels. Band intensity for both genes in brainstem was similar to that of the 200bp band of Hyperladder™ 100bp which represents 20ng of product. Hence even when bands are present for BK_{Ca}, intensity is low.

PCR controls for both brainstem and adrenal gland were negative as were RT controls (RT performed in the absence of RT enzyme) confirming the absence of genomic DNA contamination in these samples.

These data show that to get comparable band intensity between K^+ channels and β-actin, the amount of cDNA template in the PCR reaction needed to be diluted 10 times. To avoid the complication β-actin was dropped in favour of a more adequate housekeeping gene in further experiments.

Alternative Housekeeping Genes to β-actin

The difference in expression levels between K^+ channels and β-actin prompted exploration of other more adequate housekeeping genes. K^+ channels are generally expressed at low levels, requiring a housekeeping gene with similar levels of expression.

Following kind help and expert advice from Heather McClafferty (Professor Mike Shipston's group, Centre of Integrative Physiology, University of Edinburgh), three housekeeping genes were selected, namely 18S rRNA, IPO_8 and Fbxl10. Heather also kindly provided the murine primers for these genes. 18S rRNA has been suggested as a more suitable alternative to β-actin within human T lymphocytes (Bas *et al.,* 2004) however the most stably expressed housekeeping genes in adipose tissue/cells were identified as IPO_8 and Fbxl10 with 18S rRNA showing more variability (Hurtado del Pozo *et al.,* 2010).

Expression of these housekeeping genes alongside BK_{Ca} in mouse pituitary gland RNA extracts is shown in Figure 7. The RNA amount used in the RT for this experiment was 50ng.

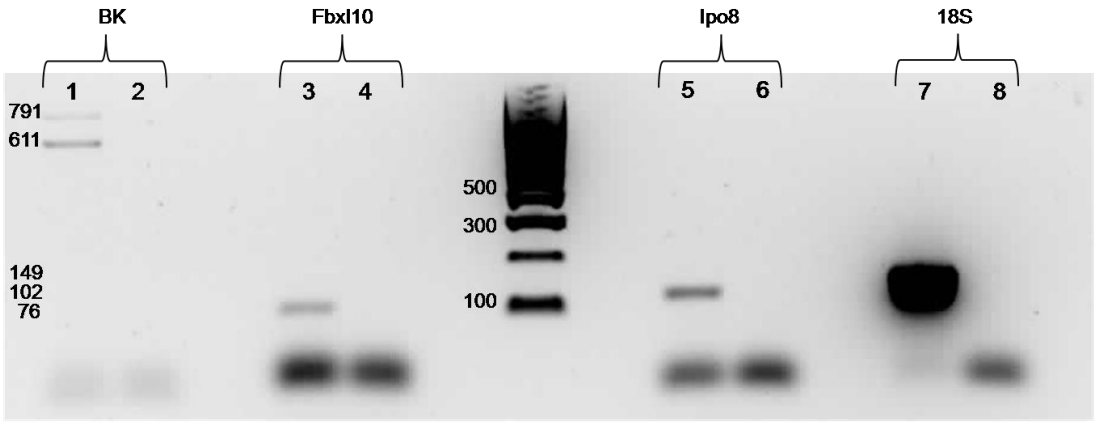

Figure 7. DNA gel comparing expression levels of BKCa with a range of housekeeping genes in murine pituitary gland. The gel was loaded in pairs of lanes: odd numbered lanes represent amplicons of BK_{Ca}, Fbxl10, IPO_8 and 18S rRNA in mouse pituitary RNA and even numbered lanes represent PCR controls for the corresponding transcripts. Ladder: HyperLadder™ 100bp.

Results from murine pituitary show bands were present although fairly weak for BK_{Ca} (two bands: STREX and ZERO - see section "PCR" for an explanation) and Fbxl10. The band for IPO_8 was robust while the band for 18S rRNA was very strong (Figure 7). Amplicon band intensity for BK_{Ca}, Fbxl10 and IPO_8 were comparable to each other as opposed to the 18S rRNA band. However, bands for BK_{Ca}, Fbxl10 and IPO_8 were of lower intensity than the 200bp (20ng) band of the HyperLadder™ 100bp,

illustrating once more the weakness of the signal. Bands on the ladder were all saturated as was the band for 18S rRNA within mouse pituitary and was more reminiscent of β-actin. PCR controls were all negative demonstrating the absence of contamination. RT controls were not performed as DNA levels were undetectable using Qubit™ (<2ng/μL DNA).

High concentrations of 18S rRNA have also been identified in human T Lymphocytes where a 1 in 10 dilution of samples was required (Bas *et al.,* 2004), as observed earlier with β-actin, making this particular gene less suitable as a housekeeping gene in this study.

Based on these findings, IPO_8 was retained as the housekeeping gene in subsequent experiments.

Renewed Attempt at K^+ Channel Profiling in Blood Vessels

As a more adequate housekeeping gene was now available, the next step was to return to gene amplification in blood vessels. Results from inferior PV are shown in Figure 8. Noteworthy is that similar amounts of RNA were used in the RT reaction for this and for the previous experiment carried out with murine pituitary (Figure 7) (48.2ng and 50ng, respectively).

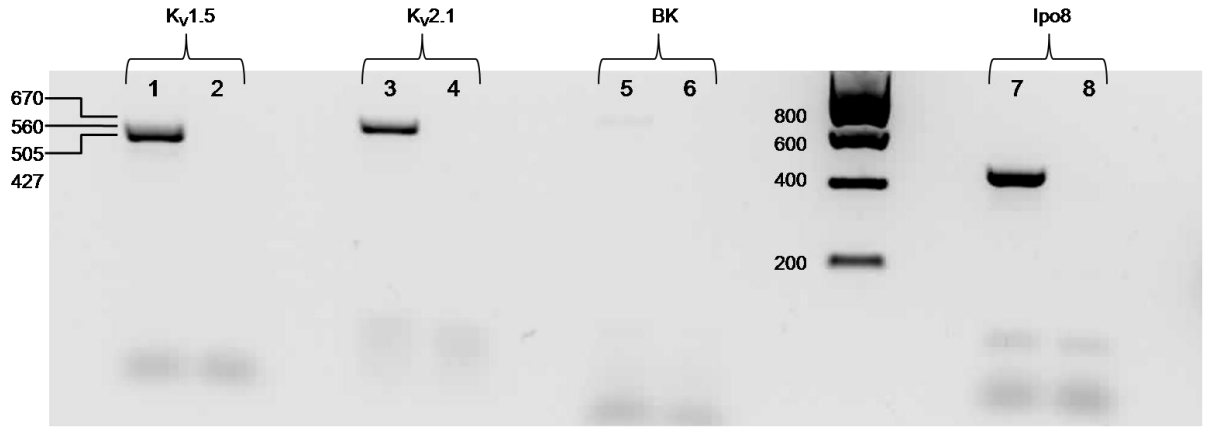

Figure 8. DNA gel showing use of K^+ channel expression in porcine inferior pulmonary vein. Lanes on gel were loaded in pairs: odd numbered lanes represent amplicons of $K_V1.5$ (1), $K_V2.1$ (3), BK_{Ca} (5), and IPO_8 (7) in pig inferior PV while even numbered lanes represent corresponding PCR controls. Ladder: HyperLadder™ 1kb.

Bands were observed for $K_V1.5$, $K_V2.1$ and IPO_8 however no band was apparent for BK_{Ca} within porcine inferior PV in this instance. In addition, the band for IPO_8 was of comparable intensity to the

bands for $K_V1.5$ and $K_V2.1$, in keeping with Figure 7 results showing that IPO_8 band intensity was of comparable to BK_{Ca} channels. Overall, all bands present were of weak intensity when compared to the ladder, a recurring finding within these studies. PCR controls were negative in this experiment demonstrating the absence of contamination. RT controls were not performed as DNA levels were undetectable using Qubit™ (<2ng/μL DNA).

In conclusion, data showed here all illustrate an ongoing issue of weakness of signal which was worse in blood vessels but could be improved in other tissues. Taken together, the data above pointed towards intrinsic difficulties when extracting RNA from blood vessels, most likely linked to the presence of thick vessel walls and high content of connective tissue and subsequent difficulty of homogenising the tissue properly.

K^+ Channel Profiling in Freshly Dissociated Cells from PVs

In an attempt to overcome the difficulty with homogenisation, PV smooth muscle cells (PVSMCs) were dissociated (see protocol in Chapter 2) in order to remove collagen and fibrous tissue prior to extracting RNA which helped with extraction columns getting blocked.

As might be expected, this new approach presented its own issues, stemming this time from the limited numbers of freshly isolated cells - 71% of extractions produced below detection RNA concentrations (14 extractions performed). A successful example of K^+ channel profiling in superior and inferior PVSMCs is shown in Figure 9. RNA amounts used in the RT were 47.4ng and 60ng for superior and inferior PVSMCs, respectively.

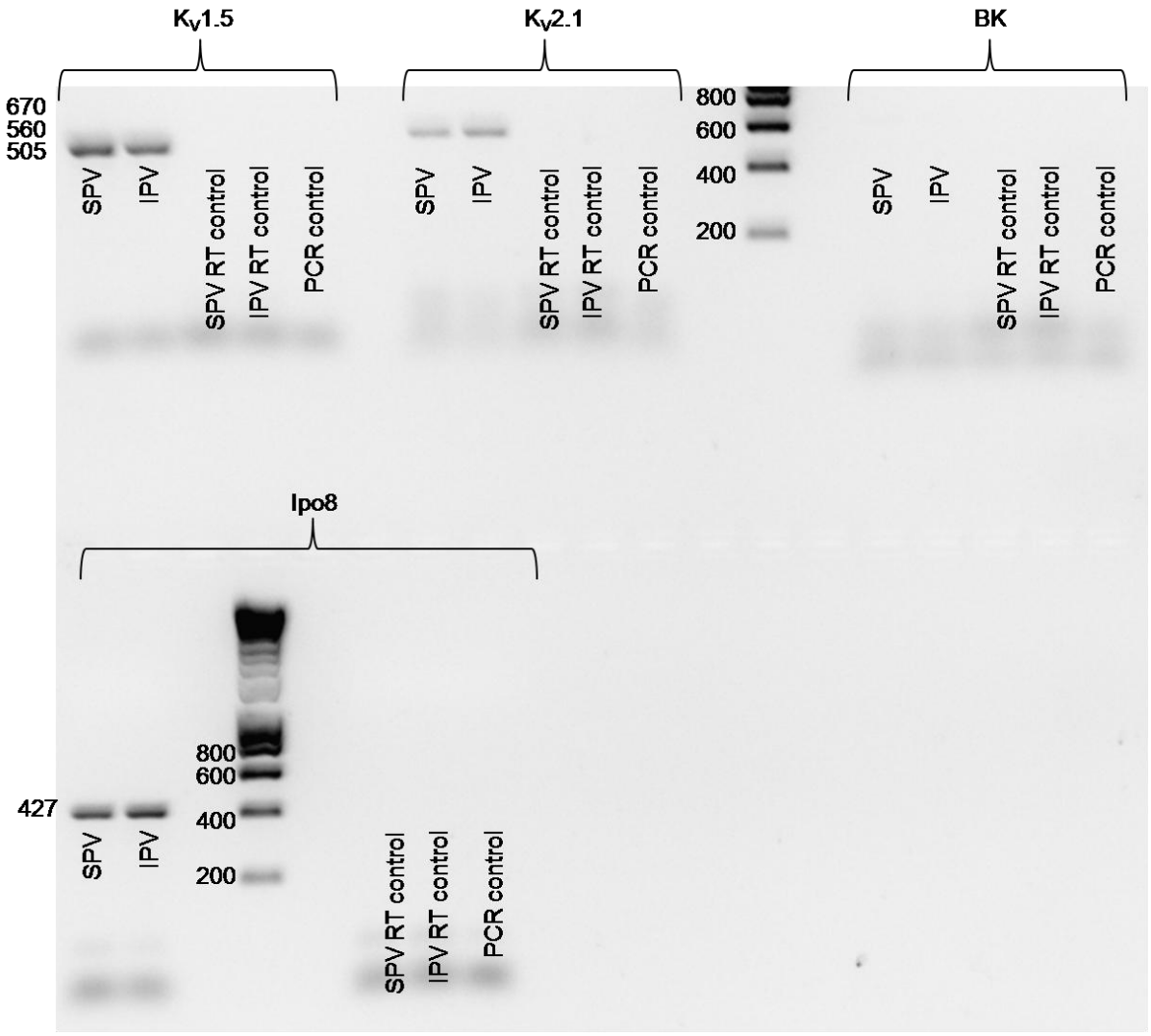

Figure 9. DNA gel showing K+ channels expression profile in dissociated pulmonary vein smooth muscle cells. Note that lanes on the gel were loaded in groups of five for K_V1.5, K_V 2.1, BK_{Ca} and IPO_8, respectively. In each group from left to right, lanes represent superior pulmonary vein smooth muscle cells (PVSMCs): SPV, inferior PVSMCs: IPV, RT control for SPV, RT control for IPV and PCR control. Ladder: HyperLadder™ 1kb.

Bands were obtained for all genes for inferior and superior PVSMCs except for BK_{Ca}. All PCR and RT controls were negative confirming the absence of contamination including genomic DNA (RT controls were a double check as DNA levels were undetectable (<2ng/µL DNA) with Qubit™). Amplicon band intensities from dissociated PVSMC RNA for IPO_8 were similar to the K^+ channels present. Although not very strong, the intensity of bands obtained here were fair, demonstrating that dissociating blood vessel cells prior to RNA extraction could improve data quality. However the high failure rate of this approach remained an issue.

Key Findings

Where RNA was successfully extracted from PVs, expression of $K_V1.5$ and $K_V2.1$ was evident at the mRNA level. Preliminary studies using murine brain tissue were successful in terms of RNA extraction and subsequent identification of BK_{Ca} expression at the mRNA level however expression of BK_{Ca} mRNA was not apparent in PVs. Despite these findings, issues with extraction of RNA of sufficient yield and quality were persistent in PVs while there was less of a problem in other tissues, pointing to an intrinsic difficulty with blood vessels. This difficulty was most likely linked to the presence of thick vessel walls and high content of connective tissue which both hampered proper homogenisation of the tissue. A range of approaches for extracting RNA from PVs were explored (see details in Annex: Tissue samples – storage and homogenisation for a more complete view), however no optimal method could be identified that would provide reproducible, reliable results. For future applications, single cell RT-PCR (as used by Platoshyn *et al.,* 2006 in PASMCs) could be considered. This technique could provide a solution to the problem whereby the whole cell is aspirated into a micropipette and used immediately for RT-PCR.

Annex: Tissue Samples – Storage and Homogenisation

Tissue storage and homogenisation are crucial steps in obtaining good quality RNA in sufficient amounts. In view of continuing limited success on both counts in this study, various approaches were tried to improve the situation. These are briefly described below.

Tissue Storage

Porcine abattoir tissue samples were obtained from either Scotch Premier Meat Ltd (Inverurie, Aberdeenshire) or Quality Pork Producers Ltd (Brechin, Angus). Tissue samples were dissected out from heart and lung tissue within 1-2 hours of kill. PVs were dissected from superior and inferior lobes. Samples were variously: i) snap frozen in liquid N_2 then stored at -80°C ii) snap frozen in liquid N_2 then used on the day or iii) stored in RNAlater (Life Technologies, UK) at 4°C or -20°C according to manufacturer's instructions.

Murine brainstem, pituitary and adrenal gland were obtained from the animal house on the University site and dissected out within 30 minutes of kill before snap freezing in liquid N_2 then storing at -80°C.

Freshly isolated cells (for details see Chapter 2) from inferior and superior PVs were spun down in a centrifuge at 300g for 5 minutes at 4°C. After supernatant elimination, the pellet was variously i)placed in a freezer at -80°C, ii) kept in the fridge or iii) used immediately.

No difference in results was observed when comparing storage methods for any of the tissues/cell samples.

Tissue Homogenisation

Homogenisation of porcine blood vessels was difficult and can partly be attributed to thick walls and high content of connective tissue. A number of different homogenisation techniques were tried including:

1. crushing whilst frozen with glass mortar and pestle and further crushing in lysis buffer
2. crushing in lysis buffer alone
3. crushing tissue directly in liquid N_2
4. mincing the tissue with a razor blade followed by addition of appropriate lysis buffer

5. mechanical homogenisation (with Stuart SHM1 with SHM/5 dispersing tool, Fisher Scientific, UK) alone and after mincing tissue with razor blades

All of these crushing methods were followed by passing tissue and lysis buffer through an 18G and/or 21G needle to further disrupt the tissue. In some experiments, the use of needle work alone was used without initial crushing.

There was a persisting difficulty in homogenisation of porcine blood vessel tissue across all approaches tried during optimisation. In contrast, other tissues were easily homogenised therefore this suggests the problem lies with blood vessels specifically and is likely due to the presence of thick vessel walls and connective tissue.